DESIGN AND TESTING OF PLANT-FIBRE COMPOSITE PROFILES FOR STRUCTURAL FACADE APPLICATIONS

Material selection, profile design and experimental validation of plant-fibre composites mullions in curtain wall applications.

TU Delft Building Technology - Master Thesis

Author
Sander Kerkdijk
Student number: 5076609

Date
04-06-2026

DESIGN AND TESTING OF PLANT-FIBRE COMPOSITE PROFILES FOR STRUCTURAL FACADE APPLICATIONS

BUILDING TECHNOLOGY GRADUATION STUDIO

MSc. Architecture, Urbanism, and Building Sciences
Building Technology Track
Technical University of Delft

Author
Sander Kerkdijk
Student number: 5076609

First mentor
Prof. Dr. M. Overend (Structural design & Mechanics)

Second mentor
Dr. Ing. M. Bilow (Façade and products innovation)

Delegate of the Board of Examiners
Ir. O. Klijn

Date
04-06-2026

ACKNOLEDGEMENT

This project marks the end of my master's programme in Building Technology at the Faculty of Architecture and the Built Environment at Delft University of Technology. This master has been a great journey, during which I have been able to further develop my passion for innovative building materials, façade engineering, and structural design. I am grateful for the knowledge and insights I have gained during this time, which will undoubtedly benefit me in my professional career after graduation.

Working on this thesis has been a challenging but rewarding experience, allowing me to push my limits while exploring new skills in the field of architectural engineering. Without the help and support of many others, this adventure would not have been possible.

First of all, I would like to express my gratitude to my thesis supervisors, Prof. Dr. M. Overend of Structural Design & mechanics and Dr. Ing. M. Bilow of Façade and products innovation, for their valuable insights and for generously sharing their expertise with me throughout this project.

In addition, I would like to thank Dr. ir. F. Veer for his supervision during the mechanical testing conducted at the Faculty of Mechanical Engineering at TU Delft.

Furthermore, I would like to thank Octatube B.V. for providing the necessary materials to manufacture the façade model used in this thesis project.

Finally, I would like to thank my family and close friends for their support during this project. In particular, I would like to thank my fellow architecture graduate student, Matt van Kessel, for taking the time to assist me with the manufacturing process. Your help has been essential in enabling me to complete this thesis.

Thank you all,
Sander Kerkdijk

ABSTRACT

This report investigates the feasibility of using non-wood plant-fibre reinforced composites as structural profile materials for stick-built curtain wall façades in low- and mid-rise buildings. The work is motivated by the need to reduce embodied carbon in building envelopes and by the absence of systematic research on plant-fibre composites in aluminium-like mullion and transom geometries. Existing studies predominantly address coupon-scale behaviour or flat panels and rarely integrate mechanical performance, manufacturability, regulatory compliance, and environmental impact at the profile level.

The study aims to determine to what extent plant-fibre composites can be developed into manufacturable façade profiles that meet the mechanical, environmental, and regulatory requirements of aluminium curtain wall systems. To this end, a structured methodology is adopted, comprising literature review and material selection, definition of performance criteria, iterative experimental manufacturing in three phases, mechanical testing (tension, bending, fastener fixation, thermal expansion), life-cycle assessment, and a basic validation against European curtain wall performance criteria (EN 13830). Cross-stitched flax fibre in a low-viscosity epoxy matrix is ultimately selected, and filament wrapping combined with vacuum bagging and oven curing is developed to produce 50 × 100 × 4 mm rectangular hollow profiles.

Results show that the flax-fibre/epoxy profiles achieve low-to-moderate tensile strengths, stiffness comparable to structural timber, exhibit progressive, damage-tolerant failure, and attain an embodied carbon of about 12.2 kg CO_2-eq/m, exceeding a 70% reduction relative to conventional aluminium profiles with ≈51.1 kg CO_2-eq/m. The profiles satisfy key criteria for wind load resistance and self-weight but remain limited by lower stiffness than aluminium, unresolved fire performance, uncertain long-term hygrothermal durability, and thermoset-driven end-of-life constraints.

The report concludes that flax-fibre/epoxy curtain wall profiles constitute a technically feasible and environmentally promising proof of concept rather than a direct drop-in replacement for aluminium. It contributes a complete, profile-scale evaluation framework and a validated manufacturing route, thereby providing a basis for further research on bio-based façade profiles in the context of low-carbon and circular construction.

KEYWORDS: *Plant-fibre reinforced composites, Curtain wall façades, Flax-fibre/epoxy profiles, Embodied carbon reduction, Bio-based structural materials, Sustainable façade engineering*

TABLE OF CONTENTS

1. INTRODUCTION

1. INTRODUCTION

1.1 BACKGROUND

As building regulations continue to become more stringent in response to climate change targets, the reduction of embodied carbon in the construction sector has gained increasing importance. Conventional load-bearing materials used in buildings are responsible for a significant share of embodied emissions, contributing approximately 48% in office buildings and 46% in residential buildings (LETI, 2020). Although building envelopes are comparatively lightweight, they still account for an estimated 10% to 30% of total embodied carbon (Clark, 2013; Cole & Kernan, 1996), which makes façade systems a relevant focus area for material optimisation.

Within this context, the use of bio-based materials in façade applications is widely recognised as a promising strategy to reduce environmental impact across the building life cycle (Pracucci et al., 2024). Plant-fibre reinforced composites (PFRCs), which combine natural fibres with polymer matrices (figure 1.0), offer a favourable strength-to-weight ratio and therefore appear suitable for lightweight engineering applications. However, their current use in architecture is mainly limited to non-structural components such as insulation or façade cladding panels. Their application in structural façade elements remains limited, partly due to a lack of standardised material data, limited understanding of long-term performance, and challenges related to the manufacturing of complex structural geometries.

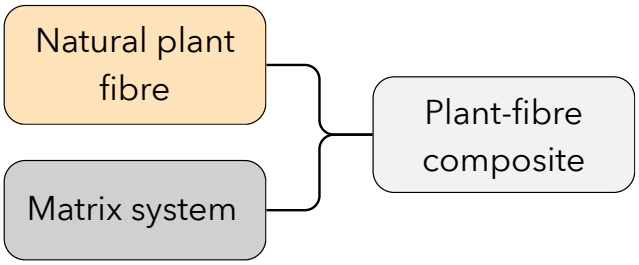

Fig. 1.0 Components of a plant-fibre reinforced composite (own work)

Stick-built curtain wall systems (figure 1.1), which are widely used in commercial and low- to mid-rise buildings, represent a relevant application field for plant-fibre composites. These systems are typically attached to the primary load-bearing structure and are commonly composed of materials such as aluminium, steel, glass, and silicon-based sealants, which are associated with relatively high embodied carbon (figure 1.2). While glazing technologies have evolved considerably through solutions such as triple glazing and adaptive systems, the supporting structural frame is still predominantly based on conventional metals. As a result, the development of low-carbon alternatives for these structural components is essential in order to reduce the overall environmental impact of façade systems.

Fig. 1.1 Aluminum curtain wall design (Aluwood, (2025) (edited image))

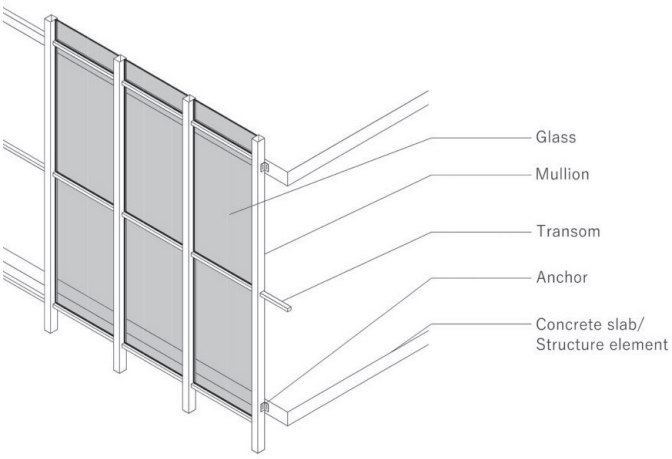

Fig. 1.2 Components of a stick-built curtain wall façade used for low- and midrise buildings in Europe (Dorji, 2024))

This need is further supported by findings from recent studies. Yan Cheong et al. (2024) report that, for a 1 m² aluminium-based curtain wall, structural components account for more than 48% of the total global warming potential. This indicates that improvements in glazing alone are

insufficient and that material substitution in the supporting frame is required to achieve substantial reductions in embodied carbon. At the same time, bio-composites are already applied in sectors such as aerospace and automotive engineering, where their high strength-to-weight ratio has an advantage.

Although interest in bio-composites for sustainable construction is increasing, their application in façade structural profiles is still insufficiently developed. In particular, there is limited research on the translation of plant-fibre composites into complex profile geometries, including aspects such as manufacturability, mechanical performance under relevant loading conditions, and comparative environmental assessment against conventional materials such as aluminium, steel, and timber.

Therefore, this thesis aims to address this research gap by developing, manufacturing, and experimentally evaluating non-wood plant-fibre composite profiles with geometries comparable to curtain wall façade members. The study focuses on optimising the manufacturing process for complex profile geometries, assessing mechanical performance through experimental testing, and comparing the resulting material system with aluminium, steel, and timber in terms of global warming potential, mechanical behaviour, durability, and visual appearance in the context of façade applications for low- and mid-rise buildings.

1.2 PROBLEM STATEMENT

The reduction of embodied carbon in the construction sector requires an increased use of bio-based materials in both new and existing building envelopes. Stick-built curtain wall systems, which have been widely applied since the Industrial Revolution and remain common in contemporary architecture, are now increasingly subject to stricter performance and sustainability requirements. Consequently, many existing façade systems require renovation or replacement to comply with current standards.

Plant-fibre reinforced composites (PFRCs) offer a promising alternative to conventional façade materials such as aluminium, primarily due to their favourable strength-to-weight ratio and potential for improved thermal and acoustic performance. Since curtain wall systems are non-load-bearing, they provide a suitable application context for the initial implementation of these emerging materials, as the structural demands are generally lower compared to primary load-bearing systems.

Despite this potential, the application of PFRCs in structural façade profiles is still limited. Current research lacks consistent mechanical characterisation of profile geometries, validated and scalable manufacturing approaches for continuous elements, and reliable data regarding long-term performance under service conditions. In particular, the development of plant-fibre composites into aluminium-like façade profiles suitable for curtain wall applications has not yet been systematically investigated. In addition, uncertainties remain regarding durability, moisture sensitivity, fire performance, and industrial scalability.

Therefore, this study aims to develop, manufacture, and experimentally evaluate plant-fibre composite façade profiles with geometries comparable to aluminium curtain wall members, and to assess their mechanical performance, manufacturing feasibility, and environmental impact in comparison with conventional materials such as aluminium, steel, and timber.

1.3 RESEARCH OBJECTIVES

The aim of this study is to evaluate the feasibility of using non-wood plant-fibre reinforced composites as structural profile materials for stick-built curtain wall façade systems in low- and mid-rise buildings in Europe. The research specifically investigates whether these composites can be developed into aluminium-like profile geometries and whether they can provide a viable alternative to conventional materials with respect to mechanical performance, durability, and environmental impact, particularly in the context of façade renovation and future low-carbon construction.

To achieve this aim, a structured set of research objectives has been defined.

First, a literature review is performed to identify suitable non-wood plant fibres, commercially available polymer matrix systems, and relevant composite manufacturing techniques for profile

production. In addition, current curtain wall design principles and applicable European performance requirements are examined to define the functional and regulatory boundary conditions for façade mullion and transom elements.

Based on these findings, an appropriate fibre–matrix system and manufacturing approach are selected and translated into a manufacturable profile geometry representative of conventional aluminium curtain wall members. This step ensures that the developed composite system is aligned with both material capabilities and façade design requirements.

Subsequently, plant-fibre composite profiles are manufactured and experimentally tested to assess their mechanical performance, including strength, stiffness, and deformation behaviour, as well as their manufacturability and geometric consistency. The durability is evaluated based on material behaviour.

Finally, the developed profiles are compared with conventional façade materials, namely aluminium, steel, and timber. This comparative assessment is based on global warming potential (GWP), mechanical performance, durability, end-of life potential and visual appearance, in order to determine the potential of plant-fibre composites as sustainable alternatives for curtain wall façade systems.

1.4 RESEARCH QUESTIONS

To address this research objectives, the following main research question is defined:

To what extent can non-wood plant-fibre reinforced composites be developed into manufacturable façade profile geometries that meet the mechanical, environmental, and regulatory requirements of aluminium curtain wall systems?

This main question is supported by the following sub-questions:

1. Which non-wood plant fibres and fibre architecture exhibit the most suitable mechanical properties and processing characteristics for use in load-transferring façade profile applications?

2. What are the requirements for a suitable polymer matrix system compatibilite with non-wood plant fibres?

3. Which composite manufacturing techniques are most suitable for producing aluminium-like profile geometries with a non-wood plant-fibre composite?

4. To what extent do the developed plant-fibre composite profiles meet the mechanical performance requirements of aluminium façade profiles in terms of strength, stiffness, and deformation behaviour?

5. What is the environmental performance of the developed plant-fibre composite profiles in terms of global warming potential and end-of-life treatment and how does this compare to aluminium, steel, and timber façade systems?

6. "To what extent can the developed manufacturing process be upscaled while maintaining structural and environmental performance?

1.5 SCIENTIFIC RELEVANCE

Existing studies into plant-fibre composites primarily focus on material characterisation or flat panel applications, while the development of PFRCs into structural, load-transferring profile geometries comparable to aluminium façade members has not yet been systematically investigated. In addition, there is a lack of integrated research combining manufacturability, mechanical performance at profile scale, compliance with EU regulations, and environmental assessment within a single coherent framework.

This defines a clear research gap: there is currently no established or validated approach for designing and manufacturing complex non-wood plant-fibre composite profiles that replicate aluminium curtain wall mullions and transoms, while simultaneously evaluating their structural performance and environmental impact in comparison to conventional materials such as aluminium, steel, and timber.

Compared to previous work, which is mainly limited to coupon-level testing or non-structural applications, this study investigates plant-fibre composites at the level of functional façade

components. In doing so, it generates new experimental data and provides a design-oriented framework for evaluating the potential of plant-fibre composites in structural façade applications.

1.6 SCOPE AND LIMITATIONS

There exists a wide range of possible plant-fibre matrix combinations for the development of bio-composites. In addition, façade design offers numerous structural applications in which such materials could potentially be implemented. In order to maintain a clear and focused scope, this study is therefore limited to non-wood, plant-derived fibres combined with commercially available polymer matrices, with application to structural components within stick-built, aluminum supported curtain wall façade systems.

Wood fibres, including both hardwood and softwood, are excluded from the scope of this research while these materials are already well-established and widely used building materials.

Figure 1.3 illustrates the three principal categories of bio-composites currently employed in construction, as identified by Ahmad et al. (2025). This research focuses solely on polymer-based bio-composites, owing to their high compatibility with natural fibres. Moreover, the availability of bio-based and biodegradable polymers allows for the development of composites that are fully bio-based and, in some cases, biodegradable as well.

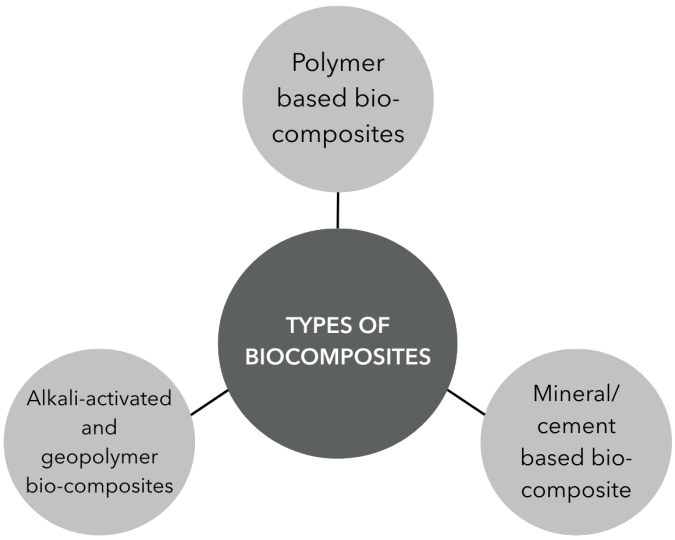

Fig. 1.3. Types of bio-composites for construction applications (adapted from Ahmad et al., 2025).

In addition, this study is limited to available university equipment. Therefore, for this research, only common and available composite manufacturing techniques are evaluated. The manufacturing techniques selected for the experimental phase are therefore selected on cost, availability and use of equipment. In addition, multiple combinations of manufacturing techniques are found in literature to achieve a particular outcome. For this study, only the most common manufacturing techniques are discussed.

2. RESEARCH METHODOLOGY

2. RESEARCH METHODOLOGY

2.1 RESEARCH APPROACH

This study is divided into three main phases: (1) the research phase, (2) the experimental phase, and (3) the validation phase. Figure 2.1 presents a schematic overview of the methodology.

The research follows a scientific-experimental approach in which iterative cycles of development, testing, and evaluation are applied within each experimental phase. Multiple iterations may be performed to improve results; however, each phase concludes with an evaluation and a defined decision point. Once completed, the research proceeds to the next phase without returning to previous stages in order to maintain project progression and ensure achievable outcomes within the available timeframe.

The research phase consists of a literature review on non-wood plant fibres, polymer matrix systems, composite manufacturing techniques, and curtain wall design principles. Particular attention is given to mullion and transom systems to define the geometric requirements and performance criteria for façade applications. Based on these findings, suitable materials and manufacturing techniques are selected for experimental investigation.

The experimental phase consists of three consecutive stages and can be described as research through experimentation. During these stages, selected materials are developed into profile geometries and evaluated through iterative cycles of manufacturing, testing, and assessment.

The first experimental phase focuses on the initial development and optimisation of material configurations and manufacturing methods. Different fibre materials, reinforcements, and production techniques are investigated. Selected samples are examined using microscopy to assess fibre–matrix bonding, material distribution, and surface quality. The most suitable material combination and manufacturing approach are then selected.

The second experimental phase consists of producing multiple specimens for the first mechanical tests. Based on the experimental results, the best-performing material and reinforcement combination is selected.

The third experimental phase focuses on manufacturing the final mullion and transom profile geometry using the selected material system and production method. The resulting profiles are subjected to a final series of mechanical tests and performance evaluations.

Finally, the validation phase consists of a Life Cycle Assessment (LCA) and a comparison with aluminium, steel, and timber profiles based on sustainability, mechanical performance, durability, and visual appearance. In addition, the developed profiles are evaluated against relevant EU curtain wall regulations.

2.1 RESEARCH PLANNING

Figure 2.2 presents the planning of the thesis project and provides an overview of the different research stages and assessment moments. The planning is structured around the assessment milestones A1, A2, A3, and A4, which serve as key decision and evaluation points throughout the project.

The period preceding the A1 assessment is characterised by the research phase, during which the research topic is defined and the theoretical foundation of the study is established. This phase includes the formulation of the background, problem statement, research objectives, research questions, relevance, scope, methodology, and planning. In addition, a substantial part of the literature review is conducted to provide the required knowledge base for the experimental work and to support the go/no-go decision at A1.

The period between A1 and A2 consists primarily of the experimental phase. During the first stage of this period, initial experiments are performed to investigate different materials, reinforcement strategies, and manufacturing techniques. Through iterative testing and evaluation, the most promising approaches are identified and selected for subsequent development. Following this initial stage, the second and third experimental phases focus on the manufacturing and optimisation of the selected profile geometry.

To maintain project progression and avoid excessive experimentation, intermediate deadlines are introduced between assessment moments.

These milestones ensure that conclusions are drawn at predefined stages and that a complete and validated final result can be achieved within the available timeframe.

The period between A2 and A3 is characterised by the final stages of the experimental work, including the development of a façade model as part of the profile evaluation process. In addition, the validation phase is conducted, during which the developed profiles are assessed through comparative analysis and validation against the established performance criteria. The A3 assessment represents the final academic presentation and thesis evaluation. Finally, A4 consists of a presentation moment intended for family and friends, during which the completed project outcomes are presented in a more accessible format.

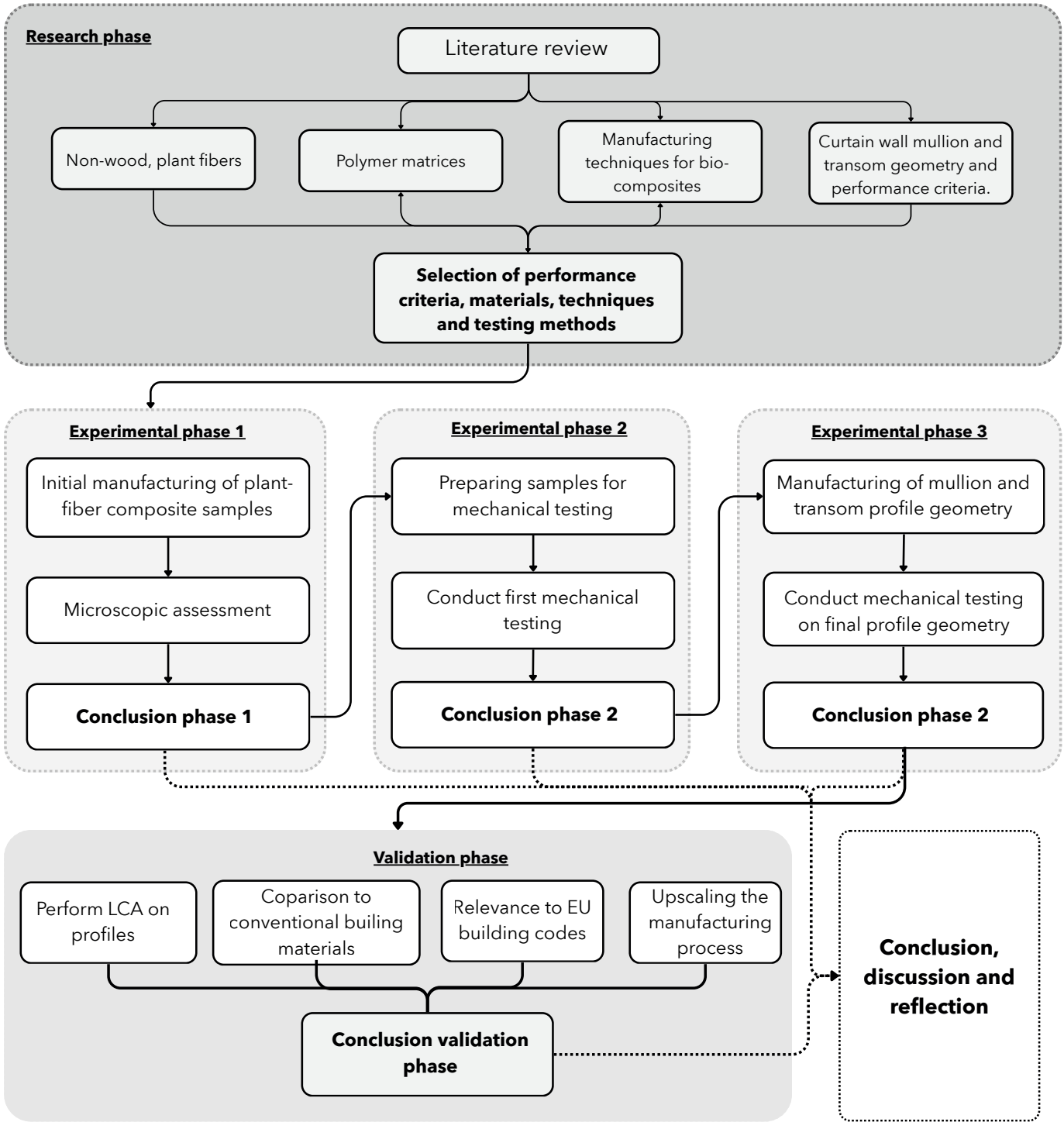

Fig. 2.1 Methodology scheme (own work)

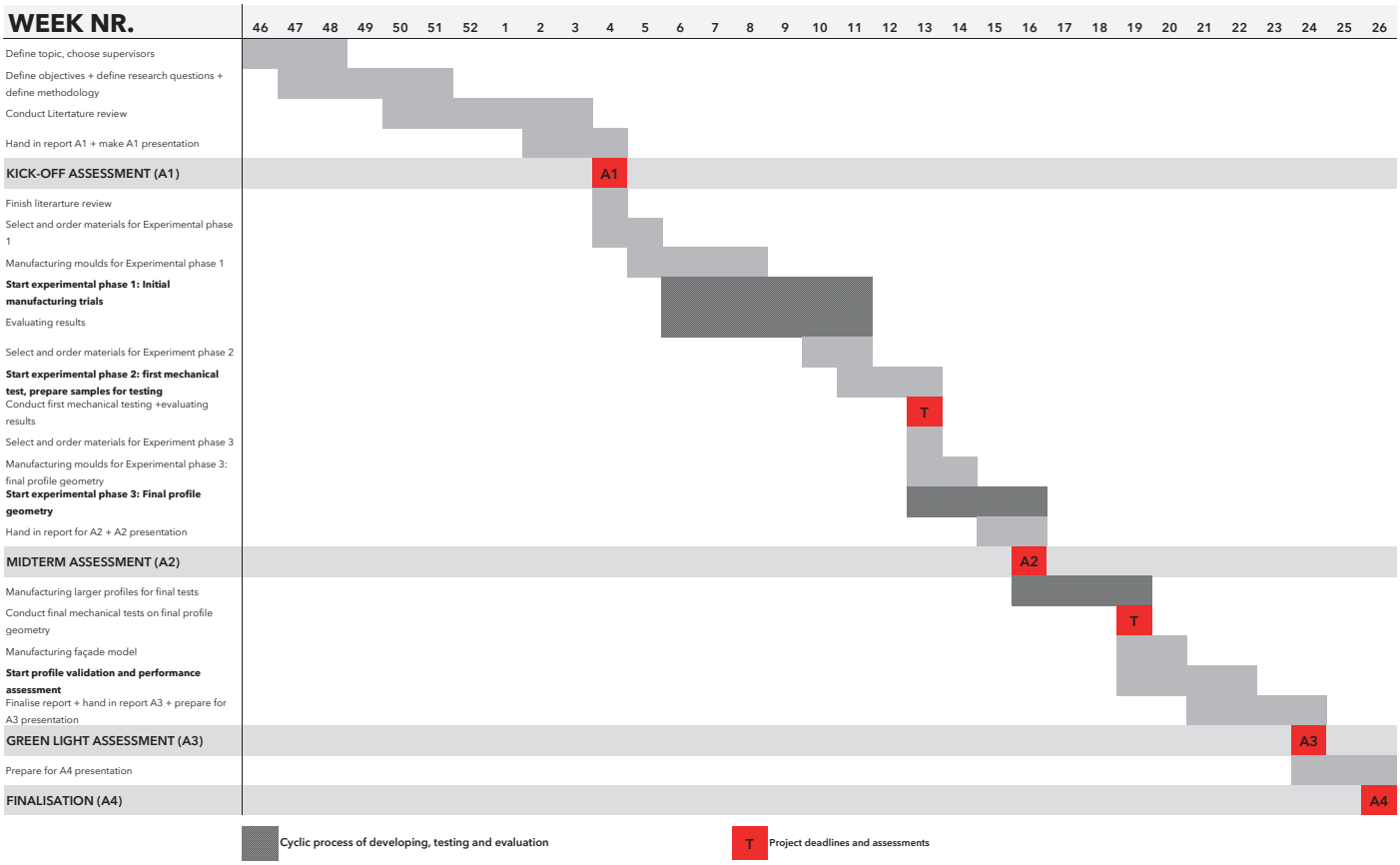

Fig. 2.2 Thesis planning (own image)

3. LITERATURE REVIEW

3.1 NON-WOOD PLANT- BASED FIBRES

This chapter addresses common types of non-wood plant-fibres that can be used for the manufacturing of a bio-composite material. First, the advantages and limitations of plant-fibres are discussed. In addition, the fibre architecture, fibre reinforcement, fibre arrangement possibilities and fibre surface treatments are discussed.

3.1.1 ADVANTAGES AND LIMITATIONS OF PLANT-FIBRES

ADVANTAGES OF PLANT-FIBRES

Natural fibre bio-composites can offer numerous advantages over traditional materials, including reduced CO^2 emissions and potential carbon neutrality, thermal insulation capabilities, effective damping performance, improved health benefits for occupants and workers, broad accessibility, and increased energy efficiency (Wimmers et al., 2019; Nechita et al., 2019; Charai et al., 2022; Livne et al., 2022; Asfaw et al., 2024; Ahmad et al., 2025). Furthermore, their low density compared to conventional materials is particularly attractive, and although their mechanical properties are generally lower, they are considered adequate for many applications in the building industry. In addition, recycling of natural fibres is theoretically simpler than that of synthetic fibres. Moreover, cost reductions of up to 60% have been reported in cases where high-performance characteristics are not critical (Biron M., 2018).

LIMITATIONS OF PLANT-FIBRES

Natural fibres also exhibit several disadvantages when compared to synthetic fibres such as carbon and glass fibres. These limitations include high moisture absorption, pronounced anisotropic behavior, limited compatibility with conventional polymer resins, and a less uniform structural composition (Jawaid & Abdul Khail, 2011; Rana et al., 2003; Khalid et al., 2021). Furthermore, the production yields of natural fibres are sometimes relatively low, which can constrain research and development efforts as well as large-scale industrial implementation (Biron M., 2018). The most important limitations are discussed further below.

MOISTURE ABSORPTION

In general, natural fibres exhibit a hydrophilic character, which causes them to absorb moisture not only from direct contact with water but also from humid air. This inherent hydrophilicity represents a significant limitation, reducing the competitiveness of natural fibres when compared to synthetic reinforcements such as glass fibres. The absorption of water leads to fibre swelling and debonding at the fibre–matrix interface. These degradation mechanisms restrict the application of natural fibre composites unless the fibres are modified. To mitigate moisture absorption, several fibre treatment techniques have been developed, of which alkali treatment and acetylation are among the most commonly applied methods (Ahmad et al., 2014). These fibre treatment methods are explained further in section 3.1.4.

FIRE RESISTANCE

Natural fibre composites generally exhibit poor fire resistance, which constitutes a significant limitation for their use in automotive and other industrial applications where fire safety and flammability performance are critical design considerations. This inherent disadvantage presents a major challenge for natural fibres in competing with synthetic fibres. Furthermore, natural fibres are non-thermoplastic in nature and possess relatively low thermal decomposition temperatures compared to their glass transition and/or melting temperatures. Despite the importance of fire performance for structural and semi-structural applications, the fire resistance of natural fibre composites has received limited attention, and only a small number of studies addressing their fire behavior are currently available in the literature (Ahmad et al., 2014).

DURABILITY

The durability of natural fibre composites under varying humidity, hygrothermal, and weathering conditions, as well as the resulting effects on their physical and mechanical properties, represents a major concern for their practical application (Mathur V.K., 2006). The durability of natural fibres is strongly associated with their resistance to both external and internal factors that contribute to a reduction in strength and service life. Despite its importance for long-term performance, particularly in structural and semi-structural applications, available data regarding the durability of natural fibres remains limited (Ahmad et al., 2014).

VARIABILITY

The inherent variability of natural fibres leads to significant fluctuations in their mechanical properties, which presents challenges in both the design process and quality assurance of natural

fibre–reinforced composites. Owing to the typically large scatter observed in the measured mechanical properties of plant-fibres, their application is often limited to low-grade composite products. Variations in fibre cross-sectional diameter are one of the contributing factors to this inconsistency, as they directly influence the mechanical performance of natural fibres (Ahmad et al., 2014).

LACK OF RESIN COMPATIBILITY

The main limitation of using natural fibres as reinforcement is the lack of compatibility between fibres and the matrix. Natural fibres' polar and hydrophilic properties are not compatible with the non-polar properties of most commercial polymers (Elfaleh et al., 2023). Therefore, improving the fibres' surface quality is often crucial to improve their adherence to the matrix and reduce moisture absorption.

3.1.2 TYPES OF PLANT-FIBRES

Figure 3.0 presents a classification of common non-wood plant-based fibres which can be used for composite manufacturing. These can be classefied into bast, fruit, grass, leaf, seed and stalk fibres. For each category, a brief overview is provided, including the most relevant fibres, typical applications and inherent limitations. The key mechanical properties like density, tensile strength and moisture absorption belonging to the fibres are found in *appendix A*.

BAST FIBRES

Bast- or stem fibres are typically obtained from the outermost layers of plant stems. These fibres are extracted through a retting process, which involves the biological or chemical degradation of the plant material to separate the fibres from the surrounding tissue (Ramesh et al., 2017).

TYPES OF BAST FIBRES

Common bast fibres are illustrated in figure 3.1. Among these, flax, hemp and jute fibres are the most extensively studied and widely available. These fibres are recognized for their fineness and flexibility relative to for example leaf fibres (The Editors of Encyclopedia Britannica, 2017). Bast fibres are typically long and exhibit high mechanical strength, properties that have traditionally made them suitable for the production of items such as bags, curtains, yarns, textiles, ropes, and sacks (Ramesh et al., 2017). Furthermore, owing to their biodegradability and natural abundance, bast fibres present promising opportunities in applications within the automotive industry, structural composites, pulp production, and textiles (Zhang et al., 2017).

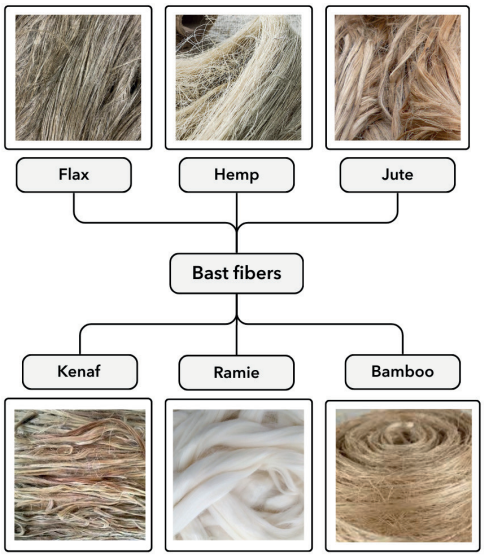

Fig. 3.1 Common bast fibres used for composites (own image)

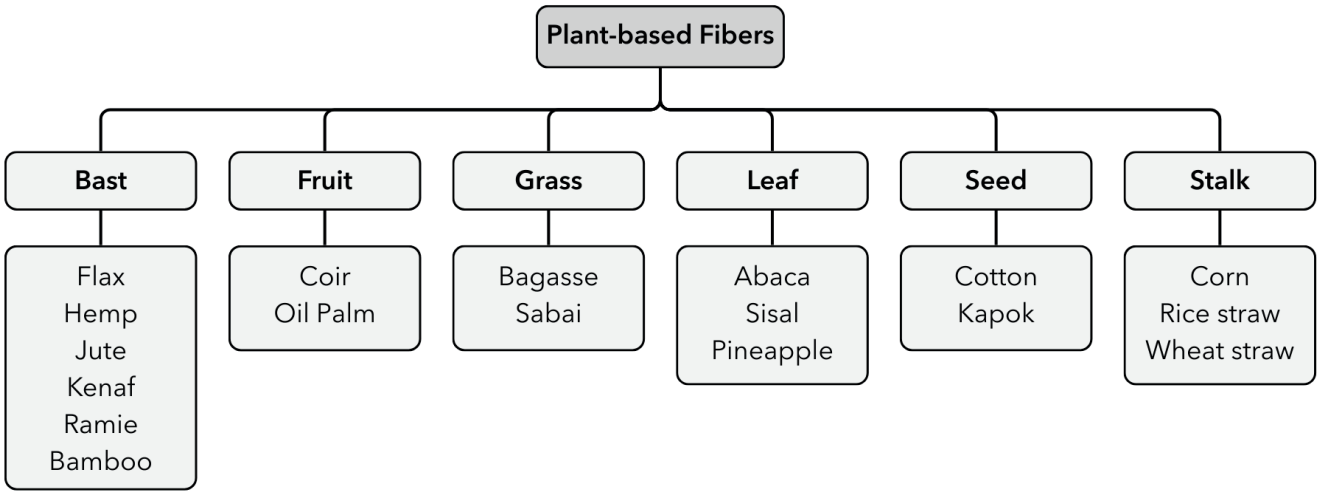

Fig. 3.0 Common plant-based fibres used in natural fibre composites (adapted from Chichane et al., 2024 and Islam et al., 2024).

FLAX FIBRE

Flax has been cultivated in Canada primarily for its seeds and seed oil. Historically, flax represents the first bast fibre employed for textile production in the Western world, with evidence of its use found in both Switzerland and ancient Egypt (Awais et al., 2021). Flax fibre possesses several advantages, including its long length (averaging 33 mm), good mechanical properties, low density, high toughness, and strength (Elfaleh et al., 2023). Flax non-woven materials are utilized by automotive manufacturers such as Opel, Renault, and Citroën for interior trim components (Biron M., 2018).

HEMP FIBRE

Hemp fibre is obtained from the Cannabis sativa plant species, which is primarily cultivated for industrial purposes. Hemp is an annual, fast-growing, herbaceous plant that produces strong and cost-effective natural bast fibres. The durability, stiffness, and low density of hemp fibres render them suitable not only for use in composite materials and wool insulation but also as effective chelating agents in various applications (Awais et al., 2021). The long bast fibres, which make up 70% of the hemp stalk, have a higher cellulose content (55–72%) and lower lignin content (2–5%) than other fibres, contributing to their high-strength mechanical properties and higher water resistance (Elfaleh et al., 2023).

JUTE FIBRE

Jute is a tropical plant from the Tiliaceae family, scientifically known as Corchorus Capsularis (Elfaleh et al., 2023). It is the second most economically significant natural fibre after cotton (Awais et al., 2021). Jute fibre is used as reinforcement in composites, and it has various applications such as packaging bags, ropes, yarns, and wall decorations (Elfaleh et al., 2023).

KENAF FIBRE

Kenaf is a herbaceous plant belonging to the genus Hibiscus and is considered one of the oldest cultivated crops in the world, with a history spanning approximately 4,000 years. It is classified as a wild dicotyledonous plant due to the three distinct layers of its stalk and is capable of thriving under ambient growing conditions (Awais et al., 2021). Although kenaf is less known then flax, hemp or jute, it is currently employed by automotive manufacturers such as Ford, Saab, and Volvo for certain interior trim components (Biron M., 2018).

RAMIE FIBRE

Ramie is a member of the family Urticaceae (Boehmeria), which comprises approximately 100 species. The use of ramie as a textile fibre has been relatively limited, primarily due to its restricted regions of cultivation and its chemical composition, which necessitates more extensive pre-treatment compared to other commercially significant bast fibres (Faruk et al., 2012). Nevertheless, in recent years, there have been numerous studies on using ramie fibres as reinforcing elements in composite materials, such as in Polypropylene-ramie and PLA-ramie composites (Elfaleh et al., 2023).

BAMBOO FIBRE

Bamboo is one of the fastest-growing bast fibres in the world, capable of growing up to 3 cm per hour and reaching heights of up to 40 m. The properties of bamboo fibres are influenced by factors such as habitat, plant size, soil moisture, and temperature. With nearly 1,000 species and wide natural availability, bamboo fibres are considered highly suitable for use as reinforcement in composite materials. The fibres are longitudinally aligned along the length of the plant, which enhances their tensile strength (Awais et al., 2021).

FRUIT FIBRES

Fruit fibres are extracted from the outer husk of the respective fruits. These fibres are lightweight and strong, making them particularly suitable for the production of ropes, mats, sacks, brushes, geotextiles, and similar applications (Ramesh et al., 2017).

TYPES OF FRUIT FIBRES

Figure 3.2 displayes two of the most common examples of fruit fibres, which are coconut coir and oil palm.

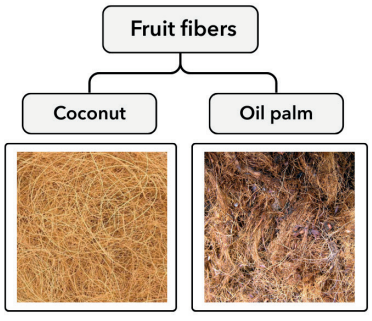

Fig. 3.2 Common fruit fibres used for bio-composites (own image)

COCONUT COIR FIBRE

Coir is a fruit fibre derived from the outer husk of coconuts. It is predominantly available in tropical regions, including Indonesia, the Philippines, Brazil, and India. Coir fibres have been combined with sodium alginate to form insulation material with great insulation value and acoustic properties (Figueiredo et al., 2025). Coir fibres are coarser than leaf and bast fibres, which restricts their suitability for delicate or high-precision applications (Awais et al., 2021).

OIL PALM FIBRE

Oil palms (Elaeis) belong to the Arecaceae, or palm, family and include two primary species. Currently, fibres derived from oil palm empty fruit bunches are recognized for their potential as reinforcement materials in plastic composites or furniture applications (Faruk et al., 2012).

GRASS FIBRES

Grass fibres are obtained from tall grasses, including rye grass, elephant grass, switchgrass. Additionally, fibrous crop residues such as bagasse, esparto, sabei, Phragmites communis, canary grass, and snake grass are primarily utilized as reinforcement materials in cement-based composites (Ramesh et al., 2017). Three of the most common grass fibres are discussed below.

TYPES OF GRASS FIBRES

Figure 3.3 displayes 3 common grass fibres used for plant-fibres for bio-composite manufacturing. These are bagasse and sabai.

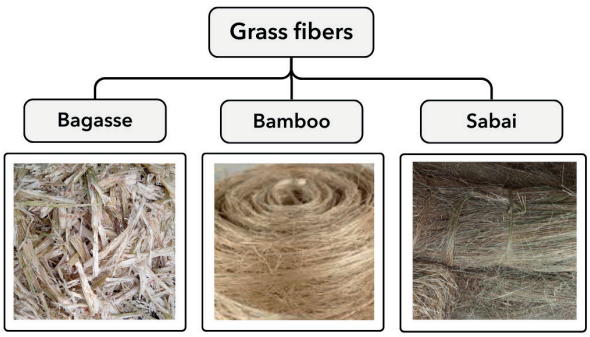

Fig. 3.3 Common grass fibres used for bio-composites (own image)

BAGASSE FIBRE

Bagasse fibre is the fibrous byproduct remaining after the extraction of juice from sugarcane stalks. It is currently employed as a renewable natural fibre in the production of composite materials (Faruk et al., 2012). It is mainly used as a burning raw material in the sugar mill furnaces. When appropriate modifications and manufacturing procedures are applied, bagasse displays improved mechanical properties such as tensile strength, flexural strength, flexural modulus, hardness, and impact strength (Balaji et al., 2015).

SABAI FIBRE

Sabai grass is native to Asia, with significant prevalence in the eastern Indian state of Odisha. Sabai grass is characterized by high cellulose content, low levels of lignin, and ash content higher than that of for example bamboo (kumar, S. et al., (2025). Despite its ease of cultivation and abundant availability, its practical applications have remained limited (Chand & Rohatgi, 1992).

LEAF FIBRES

Leaf fibres are coarse and rigid fibres obtained from plant leaves through hand scraping following a beating or retting process, or via mechanical extraction. Owing to their relatively high strength, these fibres are primarily employed in the production of woven ropes, fabrics, carpets, mats, and similar products (Ramesh et al., 2017). Leaf fibres such as abaca, sisal and pineapple are particularly strong and can even perform better than bast fibres (Elfaleh et al., 2023).

TYPES OF LEAF FIBRES

Figure 3.4 displayes 3 common leaf fibres that can be used for natural fibre composites. These are abaca, sisal and pineapple (pina) fibre.

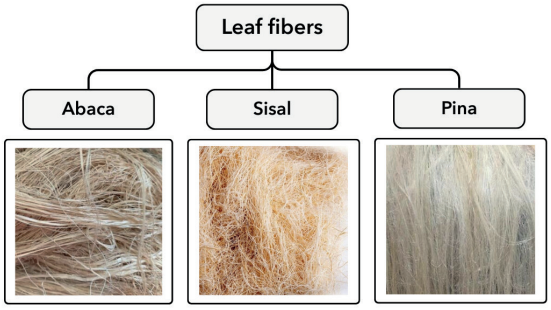

Fig. 3.4 Common leaf fibres used for bio-composites (own image)

ABACA FIBRE

Abaca, also known as banana fibre, is derived from the banana plant and is noted for its durability and resistance to seawater. Recognized as the strongest

of the commercially available cellulose fibres, abaca is native to the Philippines and is currently produced there as well as in Ecuador (Faruk et al., 2012; Elfaleh et al., 2023). Nowadays, abaca fibre is commonly used in the production of ropes, twines, and mats, and it is also used to produce floor panels in automotive manufacturing (Elfaleh et al., 2023).

SISAL FIBRE

Sisal fibres are derived from the leaves of the Agave sisalana plant and originate from Mexico. Classified as coarse and stiff leaf fibres, sisal fibres are primarily produced in East Africa, Haiti, Brazil, and India (Awais et al., 2021). Sisal offers several advantageous properties, including high strength, durability, elasticity, affinity for certain dyes, and resistance to degradation in saltwater environments (Corona Comercio Industria Ltda., 2017).

PINA (PINEAPPLE FIBRE)

Pineapple is a tropical plant native to Brazil. Its fibres are rich in cellulose, widely available, and relatively inexpensive. These fibres also exhibit potential for use as reinforcement in polymer composites. Currently, pineapple leaf fibres are considered a byproduct of pineapple cultivation, making them an economically viable resource for industrial applications (Faruk et al., 2012).

SEED FIBRES

Seed fibres are obtained from seeds or seed pods, such as those of cotton and kapok. Among these, cotton is the most significant seed fibre, possessing properties that allow it to be spun into thread or used as stuffing (S.R. Djafari Petroudy, 2017).

TYPES OF SEED FIBRES

Figure 3.5 displayes two common seed fibres that can be used for natural fibre composites. These are cotton and kapok.

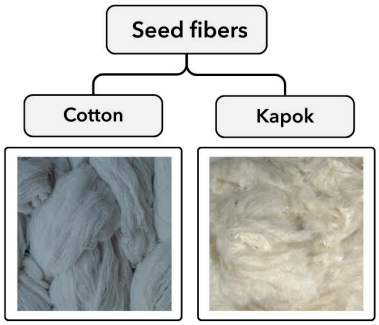

Fig. 3.5 Common grass fibres used for bio-composites (own image)

COTTON FIBRE

Cotton is cultivated in over 50 countries worldwide, with the majority of production concentrated in developing regions. Cotton fibres are regarded as the purest form of cellulose, containing approximately 90% cellulose. Additionally, cotton fibres are valued for their breathability and absorbency, properties attributed to their hollow structure (Awais et al., 2021). They are often used to make luxury papers and are widely used in the textile industry (Elfaleh et al., 2023).

KAPOK FIBRE

Kapok trees belong to the family Bombaceae and are native to regions of Asia, Africa, and South America. Kapok is a silky fibre that surrounds the seeds of Ceiba pentandra, typically exhibiting a yellowish or light-brown color with a lustrous, silk-like appearance (Zheng et al., 2013). Traditionally, kapok fibres have been employed as stuffing for bedding, upholstery, life preservers, and other water-safety equipment due to their exceptional buoyancy (Zhang et al., 2013).

STALK FIBRES

Stalk fibres are obtained from the stems of plants and are commonly extracted from species such as maize, sugarcane, corn, eggplant, sunflower, and wood, as well as from the straws of various cereal crops including barley, wheat, and rice (Ramesh et al., 2017).

TYPES OF STALK FIBRES

Figure 3.6 displayes common stalk fibres that can be used for natural fibre composites. These are corn, Rice and wheat.

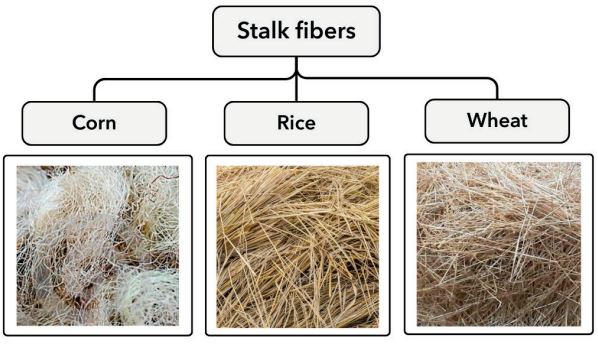

Fig. 3.6. Common grass fibres used for composites (own image)

CORN FIBRE

Corn is among the most widely cultivated crops globally. According to the United States

Department of Agriculture, global corn production reached 1,110.84 million metric tons in 2019 (World Agricultural Production, 2025). Cornhusk fibre, being one of the most economical natural cellulosic fibres, holds significant potential for use in textiles and value-added products such as carpets, rugs, and cordage, with applications determined largely by the fibre's staple length (Kambli et al., 2021).

RICE STRAW

Rice is one of the major cereal grains used for the production of hull fibres and is among the most widely cultivated crops, with a global production of approximately 720 million tons in 2012 (Faruk et al., 2012). Rice husk fibres and rice straws exhibit significant potential for reinforcement in polymer composites, owing to the strong interfacial adhesion between the husk and straw, which enhances stress transfer and facilitates uniform load distribution across the interface (Yang et al., 2004).

WHEAT STRAW

Wheat straw exhibits a favorable capacity for fibre-to-fibre bonding, and approximately one-third of the straw can be sustainably harvested from fields without adversely affecting soil humus levels. These characteristics make wheat straw a promising source of reinforcement fibres for the production of packaging paper (Hagel & Schütt, 2024). However, its use as a raw material for fibre production also presents notable challenges, including high transportation and storage costs due to its low bulk density and its susceptibility to rapid deterioration (Puițel et al., 2020).

3.1.3 PLANT-FIBRE ARCHITECTURE AND REINFORCEMENT STRATEGIES

PLANT-FIBRE ARCHITECTURE

Natural fibres can be characterized as composite structures, in which individual hollow cellulose fibrils are embedded within a matrix of hemicellulose and lignin. The performance of natural fibres as reinforcement in composites is largely determined by their cellulose content. Higher proportions of non-cellulosic components typically reduce both the strength and flexibility of the fibres, thereby adversely affecting the mechanical performance of natural fibre-reinforced composites (Shelly et al., 2025).

Figure 3.7 illustrates the microstructure of natural fibres. Fibre cell walls are heterogeneous membranes composed of multiple layers. During cell growth, the initial layer formed is the thin primary wall, which surrounds the secondary wall. The mechanical properties of the fibre are largely determined by the central layer of the secondary wall, which itself comprises three distinct sub-layers. Within the middle layer, long-chain cellulose molecules are helically arranged to form cellular microfibrils (Shelly et al., 2025).

The amorphous matrix phase of the cell wall contains hemicellulose, lignin, and, in some cases, pectin, waxes, and other minor constituents. Hemicellulose molecules form hydrogen bonds with cellulose, generating a cohesive matrix that integrates the cellulose microfibrils into a robust cellulose–hemicellulose network. This network serves as the primary structural framework of the fibre cell. The hydrophobic lignin network further reinforces the composite by acting as a coupling agent and enhancing the rigidity of the cellulose/hemicellulose structure (Shelly et al., 2025).

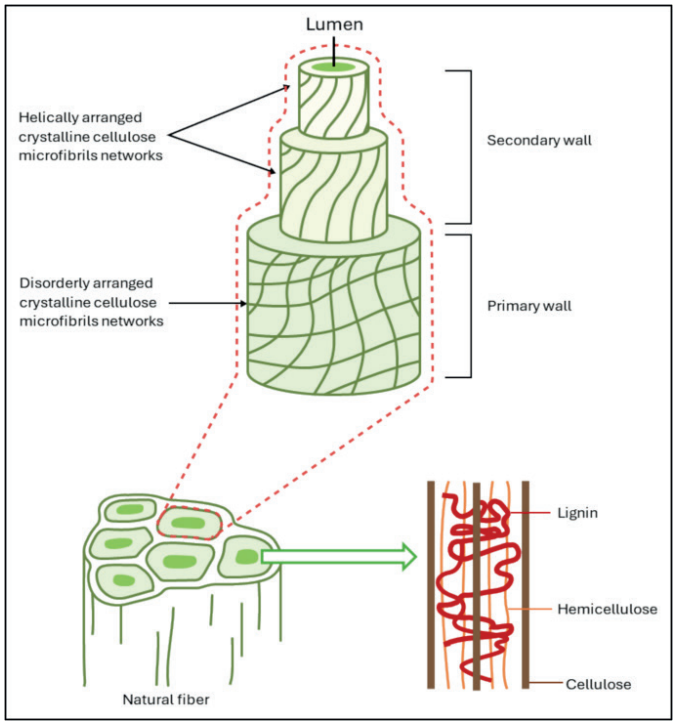

Fig. 3.7 Schematic illustration of natural fibre (Shelly et al., 2025)

FIBRE REINFORCEMENT STRATEGIES

Figure 3.8 illustrates the possible fibre arrangements as reported by Hu (2008), Ciobanu (2011), and Cho & Jo (1980). Fibre arrangement, also referred to as fibre configuration or architecture, plays a critical

LEVEL	*REINFORCEMENT*	*ARCHITECTURE*	*ARRANGEMENT*	*ORIENTATION*	*ENTANGLEMENT*
1	Discrete	Chopped fibres	Discontinuous	Uncontrolled (2D)	None
2	Linear	Filaments	Continuous	Linear (2D)	None
3	Laminar	Simple fabric	Continuous	Planar (2D)	Planar
4	Integrated	Advanced fabric	Continuous	3D	3D

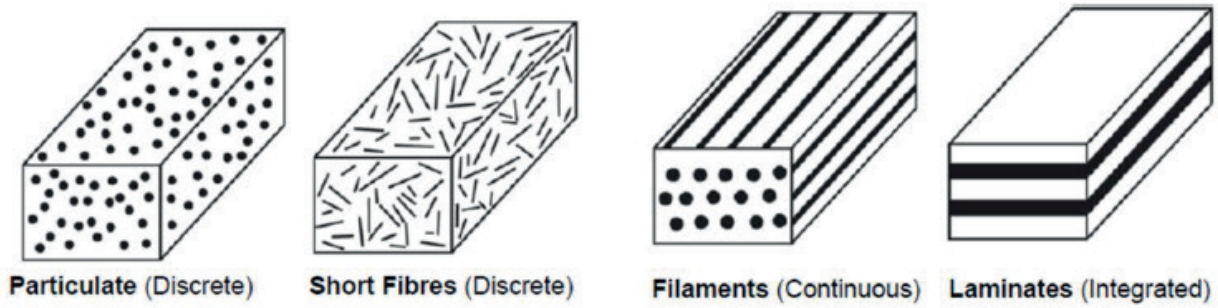

Fig. 3.8 Fibre architecture and arrangement (adapted from Hu, 2008, Ciobanu, 2011 and cho&Jo, 1980).

role in determining the final physical and mechanical properties of composite materials. Based on their structural organization, fibre architectures can be classified into four main types: (1) discrete, (2) continuous, (3) planar interlaced (2D), and (4) fully integrated (3D) structures (Chou & Ko, 1989).

1. DISCRETE FIBRE EINFORCEMENT

Discrete fibre arrangement is characterized by the use of discrete or chopped fibres with a discontinuous distribution and largely uncontrolled fibre orientation. The main advantages of this configuration include cost-effectiveness, ease of manufacturing complex shapes, and reduced sensitivity to defects when compared to continuous fibre systems (Alsuhaibani, 2025). However, short-fibre reinforcement in high-density polymer matrices presents several challenges. Achieving a uniform fibre distribution is difficult, which can significantly diminish the reinforcing efficiency of natural fibre composites and limit their suitability for structural applications. In addition, randomly distributed short natural fibres may lead to polymer matrix agglomeration, adversely affecting the overall composite properties (Arumugam et al., 2022). Furthermore, short fibres can be converted into mats and used as randomly distributed reinforcement in composite production, such as compression moulding (Fan & Weclawski, 2017).

2. LINEAR FIBRE RINFORCEMENT

To overcome the disadvantages associated with discrete fibre arrangements, linear fibre reinforcement was introduced. Linear reinforcement is characterized by the use of continuous filaments aligned in a predominantly linear orientation. Among these, flax and hemp bast fibres are considered the most promising linear reinforcements for composite materials (Fan & Weclawski, 2017).

3. LAMINAR FIBRE REINFORCEMENT

Planar interlaced reinforcement refers to the intentional entanglement of fibres within a plane. In contrast to discrete and linear fibre reinforcements, which exhibit no entanglement, planar interlaced (laminar) reinforcement features a two-dimensional network of interwoven fibres. This reinforcement method produces simple 2D fabrics composed of continuous fibres arranged in woven, braided, or knitted architectures, as illustrated in Figure 3.9.

Studies have shown that natural fibre–reinforced composites with different weaving patterns demonstrate enhanced mechanical properties compared to composites reinforced with discrete or linear fibre arrangements. The continuous and interlaced nature of the fibres improves load transfer and stress distribution within the composite (Arumugam et al., 2022).

4. INTEGRATED FIBRE REINFORCEMENT

Lastly, integrated fibre reinforcement produces advanced fabrics with a continuous arrangement

of fibres in a three-dimensional (3D) orientation with through-thickness entanglement. This method results in fabrics with superior mechanical properties, particularly improved interlaminar strength, damage tolerance, and resistance to delamination compared to 2D reinforcements.

Three-dimensional reinforcement architectures include woven, braided, stitched, and knitted structures, as illustrated in Figure 3.9. These 3D patterns enable enhanced load transfer in multiple directions and provide advanced structural integrity, making integrated fibre reinforcements especially suitable for high-performance and load-bearing composite applications.

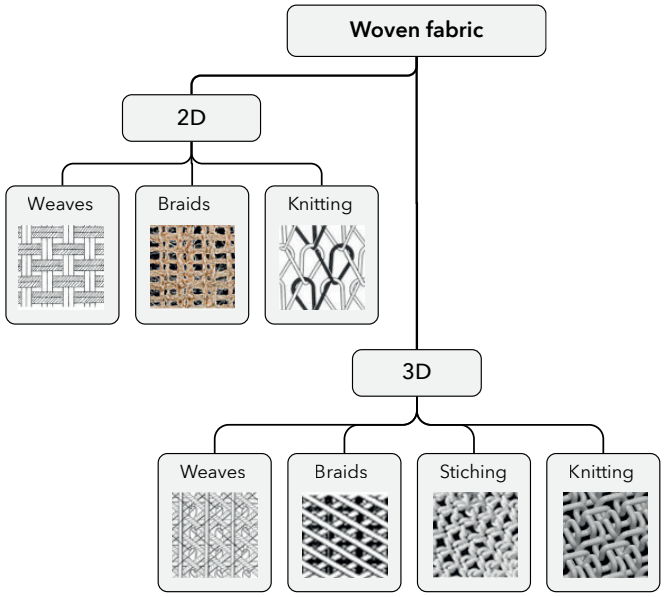

Fig. 3.9 Composite fabric reinforcements and preforms (adapted from Fan & Weclawski, 2017).

3.1.4 SURFACE TREATMENTS OF PLANT-FIBRES

This section discusses surface treatments of plant-fibres to enhance resin bonding or surface quality. There are biological and chemical treatments available.

BIOLOGICAL TREATMENTS

Natural fibres can be treated naturally using micro-organisms like bacteria and funghi. This is a low-cost, ecological way to treat the fibres but requires a longer time than chemical treatment. Fungal treatment creates cavities on the fibre surface providing a rough interface and enhanced interlocking with the matrix. Enzymes like peroxidases can be used to improve the functions of lignocellulose and the lignin content can be decreased to a large extent (Samanth & Bhat, 2023).

CHEMICAL TREATMENTS

The selection of chemical treatment method depends on the availability of reagents, functional group modification desired and need of active groups that are able to interact with natural fibre structures (Samanth & Bhat, 2023). The most common chemical treatments for natural fibres are an alkali treatent, a silane treatment, acetylation treatment, benzoylation treatment and peroxide treatment. Most of these treatments are used as a surface modification of the fibres and enhance the bonding to a matrix. The most common chemical treatments are discussed further below.

ALKALINE TREATMENT

Alkaline treatment is the most common chemical treatment for natural fibres and is also known as mercerization of cellulose fibres. It depends on the concentration of the alkaline solution, its temperature and treatment time (Samanth & Bhat, 2023). This treatment increases the surface roughness of the fibre by interrupting the hydrogen bonds in the fibre. This will increase the bonding of the fibre to a matrix (Samanth & Bhat, 2023). Figure 3.10 displayes the structure of untreated fibres (i) and alkaline treated fibres (ii).

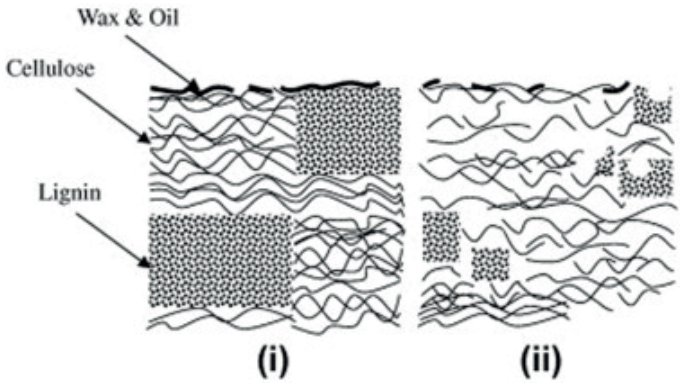

Fig. 3.10 untreated fbers (i) and alkali treated fibres (ii) (Samanth & Bhat, 2023).

SILANE TREATMENT

Silane treatment involves different steps like hydrolysis, self-condensation, and chemical grafting and improves the strength and heat stability of the composites. Here, silyl reagent is used as an adhesion promoter to change the exterior of the fibrils and decreases the cellulose hydroxyl groups, it increases the bond strength which reduces debonding in the surface (Samanth & Bhat, 2023).

ACETYLATION TREATMENT

With an acetylation treatment, typically, the fibres are first dipped in acetic acid and then treated with acetic anhydride with or without the use of an acid catalyst. Acetylation effectively reduces surface -OH groups of the fibres which helps to reduce moisture absorption. The reaction leads to the formation of acetic acid as a byproduct which can be removed by washing with water. Major drawback of this method is the reagent, which is comparatively expensive and relatively toxic (Samanth & Bhat, 2023).

BENZOYLATION TREATMENT

This method uses alkali pretreatment where the extractable materials other than cellulose are eliminated and greater susceptible hydroxyl (OH) groups are exhibited on the exterior fibril. Later the fibres are replaced by benzoyl group. After treating with benzoyl chloride, the hydrophobic character of the fibre is enhanced. It improved fibre-lattice adhesion, fibre-matrix strength and its thermal resistance and further decreased the water absorption of the fibres (Samanth & Bhat, 2023).

PEROXIDE TREATMENT

Benzoyl Peroxide (BP) and Dicumyl Peroxide (DCP) are the organic peroxides that can be used in altering the fibre surface. This treatment results in decreased hydrophilicity of the fibre and increased tensile strength (Samanth & Bhat, 2023).

MALEATED COUPLING AGENTS

Maleated coupling agents helps to reinforce fillers and fibre reinforcement. This process results in greater porosity of the fibril and the tendency to absorb water can also be decreased. In addiion, the mechanical properties like impact strength of the fibre, Young's modulus and flexural modulus can be enhanced (Samanth & Bhat, 2023).

3.2 POLYMER REINFORCEMENT MATRIX

This chapter discusses the various polymer matrices employed as reinforcement for plant-fibre composites. A selection is made based on resin availability and workability. Figure 3.11 displayes the different polymers used for making composites. These an be classified into fossil-based polymers (synthetic thermosets and synthetic thermoplastics) and Bio-polymers (Biodegradable, bio-based and combinations). The properties of the matrices discussed can be found in *appendix B.*

3.2.1 FOSSIL-BASED THERMOSETS

Synthetic thermosets are petroleum-based polymers. The most commonly used synthetic thermosets for reinforcing composites include polyesters, vinyl esters, epoxy resins, and polyurethane (PU).

POLYESTERS

Polyesters are the most widely used resin type in composite fabrication. They are cost-effective, easy to process, and provide satisfactory basic mechanical properties compared to other thermosets (Excel Composites, 2024). Their low cost and excellent weathering resistance make them particularly suitable for applications such as flat roofing, waterproofing, and pond lining, as well as conventional fibreglass projects including boat construction, enclosures, and molded components for transportation applications (EasyComposites, 2025).

VINYL ESTERS

Vinyl esters offer superior chemical resistance and generally higher strength compared to polyesters. They are compatible with all fibre types, which contributes to their higher cost relative to polyester resins (Excel Composites, 2024). Vinyl ester resins exhibit behavior similar to polyester resins but provide enhanced mechanical properties and chemical resistance, making them a preferred choice for tooling and mold-making applications. Additionally, vinyl ester and polyester resins, along with their gelcoats, are fully compatible and can be used in combination (EasyComposites, 2025).

EPOXY RESIN

Thermosetting epoxy resins are extensively used across diverse applications, including printed circuit boards, semiconductor encapsulation, coatings, adhesives, and composite materials, owing to their excellent chemical resistance, adhesion, electrical insulation, heat resistance, and mechanical performance (Dai et al., 2018). Epoxy resins are generally regarded as the highest-performance resin type for composites and are available in a wide range of formulations tailored for specific applications, such as hand-laminating, resin infusion, coating, casting, flexible components, repair, and high-temperature use (EasyComposites, 2025). Their capacity to accommodate higher fibre content results in superior stiffness and strength compared to polyester and vinyl ester resins, which also contributes to their higher cost (Excel Composites, 2024).

POLYMER REINFORCEMENT				
FOSSIL-BASED POLYMERS		BIO-POLYMERS		
SYNTHETIC THERMOSETS	SYNTHETIC THERMOPLASTICS	DEGRADABLE FOSSIL-BASED POLYMERS	NON-DEGRADABLE BIO-BASED POLYMERS	DEGRADABLE BIO-BASED POLYMERS
Polyesters *Vinyl esters* *Epoxy resin* *Polyutherane (PU)*	*Polyethylene (PE)* *Polypropylene (PP)* *Polyvinyl chloride(PVC)* *Polymethyl methacrylate (PMMA* *Polystyrene (PS)* *High Density Polyethene (HDPE)* *Polyether-ether ketone (PEEK)* *Acrylonitrile-butadiene-styrene (ABS)*	*Poly(butylene adipate-co-terephtalate) (PBAT)* *Bio-Epoxy resin* *Polyaprolactone (PCL)* *Polybutylene succinate (PBS)* *Polyvinyl Alcohol (PVOH)*	*BIO-PE* *Polyethylene furanoate (PEF)* *BIO-PET*	*Polyactic acid (PLA)* *Poly-B hydroxyalkanoates (PHA)* *Polyglycolic acid (PGA)* *Starch blends*

Fig. 3.11 Widely used matrices in fibre-reinforced polymers (adapted from Faruk et al., 2012; Vaisanen et al., 2017; Andrew & Dhakal., 2022)

POLYUTHERANE (PU)
Polyurethanes are among the most widely used casting resins, finding applications that range from miniatures and figurines to rapid prototyping and structural components such as skateboard wheels and engine mounts (EasyComposites, 2025). Polyurethane offers increased transverse strength and faster processing times; however, it imposes limitations on the complexity of achievable profiles (Excel Composites, 2024).

3.2.2 FOSSIL-BASED THERMOPLASTICS

Synthetic thermoplastics generally accommodate higher fibre content, are recyclable, and, unlike thermosets, can be post-formed after processing (Excel Composites, 2024). A wide range of plastics is employed for composite reinforcement, with the most commonly used thermoplastics including polyethylen (PE), polypropylene (PP), polyvinyl chloride (PVC), polymethyl methacrylate (PMMA), polystyrene (PS), high-density polyethylene (HDPE), polyether-ether ketone (PEEK) and acrylonitrile-butadiene-styrene (ABS).

POLYPROPYLENE (PP)
Polypropylene is widely regarded as a preferred matrix material for advanced composites in the aerospace, civil, and automotive sectors (Wang Z., Zhu G., 2023) and currently dominates the production of natural fibre composites, alongside polyethylene and polyvinyl chloride (Arinze R.U., et al., 2023). Among the various types of polypropylene, homopolymers, produced through the polymerization of propylene alone, are the most commonly utilized (Biron, 2018).

POLYVINYL CHLORIDE (PVC)
Pure polyvinyl chloride (PVC) is the linear homopolymer of vinyl chloride. PVC is considered one of the most versatile thermoplastic resins due to its capacity to incorporate a wide range of additives, including plasticizers, stabilizers, fillers, processing aids, impact modifiers, lubricants, foaming agents, biocides, pigments, and reinforcements. However, PVC cannot be processed in its pure form and requires the addition of stabilizers and lubricants, as well as plasticizers if flexibility is desired (Biron, 2018).

POLYMETHYL METHACRYLATE (PMMA)
The primary advantages of polymethyl methacrylate (PMMA) include its excellent optical properties, high transparency, brightness, color stability, and outstanding weathering resistance, making it a preferred material for optical and transparent components in both technical and aesthetic applications. However, PMMA exhibits several limitations, including low impact resistance, restricted thermal performance (except for acrylic imides), inherent flammability, susceptibility to environmental stress cracking in the presence of certain chemicals, and vulnerability to chemical attack by specific solvents (Biron, 2018).

POLYSTYRENE (PS)
Polystyrene (PS) is valued for its transparency, favorable mechanical properties, rigidity at room temperature, low cost, and attractive price-to-performance ratio. Additional advantages include adequate dimensional stability, ease of processing, chemical inertness to certain substances, low water absorption, moderate density and good electrical insulation even under wet conditions. The foaming capability of polystyrene has facilitated the large-scale production of foamed materials used for insulation and vibration damping applications (Biron, 2018).

HIGH-DENSITY POLYETHYLENE (HDPE)
High-density polyethylene (HDPE) is a high-density variant of polyethylene (PE) that exhibits good mechanical properties, flexibility, and impact resistance at ambient temperatures. It also functions as an effective electrical insulator, even in wet conditions, and demonstrates excellent thermal and creep performance. However, HDPE has several limitations, including inherent sensitivity to heat, ultraviolet light, and weathering (although stabilized grades are available), susceptibility to stress cracking and creep, low rigidity, significant shrinkage, and limited transparency (Biron, 2018).

POLYETHER-ETHER-KETONE (PEEK)
Polyether-ether-ketones (PEEKs) are valued for their excellent mechanical, chemical, and electrical properties, high service temperatures (up to 250 °C), rigidity, favorable creep behavior, wear resistance, fatigue endurance, moderate shrinkage and moisture absorption. However, PEEKs have certain limitations, including sensitivity to light and UV radiation, necessitating protective measures for outdoor use, high cost, which is generally justified by their performance, and, in some cases, insufficient fire resistance (Biron, 2018).

ACRYLONITRILE-BUTADIENE-STYRENE (ABS)

Acrylonitrile-butadiene-styrene (ABS) is valued for its good mechanical properties, including impact strength, favorable price-to-performance ratio, dimensional stability, surface gloss and low-temperature performance. However, ABS also presents several limitations, including inherent sensitivity to heat, UV light, and weathering (though stabilized grades are available), relatively high cost, poor scratch resistance, creep at elevated temperatures, flammability with dripping and electrostatic charge accumulation (Biron, 2018).

3.2.3 BIOBASED ALTERNATIVES

The considerable environmental impact of petroleum-based thermosets and thermoplastics has prompted the development of bio-based alternatives to conventional petroleum-derived resins (Deghani, A., et al., 2013; Mustapha, R., et al., 2019). Bio-based thermosets are obtained from renewable sources, including plant oils, polylactic acid (PLA), epoxidized plant oils, cardanol, glycerol, furan, gallic acid, and corn (Islam, S., et al., 2025).

BIOPLASTICS

Figure 3.12 displayes the different classes of biopolymers. Biopolymers, in contrast to conventional fossil-based, non-biodegradable polymers, are increasingly used as matrices for natural fibre reinforcement. Biopolymers can be further classified into three categories: biobased polymers, biodegradable polymers, and polymers that are both biobased and biodegradable. Notably, some polymers produced entirely or partially from petroleum-based feedstocks can also exhibit biodegradability (Gowman et al., 2019).

1. DEGRADABLE FOSSIL-BASED PLASTICS

The most commonly used fossil-based, biodegradable polymers include poly(butylene adipate-co-terephthalate) (PBAT), bio-based epoxy resins, polycaprolactone (PCL), polyethylene succinate (PBS), polyethylene adipate (PEA), and polyvinyl alcohol (PVA).

POLY (BUTYLENE-ADIPATE-CO TEREPHTALATE (PBAT)

Poly(butylene adipate-co-terephthalate(PBAT) is synthesized via polycondensation of 1,4-butanediol, adipic acid, and terephthalic acid (Gowman et al., 2019). PBAT can be processed using standard polymer processing techniques; however, a notable limitation is its relatively low degradation temperature range (140 °C to 230 °C), which can result in thermal degradation during processing (Costa et al., 2015).

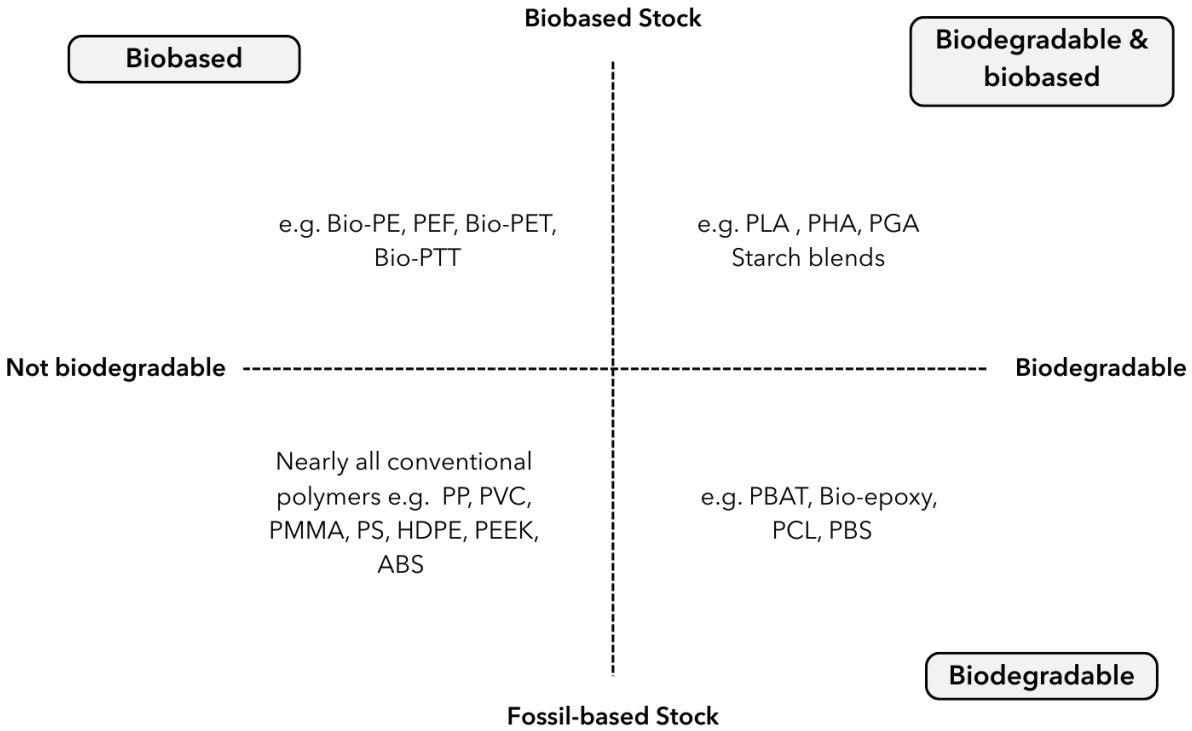

Fig. 3.12 Classes of biopolymers (adapted from European Bioplastics, 2020)

BIO-EPOXY
Bio-based epoxy resins are primarily derived from renewable raw materials such as magnolol, resveratrol, vanillin, and ferulic acid. Considerable research and development efforts have focused on improving their thermal and mechanical properties. However, certain limitations restrict their broader adoption, including the high cost of biomass feedstocks and the challenges associated with processing bio-based epoxy monomers (Zhang et al., 2024).

POLYCAPROLACTONE (PCL)
Polycaprolactone (PCL) is a semi-crystalline, biodegradable polymer synthesized from ε-caprolactone through a ring-opening polymerization reaction. It exhibits a low melting temperature of approximately 60 °C and a glass transition temperature of around –60 °C (Gowman et al., 2019). PCL is utilized in biomedical applications, including implants and drug delivery systems, as well as in sustainable packaging solutions (McKeen, 2012; Ahmad et al., 2018).

POLYETHYLENE SUCCINATE (PBS)
Polyethylene succinate (PBS) is a biodegradable polymer that can be synthesized entirely from petroleum-based feedstocks or partially from biobased sources using biobased succinic acid (Gowman et al., 2019). Its properties are comparable to those of polypropylene (PP) and polyethylene (PE) (Fujimaki, 1998).

POLYVINYL ALCOHOL (PVOH)
Polyvinyl alcohol (PVOH) is synthesized from poly(vinyl acetate) through full or partial hydroxylation (Gowman et al., 2019). Owing to its biocompatibility, chemical resistance, high water solubility, and absorption properties, PVOH is frequently employed in medical applications such as contact lenses, artificial cartilage and menisci (Baker et al., 2012).

2. NON-DEGRADABLE BIO-BASED PLASTICS
The most commonly used bio-based polymers that are not biodegradable include bio-polyethylene (Bio-PE), polyethylene furanoate (PEF), bio-polyethylene terephthalate (Bio-PET), and polytrimethylene terephthalate (PTT).

BIO-POLYETHYLENE (BIO-PE)
Bio-polyethylene (Bio-PE) is produced by converting bioethanol into bio-ethylene, which is subsequently polymerized into polyethylene (Rahman & Bhoi, 2021). Companies such as Dow and Braskem currently manufacture Bio-PE from bioethanol (Isikgor & Becer, 2015).

POLYETHYLENE FURANOATE (PEF)
Polyethylene furanoate (PEF) is a fully recyclable, bio-based polymer derived from renewable plant sugars. Its production involves the polymerization of 2,5-furan dicarboxylic acid (FDCA) and ethylene glycol, following a process similar to that of PET production, but substituting terephthalic acid with FDCA. Although PEF is not inherently biodegradable, it is designed to decompose under industrial composting conditions, breaking down significantly faster than conventional plastics such as PET (SpecialChem, 2021).

BIO-POLYETHYLENE TEREPHTALATE (BIO-PET)
Bio-polyethylene terephthalate (Bio-PET) is produced via a multi-step process beginning with bioethylene. Shell's OMEGA technology converts ethylene oxide and CO^2 into ethylene carbonate, which is subsequently hydrolyzed to form ethylene glycol (EG). The ethylene glycol then reacts with terephthalic acid to produce PET monomers through a dehydration reaction. These monomers undergo polycondensation at 260–300 °C, typically in the presence of catalysts such as antimony(III) oxide. Excess ethylene glycol is recycled, resulting in the final PET polymer (Rahman & Bhoi, 2021).

3. DEGRADABLE BIO-BASED PLASTICS
The most commonly used bio-based thermoplastics include polylactic acid (PLA), polyhydroxyalkanoates (PHA), polyglycolic acid (PGA), and starch-based blends.

POLYATCTIC ACID (PLA)
Polylactic acid (PLA) is a widely used, fully bio-based thermoplastic polymer derived from renewable sources such as cassava, sugarcane, or corn. It is favored for its good mechanical properties and relatively low cost (Gowman et al., 2019). PLA is also a versatile material that can be processed using a variety of techniques, including injection molding, thermoforming, blow molding, extrusion blowing, foaming, sheet extrusion, and film extrusion (Auras et al., 2010). The primary limitations of PLA are its low impact strength and low heat distortion temperature (Gowman et al., 2019).

POLY-B HYDROXYALKANOATES (PHA)
Polyhydroxyalkanoates (PHAs) are polyesters produced through bacterial fermentation. Although numerous types of PHAs can be synthesized, the majority are not commercially available (Gowman et al., 2019). PHAs exhibit poor melt processability and thermal stability, slow crystallization, and brittleness (Muthurai et al., 2018). Their primary applications include plastic shopping bags, medical devices, agricultural films, fishing nets, and cosmetic packaging (Philip et al., 2007).

POLYGLYCOLIC ACID (PGA)
Polyglycolic acid (PGA) has a chemical structure similar to polylactic acid (PLA) but exhibits a higher heat distortion temperature, excellent mechanical properties, and notably superior gas barrier performance. Its exceptional mechanical strength, thermal stability, chemical resistance, and gas barrier properties make PGA highly attractive for applications in the oil and gas industry as well as packaging, where performance comparable to engineering polymers such as PET, PPO, and Nylon 6 is required (Samantaray et al., 2020).

STARCH BLENDS
Starch is a carbohydrate polymer composed of numerous glucose units linked by glycosidic bonds and is naturally present in plants such as potatoes, cereal grains, rice, maize, and cassava (Gowman et al., 2019). Its intrinsic properties, including a high glass transition temperature, strong inter- and intra-molecular hydrogen bonding, water sensitivity, and poor flowability of starch granules, can limit processability and consequently restrict its range of applications (Mekonnen et al., 2013). While chemical modification can enhance starch properties, it is typically expensive and may generate harmful by-products. Plasticization is generally considered the most effective method for improving the processability and performance of starch (Gowman et al., 2019).

3.2.4 COMMONLY STUDIED PLANT-FIBRE COMPOSITES

Numerous studies have investigated the combination of natural fibres with various polymer matrix systems to develop plant-fibre composites with improved mechanical and environmental performance. Among the different categories of natural fibres, bast fibres are the most extensively studied due to their comparatively superior mechanical properties. The material properties of commonly used plant-fibre composites based on flax, hemp, jute, and kenaf fibres are presented in Appendix B.

Contemporary flax fibre composites commonly consist of combinations such as flax fibre/polypropylene, flax fibre/epoxy resin, and flax fibre/polylactic acid (PLA). Frequently studied hemp fibre composites include hemp/polypropylene, hemp/high-density polyethylene (HDPE), hemp/polyester, and hemp/PLA systems. Common jute fibre composites primarily comprise jute/epoxy and jute/PLA combinations, while kenaf fibres are most often combined with polypropylene and polyester matrices.

3.3 COMPOSITE MANUFACTURING

Figure 3.13 illustrates the various processing techniques employed for composites comprising fibres and either thermoplastic or thermoset polymers. Certain processing methods are compatible with both thermoplastics and thermosets. As noted in Section 3.2, a key distinction between these polymer types is that thermoplastics can be reshaped after curing, whereas thermosets cannot.

The choice of processing method generally depends on the manner in which biofillers or fibres are incorporated. Woven fibres are typically processed using compression molding, while short fibres are commonly used in injection molding. Additionally, many naturally derived fibres exhibit limited thermal stability, which restricts processing temperatures to approximately 200 °C or below (Gowman et al., 2019).

From the manufacturing techniques, hand and auto lay-up, filament winding, pultrusion and extrusion are also known as fibre placement techniques or primary processing techniques. After these techniques, the composite material can be processed further with for example oven curing or thermoforming. Figure 3.15 displayes an additional diagram that can be used to choose suitable manufacturing techniques of plant-fibre composites.

3.3.1 COMPOSITE MANUFACTURING TECHNIQUES

COMPRESSION MOLDING

Compression molding is a widely employed composite fabrication technique due to its low cost and simplicity. It allows for precise control over fibre orientation; however, certain natural fibres can be challenging to disperse uniformly during the process (Gowman et al., 2019). The compression molding of thermoplastics generally involves two main steps: (1) the required amount of thermoplastic is placed into the mold cavity and compressed under high pressure between the heated mold halves, and (2) once the thermoplastic softens and conforms to the mold shape, the mold is cooled to solidify the material and enable demolding (Biron, 2018). Figure 3.14 illustrates the principle of compression molding for thermoplastics.

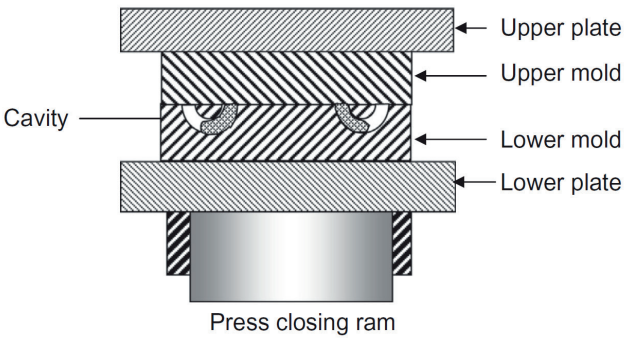

Fig. 3.14 Principle of compression molding (Biron M., 2018).

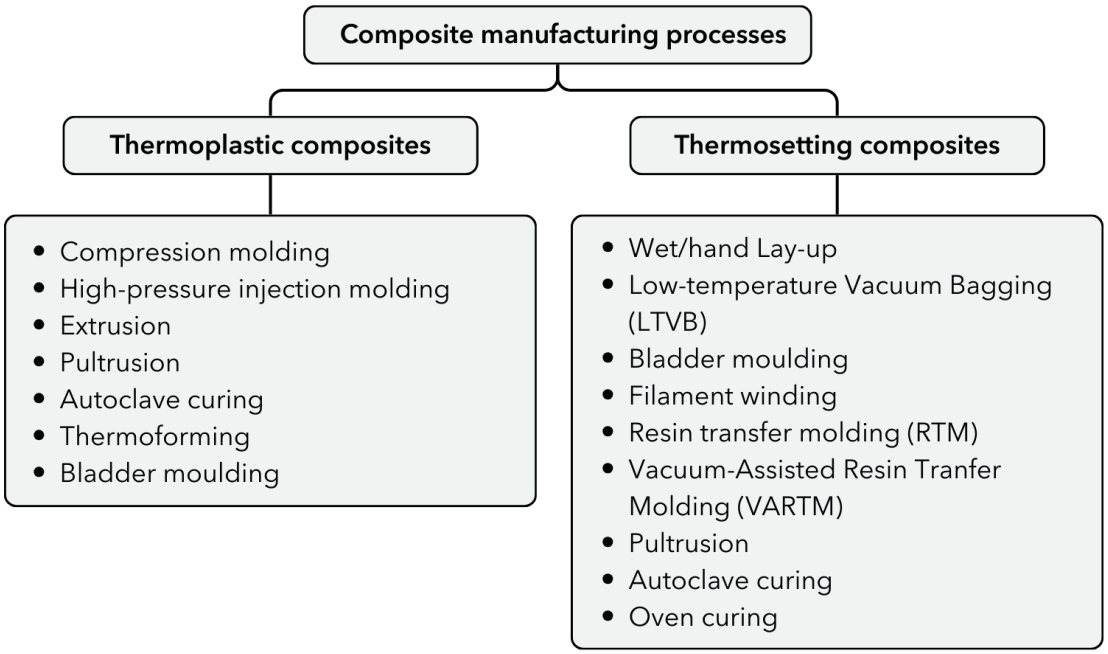

Fig. 3.13 Recent & widely used production methods for fibre composites (adapted from Aravindh et al., 2022).

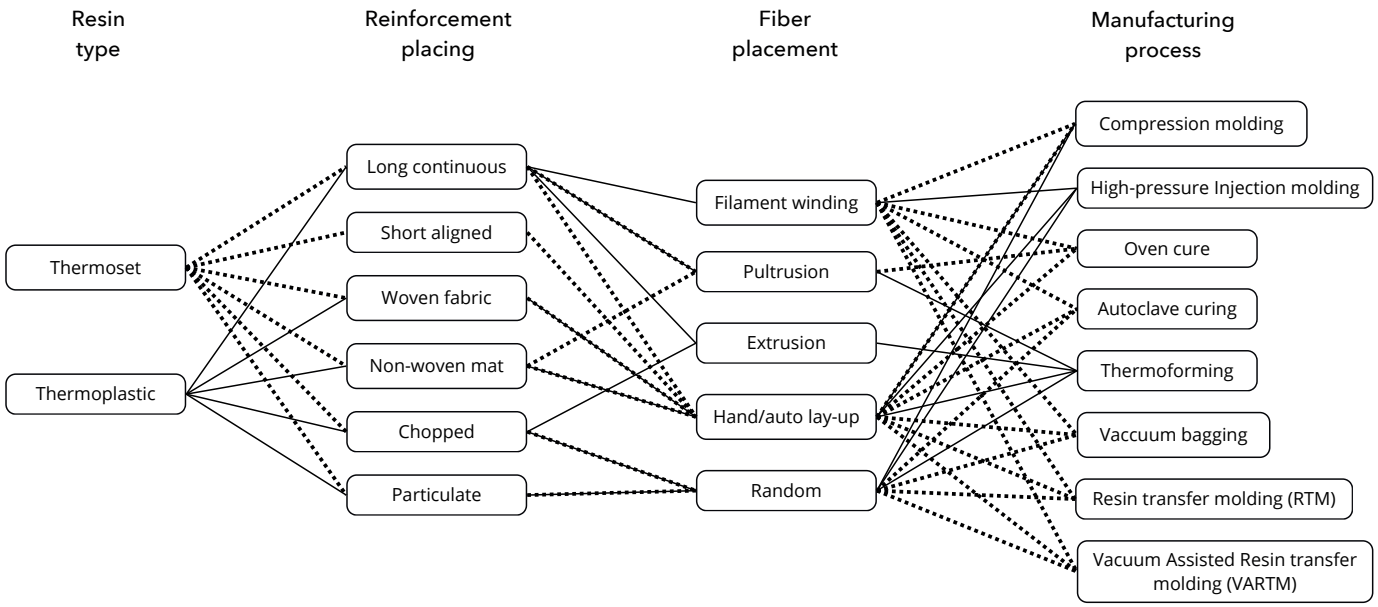

Fig. 3.15 Composite constituent materials and manufacturing options (adapted from Peters, 2013, modified).

HIGH-PRESSURE INJECTION MOLDING

With injection molding, the softened or melted thermoplastic is injected into a mold cavity and subsequently cooled to solidify, achieving its final properties. Except for dimensional changes such as shrinkage or potential warpage, the molded part replicates the shape of the cavity (Biron, 2018). Figure 3.16 illustrates the principle of high-pressure injection molding for thermoplastics.

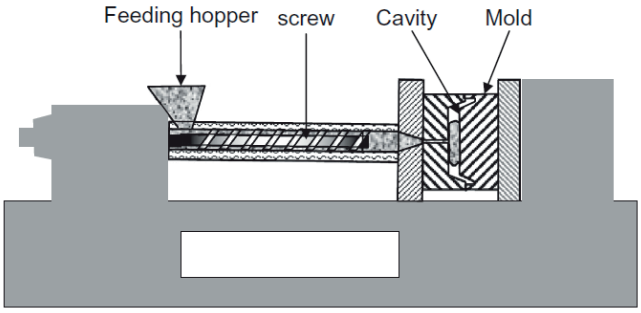

Fig. 3.16 Principle of high-pressure injection molding (Biron M., 2018).

EXTRUSION

Extrusion is a process in which plasticized or melted thermoplastic material is forced through a die, and optionally a punch forming an air gap, to produce a shape that approximates the final cross-sectional profile of the product (Biron, 2018). Figure 3.17 illustrates the principle of extrusion for thermoplastics.

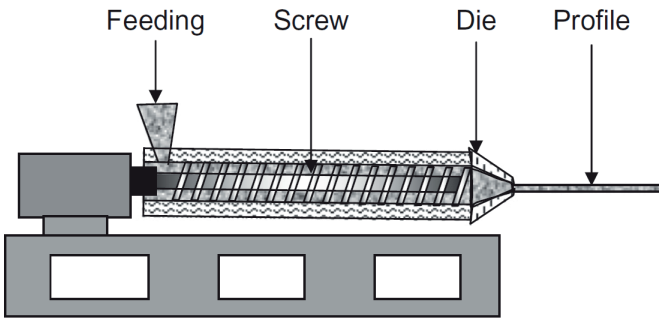

Fig. 3.17 Principle of extrudion (Biron M., 2018).

AUTOCLAVE CURING

Autoclave curing is the most commonly employed method for producing high-quality laminates (Campbell, 2010). The process utilizes elevated temperatures and pressures, resulting in composites that are denser and largely free of voids (Balasubramanian et al., 2018). Typically, prepreg layers are arranged in a mold according to the desired layup, after which the assembly is vacuum-bagged prior to autoclave processing. Figure 3.18 shows this autoclave curing process.

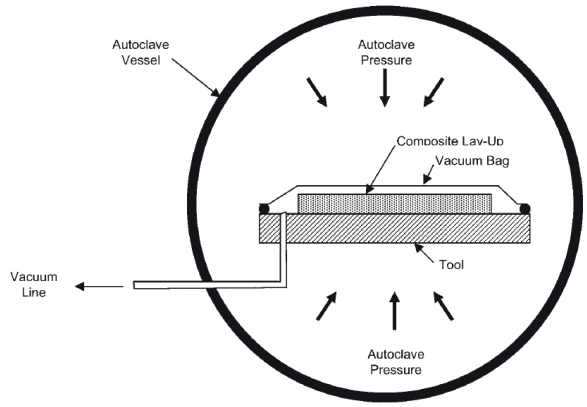

Fig.3.18. Autoclave working principle (Campbell, 2010).

OVEN CURING

Oven curing is similar to autoclave curing without the added pressure. The only limitation to the oven cure are the dimension of the oven. Oven cure is primarely used to fasten the curing time of the composite.

THERMOFORMING

A key advantage of thermoplastic composites is their ability to be rapidly formed into structural shapes through thermoforming (Campbell, 2010). Thermoforming involves heating a thermoplastic sheet until softened and then pressing it onto the walls of a mold to achieve the desired shape. Depending on processing conditions, the resulting shapes and tolerances can range from coarse to highly precise. Under optimal conditions, fine tolerances and sharp details are achievable, and with appropriate finishing techniques, thermoformed parts can attain quality comparable to that of injection-molded components (Biron, 2018). Figure 3.19 shows the principles of thermoforming of thermoplastics.

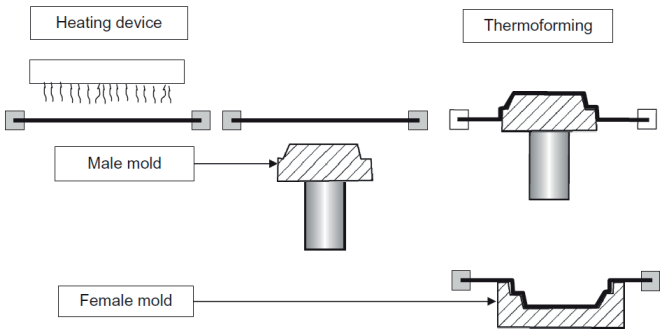

Fig. 3.19 Principle of thermoforming (Biron M., 2018).

WET HAND LAY-UP

The hand lay-up method (figure 3.20), also referred to as the wet lay-up method, is one of the oldest and most traditional composite fabrication techniques in the industry. It is a straightforward process in which each ply is handled manually and stacked layer by layer until the desired thickness is achieved (Balasubramanian et al., 2018). A dry reinforcement, typically a woven glass cloth, is placed on the mold by hand, after which a low-viscosity liquid resin is applied through pouring, brushing, or spraying. No external heat is required for curing, which generally occurs at room temperature. To improve laminate quality, this method can be combined with vacuum bagging or applied pressure to minimize voids and porosity (Campbell, 2010).

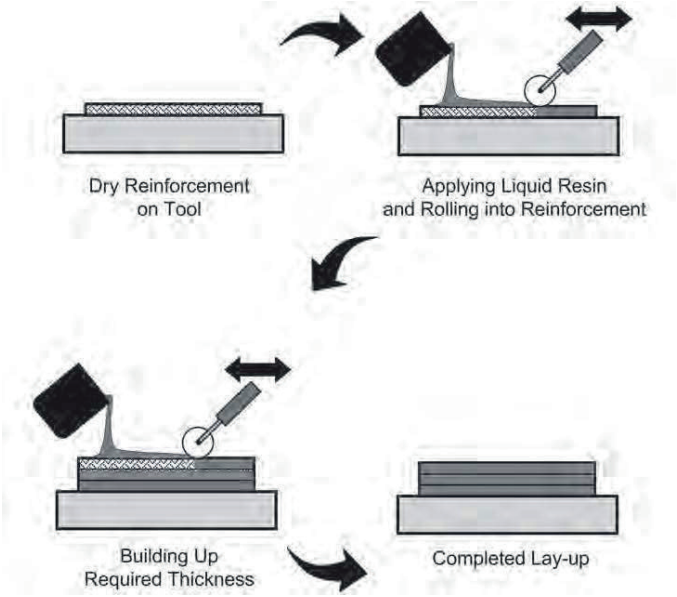

Fig. 3.20 Hand/auto lay-up working principle (Campbell, 2010).

FILAMENT WINDING

Filament winding (figure 3.21) is a widely used technique for integrating two-dimensional reinforcements with additional processes and for producing three-dimensional reinforcement structures. It is a well-established method capable of creating symmetrical shapes (Balasubramanian et al., 2018). In this high-throughput process, a continuous fibre band is wound onto a rotating mandrel. Filament winding is highly repeatable and allows the fabrication of large, thick-walled composite structures (Campbell, 2010). Carbon-fibre tubes are made using prepegs of carbon-fiber with a resin matrix and cured using an autoclave process.

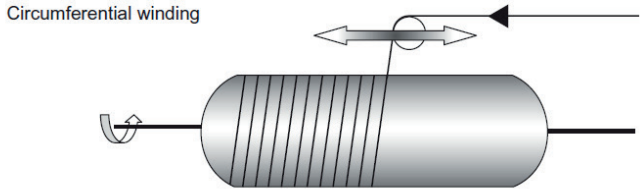

Fig. 3.21 Principle of filament winding (Biron M., 2018).

PULTRUSION

Pultrusion is a well-established manufacturing process that has been employed in commercial applications since the 1950s. In this process, continuous fibrous reinforcement is impregnated with a polymer matrix and continuously consolidated into a solid composite (Campbell, 2010). A heating system softens the pre-impregnated rovings, after which rollers consolidate the material before it passes through a cooled die to solidify the thermoplastic matrix (Biron, 2018). The studies conducted on manufacturing profile geometry with plant-fibre composites are done with pultrusion. The only downside to this process is the specialised equipment needed. Figure 3.22 shows the pultrusion process.

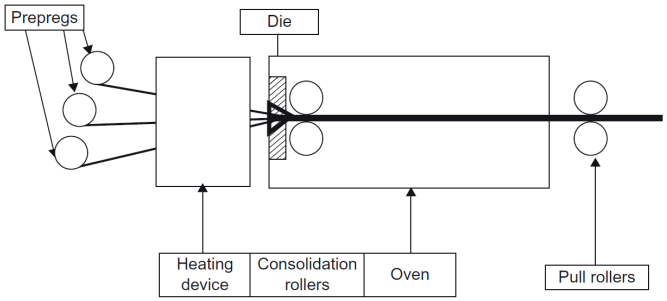

Fig. 3.22. Principle of thermoplastic pultrusion (Biron M., 2018)

LOW-TEMPERATURE VACUUM BAGGING

Low-temperature vacuum bagging (LTVB) prepregs were initially developed for the fabrication of composite tooling. Over the past 15 years, however, their applications have expanded, making them suitable for the production of composite structural components (Campbell, 2010). Vacuum bagging can be combined with multiple other techniques like oven curing and resin transfer molding (RTM). Figure 3.23 displayes the vacuum bagging technique.

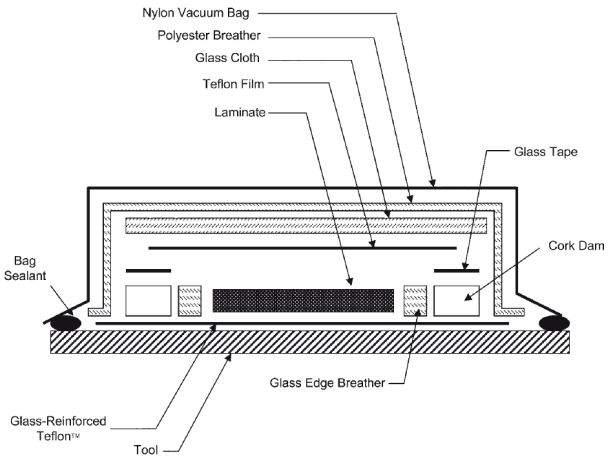

Fig. 3.23 Principle of Low-temperature vacuum bagging (LTVB) (Campbell, 2010).

RESIN TRANSFER MOLDING (RTM)

Resin transfer molding (RTM) is a widely used processing technique for plastics, valued for its versatility in accommodating a broad range of materials and its operational simplicity. This method has been shown to enhance fibre dispersion and improve both tensile and flexural properties of composites (Mohanty et al., 2004). Figure 3.24 illustrates the principle of resin transfer molding, a process primarily applied to thermosets but also compatible with certain thermoplastics.

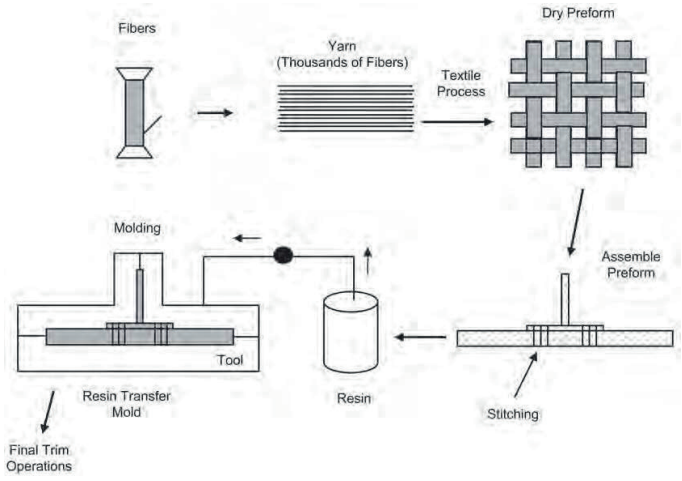

Fig. 3.24 Principle of Resin Transfer Molding (RTM) (Balasubramanian et al., 2018).

VACUUM ASSISTED RESIN TRANSFER MOLDING (VARTM)

Next to conventional resin transfer molding, vacuum-assisted resin transfer molding (VARTM) relies solely on vacuum pressure for both resin infusion and curing, its primary advantage is that the tooling is significantly less expensive and simpler

to design compared to conventional resin transfer molding (RTM) processes. Furthermore, because an autoclave is not required for curing, VARTM enables the fabrication of very large composite structures (Campbell, 2010). VARTM is displayed below in figure 3.25.

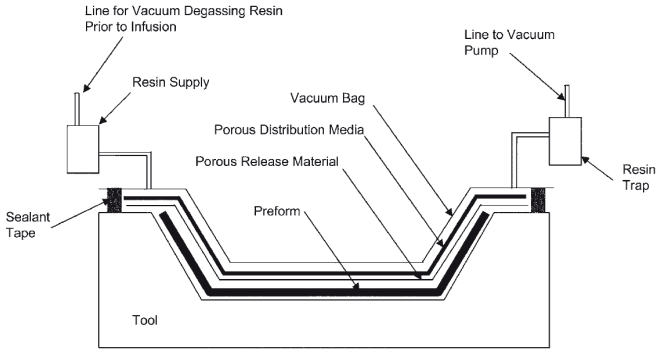

Fig. 3.25 Principle of Vacuum-Assisted Resin Transfer Molding (VARTM) (Balasubramanian et al., 2018).

3.3.2 MANUFACTURING OF PLANT-FIBRE COMPOSITE PROFILES

The limited studies on manufacturing plant-fibre reinforced polymers into complex profile geometry used for load-bearing applications are all done by pultrusion technique with specialised build machinery and highly manipulated natural fibres not available during this research. Two examples where found of application of plant-fibre composites used for load-bearing applications, the LeichtPRO project and the BasajaunH2020 project.

LeichtPRO Project

This study delves into the pultrusion technology, introducing a novel bio-composite product, a round profile engineered as a load-bearing element for structural applications. This product emerged through the LeichtPRO research project (Pultruded load-bearing lightweight profiles from natural fibre composites), led by the Bio- Mat Department at the ITKE Institute at the University of (Stuttgart) (Spyridonos, E., & Dahy, H., 2025).

Here, the profiles were made of kemafil hemp bast strips with a customised matrix formulation consisting of a plant-based resin component, a hardener, an accelerator, and the aluminum trihydrate (ATH) additive which acts as a mineral filler and flame retardant (Spyridonos, & Dahy, 2025). Figure 3.26 displayes the obtained profiles.

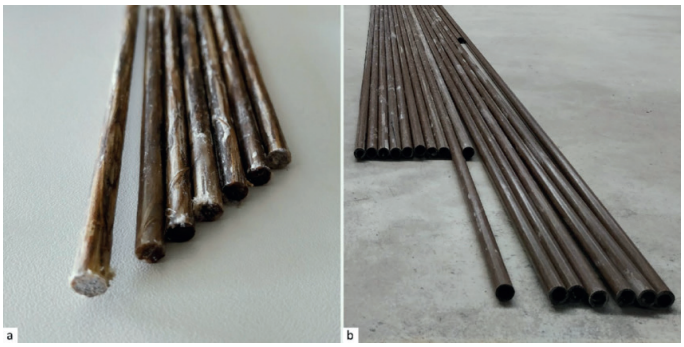

Fig. 3.26. Natural fibre pultruded profiles (Spyridonos, & Dahy, 2025).

Basajaun H2020 Project

This project funded by the European Union aimed to demonstrate the feasibility of introducing environmentally friendly bio-based components into the mature curtain wall façade industry. The project focuses on identifying technological solutions for replacing key components such as profiles, insulation, and the tightness system with bio-based and less environmental impact alternatives (Guedes S.C. & Salvado, F.C., 2026).

For this particular project, pultrusion emerges as a cost-effective and competitive method to conventional profile manufacturing techniques like extrusion for metals. The project manages to transform a thermoset matrix and natural reinforcement into a consistent composite profile by doing raw material analysis, balanced composition and comprehensive testing. The profiles were made of a polyester matrix combined with basalt fibres from the basalt quarry stone (melted at about 1400°C) and wood material (Pracucci et al., 2024). Figure 3.28 shows a section of the pultruded profiles.

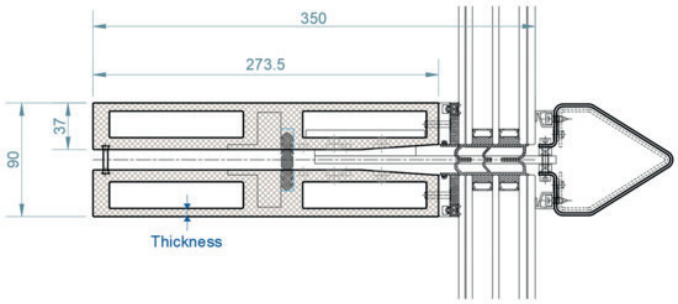

Fig. 3.27. Cross-section of basalt and wood fibre pultruded profiles (Pracucci et al., 2024)

4. FACADE APPLICATION CONTEXT

4. FACADE APPLICATION CONTEXT

For the implementaton of a structurally performing plant-fibre reinforced composite, mullion and transoms are chosen of the stick-built curtain wall façade system of low-rise and mid-rise buildings in the European Union. This façade typology allows for the plant-fibre reinforced composite to still have a structural function but with less strict performance criteria related to structural performance and fire regulations. This is also due to the applications of this façade in low- and mid-rise buildings. In addition, because of the high moisture absorption and poor UV-stability of plant-fibres (see section 3.1), curtain wall mullion and transoms are a suitable application because these components are situated inside of the thermal envelope of the building (behind glazing panels and gaskets).

This alternatively means, the plant-fibre reinforced composite only has to:

- redirect horizontal windloads to the main building structure;
- carry its own self-weight;
- provide stability to the façade system

This chapter discusses curtain wall façades, its performance criteria and accompanying mullion and transom design.

4.1 CURTAIN WALL FACADE SYSTEM

Curtain wall façades are widely recognized as a defining element of modern architecture across the globe. At present, the skylines of most major cities are characterized by high-rise landmark buildings that incorporate curtain wall systems (CWS) to some extent. The widespread adoption of these systems can largely be attributed to their ability to enhance indoor daylight availability, deliver high aesthetic quality, accelerate construction processes, improve construction precision, and promote material efficiency through lightweight structural solutions and prefabrication techniques, among other advantages (Boafo et al., 2021).

4.1.1 HISTORICAL DEVELOPMENT OF CURTAIN WALLS

Historically, the emergence of curtain wall systems was driven by the demand for reduced wall thickness, which allowed for increased usable floor area, as well as the possibility of parallel construction scheduling, leading to shorter construction timelines. Additional motivating factors included the adoption of lighter structural solutions, resulting in savings in both material usage and transportation, enhanced structural flexibility that facilitated seismic design and engineering, improved daylight penetration enabling more adaptable and cost-effective architectural layouts, and the structural independence of the façade from the primary load-bearing system (Kazmierczak & Hershfi, 2010).

The Crystal Palace in London, designed by Sir Joseph Paxton and completed in 1851 (figure 4.1), is widely regarded as the first fully glazed structure employing a curtain wall façade system (Boafo et al., 2021).

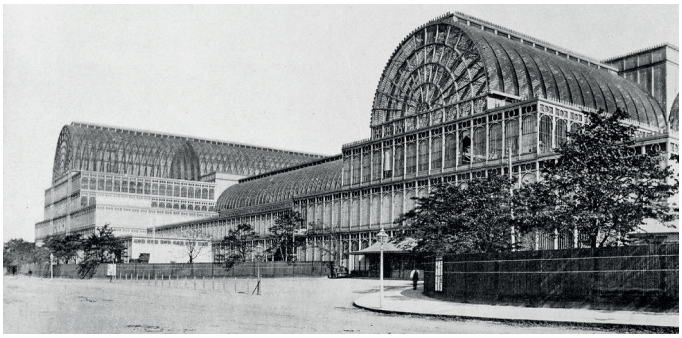

Fig. 4.1 The Crystal Palace, London (Kelly, 2024).

4.1.2 TYPES OF CURTAIN WALL FACADES

Based on the degree of prefabrication and construction methodology, curtain wall systems may be broadly classified into stick-built, unitized, semi-unitized, and structural glazing systems (Boafo et al., 2021).

STICK-BUILT SYSTEMS

''The stick system is the oldest type of curtain wall system'' (Sanders, 2006). This system consists of standard, factory-produced components, including vertical and horizontal curtain wall framing members (mullions and transoms) as well as glass or opaque spandrel panels, which are assembled incrementally on site. Figure 4.2 shows a typical stick-built curtain wall sequence. Stick-built systems provide a high degree of flexibility in terms of assembly and glazing techniques and can readily accommodate diverse site conditions. While the initial material costs are relatively low and lead times are short due to the use of off-the-shelf components, on-site labor requirements are generally higher, resulting in longer installation durations, as the entire system is constructed in situ (Boafo et al., 2021).

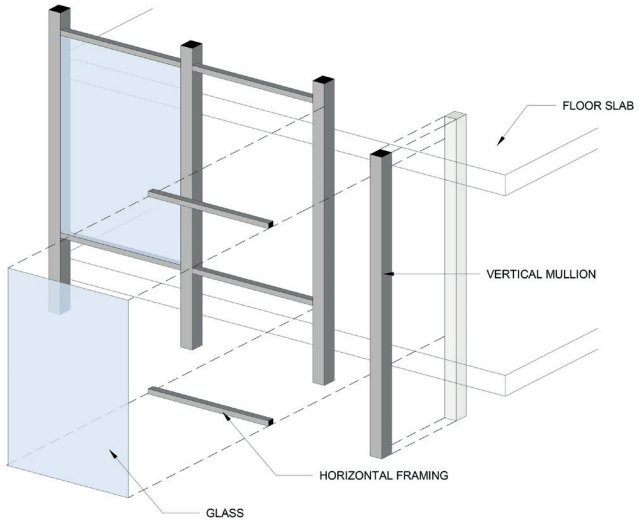

Fig. 4.2 Stick-built curtain wall sequence (Raggousis, 2016).

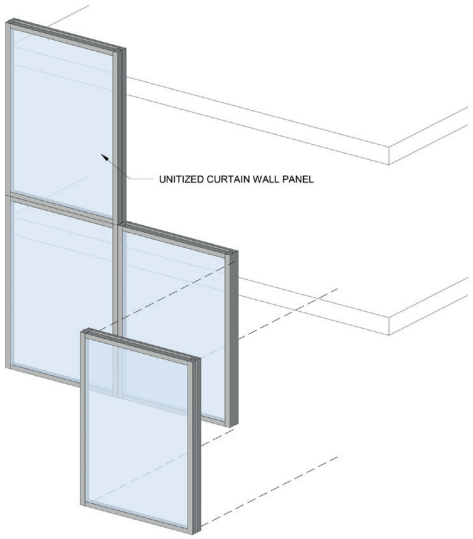

Fig. 4.3 Unitized curtain wall sequence (Raggousis, 2016).

UNITIZED SYSTEMS

A unitized curtain wall façade consists of fully prefabricated modules that are manufactured off site and transported to the construction site as complete assemblies. Prefabrication is defined as an off-site manufacturing process conducted in specialized facilities, where different materials and building systems are integrated into large components that are later delivered and installed as part of the final building assembly (Boafo et al., 2016).

Existing studies indicate that prefabrication can significantly enhance construction quality and safety, while simultaneously reducing construction duration, overall costs, material waste, and environmental impacts. Furthermore, when unitized modules are relatively small in size, installation can be carried out from within the building, eliminating the need for crane operations (Boafo et al., 2021). Figure 4.3 displayes a typical unitized curtain wall sequence.

SEMI-UNITIZED SYSTEMS

In addition to stick-built, unitized, and structural glazing curtain wall systems, the unit mullion system represents a hybrid solution that combines features of both stick and unitized approaches. In this system, pre-assembled units are installed behind individual mullions spanning one or two stories. As a result, the system retains several advantages commonly associated with unitized construction, including improved factory-controlled quality. At the same time, it typically involves slightly lower costs and shorter lead times due to reduced customization when compared to fully unitized systems, while also benefiting from the comparatively lower installation costs characteristic of stick-built systems (Boafo et al., 2021).

STRUCTURAL GLAZING SYSTEMS

Point-loaded structural glazing systems are a type of curtain wall façade composed of structural-grade glass, such as tempered or heat-strengthened glass. The glass is supported by specialized fixing systems that minimize or entirely eliminate the visible metal framing typical of conventional frame-supported curtain wall systems (Boafo et al., 2021). Various support configurations, including tension cable systems, trusses, and glass mullions offer substantial design flexibility and a wide range of aesthetic possibilities, while accommodating different levels of transparency, structural stiffness, and cost. However, both product and installation costs for these systems are generally higher than those associated with traditional framed curtain wall solutions (Boafo et al., 2021).

4.2 MULLION AND TRANSOM CURTAIN WALL SYSTEMS

The mullion-and-transom curtain walling system is a stick-system and is defined by a load-bearing framework arranged according to structural, morphological, and enclosure requirements, onto which the glass elements are attached. In contrast to unitized curtain wall systems, the mullion-and-transom curtain wall system is predominantly used for low- to mid-rise buildings due to its on-site fabrication and greater design flexibility (Paoletti & Nastri, 2024).

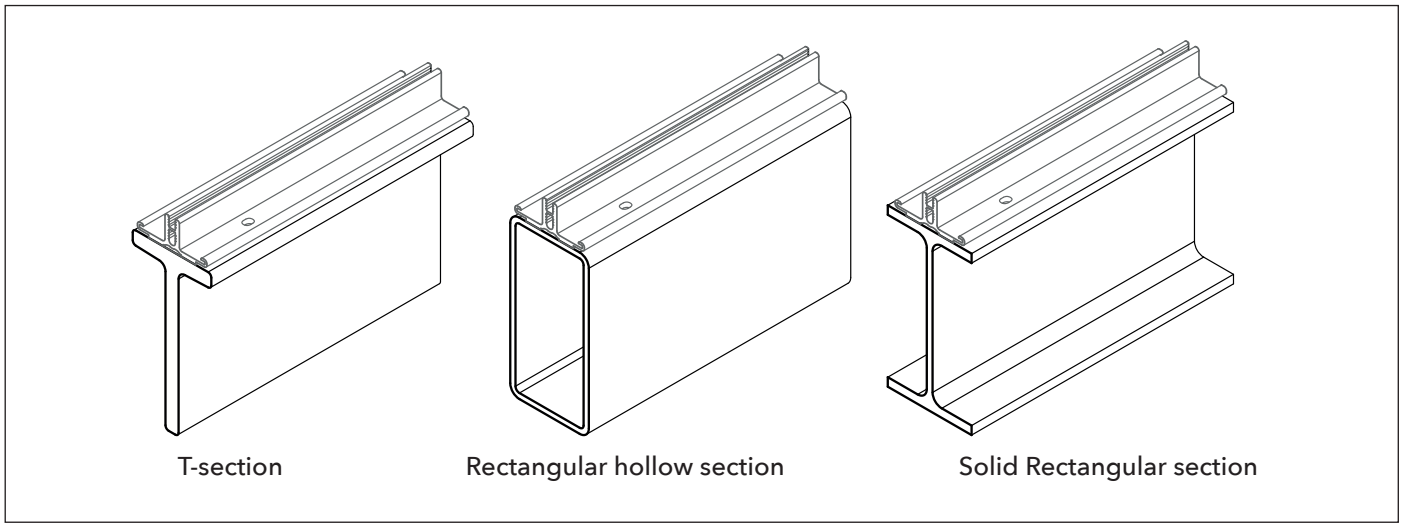

Fig. 4.4 Different mullion and transom profile geometries used for curtain wall façades (STABALUX, 2025).

This system, suitable for flat or polygonal façades, is assembled on site following the preparation of the structural components. These preparations involve cutting and machining the profiles to enable:

- the connection of the vertical profiles (mullions) to the primary load-bearing structure;
- the installation of the horizontal elements (transoms) onto the mullions;
- the assembly of vertical enclosure elements, including insulating glass units or spandrel panels

Specifically, the mullion-and-transom façade system consists of a frame formed by mullion profiles with a quadrangular, homogeneous tubular cross-section, characterized by a rear rib that is larger than the lateral ribs. The front rib of the mullion profile is equipped with:

- a continuous threaded linear pin for fastening the pressure plate;
- a pair of parallel grooves designed to house internal gaskets, typically made out of EPDM (Paoletti & Nastri, 2024).

Curtain wall façades can be constructed using a wide variety of materials, including glass, wood, stone, stainless steel, aluminum, polyvinyl chloride (PVC), and concrete, among others. Due to its widespread availability, favorable strength-to-weight ratio, corrosion resistance, and ease of fabrication, lightweight aluminum framing is the most commonly used material in curtain wall systems (Boafo et al., 2021).

4.2.1 MULLION AND TRANSOM PROFILE GEOMETRY

As a reference for mullion and transom profile geometry to use for this research, different metal profile geometries are chosen from the Stabalux website. Stabalux is a façade manufacturer producing curtain wall façades of aluminum, steel, wood and bamboo. All the products apply to the passive house standard norms. For this study, only the metal profiles are looked at while the wood and bamboo profiles already exhibid a significantly lower embodied carbon than the aluminum or steel profiles.

The metal profile geometries of Stabalux are displayed in figure 4.4. The geometry include a T-profile, a rectangular hollow pofile and an I- or H profile. These profile geometries are discussed further.

T-SECTION MULLION AND TRANSOM

Figure 4.5 presents the profile geometry of the T-section profiles developed by STABALUX. These profiles are primarily manufactured from steel, as the slender profile geometry often requires higher structural strength and stiffness. A disadvantage of this profile configuration is the visible connection between the aluminium base profile and the steel T-profile, which may negatively affect the visual appearance and architectural integration of the façade system.

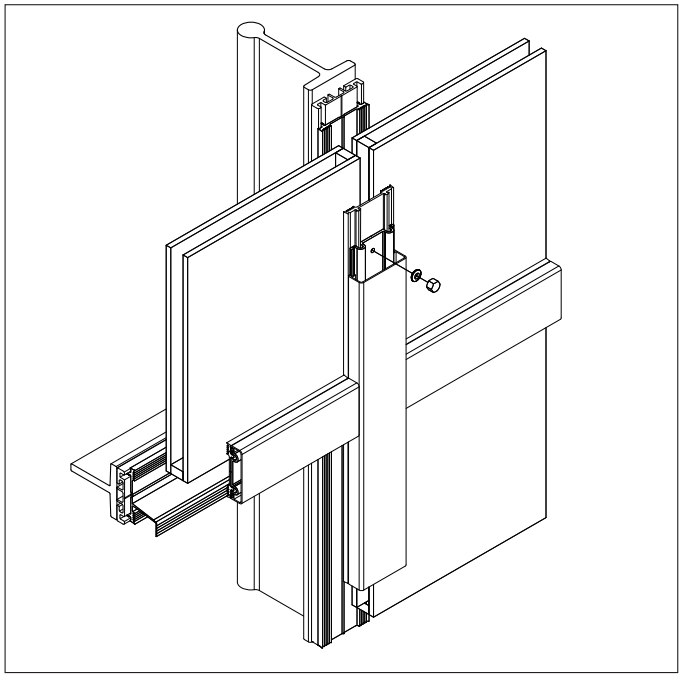

Fig. 4.5 STABALUX-T systems (STABALUX, 2025).

RECTANGULAR HOLLOW SECTION

Figure 4.6 displayes the most common profile of a mullion and transom. Which are hollow rectangular sections. The transverse dimensions of the mullions (typically ranging from 50mm to 85mm in width and 60mm to225 mm in depth) are determined based on anticipated mechanical loads, the overall module geometry, and the required moment of inertia to ensure adequate structural performance (Paoletti & Nastri, 2024).

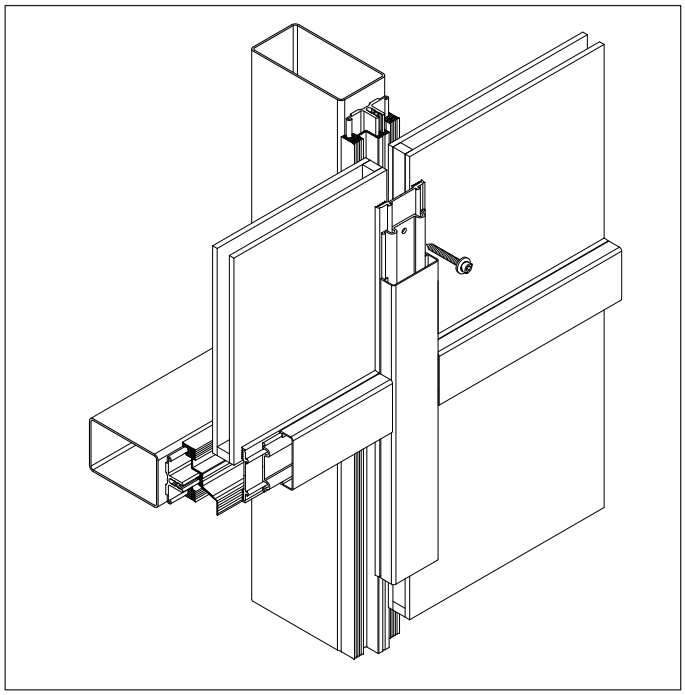

Fig. 4.6. STABALUX AK-S system (STABALUX, 2025).

I-SECTION AND H-SECTION

In addition to T-sections and rectangular hollow sections, I-sections and H-sections can also be applied in the design of mullions and transoms. Similar to T-profile geometries, these sections are manufactured through extrusion processes. Although these profile configurations are less commonly adopted in standard curtain wall systems, they can be produced and implemented upon specific client request to meet project-specific structural or architectural requirements.

4.2.2 STRUCTURAL PROPERTIES OF MULLIONS AND TRANSOMS

The metal STABALUX profiles are made of galvanized steel class S280 or aluminum 6060 T-66. The profiles are produced through an extrusion process according to DIN EN 12020. This code discribes tolerances on dimensions and form of extruded precision profiles in alloys EN AW-6060 (NEN., 2023). The aluminum used for these profiles is 6060 T66 aluminum (STABALUX, 2025). 6060-T66 aluminum is 6060 aluminum in the T66 temper. To achieve this temper, the metal is solution heat-treated and artificially aged, with additional process control to yield more favourable properties (Makeitfrom, 2020). The properties of 6060-T66 aluminium are displayed in table 4.0.

MECHANICAL PROPERTIES	VALUE
Density	*2.7 g/cm^3*
Youngs modulus	*68 GPa*
Yield strength	*170 MPa*
Shear strenth	*130 MPa*
Elongation at break	*9.1 %*
Specific heat Capacity	*900 J/kg-K*
Thermal expansion	*24 µm/m-K*
Embodied Carbon	*8.3 kg CO_2/ kg material*

Table 4.0 Properties 6060-T66 aluminum (STABALUX, 2025; Makeitfrom, 2020).

4.3 EUROPEAN CURTAIN WALL REGULATIONS

The European Union has requirements for curtain wall façades. These requirements and performance creteria are defined in building code EN 13830: Curtain wailling- product standard. This European Standard specifies requirements of curtain walling kit intended to be used as a building envelope to provide weather resistance, safety in use, energy economy and heat retention and provides test, assessments, calculation methods and compliance criteria of the related performances (STABALUX, 2025).

The curtain walling kit covered by this standard should fulfil its own integrity and mechanical stability but does not contribute to the load bearing or stability of the main building structure, and could be replaced independently of it. This standard applies to curtain walling kit ranging from a vertical position to ± 15° from the vertical. Any sloping parts should be contained within the curtain walling kit (Intertek, 2024). This building code specifies performance requirements for curtain wall systems, including (STABALUX, 2025):

- *Resistance to wind load*
- *Self-weight*
- *Air permeability*
- *Impact resistance*
- *Driving rain resistance*
- *Heat transition*
- *Airborne sound insulation*
- *Fire resistance*
- *Fire behavior*
- *Fire spread*
- *Durability*
- *Water vapor permeability*
- *Potential equalization*
- *Seismic safety*
- *Thermal shock resistance*
- *Building and thermal movement*
- *Resistance to dynamic horizontal loads*

Of these performance requirements, the following are especially important for the structural mullions and transoms:

- *Resistance to wind load*
- *Resistance to self-weight*
- *Impact resistance*
- *Fire resistance*
- *Seismic safety*
- *Building and thermal movement*
- *Resistance to dynamic horizontal loads*

The European standards with their accompanying performance criteria are found in *Appendix D*. The necessary tests to determine these performance criteria are also discribed in building code EN 13830.

4.4 EMBODIED CARBON OF CURTAIN WALL FACADES

The main components of curtain wall façades that contribute to embodied carbon emissions are the structural profiles, insulation materials, glazing systems, and the tightness and stiffness layers. Although glazing often represents a significant proportion of the embodied carbon of curtain wall façades, it is also the component most readily replaced after several years of operation with higher-performing glazing technologies. In many cases, glazing is the only façade component replaced during the building's service life. Consequently, the total embodied carbon of the façade system is primarily determined by the structural profiles, insulation materials, and tightness layers, which are generally not replaced throughout the lifespan of the system.

STRUCTURAL PROFILES

Conventional commercially available aluminium curtain wall façades utilise aluminium profiles with an average recycled content of approximately 36% in Europe and an embodied carbon value of around 44 $kgCO_2$-eq/m (Pracucci et al., 2024). Similarly, Gannon (2021) assessed the Global Warming Potential (GWP) of aluminium profiles within a unitised curtain wall system and reported a value of 59 $kgCO_2$-eq/m of profile. The average value of 51.1 $kgCO_2$-eq/m is taken as a general value for the embodied carbon of the structural profiles of the façade.

INSULATION MATERIAL

Conventional curtain wall systems typically employ rock wool insulation, which has an average Global Warming Potential (GWP) of approximately 45 $kgCO_2$-eq/m^3 based on Environmental Product Declarations (EPDs) (Pracucci et al., 2024). In addition, Gannon (2021) evaluated the GWP of mineral wool insulation within a unitised curtain

wall system and reported a value of 167 kgCO_2-eq/m².

TIGHTNESS- AND STIFFNESS LAYERS

Conventional curtain wall façades generally incorporate silicones, sealants, and aluminium sheets as part of their tightness and stiffness layers. For an opaque façade module, these materials have an estimated average embodied carbon of approximately 38 kgCO_2-eq/m² (Pracucci et al, 2024). Overall, the structural components account for approximately one-third of the embodied carbon within the façade system. Therefore, considerable reductions in embodied carbon may be achieved through the implementation of more sustainable alternatives for these components.

5. MATERIAL AND GEOMETRY SELECTION

5. MATERIAL AND GEOMETRY SELECTION

This chapter presents the selection of plant-based fibres, resin matrices, processing methods, and testing procedures that will be applied during the experimental phase of this research. The objective is to manufacture plant-fibre composite mullion and transom profile geometries with sufficient mechanical performance to satisfy the structural and functional requirements of curtain wall façade systems.

5.1 PERFORMANCE CRITERIA FOR PROFILES

MATERIAL PERFORMANCE

The performance criteria for the plant-fibre composites consist of the key material properties that the developed composites should aim to achieve. Within the scope of this research, the intended application of the plant-fibre composite profiles is the replacement of aluminium mullions and transoms used in curtain wall façades. Therefore, the properties of the aluminium alloy applied in the STABALUX AL mullion and transom profiles have been selected as the reference benchmark.

The selected material properties are based on the principal loading conditions acting on mullion and transom profiles, which predominantly experience tensile stresses. Furthermore, the elongation at break is considered an important parameter, as it provides insight into the material failure behaviour and ductility characteristics. In addition, embodied carbon is included as an evaluation criterion to assess the environmental performance and sustainability potential of the material. The selected performance criteria are presented in table 5.0.

MECHANICAL PROPERTIES	VALUE
Tensile strength	*220 MPa*
Yield strength	*160 MPa*
Young's modulus	*68 GPa*
Thermal expansion	*24 µm/m°C*
Embodied Carbon	*8.3 kg CO_2-eq/kg material*
Price	+++

Table 5.0 Mechanical properties of 6060-T66 aluminum (STABALUX, 2025; Makeitfrom, 2020).

EUROPEAN CURTAIN WALL PERFORMANCE

In addition to material performance, Table 5.1 presents the relevant performance criteria applicable to curtain wall systems in Europe. Although comprehensive testing of all relevant properties would be preferable, constraints in available equipment and project time frame limit the scope of mechanical testing that can be performed within this research. Consequently, only the following performance criteria are selected and considered within the scope of this study:

PROPERTY	VALUE
Resistance to windload of 2 kN/m^2	*Allowed profile deflection: Must not exceed L/200 or 15mm if L ≤ 3000mm*
Building and thermal movement	*"The design of the curtain wall must be capable of absorbing thermal movements and movements of the structure in such a way that destruction of facade elements or impairment of the performance characteristics do not occur.*

Table 5.1 Relevant curtain wall design criteria (STABALUX, 2025; Intertek, 2024).

In this context, resistance to wind loads can be evaluated through three-point bending tests. These tests provide insight into the material's flexural strength, stiffness, and failure mechanisms. Building-related and thermal movements can be assessed by determining the coefficient of thermal expansion, in combination with the evaluation of Young's modulus.

DURABILITY AND VISUAL PERFORMANCE

In addition to the mechanical properties of the mullion and transom profiles, durability and visual performance criteria were defined to guide the selection of suitable fibre materials for façade applications. These criteria include embodied carbon and surface quality.

Based on Section 4.4, the embodied carbon of the aluminium structural members used in conventional curtain wall façades is approximately 51.1 kgCO_2-eq/m. In this study, a durability-related performance target is defined, aiming to reduce this embodied carbon by 70%, resulting in a target

value of 15.3 kgCO_2-eq/m for the manufactured plant-fibre composite profiles.

The surface of the material should exhibit minimal porosity or perforations to prevent water ingress into the fibre structure. Such ingress may lead to fibre swelling over time, which can in turn induce resin–fibre debonding at the interface and ultimately compromise the composite's structural integrity.

PROPERTIES	VALUE
Embodied carbon profile	*< 15.3 kg CO_2-eq/m*[1]
Surface quality	*Minimal porosity or perforations*

Table 5.2 Additional performance criteria (own work).

5.2 MATERIAL SELECTION PROCESS

The mechanical properties of natural fibre composites, including impact, flexural, and tensile strength, are governed by several interrelated factors, such as fibre content within the matrix, intrinsic fibre strength, fibre–matrix adhesion, fibre orientation, fibre concentration, and the type of fibre surface treatment applied (Arumugam et al., 2022).

In addition, the physical performance, surface quality, scalability, cost efficiency, and environmental impact of plant-fibre reinforced polymer composites are primarily determined by three interdependent parameters: the matrix, the fibre and the manufacturing process, as illustrated in Figure 5.0 (Overend, M., et al. (unpublished) Consequently, during the design and development process, careful material selection that accounts for functional requirements, economic feasibility, and environmental sustainability represents a fundamental step in composite material engineering (Mahajan et al., 2022).

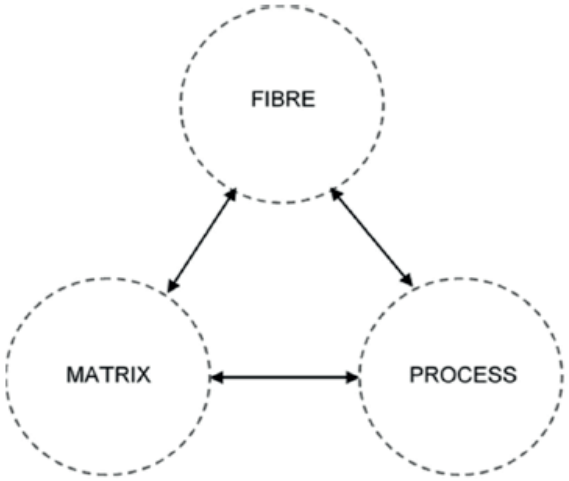

Fig. 5.0. Principal desicion factors (Overend, M., et al., unpublished)

5.2.1 RESIN MATERIX SELECTION

This section focuses on the selection of a suitable polymer matrix to manufacture a plant-fibre composite. Various criteria have been established to identify the optimal resin matrix for the intended application. The main selection criteria are:

1. Polymer type: thermoset or thermoplastic
2. Resin availability and cost
3. Required equipment and ease of use
4. Resin mechanical performance: including tensile strength, tensile modulus, elongation at break, and melting temperature

1. POLYMER TYPE

Table 5.3 presents a comparative overview of the advantages and limitations of thermoset and thermoplastic matrix systems, thereby supporting an informed material selection for the intended composite application.

MATRIX	ADVANTAGES / LIMITATIONS
Thermoset polymer	*> Lamination techniques* *> Mechanical properties* *> Thermal stability* *> Chemical resistance* *< Creep resistance* *< Stress relaxation* *> Wettability of reïnforcement* *< Working conditions (some solvent fumes)* *< Complex geometry*

Thermoplastic polymer	> *Impact strength* > *Fracture toughness* > *Elongation at break* > *Storage life* > *Post-formability* < *Fabrication time* > *Complex geometry possible* > *Surface quality*

Table 5.3 Performance of thermoplastics vs thermosets (adapted from Overend, M., et al., unpublished)

Thermoset matrix systems offer several advantages over thermoplastic matrix systems, including compatibility with established lamination techniques, superior mechanical performance compared to thermoplastic matrices, and enhanced thermal stability (Fan & Weclawski, 2017). In addition, thermosetting polymers are considered particularly suitable for plant-fibre-reinforced composites due to their relatively low processing temperatures, which reduce the risk of thermal degradation of natural fibres (Shelly et al., 2025). Furthermore, the manufacturing of complex profile geometries requires sufficient formability during processing to ensure accurate shaping without compromising structural integrity (Overend, M., et al. (2026) unpublished). Certain thermoset systems also exhibit extended curing times, during which the material remains workable, thereby enabling improved control over forming processes.

However, thermoset systems also present limitations, including the emission of volatile organic compounds (VOCs), challenges related to recycling and end-of-life recovery, limited pot and shelf life, and potential difficulties in achieving high-quality surface finishes, depending on the processing route (Fan & Weclawski, 2017).

Nevertheless, for structural applications, thermoset matrices in the form of low-viscosity liquid resins with relatively slow curing kinetics are particularly suitable. Such systems facilitate the fabrication of the curvilinear geometries required for curtain wall mullions and transoms, as described in Section 4.2.1. In particular, two-component epoxy systems consisting of a resin and hardener are well suited, as they provide sufficient working time to accommodate the complexity of the geometry while ensuring uniform resin distribution and consistent surface quality throughout the composite (Overend, M., et al. (unpublished).

5.2.2 PLANT FIBRE SELECTION

The following section outlines the selection process for plant fibres using a multi-criteria decision-making (MCDM) approach.

PLANT-FIBRE SELECTION CRITERIA

The performance of natural fibres is influenced by a wide range of factors, including, but not limited to, geographic location and climatic conditions, agricultural practices such as crop variety, seed density, and soil quality, as well as the methods used for fibre extraction and subsequent treatment. Furthermore, the literature indicates substantial variability in natural fibre properties, with significant differences in performance observed even within the same fibre type. Consequently, no single natural fibre can be considered universally optimal, and fibre selection must therefore be governed by the specific requirements of the intended application (Mahajan et al., 2022).

Accordingly, the selection of suitable plant fibres for a given application requires a multi-criteria decision-making (MCDM) approach. Mahajan et al. (2022) developed an MCDM framework for plant fibre selection based on application-specific requirements. In the present study, which focuses on functional and structural applications in façade design, mechanical performance is identified as the most critical parameter, as it directly governs the resulting properties of the composite material.

The criteria applied in the MCDM method for plant fibre selection are presented in Table 5.4 (Mahajan et al., 2022).

CRITERIA	EXPLANATION
Elongation at break	*The material must exhibit sufficient elongation at break values to ensure adequate toughness characteristics, as this parameter is indicative of the material's ductility.*
Specific strength	*The ratio between yield strength and material density, commonly referred to as specific strength, should be high in order to achieve a structurally efficient and mechanically robust material.*
Specific modulus	*The ratio between Young's modulus and material density, commonly referred to as the specific modulus, should be high to obtain a material with high stiffness relative to its weight.*

Aspect ratio (length to diameter)	*An optimum fibre aspect ratio is preferred, as the reinforcing efficiency of the fibre is limited at low values. Higher aspect ratios are generally associated with improved tensile and flexural strength of the composite material due to enhanced stress transfer between the fibre and the matrix.*
Moisture absorption	*The material should exhibit low moisture absorption to minimise the risk of crack formation and associated degradation mechanisms.*
Material cost and availability	*Cost is a crucial criterion in material selection, as economic constraints must be carefully considered throughout the design process.*

Table 5.4 Plant-fibre selection criteria (adapted from Mahajanet al., 2022).

Appendix A presents the mechanical properties of the selected plant fibres introduced in Section 3.1.2, in comparison with aluminium alloy 6060-T66. The selection of plant fibres is based on mechanical strength, fibre aspect ratio, moisture content, availability, and cost. Subsequently, an appropriate fibre reinforcement strategy and fibre placement configuration are defined for the experimental phase of this research.

MECHANICAL STRENGTH

A preliminary selection was conducted by excluding fibres that do not satisfy the defined performance criteria for (1) elongation at break, (2) specific strength, and (3) specific modulus in comparison to aluminium.

The following fibres were excluded:

Fruit fibres: All fruit-derived fibres, including coir, oil palm, bagasse, and sabai, were excluded due to their relatively high elongation at break and low specific modulus compared to aluminium.

Leaf fibres: Abaca and sisal fibres were excluded due to their lower specific modulus and elevated moisture absorption.

Seed fibres: Cotton and kapok fibres were excluded because of their insufficient specific modulus in relation to aluminium.

Stalk fibres: Maize, rice, and wheat fibres were excluded due to a combination of low specific modulus, high moisture absorption, and/or insufficient availability of reliable mechanical property data.

Following this initial screening, the following plant fibres remained under consideration for further analysis:

Bastfibres: Flax, hemp, jute, kenaf, ramie, and bamboo
Leaf fibres: Pineapple (pina)

ASPECT RATIO

The fibre aspect ratio, defined as the ratio of fibre length to fibre diameter, is a critical parameter influencing composite performance. A higher aspect ratio generally contributes to improved tensile and flexural strength of the resulting composite material (Mahajan et al., 2022). Longitudinal fibres are preferred as reinforcement in laminate applications due to their high strength and versatility, particularly their ability to provide reinforcement in multiple directions, improve through-thickness properties, and conform to complex geometries during manufacturing (Overend, M., et al. (unpublished).

Accordingly, a high fibre aspect ratio is identified as a critical selection criterion. In this study, fibres are required to exhibit an aspect ratio greater than 250 µm. Based on this requirement, bamboo fibre does not satisfy the defined threshold and is therefore excluded from further consideration.

MOISTURE CONTENT

Moisture absorption is another key parameter, as increased moisture uptake negatively affects the mechanical properties of plant fibres. Therefore, only fibres with a moisture absorption below 10% are considered suitable for this research. Application of this criterion to the previously shortlisted fibres resulted in the exclusion of ramie, and pineapple fibres. Consequently, only flax, hemp,jute and kenaf fibres remain as candidates for further evaluation.

FIBRE AVAILABILITY AND COST

After applying the mechanical strength, aspect ratio, and moisture absorption criteria, the remaining candidate fibres are the bast fibres flax, hemp, jute and kenaf. This outcome is consistent with the literature, as among natural fibres, hemp, jute, flax, kenaf, sisal, and bamboo are generally recognised as the most promising reinforcements for structural applications due to their high cellulose content, favourable strength-to-weight ratios, and

biodegradability (Belaguli Mahesh et al., 2026).

From this selection, kenaf fibre is only available as separate fibres, which limits reinforcement possibilities compared to flax (linen), hemp fibres and jute fibres which are commercially available in multiple forms, including individual fibres, mats, and woven fabrics. Therefore, kenaf fibre is excluded from further consideration, leaving flax, hemp and jute as the primary candidate bast fibres.

Although flax is generally associated with a higher cost than hemp- or jute fibre, this difference is strongly dependent on the reinforcement form and processing route. Consequently, cost alone is not considered a sufficient criterion to exclude either fibre at this stage of the selection process.

FIBRE REINFORCEMENT SELECTION

Table 5.5 illustrates the different reinforcement types of natural fibres. Discrete fibres present challenges in achieving a uniform fibre distribution, which can significantly reduce the reinforcing efficiency of natural fibre composites and limit their suitability for structural applications (Arumugam et al., 2022). In addition, the literature indicates that discrete fibre systems generally exhibit substantially lower mechanical performance compared to continuous fibre reinforcements or woven fabric architectures. As higher strength is required for structural façade applications, discrete fibre reinforcements are excluded from further consideration.

Integrated three-dimensional (3D) woven preforms as illustrated in figure 5.1, provide the highest mechanical performance. However, they are also associated with high production costs and require specialised manufacturing equipment. Consequently, they are deemed unsuitable for this research due to budgetary constraints and the absence of dedicated processing facilities. Accordingly, linear and laminar reinforcement systems are considered more appropriate for the intended structural application. Woven reinforcement systems are particularly suitable due to their interlocking architecture, which enhances structural integrity, fibre–matrix adhesion, and overall mechanical performance compared to non-woven alternatives. The selection of a specific weave architecture is dependent on end-use requirements, including multi-directional mechanical performance (e.g., strength, stiffness, and fracture toughness), durability, and aesthetic considerations (Overend, M., et al. (unpublished). Furthermore, 2D woven preforms are readily available from commercial suppliers, thereby reducing the need for specialised manufacturing equipment.

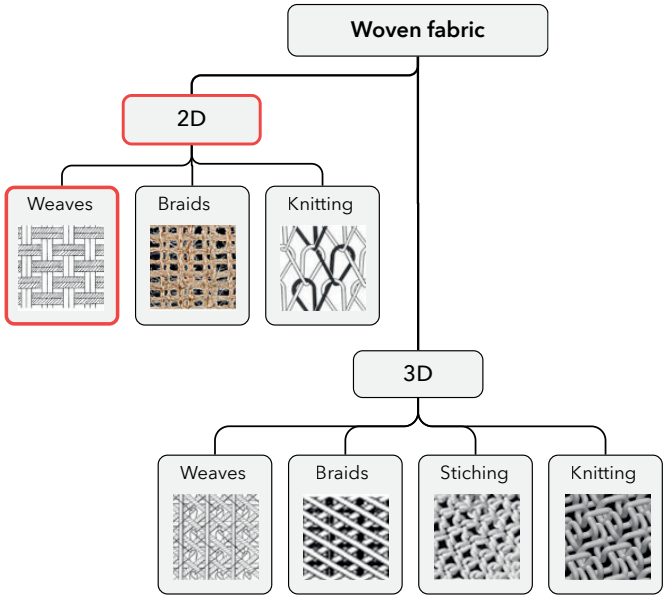

Fig. 5.1 Selection of composite fabric reinforcements and preforms for experimental phase (adapted from Fan & Weclawski, 2017).

For structural applications where extreme strength, such as that required in aerospace or primary load-

LEVEL	REINFORCEMENT	ARCHITECTURE	ARRANGEMENT	ORIENTATION	ENTANGLEMENT
1	*Discrete*	*Chopped fibres*	*Discontinuous*	*Uncontrolled (2D)*	*None*
2	*Linear*	*Filaments*	*Continuous*	*Linear (2D)*	*None*
3	*Laminar*	*Simple fabric*	*Continuous*	*Planar (2D)*	*Planar*
4	*Integrated*	*Advanced fabric*	*Continuous*	*3D*	*3D*

Table 5.5 Fibre arrangement (adapted from Hu, 2008, Ciobanu, 2011 and cho&Jo, 1980).

bearing structural elements in buildings, is not necessary, non-woven mats may also be considered. These mats consist of unidirectional short fibres and are compatible with common laminating processes, including hand lay-up, vacuum bagging, and resin infusion (EasyComposites Europe, 2025).

For this study, three types of fibre reinforcements will be used in the experimental phase as illiustrated in the diagram in figure 5.2: long continuous fibres, non-woven mats composed of short unidirectional fibres, and 2D woven fabrics consisting of long woven fibres.

FIBRE PLACEMENT SELECTION

Figure 5.2 presents a schematic overview of composite constituent materials and their associated manufacturing routes. Based on this diagram, it can be concluded that the use of a thermoset resin in combination with long continuous fibres, non-woven mats, or woven fabrics enables fibre placement through several manufacturing techniques, including hand or automated lay-up, filament winding, and pultrusion.

However, among the available options, pultrusion and filament winding requires expensive and specialised equipment and is therefore excluded from the experimental phase due to practical and financial constraints.

Consequently, the fibre placement techniques applied in the experimental phase are limited to hand or auto lay-up.

5.2.3 COMPOSITE MANUFACTURING TECHNIQUE SELECTION

In the context of composite manufacturing, several techniques such as compression moulding, extrusion moulding, injection moulding, and resin transfer moulding are commonly applied, each offering specific advantages for shaping natural-fibre composites into functional components (Shelly et al., 2025). In addition, the selected thermoset resin enables the use of advanced closed-mould processes, such as Resin Transfer Moulding (RTM), which offer reduced environmental impact during processing while still allowing high reinforcement content and improved mechanical performance (Di Landro & Janszen, 2014). Figure 5.2 illustrates the range of manufacturing processes applicable when using a thermoset epoxy resin in combination with long continuous fibres, non-woven mats, woven fabrics, and hand lay-up fibre placement.

Among the thermoset manufacturing processes considered, autoclave curing and RTM are the only methods that require costly machinery and tooling that are not available within the scope of this project (see manufacturing technique comparison in Appendix C). Although lower pressure levels are applied, the combination of vacuum bagging and oven curing can achieve comparable results to autoclave processing in terms of consolidation and mechanical performance.

Vacuum-Assisted Resin Transfer Moulding (VARTM) is a variation of conventional RTM that utilises

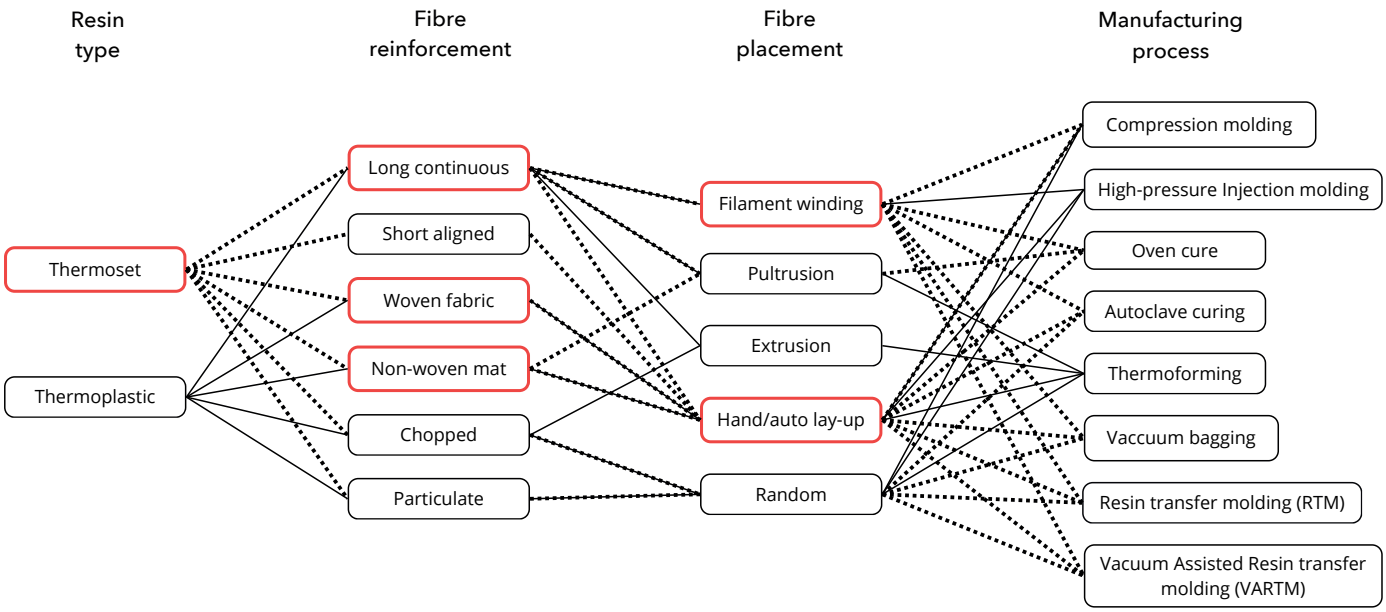

Fig. 5.2 Composite constituent materials and manufacturing options: fibre placement selection (adapted from Peters, 2013, modified).

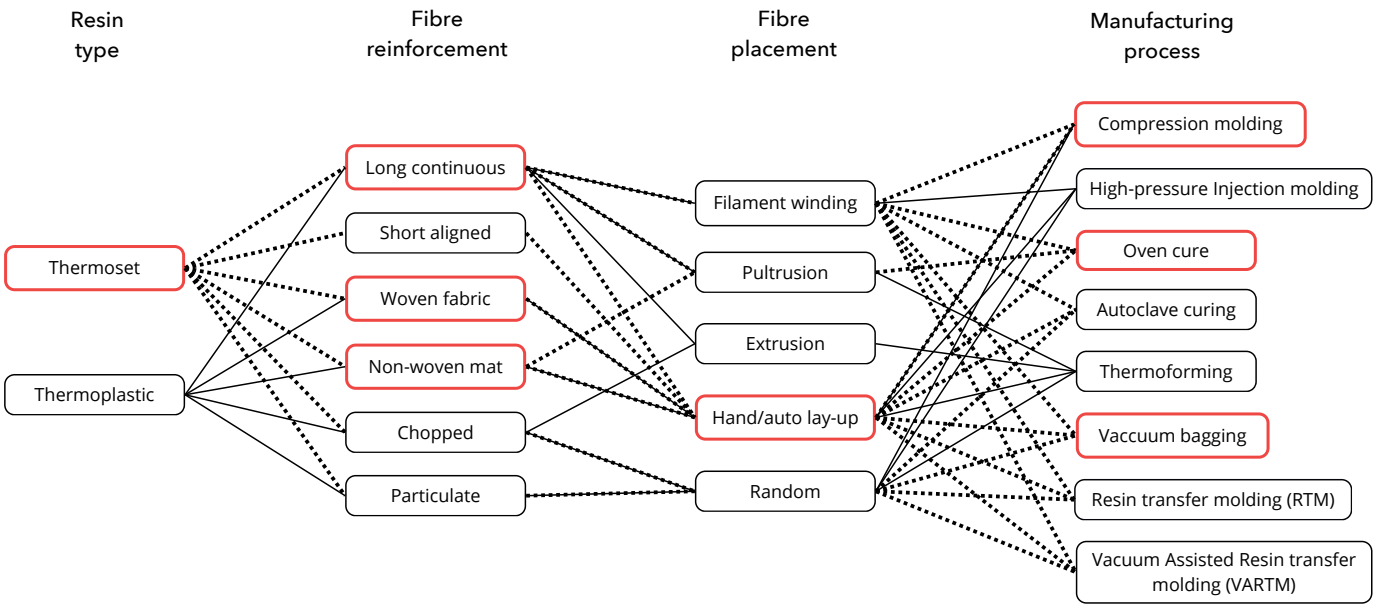

Fig. 5.3 Composite constituent materials and manufacturing options: manufacturing process selection (adapted from Peters, 2013, modified).

less expensive equipment and mould materials. Although this method is technically available, its main disadvantages include the requirement for precisely manufactured internal and external moulds and a reduced level of manual control during processing, as the outcome is highly dependent on resin flow behaviour.

Therefore, for the fabrication of complex profile geometries using hand or automated lay-up or filament winding fibre placement, the following manufacturing processes are selected for the experimental phase: vacuum bagging, compression moulding, and oven curing (figure 5.3). These techniques provide external pressure during curing and enable the production of surfaces with minimal porosity. In addition, improved fibre-to-resin ratios can be achieved through the application of external compression during curing. Oven curing may be applied to accelerate the curing process when required.

A key focus during processing is the successful demoulding of the cured composite. The use of an appropriate release agent is therefore essential to ensure clean separation from the mould without damaging the final component.

5.3 PROFILE GEOMETRY SELECTION

This section discusses the selected mullion profile geometry to be manufactured in the experimental phase. In addition, the dimensions of an aluminium profile are calculated for a curtain wall section with a height of 3 m and a width of 1.5 m, in order to enable a comparison between the structural performance of the resulting plant-fibre composite profile and the reference aluminium system at the end of this study.

SELECTION OF MULION PROFILE GEOMETRY

For this study, a rectangular hollow section (RHS) mullion profile is selected as the representative geometry for the plant-fibre composite profiles (Figure 5.4). Transom profiles, as well as I-section and H-section geometries, are excluded from the selection, as these sections are less commonly applied in standard façade systems.

In addition, the fabrication of a rectangular hollow section requires the use of a removable internal mould, which introduces an additional level of complexity during the manufacturing process.

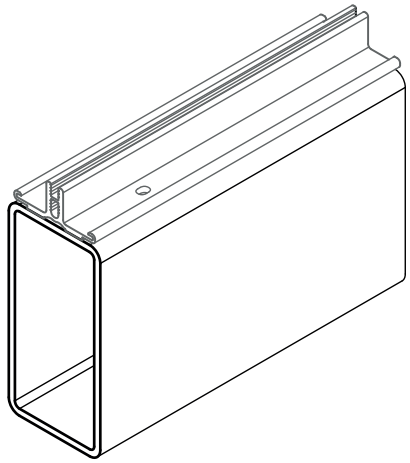

Fig. 5.4 Rectangular hollow section (STABALUX, 2025).

PROFILE GEOMETRY CALCULATION

To enable a comparison between the developed plant-fibre composite profiles and conventional aluminium profiles, the dimensions of the mullion system are calculated for a curtain wall section with a height of 3 m and a width of 1.5 m. This implies that the vertical mullion has a length of 3 m. The wind load acting on a vertical mullion is illustrated in Figure 5.5.

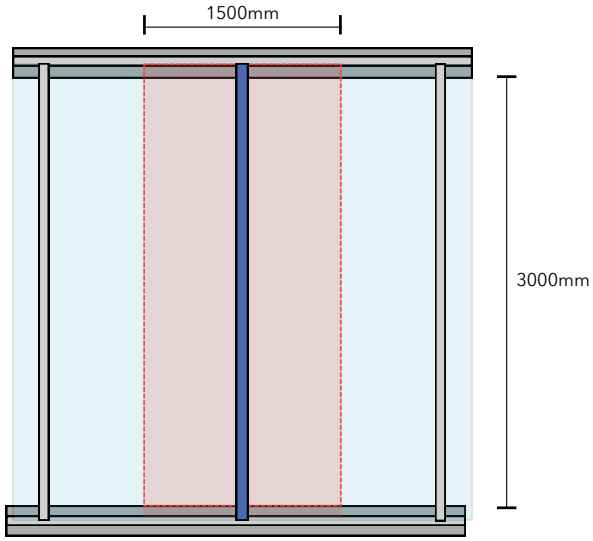

Fig. 5.5 Windload area on vertical mullion (own image).

In this configuration, the vertical mullions transfer wind loads to the primary load-bearing structure of the building and also support their own self-weight.

To determine the required mullion profile geometry for this curtain wall façade section, a calculation has been performed to establish the moment of inertia required for the mullions to resist wind loads and support the self-weight of the glazing system.

For this calculation, the following boundary conditions are assumed for the rectangular hollow section, as presented in Table 5.6:

PROPERTY	VALUE
Support type	*Fixed connections on top and bottom with brackets to the load-bearing structure.*
Length mullion	*3m*
Tributary width mullion	*1.5m*
Loads	*- Windforce (2kN/m²)* *- Self-weight (minor, but included)*
Max deflection	*15 mm*
Width of mullion profile	*50 mm*
Thickness profile	*4 mm*

Table 5.6 Curtain wall square hollow section properties (Intertek, 2024)

For this calculation, the following material properties of aluminum are assumed for the rectangular hollow section, as presented in Table 5.7:

PROPERTY	VALUE
Aluminum alloy	*EN AW-6060 T66*
E-modulus	*70,000 N/mm²*
Yield strength	$f_{y,k}$ *= 160 N/mm²*

Table 5.7 Aluminum EN AW-6060 T66 material properties (Makeitfrom, 2020)

CALCULATION RECTANGULAR HOLLOW SECTION

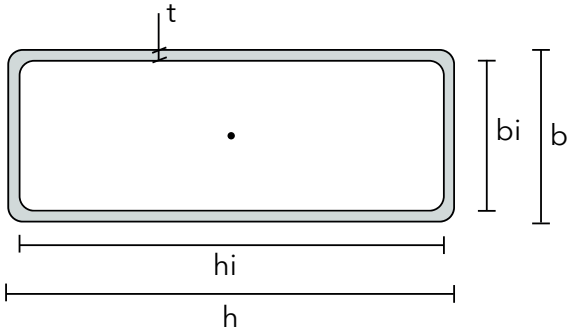

Fig. 5.6 Profile geometry of rectangular hollow section (own image).

Wind load on mullion:
$q = 2.0\ kN/m^2$
Tributary width per mullion:
$b=1.5m$

Line load on mullion:
$w = q \times b = 2.0 \cdot 1.5 = 3.0\ kN/m$

Beam length: $L = 3.0\ m$
Load: uniformly distributed
Support: fixed–fixed

Maximum bending moment:
$M_{max} = wL^2 / 12 = (3.0 \cdot 3.0^2) / 12 = 2.25\ kNm$

Deflection check (according to DIN EN 13116):
$w = 3.0\ N/mm$
$L = 3000\ mm$
$E = 70{,}000\ N/mm^2$
$\delta = 15\ mm$

$\delta_{max} = wL^4 / 185\ EI$
$I_{req} = wL^4 / 185E\delta$
$I_{req} = (3.0 \cdot 3000^4) / (185 \cdot 70{,}000 \cdot 15) \approx 1.25 \cdot 10^6\ mm^4$

Second moment of inertia of a rectangular hollow section:
$I_x = (b \cdot h^3 - b_i \cdot h_i^3) / 12$

Inner width: $b_i = b - 2t$
Inner heigth: $h_i = h - 2t$

$b_i = 50 - 2(4) = 42mm$
$h_i = h - 8$
$I_x = (50 \cdot h^3 - 42(h-8)^3 / 12$
$1.25 \cdot 10^6 = (50 \cdot h^3 - 42(h-8)^3 / 12$

Solving this equation yields a required profile height of approximately h ≈ 96 mm. As this does not correspond to a standardised or commonly available profile dimension, a practical profile depth of 100 mm is adopted.

Final profile dimensions: 50 × 100 × 4 mm

Strength (yield) check:
$I_x = 1.25 \cdot 10^6\ mm^4$
$M_{max} = 2.25\ kNm$

Maximum bending stress:
$y_{max} = h / 2 = 100 / 2 = 50\ mm$
$\sigma_{max} = (M_{max} \cdot y_{max}) / I_x$
$\sigma_{max} = (2.25 \cdot 10^6 \cdot 50) / (1.25 \cdot 10^6) \approx 90\ N/mm^2$
$fy = 160\ N/mm^2$ --> *strength OK (≈ 0.56 utilization)*

Factor of safety ≈ 2.0

5.4 TESTING METHODS AND STANDARDS

To enable a comparison between the manufactured plant-fibre composite and the selected properties of the aluminium alloy, as well as the relevant EU building codes for curtain wall systems outlined in Section 5.1, a series of mechanical tests must be conducted on the produced profiles. These tests are intended to evaluate both the mechanical performance and durability of the plant-fibre composite and the proposed profile geometry.

The following mechanical properties will be assessed on the initial samples and geometries:

- Ultimate tensile strength
- Flexural strength
- Thermal stability
- Fastener fixation capacity

For the final specimens and profile geometries, the following tests will be conducted:

- Ultimate tensile strength
- Flexural strength
- Connection performance with other curtain wall system components

All specimens will be tested in accordance with the following ISO standards:

- ISO 527-5:2021(E). "Determination of tensile properties – Test conditions for unidirectional fibre-reinforced plastic composites"
- ISO 14125: "Fibrereinforced plastic composites – Determination of flexural properties".
- ISO 1268 Part 5: Fibre-reinforced plastics - Methods of producing test plate- Filament winding.

Although the relevant standards specify a minimum of five specimens per mechanical test, this study will employ a reduced sample size of three specimens per test due to limitations in time and material availability. Prior to mechanical testing, the density of each specimen will be determined with precision.

The applied mechanical testing procedures are further described in the following sections.

DENSITY

The density of composite laminates can be calculated in a simple way by the formula below.

$$\rho_c = m_{c,dry} / V_{c,\,dry}$$

Where ρ_c is the density of the plant-fibre composite laminates. $m_{c,dry}$ is the weight of specimens at dry state and $V_{c,\,dry}$ is the correspondent volume of the rectangular specimens (Jia Y. ,2020). The density of each specimen is measured prior to every mechanical testing procedure to ensure accurate and consistent results.

FIBRE VOLUME FRACTION

The fibre volume fraction is determined to quantify the relative proportion of reinforcement within the composite laminate. This parameter is essential for comparing mechanical performance between specimens and for assessing manufacturing consistency. The fibre volume fraction can be estimated using the relation:

$$V_f = (m_f / \rho_f) / ((m_f / \rho_f) + (m_r / \rho_r))$$

Where m_f and m_r are the masses of fibre and resin respectively, and ρ_f and ρ_r are their corresponding densities.

TENSILE TESTING

Mullions are primarily responsible for supporting the weight of transoms, glazing panels, and their own self-weight, as they are suspended vertically from the building's primary structural system. Consequently, high tensile strength is required to ensure that the mullions can safely resist these vertical loads without failure.

Tensile testing will be performed to determine the tensile strength of the specimens. In addition, the yield strength will be evaluated. The strain at break is used as an indicator of ductility and fibre–matrix adhesion within the composite system. A higher strain at break generally reflects improved load transfer between the plant fibres and the epoxy matrix and provides insight into the overall toughness of the composite material.

Figure 5.7 illustrates a schematic representation of the tensile test setup.

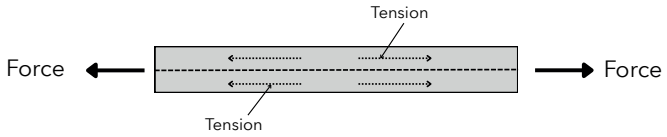

Fig. 5.7 Three-point bending test schematic (own image)

Tensile tests will be conducted using a 100 kN universal testing machine located at the Faculty of Mechanical Engineering under the supervision.

THREE-POINT BENDING TEST

In addition to vertical loading, mullions are required to transfer horizontal wind loads to the building's primary load-bearing structure. These loads induce bending stresses along the length of the profiles. The maximum allowable deflection under such conditions is predefined (see Table 5.1). Ensuring sufficient bending stiffness and strength is therefore essential to prevent excessive deflection and potential structural failure.

To evaluate the bending performance of the profiles, three-point bending tests will be conducted. From these tests, the flexural strength, strain at break, and Young's modulus can be determined based on the resulting stress–strain response. Figure 5.8 illustrates a schematic representation of the three-point bending test, in which the load is applied at the midpoint of the specimen.

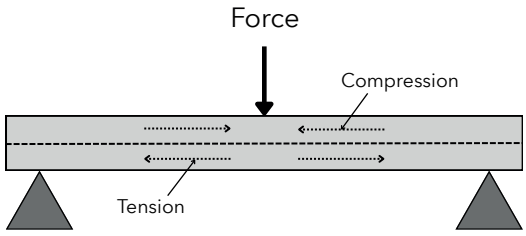

Fig. 5.8 Three-point bending test schematic (own image)

The three-point bending tests will be performed using a 100 kN universal testing machine located at the Faculty of Mechanical Engineering under the supervision.

THERMAL EXPANSION TEST

To enable comparison of the thermal stability of the plant-fibre composite with aluminium, a thermal expansion test will be conducted using the Heraeus oven at the Faculty of Architecture and the Built Environment at TU Delft.

Thermal expansion is determined by measuring the dimensions of a specimen at room temperature using a precision caliper. The specimen is subsequently heated in an oven to 100 °C, after which its dimensions are measured again using the same precision caliper.

From the resulting measurements, the themal expansion coefficient (*α)* can be calculated using the following formula:

$dl = L_0 * \alpha (\Delta T)$

Where:
dl = change in object length (m)
L_0 *= initial length of the sample (m)*
α = linear exapansion coefficient (m/m°C)
ΔT = change in temperature (°C)

TESTING FASTENER FIXATION CAPACITY
In addition to the mechanical testing of the composite material, the connection between the aluminium curtain wall profiles and the plant-fibre composite mullions must also be evaluated. In conventional systems, these profiles are typically connected by means of screw fastenings into steel, aluminium, or timber mullions and transoms.

To assess the performance of these connections, tests will be conducted to determine the load-bearing capacity of different fasteners installed in the manufactured plant-fibre composite profiles. The connected components will subsequently be subjected to tensile loading until separation occurs, in order to evaluate the connection strength and failure behaviour.

5.5 SUMMARY OF MATERIAL AND GEOMETRY SELECTION

Table 5.8 presents the results of the material selection process.

PROPERTY	SELECTION
Polymer matrix	*- a low viscosity two-component epoxy resin (epoxy + hardener)*
Plant-fibre	*Hemp fibre, flax fibre and jute fibre*
Fibre reinforcement	*Linear / laminar*
Fibre arrangement	*- Long continuous fibres* *- Non-woven mat (short unidirectional fibres)* *- woven cloth*
Fibre placement	*- Hand/ auto lay-up*
Manufacturing process	*- Compression molding* *- Vacuum bagging* *- Oven curing*
Testing methods	*- Tensile testing* *- Three-point bending test* *- Thermal expansion test* *- Fastener fixation capacity*

Table 5.7 Result of chapter 5: material selection (own work)

6. EXPERIMENTAL PHASE 1: INITIAL MANUFACTURING TRIALS

6. EXPERIMENTAL PHASE 1: INITIAL MANUFACTURING TRIALS

This chapter presents the materials and equipment used in the initial experimental phase of the study. In addition, the preliminary experimental work is described, in which different fibre materials, fibre lay-ups, and manufacturing techniques are investigated with the aim of producing a rectangular hollow section profile.

The results of these trials are evaluated to determine their suitability for further development. Furthermore, selected samples are examined using microscopy to assess fibre–matrix bonding quality, fibre distribution within the matrix, and overall surface characteristics. Based on the outcomes of these initial experiments, the most suitable fibre material, reinforcement configuration, and manufacturing method are identified. These findings form the basis for the second experimental phase, in which the first mechanical testing of the optimised composite profiles is conducted.

6.1 MATERIALS AND EQUIPMENT

Table 6.0 presents the fibre reinforcement configurations selected for the first experimental phase:

FIBRE REINFORCEMENT	PRODUCT
Long continuous fibres	*Flax fibre yarn on a spool*
Non-woven mat	*Short, undirectional hemp fibres from EcoTechnilin processed into a non-woven mat.*
Cross-stitched woven cloth	*A flax cross-stitched woven cloth from EcoTechnilin (long, unidirectional fibres)*
Plain woven cloth	*A jute plain woven cloth (long, plain woven fibres) from natuurlijkjute.nl*

Table 6.0 Selected fibre materials for experimental phase 1 (own table)

LONG CONTINUOUS FLAX FIBRES

Figure 6.0 illustrates the flax fibre yarn selected for use in the experimental phase. This reinforcement consists of long continuous flax fibres wound onto a spool. The yarn has an approximate thickness of 0.1 mm and a width of 10 mm, making it suitable for application through a manufacturing approach comparable to filament winding.

Fig. 6.0 Long continuous flax fibre yarn on a spool (own image)

NON-WOVEN HEMP FIBRE MAT

Figure 6.1 illustrates the 150 g non-woven hemp fibre mat supplied by Eco-Technilin, which is selected for use in the first experimental phase. This relatively low-cost material is compatible with a wide range of laminating processes, including hand lay-up, vacuum bagging, and resin transfer techniques.

The non-woven hemp fibre mat is naturally sourced in a manner comparable to flax fibres and can be applied in many similar applications (EasyComposites, 2025).

Fig. 6.1 Non-woven hemp fibre mat from Eco-Technilin (Easycomposites, 2025)

The technical specifications of the non-woven hemp fibre mat supplied by Eco-Technilin were obtained from the product datasheet available on the supplier's website. The corresponding material properties are presented in Table 6.1.

PROPERTY	VALUES
Nature of product	*Non-woven mat*
Nature/proportion/ quality of fibres	*Short fibres of European hemp*
Consolidation method	*Exclusive consolidation process*
Moisture content	*≈ 9 %*
Fibre density	*1.45 g/cm³*
Tensile strength	*≈ 46-108 MPa*
Young's Modulus	*≈ 6-11 GPA*
Elongation at break	*≈ 1.5 %*
Thickness of 1 impregnated ply	*0.29 mm*
Additional information	*Store dry and avoid direct sunlight*
Manufacture methods	*Infusion, VARTM, thermo compression, hand lay-up and more.*

Table 6.1 FIBRILIGHT-F150 technical data *(Easycomposites, 2025)*

CROSS-STITCHED FLAX FIBRE CLOTH

For the woven reinforcement, a cross-stitched flax fibre fabric is selected for use in the first experimental phase. Cross-stitched fabrics provide particularly high strength in a preferred direction and can be combined with additional woven layers or identical fabrics to achieve the desired fibre orientation. Another reason for selecting this reinforcement is its relatively low thickness, which facilitates the manufacturing of complex geometries with sharp corners and pronounced angles.

A disadvantage of this material is its higher cost compared to the non-woven hemp mat. Figure 6.2 illustrates the 180 g cross-stitched unidirectional flax fibre reinforcement supplied by Eco-Technilin. The fully unidirectional construction of this material results in a highly dense reinforcement architecture, which may lead to slower resin infusion compared to conventional woven alternatives (EasyComposites, 2025).

Fig. 6.2 Cross-stiched flax fibre cloth obtained from Easycomposites.nl (Easycomposites, 2025)

The technical specifications of the non-woven hemp fibre mat supplied by Eco-Technilin were obtained from the product datasheet available on the supplier's website. The corresponding material properties are presented in Table 6.2.

PROPERTY	VALUES
Nature of product	*Cross-stiched flax fibre*
Nature/proportion/ quality of fibres	*100% european flax from Normandy region, France*
Consolidation method	*Exclusive consolidation process*
Moisture content	*≈ 9 %*
Fibre density	*1.45 g/cm³*
Tensile strength	*≈ 255 MPa (warp direction)*
Young's Modulus	*≈ 23 GPA (warp direction)*
Elongation at break	*≈ 2 %*
Thickness of 1 impregnated ply	*0.36 mm*
Additional information	*Store dry and avoid direct sunlight*
Manufacture methods	*Infusion, VARTM, thermo-compression, hand lay-up and more.*

Table 6.2 FLAXDRY-UD180 technical data *(Easycomposites, 2025)*

JUTE PLAIN WOVEN CLOTH

As a plain woven reinforcement, a 366 g/m² jute woven fabric supplied by Natuurlijkjute.nl is selected for use in the first experimental phase, as shown in Figure 6.3.

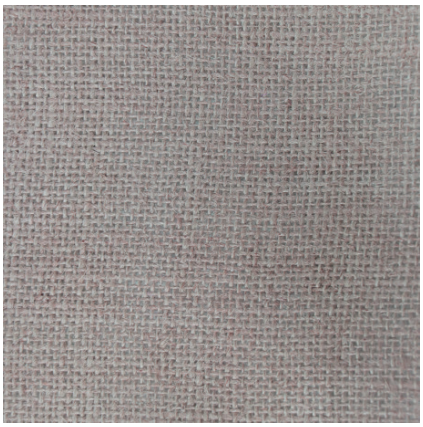

Fig. 6.3 Jute plain woven cloth obtained from natuurlijkjute.nl (Natuurlijkjute, 2025)

The fabric has an approximate thickness of 0.6 mm and a width of 120 cm and can be cut to the required length. However, no detailed technical data is available for this material, as it is primarily intended for decorative applications rather than engineered structural use.

LOW VISCOSITY 2-COMPONENT EPOXY RESIN

The epoxy resin used for the experiments is the EL2 epoxy laminating resin supplied by EasyComposites.nl. This resin is suitable for wet lay-up and vacuum bagging processes. The technical specifications of this laminating epoxy system are presented in Table 6.3 and Table 6.4

PROPERTY	RESIN	HARDENER	COMBINED
Material	*Epoxy resin*	*Formulated Amine*	*Epoxy*
Appearnace	*Clear liquid*	*amber-liquid*	*clear liquid*
Viscosity at 20°C (mPa.s)	*1200 -1800*	*5-80*	*1000-1400*
Density (g/cm^3)	*1.13-1.17*	*0.90 - 1.06*	*1.05 - 1.15*

Table 6.3 EL2 laminating epoxy resin specification *(Easycomposites, 2025)*

In combination with the epoxy resin, a hardener is required to initiate and complete the curing process. The AT30 slow hardener, supplied by EasyComposites, is selected for this study. It has a pot life at 25 °C of approximately 95–115 minutes and a demoulding time at 25 °C of 24–30 hours. The curing duration is dependent on temperature and can be reduced from approximately 24 hours at room temperature to around 6 hours at 60 °C.

The properties of the AT30 slow hardener used in this study are presented in Table 6.4.

PROPERTY	AT30 SLOW
Hardness	*84 - 88 shore D*
Flexural strength	*103 - 117 MPa*
Flexural modulus	*2600 - 3600 MPa*
Tensile strength	*70 - 80 MPa*
Elongation at break	*6 - 10 %*
Linear shrinkage	*0.5 %*
Heat deflection temperature (H.D.T)	*82-88 °C*

Table 6.4 EL2 laminating resin technical data *(Easycomposites, 2025*

MOULD MATERIALS

To manufacture hollow geometries, removable moulds are required for the experimental work. The selected mould materials are readily available and consist of high-density polyethylene (HDPE), aluminium, and PET-G.

To ensure that the epoxy does not adhere to the mould surface during manufacturing, a mould release agent must be applied. For this study, the RW4 High Build Spray Wax release agent supplied by EasyComposites.nl is used. It is essential that the application of the release agent is carried out in a well-ventilated area, using appropriate personal protective equipment (PPE), as the spray may cause skin irritation.

PERSONAL PROTECTIVE EQUIPMENT (PPE)

Working with materials such as epoxy resin and wax spray can cause skin irritation and allergic reactions upon direct contact, as well as adverse health effects through inhalation of vapours. Therefore, all manufacturing activities must be conducted in a well-ventilated area, and appropriate personal protective equipment (PPE) is required throughout the process. The experiments during this project are all conducted in the Thinklab lab at the faculty of Architecture and the Built Environments at TU Delft.

The required PPE includes nitrile gloves, a laboratory coat or disposable coveralls, and safety goggles.

RELEASE FILM AND BREATHER CLOTH

The surface condition of the mould has a direct influence on the final surface finish of the composite material. In other words, the surface quality of the mould is replicated in the outer surface of the cured composite. Therefore, as a final layer prior to the application of compression, different auxiliary materials will be applied to assess their effect on the surface quality of the specimens.

The following materials will be used as the final surface layer:

- A non-perforated transparent polyethylene (PE) cover film
- Peel ply, used to produce a controlled roughened surface finish
- A thin perforated release film to allow excess resin to escape from the specimen during curing

For configurations involving peel ply and perforated release film, a breather cloth will be applied as the outermost layer. This layer serves to absorb excess resin during curing and to protect the vacuum bag from damage.

CURING OF SAMPLES

A portable curing oven is manufactured to enable overnight curing of the specimens at elevated temperatures. A platinum heating mat (35 cm × 55 cm) with an external temperature controller, supplied by GreenTradingXXL.com, is used as the heat source. This heating mat is capable of reaching temperatures up to 50 °C and is placed inside a plastic crate.

The interior walls of the crate are lined with 10 mm thick Styrofoam insulation to minimise heat loss and improve temperature stability. A digital thermometer with an external sensor is used to monitor the actual internal temperature of the system, positioned at a height of 10 cm above the base of the setup.

Figure 6.4 illustrates the constructed portable curing oven used in the first experimental phase.

Fig. 6.4 Portabel curing oven (own image)

ADDITIONAL MATERIALS AND EQUIPMENT

In addition to the natural fibres, epoxy resin, mould materials, personal protective equipment (PPE), release films, and the portable curing oven, several supplementary materials are required for the manufacturing of the specimens. The following materials are used during the fabrication process:

- a digital precision scale (capacity 10kg)
- small cardboard cups to mix resin and hardener
- airtight sealing bags to store the natural fibres and manufactured specimens.
- Vacuum bags (40 x 60cm) which can be put into vacuum with a vacuum cleaner for the vacuum bagging process.
- laminating brushes to apply epoxy resin to fibres
- fabric scissors to cut fibres and fabrics
- sandpaper (multiple different grades)
- wooden mixing sticks to mix resin and hardener

6.2 INITIAL EXPERIMENTS

The first 6 weeks of the experimental phase consist of getting familiar with the materials and manufacturing techniques. In the first week, moulds are obtained of PETG, aluminum and HDPE. The correct resin to fibre proportions are obtained to make sure manufacturing errors will be minimized during the manufacturing of the final specimens for mechanical testing. After 6 weeks, the most promising results will be taken to the next experimental phase to prepare for mechanical testing.

MIXING AND CURING CONSTANTS PHASE 1

The following mixing and curing constantes are used during the first experimental phase to make sure a well- considered comparison can be made between the tested manufacturing processes:

- *An initial fibre to resin ratio of 33% fibre and 66% resin is used as advised on the Easycomposites.nl website.*

- *A resin to hardener ratio of 100/30 by weight is used as advised by the supplier of the epoxy resin.*
- *The fibre material is dried for 2 hours at 60°C in an oven before every manufacturing to drive out most of the excess moisture.*
- *The fibres are cooled down to room temperature for 2 minutes after drying in the oven.*
- *All samples are cured for at least 18 hours at 40°C in the manufactured oven.*
- *After manufacturing, the samples are stored in an airsealed bag to keep the samples dry.*

SPECIMEN 1 AND 2

The first week focused on the collection of materials and the fabrication of internal moulds made from aluminium, PETG, and HDPE. These moulds were sourced from the Faculty of Architecture and the Built Environment at TU Delft and the LAMA-Lab (3D printing laboratory). All moulds were cut to a uniform length of 150 mm. The 3D-printed PETG mould has dimensions of 50 × 50 mm with 90° corners, the aluminium mould is a rectangular hollow section of 60 × 30 × 5 mm with sharp 90° corners, and the HDPE mould measures 50 × 40 mm with rounded corners.

PETG was selected instead of PLA for the 3D-printed mould due to its higher glass transition temperature. PLA begins to deform at approximately 50–60 °C, whereas PETG remains stable up to around 75 °C. This makes PETG suitable for curing processes conducted at temperatures between 40–50 °C.

The first step in each manufacturing process involved cleaning the fibres and cutting them to the required dimensions. The fibres were then dried in an oven at 60 °C for 2 hours to remove excess moisture, as shown in Figure 6.5. A Heraeus UT 12P oven was used for this purpose. Prior to fabrication, the dry fibre mass was measured using a high-precision balance to determine the required epoxy resin content.

Fig.6.5 Drying the fibres for 2hrs at 60 °C (own image)

During fibre drying, the mould surfaces were coated with multiple layers of release agent, applied in intervals of 10–15 minutes between coats. The manufacturing parameters for Specimen 1 and Specimen 2 are summarised in Tables 6.5 and 6.6.

MANUFACTURING PROPERTIES SPECIMEN 1	
Fibre type	*Jute plain woven cloth*
Mould	*PETG (3D-printed, non-sanded) (50 x 50mm)*
Layers of release agent	4
Fibre length	*150cm*
Rotations around mould	*5/0.59 ≈ 8.5*
Fibre weight	*73gr*
Amount of EL2 epoxy laminating resin	*73 x 2 = 146 gr (as advised by the supplier)*
Amount of AT30 slow hardener	*146 x 0.3 = 43.8gr*
Fibre volume fraction (uncut specimen)	*23.3%*
Manufacturing time	*30 minutes*
Weight of specimen	*255gr (including PET-G mould)*
Length of sample	*15 cm*
Thickness of sample	5 - 12 mm

Table 6.5 Fabrication details specimen 1 (own work).

MANUFACTURING PROPERTIES SPECIMEN 2	
Fibre type	*non-woven hemp fibre mat*
Mould	*aluminum (30 x 60 x 3mm)*
Layers of release agent	4

Fibre length	*150cm*
Rotations around mould	*5/0.29 ≈ 8.5*
Fibre weight	*35gr*
Amount of EL2 epoxy laminating resin	*35 x 2 = 70 gr*
Amount of AT30 slow hardener	*70 x 0.3 = 21gr*
Fibre volume fraction (uncut specimen)	*23.3%*
Manufacturing time	*25 minutes*
Weight of sample	*91gr*
Length of sample	*15 cm*
Thickness of sample	3 - 8 mm

Table 6.6 Fabrication details specimen 2 (own work).

MANUFACTURING OF SPECIMEN 1 AND 2

Both specimens were manufactured by wrapping fibre reinforcements around PETG and aluminium moulds. This method was selected as a first approach, as it resembles a filament winding process commonly used for tubular composite structures. A key challenge in this process was achieving sufficient fibre tension and uniform wrapping, particularly around sharp corners.

Initially, a thin layer of epoxy resin was applied to the mould surface. The jute woven fabric (Specimen 1) and the non-woven hemp mat (Specimen 2) were then manually wrapped around the respective moulds. During each rotation, a thin layer of epoxy was applied using a laminating brush to ensure impregnation.

As a final surface layer, a non-perforated 60 µm polyethylene (PE) film was applied to protect the vacuum bag from epoxy contamination during curing.

External compression was applied using a small 3 L vacuum bag connected to a manual vacuum pump. The specimens were then cured overnight in a portable curing oven at 40 °C for approximately 18 hours.

DEMOULDING OF SPECIMEN 1 AND 2

Specimen 1 could not be successfully demoulded. The applied vacuum caused the jute fabric and epoxy to bond strongly around the edges of the PETG mould. As a result, the composite had to be cut at the mould boundaries, which compromised clean release. In addition, the PETG mould did not allow sufficient mechanical force for extraction without damage. Figure 6.6 shows the uncut and cut cross-sections of Specimen 1.

Fig. 6.6 Uncut view (left) and cutted cross section (right) of sample 1 (own image)

The final result of Specimen 1 is shown in Figure 6.7.

Fig. 6.7 Result sample 1 (own image)

Specimen 2 also required cutting at the mould edge to facilitate removal. Figure 6.8 shows the uncut and cut cross-sections of Specimen 2.

Fig. 6.8 Uncut view (left) and cutted cross section (right) of sample 2 (own image)

Using a hammer and chisel, the specimen was successfully separated from the aluminium mould. The final specimen is shown in Figure 6.9, while Figure 6.10 presents the cross-section.

Fig. 6.9. Result specimen 2 (own image)

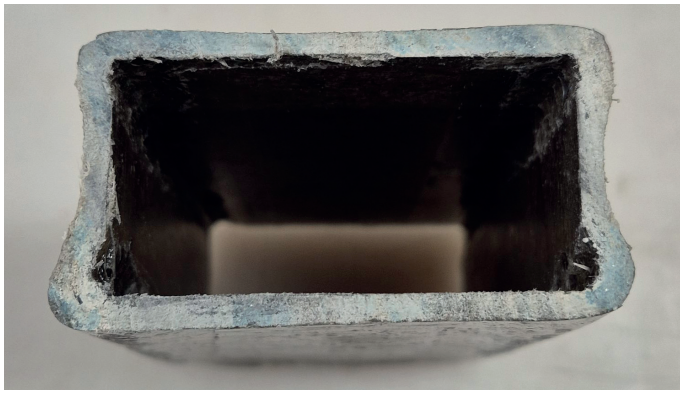

Fig. 6.10 Cross-section of specimen 2 (own image)

The thickness of Specimen 2 varies between 3–5 mm along straight sections and 4–8 mm at the corners. A notable observation is the accumulation of fibres in the corner regions.

EVALUATION OF SPECIMEN 1 AND 2

The roll-wrapping of jute woven fabric around the PETG mould proved difficult due to its thickness, particularly at 90° corners. In contrast, the thinner non-woven hemp mat (0.29 mm) conformed more effectively to the mould geometry, indicating that sharper corners are feasible when using thinner reinforcements. Future work should therefore investigate finer fibre systems, such as yarn-based reinforcements. As corners may act as stress concentration zones, subsequent specimens will also incorporate slightly rounded geometries, with mechanical testing used to evaluate their influence.

Applying epoxy during rotation of the mould was challenging, as fibre slippage occurred and resin spillage was observed. Improved fibre fixation is therefore required to maintain uniform tension during manufacturing. The use of a non-stick polyethylene (PE) tape is proposed to stabilise the fibre position.

The fibre-to-resin ratio was generally acceptable; however, the non-woven hemp mat exhibited higher resin absorption compared to the woven fabric.

The vacuum bagging system provided a low-cost compression method but did not achieve fully uniform consolidation. Limited vacuum efficiency was further affected by residual moisture in the fibres and resin system. The PE cover film successfully protected the vacuum bag but resulted in resin accumulation and limited resin drainage.

Curing in the portable oven was generally effective. Although the target temperature was 40 °C, the internal temperature dropped to approximately 32 °C overnight due to ambient conditions. Future curing will be conducted at 50 °C to improve consistency. A temporary temperature increase was observed after placement in the oven, consistent with the exothermic nature of epoxy curing.

Demoulding proved to be a major limitation. PETG mould removal resulted in damage to both mould and composite, while aluminium mould extraction required high force and caused edge damage. These results indicate that smoother mould surfaces and improved release strategies are necessary. Increasing the number of release agent layers is therefore recommended.

Furthermore, PETG is deemed unsuitable for future experiments due to its low mechanical resistance during demoulding.

SURFACE QUALITY ASSESSMENT

For both specimens, the non-perforated PE cover film prevented air and excess resin from escaping during curing. This resulted in a thick outer resin-rich layer containing small air bubbles and local fibre accumulation, as shown in Figures 6.11 and 6.12.

Fig. 6.11 Close-up of the surface of sample 1 (own image)

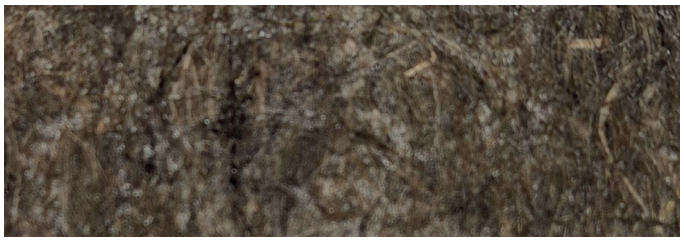

Fig. 6.12 Surface quality of sample 2 (own image)

These defects can be mitigated by replacing the PE film with a peel ply or perforated release film to allow resin bleed and controlled surface roughness. In addition, the use of a breather cloth is recommended to absorb excess resin and protect the vacuum bag from contamination.

SPECIMEN 3 AND 4

The roll wrapping manufacturing technique and vacuum bagging was tested further to improve the results of specimen 1 and 2. The following changes are made to the manufacturing process to improve the results of the samples:

- 6 rounds of release agent will be applied to the moulds every 15 minutes instead of 4 rounds every 10 minutes.
- HDPE will be used with rounded corners as internal moulds for the next samples. This material is easier to manipulate with low-budget tools compared to aluminum.
- The fibres are cut better to size
- The mould is placed in a stationary vicebench to avoid hand-turning the mould causing resin spillage.
- The fibres will be attached to the mould with non-stick PVC tape to avoid slipping of the fibres while applying the epoxy resin with a brush.
- A thinner woven cloth will be used to avoid heavy accumulation of fibres in the corners.
- A perforated release foil is applied around the sample for air to escape from the samples during the vacuum bagging process.
- A breather cloth will be added as a final layer to catch excess resin escaping from the samples and protect the vacuum bag from resin.

Table 6.7 and table 6.8 display the manufacturing properties of specimen 3 and 4.

MANUFACTURING PROPERTIES SPECIMEN 3	
Fibre type	*Cross-stiched flax fibre cloth*
Mould	*HDPE (rounded corners) (50 x 40mm)*
Layers of release agent	*6*
Fibre length	*240cm x 15cm*
Rotations around mould	*5/0.36 ≈ 13*
Fibre weight	*72gr*
Amount of EL2 epoxy laminating resin	*72 x 2 = 144gr*
Amount of AT30 slow hardene	*144 x 0.3 ≈ 43gr*
Fibre volume fraction (uncut specimen)	*23.3%*
Manufacturing time	*30 minutes*
Weight of sample	*127gr*
Length of sample	*11.5 cm*
Thickness of sample	*5 - 8mm*

Table 6.7 Fabrication details specimen 3 (own work).

MANUFACTURING PROPERTIES SPECIMEN 4	
Fibre type	*Non-woven hemp fibre mat*
Mould	*HDPE (rounded corners) (50 x 40mm)*
Layers of release agent	*6*
Fibre length	*150cm x 15cm*
Rotations around mould	*3/0.29 ≈13*
Fibre weight	*35gr*
Amount of EL2 epoxy laminating resin	*35 x 2 = 70 gr*
Amount of AT30 slow hardener	*70 x 0.3 = 21 gr*
Fibre volume fraction (uncut specimen)	*23.3%*
Manufacturing time	*25 minutes*
Weight of sample	*73gr*
Length of sample	*13.5cm*
Thickness of sample	*2.3 - 3.5mm*

Table 6.8 Fabrication details specimen 4 (own work).

MANUFACTURING OF SAMPLE 3 AND 4

The HDPE mould was fixed in a portable vice bench, as shown in Figure 6.13.

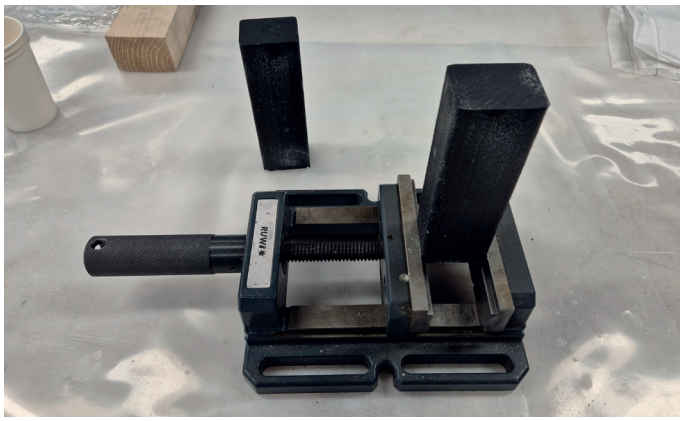

Fig. 6.13 HDPE mould clamped in a portable vice bench (own image)

The fibres were secured using yellow PVC tape before being wrapped around the HDPE mould. During wrapping, a thin layer of epoxy resin was applied with a brush after each fibre layer until the final reinforcement layer was completed.

A peel ply was applied as the second-to-last layer, followed by a breather cloth wrapped around the specimen to absorb excess resin. The assembly was then placed inside a vacuum bag, evacuated using a vacuum cleaner, and cured overnight in a heated thermobox at 45 °C.

The vacuum level was checked two hours after manufacturing and remained sufficient. At this point, the oven temperature was 37 °C. A second inspection was carried out after four hours; additional vacuum was applied using a vacuum cleaner, and the temperature had increased to 42 °C.

DEMOULDING OF SPECIMEN 3 AND 4

Specimens 3 and 4 were demoulded after 18 hours of curing. Compared to the first manufacturing series (Week 7), demoulding was easier due to the presence of peel ply, which improved release behaviour. The HDPE mould was removed using controlled force with a hammer.

In both specimens, the breather cloth was fully saturated with epoxy resin, as shown in Figure 6.14.

Fig. 6.14 Specimen 4 and 5 before demoulding (own image)

Figure 6.15 shows the demoulded cross-stitched flax fibre specimen manufactured using filament wrapping, vacuum bagging, peel ply, and breather cloth, cured in the heated thermobox. Figure 6.16 presents the final result of Specimen 3..

Fig. 6.15 Result of sample 3 using vacuum bagging, a peel-ply and a breather cloth (own image)

Figure 6.16 presents the final result of Specimen 4.

Fig. 6.16 Result specimen 4 using vacuum bagging, a peel-ply and a breather cloth (own image)

EVALUATION OF SPECIMEN 3 AND 4

Clamping the mould in a portable vice bench proved more effective than manual rotation; however, further improvement is required to achieve a more uniform and tighter fibre wrap. The yellow PVC tape was insufficient to fully secure the cross-stitched flax fabric and non-woven hemp mat, as the waxed mould surface reduced adhesion. Nevertheless, improved fibre compaction was achieved compared to earlier specimens due to the lower reinforcement thickness. Specimen 4

showed that achieving a tight wrap with the non-woven mat remains difficult, as the short fibres tend to loosen during processing.

Local fibre detachment was observed at the edges of the cross-stitched fabric, requiring post-trimming. The use of peel ply and breather cloth improved resin distribution and surface consistency. However, complete saturation of the breather cloth indicated excessive resin use, with resin leakage into the vacuum bag. Removal of the saturated layers was difficult and required progressive cutting until the peel ply was exposed. Future specimens should therefore use a reduced resin quantity to prevent oversaturation and improve demoulding efficiency.

The curing process remained stable and consistent with previous specimens, resulting in full curing after approximately 18 hours. Vacuum levels were monitored periodically and adjusted where necessary.

SURFACE QUALITY ASSESSMENT

Both specimens exhibit a rough, matte surface finish. The peel ply effectively facilitated resin bleed and air evacuation, resulting in improved fibre–resin distribution and reduced surface resin accumulation compared to Specimens 1 and 2.

However, the resulting surface roughness is not desirable for façade applications, as increased surface porosity may promote moisture ingress and subsequent fibre swelling. In future specimens, the peel ply will therefore be replaced by a perforated release film to achieve a smoother surface finish while still allowing controlled resin and air evacuation.

SPECIMEN 5 AND 6

Results from the previous experiments indicate that manufacturing is more effective when using thin, flexible reinforcements that can conform to the mould without fibre breakage. Consequently, filament winding using a thin yarn with long continuous fibres is expected to enable a tighter and more controlled wrap around the mould. To achieve this, a dedicated filament winding setup was developed, as shown in Figure 6.17.

For this configuration, the fibre spool is mounted on a rotating wheel fixed to a portable vice bench. The flax fibre yarn is guided through an HDPE resin bath, allowing full impregnation during processing. The yarn enters the resin container through an opening in the bottom and exits through a hole in the cap, as illustrated in Figure 6.18.

The impregnated fibre is then attached to the mould, which is supported and rotated by a filament winding apparatus incorporating 3D-printed PLA components (Figure 6.21). The frame of the setup is constructed from plywood panels connected using L-shaped aluminium profiles. All rotating components are fabricated using PLA via 3D printing at the LAMA-Lab of the Faculty of Architecture and the Built Environment at TU Delft.

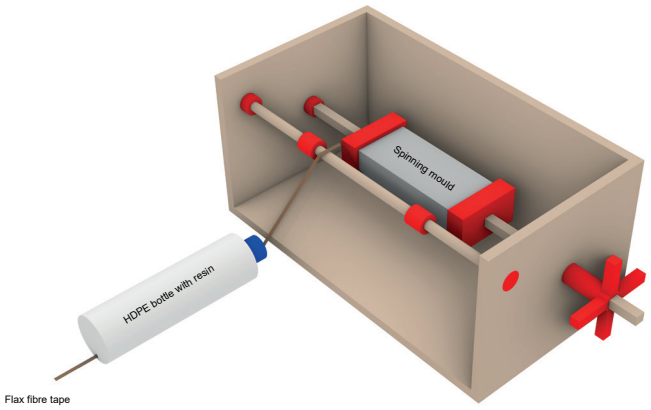

Fig. 6.17 Filament winding set-up (3D-printed parts displayed in red) (own image)

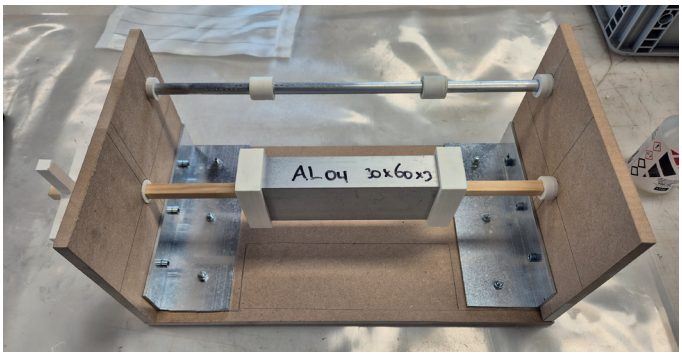

Fig. 6.18 Filament winding machine (right) (own image)

Fig. 6.19 Filament winding set-up with left the spool of flax fibre yarn and right the manufactured winding machine (own image)

The manufacturing properties of specimen 5 and 6 are displayed in table 6.9 and table 6.10.

MANUFACTURING PROPERTIES SPECIMEN 5	
Fibre type	*Flax fibre yarn*
Mould	*aluminum (30 x 60 x 3mm)*
Layers of release agent	*6*
Fibre length	*Width flax fibre yarn: 3 mm - 4 mm*
Rotations around mould	*5/0.30 ≈ 10 layers (14/0.3 ≈ 45 mould rotations per layer)*
Fibre weight	*7gr*
Amount of EL2 epoxy laminating resin	*60gr (estimation based on previous experiments of the non-woven mat around the aluminum mould)*
Amount of AT30 slow hardener	*60x0.3 = 18gr*
Fibre volume fraction (uncut specimen)	*67.8%*
Manufacturing time	*50 minutes*
Weight of sample	*94 gr*
Length of sample	*13.5 cm*
Thickness of sample	*3 - 5 mm*

Table 6.9 Fabrication details specimen 5 (own work).

MANUFACTURING PROPERTIES SPECIMEN 6	
Fibre type	*Cross-stiched flax fibre cloth*
Mould	*aluminum (30 x 60 x 3mm)*
Layers of release agent	*6*
Fibre length	*240cm x 10cm*
Rotations around mould	*5/0.36 ≈ 13*
Fibre weight	*57 gr*
Amount of EL2 epoxy laminating resin	*57 x 1.8 ≈ 102 gr*
Amount of AT30 slow hardener	*102 x 0.3 ≈ 30.6gr*
Fibre volume fraction (uncut specimen)	*25.4%*
Manufacturing time	*35 minutes*
Weight of sample	*121 gr*
Length of sample	*10.5 cm*
Thickness of sample	*5 - 6mm*

Table 6.10 Fabrication details specimen 6 (own work).

MANUFACTURING OF SPECIMEN 5 AND 6

For Specimen 5, the flax fibre yarn spool was mounted on the rotating wheel of the portable vice bench. The yarn was guided through an HDPE bottle serving as a resin bath and subsequently attached to the aluminium mould using a knot and release tape at the far end.

Prior to filling the resin bath, a thin layer of epoxy was applied to the aluminium mould surface using a brush to ensure initial impregnation. The remaining epoxy resin was then poured into the HDPE bottle, which was sealed with a cap. Filament winding was initiated by rotating the 3D-printed wheel, while the resin bath was moved laterally to ensure uniform fibre deposition along the mould.

A total of approximately 45 rotations per layer were applied, with 10 layers required to achieve a final thickness of approximately 3 mm. Figure 6.20 illustrates the manufacturing process of Specimen 5.

Fig.6.20 Manufacturing of sample 5 with filament winding set-up (own image)

After reaching the target thickness, the yarn was cut and the specimen removed from the setup. A second mould was then installed for the production of Specimen 6.

For Specimen 6, the cross-stitched flax fibre fabric was positioned over the mould and secured using release tape, as shown in Figure 6.21. A thin epoxy layer was first applied to the mould surface. The fabric was then wound tightly around the mould, with a thin layer of epoxy applied after each rotation. A total of 13 rotations were required to achieve a final thickness of approximately 5 mm. Excess material was trimmed, and loose edge fibres were removed with scissors.

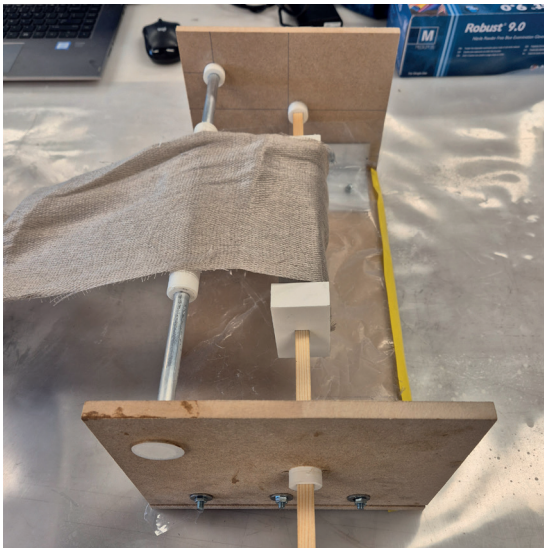

Fig. 6.21 Manufacturing of sample 6 with the filament winding set-up (own image)

Both specimens were completed by applying a thin perforated release film as the second-to-last layer, followed by a breather cloth as the outermost layer. The specimens were then placed in a vacuum bag, evacuated using a vacuum cleaner, and cured in a heated thermobox at 45 °C.

DEMOULDING OF SPECIMEN 5 AND 6

Removal of the breather cloth and perforated release film was straightforward for both specimens. Only minimal resin was observed in the breather cloth, as shown in Figure 6.22.

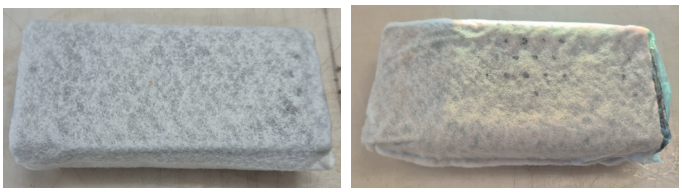

Fig. 6.22 Specimen 5 (left) and specimen 6 (right) out of vacuum bag with breather cloth (own image)

The final result of Specimen 5 is shown in Figure 6.23.

Fig. 6.23 Result specimen 5 (own image)

The demoulded Specimen 6 is presented in Figure 6.24.

Fig. 6.24 Result specimen 6 (own image)

EVALUATION OF SPECIMEN 5 AND 6

During the manufacture of Specimen 5, an insufficient initial resin volume was prepared. As a result, an additional 30 g of epoxy and 9 g of hardener were mixed during processing. In total, 31 g of resin remained unused, resulting in a total

resin consumption of 87 g.

For Specimen 6, the resin content was adjusted based on previous results (Specimen 3), using a resin-to-fibre ratio of 1.8 instead of 2.0 to reduce oversaturation of the breather cloth. Despite this adjustment, 37 g of resin remained unused, resulting in a total consumption of 95.6 g.

The filament winding setup improved manufacturing by enabling controlled rotation and increasing fibre tension, resulting in a tighter wrap. The addition of a guide bar further stabilised fibre deposition and reduced excess resin accumulation. However, the HDPE bottle configuration was suboptimal, as its geometry caused irregular resin flow and local oversaturation of the flax yarn. To mitigate this, alternating wet and dry fibre deposition was applied. After approximately seven layers, resin flow became inconsistent due to the bottle geometry, requiring additional resin preparation during processing.

Manufacturing time for Specimen 5 was approximately twice that of Specimen 6, indicating that fabric-based reinforcement significantly improves production efficiency. However, scaling the yarn-based process to larger geometries may exceed epoxy pot life, which could compromise manufacturing feasibility.

The fabric-based process, while faster, was less precise. Limited flexibility of the cloth made tight wrapping more difficult, and variations in width as well as fibre detachment at the edges resulted in uneven fibre distribution and required post-trimming. Improved pre-cutting and controlled edge management are necessary to enhance surface quality.

Demoulding of Specimen 5 was particularly challenging due to tight compaction and limited access, requiring approximately 30 minutes and a secondary mould. Specimen 6 was demoulded more efficiently within approximately 15 minutes.

Curing conditions were consistent with previous specimens, resulting in full curing after 18 hours. Vacuum levels remained stable throughout the curing process.

SURFACE QUALITY ASSESSMENT

The perforated release film had minimal influence on the final surface texture, as its thickness was negligible and it closely conformed to the specimen surface. A close-up of Specimen 5 is shown in Figure 6.25, and Specimen 6 in Figure 6.26.

Fig.6.25 Surface of specimen 5 (own image)

Fig.6.26 Surface of specimen 6 (own image)

The surface of Specimen 5 is irregular due to non-uniform filament distribution. In an automated process, improved consistency and surface regularity would be expected. Manual winding inevitably introduces small variations in fibre tension and thickness. Air bubble formation was limited, indicating that the release film facilitated adequate air evacuation. However, further improvement could be achieved by applying higher external pressure than that provided by vacuum bagging alone.

The surface of Specimen 6 is also irregular and reflects the texture of the cross-stitched fabric. The release film had limited effect on smoothing the surface. Areas secured with release tape exhibited a smoother finish but also contained a higher concentration of air bubbles, as air evacuation was restricted. In contrast, areas without tape, where only release film was used, showed fewer air inclusions and improved porosity control.

SPECIMEN 7 AND 8

The final experimental specimens were manufactured using the cross-stitched flax fibre fabric and the non-woven hemp fibre mat, as these materials demonstrated sufficient performance in previous trials for further investigation. For Specimen 7, the cross-stitched flax fibre was wound around a smaller aluminium mould with dimensions

15 × 40 × 2 mm. For Specimen 8, the non-woven hemp fibre mat was applied to an identical mould geometry.

The manufacturing parameters for Specimen 7 are presented in Table 6.11, and those for Specimen 8 in Table 6.12.

MANUFACTURING PROPERTIES OF SPECIMEN 7	
Fibre type	*Cross-stiched flax fibre cloth (fibre direction parallel to force)*
Mould	*aluminum (15x40x2mm)*
Layers of release agent	*6*
Total fibre length	*60 cm*
Rotations around mould	*2/0.39 ≈ 5.1*
Fibre weight	*29 gr*
Amount of EL2 epoxy laminating resin	*29 x 1.4 = 40.6 gr*
Amount of AT30 slow epoxy hardener	*40.6 x 0.3 = 12.2 gr*
Fibre volume fraction (uncut sample)	*30.3%*
Manufacturing time per sample	*25 min*

Table 6.11 Properties of specimen 7 (cross-stitched flax fibre cloth) (own work).

MANUFACTURING PROPERTIES OF SPECIMENS 8	
Fibre type	*Non-woven hemp fibre mat*
Mould	*aluminum (15x40x2mm)*
Layers of release agent	*6*
Fibre length	*80 cm*
Rotations around mould	*2/0.29 ≈ 6.9*
Fibre weight	*35 gr*
Amount of EL2 epoxy laminating resin	*35 x 2 = 70gr*
Amount of AT30 slow epoxy hardener	*70 x 0.3 = 21gr*
Fibre volume fraction (uncut sample)	*23.4%*
Manufacturing time per sample	*35 minutes*

Table 6.12 Properties of specimen 8 (non-woven hemp fibre mat) (own work).

MANUFACTURING OF SPECIMEN 7 AND 8

The manufacturing procedure for Specimens 7 and 8 followed the same filament winding-based approach as Specimen 6, as both reinforcements consist of fabric-based materials. The filament winding setup was again used; however, the results indicate that further optimisation is still required to improve consistency for mechanical testing specimens.

For Specimen 7, a reduced fibre-to-resin ratio of 1.4 was applied to limit resin consumption. For Specimen 8, an additional final layer of flax fibre yarn was applied to increase surface compaction and improve surface quality.

Both specimens were finished with a perforated release film as the second-to-last layer and a breather cloth as the outer layer. The breather cloth was secured using PVC tape. Subsequently, both specimens were placed in a vacuum bag, evacuated using a vacuum cleaner, and cured for 18 hours at 40 °C.

DEMOULDING OF SPECIMEN 7 AND 8

Demoulding was comparable to Specimen 6 and proceeded without major difficulties. The specimens were clamped in a vice bench, after which controlled force was applied to one end of the mould to release the composite.

Figure 6.27 shows the final result of Specimen 7, and Figure 6.28 shows Specimen 8.

Fig. 6.27 Result of specimen 7 (own image)

Fig. 6.28 Result of specimen 8 (own image)

EVALUATION OF SPECIMEN 7 AND 8
Specimen 7 achieved the most favourable result to date, exhibiting a relatively smooth outer surface and well-defined edges that closely replicate the mould geometry. The cross-section shows minimal void content, with smooth inner and outer surfaces. However, a reduced fibre presence was observed in the corner regions due to the sharp 90° geometry of the mould, which may negatively influence local mechanical performance.

Specimen 8 shows a less uniform structure, with fibre accumulation in central regions and localised voids where insufficient fibre and resin were present. The additional flax yarn layer improved compaction and surface quality but increased manufacturing time by approximately 10 minutes, which may become a limiting factor for upscaling.

SURFACE QUALITY ASSESSMENT
The surface of Specimen 7 is comparable to Specimen 6 (Figure 6.26), showing minor perforations and a mixed surface texture. Regions where PVC tape was applied exhibit smoother finishes, while areas covered only by perforated film are more irregular.

The surface of Specimen 8 is comparable to Specimen 5 (Figure 6.25), although the additional flax yarn layer provided improved compaction and slightly enhanced surface quality.

Figure 6.29 and 6.30 display an overview of samples 1-8 manufactured in the first experimental phase.

6.3 MICROSCOPIC ASSESSMENT

The mechanical properties of the specimens are strongly influenced by fibre–resin bonding quality, edge conditions, and the overall fibre-to-resin distribution within the composite. To assess these aspects, multiple samples from the manufactured specimens were examined using an electronic microscope in collaboration with Dr. ir. Fred Veer at the Faculty of Architecture and the Built Environment, TU Delft.

Small sections of approximately 10 mm thickness were cut from the manufactured specimens. The cut edges were intentionally left unsanded to avoid obscuring the fibre structure. For each specimen, the centre of the cross-section, the outer edges, and the internal interfaces were analysed. In addition, corner regions were examined for all specimens intended for mechanical testing.
The analysed samples include:
- A sample from Specimen 7 (cross-stitched flax fibre cloth) (Figure 6.27)
- A sample from Specimen 8 (non-woven hemp fibre mat) (Figure 6.28)
- A sample from Specimen 5 (flax fibre yarn) (Figure 6.23)

The results of the microscopic analysis acan be found in Appendix E.

FINDINGS MICROSCOPIC ASSESSMENT
From the microscopic analysis, the following observations can be made:

1. The cross-stitched flax fibre sample exhibits an uneven fibre-to-resin distribution and clear fibre layering. In the corner regions, significant fibre-deficient zones are observed, which may reduce local mechanical performance. This behaviour is attributed to the fabric thickness and the woven architecture of the reinforcement. The sharp 90° geometry of the mould likely caused fibre displacement away from the corners during compaction. This issue could be mitigated by using rounded corner geometries.

2. Both the non-woven hemp mat and the flax fibre yarn samples show a more homogeneous fibre-to-resin distribution compared to the cross-stitched flax fabric. This is consistent with expectations, as the non-woven mat consists of short, randomly oriented fibres that allow more uniform resin penetration and reduced fibre clustering. In addition, these samples were manufactured with relatively higher resin uptake. The flax yarn configuration, due to its thin geometry and high number of layers, also results in a comparatively dense and well-distributed composite structure.

3. The outer edges of the cross-stitched flax fibre sample appear rougher than the interior regions. This is attributed to reduced compaction in the final wrapping layers, resulting in locally lower fibre packing density and increased resin variation.

4. The flax fibre yarn sample shows localised signs of delamination in some outer layers, while other regions exhibit a smooth and consistent surface. Overall, however, the yarn-based specimens achieve the smoothest surface finish among the

tested configurations. This suggests that insufficient compaction or locally reduced resin application occurred in certain regions during the final winding stages.

5. The non-woven hemp fibre mat sample exhibits variations in fibre coloration, indicating possible contamination of the reinforcement material. This is consistent with observations during specimen preparation, where minor cross-contamination could not be fully eliminated despite cleaning efforts.

6. The cutting process using a jigsaw introduced local thermal damage to the specimens, resulting in colour variation between cut surfaces. This effect is particularly visible in the corner regions, where increased material thickness led to higher heat accumulation and partial burning of the fibre material.

Fig. 6.29 Overview of result of Experimental Phase 1 (own image)

Fig. 6.30 Overview of result of Experimental Phase 1 (own image)

6.4 SUMMARY OF PHASE 1 FINDINGS

The initial experiments demonstrated the potential of the filament wrapping technique, in which fibre material is tightly wrapped around a mould. Early trials (specimens 1–4), using manual rotation or a stationary vice bench, resulted in insufficient fibre tension and excessive movement, leading to fibre slippage and resin spillage. In contrast, the use of a custom-built filament winding machine (specimens 5–8) significantly improved process stability and product quality.

Vacuum-assisted resin transfer moulding (VARTM) was not applied in this phase, as its limited process control and requirement for dry fibre placement make it unsuitable for rectangular hollow geometries.

Regarding mould materials, aluminium proved most effective compared to PETG and HDPE. Its combination of low weight and high strength allows for greater demoulding forces without deformation. Additionally, thermal expansion during curing enhances internal compression, resulting in improved consolidation, while the shrinkage of the aluminum mould facilitates easier demoulding. PETG moulds failed under demoulding loads, and HDPE, although viable, exhibited a rougher surface that complicated release.

Among the tested fibre materials, the non-woven hemp mat and cross-stitched flax fibre yielded the best results. The jute plain weave was too thick and stiff for complex geometries, while flax fibre yarn, although suitable for intricate shapes, significantly increased manufacturing time. This extended processing time risks premature resin curing and limits scalability, making it less suitable for upscaled production.

Demoulding was performed by clamping the specimen and applying axial force, using a secondary mould to push out the primary core. The application of five layers of release agent enabled consistent and relatively efficient demoulding. However, PETG moulds could not be removed due to insufficient material strength. For larger geometries, higher demoulding forces are expected, particularly when tighter fibre wrapping is achieved.

Surface quality was strongly influenced by the choice of final layer. A perforated release film combined with breather cloth enabled excess resin removal during curing, resulting in a smooth, glossy finish. In contrast, peel ply produced a rough, matte surface suitable for secondary bonding. For structural applications, a smooth, unperforated outer surface is preferred to prevent moisture ingress and fibre degradation. This can be achieved by applying an additional epoxy coating after manufacturing.

7. EXPERIMENTAL PHASE 2: FIRST MECHANICAL TESTS

7. EXPERIMENTAL PHASE 2: FIRST MECHANICAL TESTS

Based on the results of the first experimental phase, the two most suitable fibre materials and reinforcement configurations are selected for the preparation of samples used in the initial mechanical tests. This chapter describes the manufacturing process of these test specimens as well as the experimental setup employed for mechanical testing. Subsequently, the obtained test results are analysed and evaluated in order to identify the most suitable combination of fibre material and reinforcement. On the basis of this evaluation, a final decision is made regarding the material system that will be used to manufacture the final profile geometry in the third experimental phase.

7.1 PREPARATION OF SPECIMENS FOR MECHANICAL TESTING

MATERIAL SELECTION PHASE 2

Based on the outcomes of the preliminary experimental phase, two fibre systems were selected for the second stage of mechanical testing: a cross-stitched flax fibre fabric and a non-woven hemp fibre mat. These materials were chosen due to their contrasting structural characteristics, manufacturing behaviour, and anticipated mechanical performance.

The cross-stitched flax fibre fabric was selected because of its relatively stable handling properties during processing, its comparatively low laminate thickness, and its ability to produce a consistent surface finish. In the present configuration, the fibre orientation was deliberately aligned such that the primary fibre direction was oriented parallel to the expected loading direction during mechanical testing (see Figure 7.0). This was done to ensure that the applied load acts predominantly along the fibre-dominant direction of the composite.

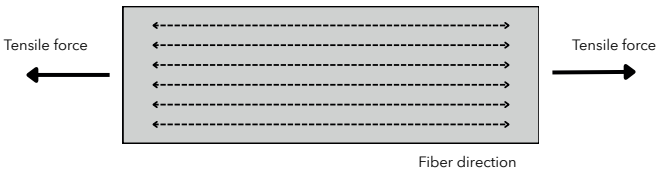

Figure 7.0 Fibre direction parallel to tensile forces (own image).

The non-woven hemp fibre mat was selected as a second material system due to its low material cost, ease of conformability, and suitability for producing geometrically complex profiles. However, previous observations indicated that this material system exhibits limited surface consolidation when processed in isolation. To improve surface integrity and compaction, an additional outer layer consisting of tightly wound flax fibre yarn was applied in the final wrapping stage of the specimen.

Flax fibre yarn as a standalone reinforcement system was excluded from the second experimental phase. This decision was based on significantly longer manufacturing times compared to the other reinforcement systems, which would be incompatible with the epoxy resin pot life when considering potential scale-up. Furthermore, the filament winding configuration constrains fibre alignment predominantly in a direction transverse to the primary loading direction, which reduces its structural efficiency for the intended loading case.

A jute plain woven fabric was also excluded from further testing due to its relatively high thickness and stiffness, which limited its ability to conform to the mould geometry during manufacturing.

MANUFACTURING TECHNIQUE PHASE 2

The specimens were manufactured using a filament winding–based roll-wrapping process around an aluminium mould. During fabrication, epoxy resin was applied manually using a brush after each wrapping cycle to ensure uniform impregnation of the fibre layers.

To improve consolidation during curing, a vacuum-assisted compression method was applied. The specimens were sealed using a simple vacuum bagging system connected to a vacuum cleaner. This approach ensured sufficient compaction of the laminate while still allowing the aluminium mould to be removed after curing without damage to the composite structure.

A key limitation of this manufacturing method is the geometric restriction imposed by the filament winding setup, as the mould dimensions must remain compatible with the winding apparatus.

MIXING AND CURING CONSTANTS PHASE 2

To ensure consistency across all manufactured specimens, the following processing parameters were maintained throughout the second experimental phase:

- *All fibre reinforcements were dried at 60°C for*

2 hours prior to processing to reduce moisture content.
- *After drying, fibres were cooled to ambient temperature for approximately 2 minutes before resin application.*
- *A resin-to-hardener ratio of 100:30 by weight was used, in accordance with the manufacturer's specification.*
- *All specimens were cured for a minimum of 18 hours at 40°C in a controlled oven environment.*
- *After curing, specimens were stored in sealed airtight packaging to prevent moisture uptake prior to testing.*

These parameters were kept constant to minimise variability between specimens and ensure comparability across test results.

7.2 MECHANICAL TEST SET-UP

All mechanical tests were conducted in accordance with the relevant ISO standards as described in Section 5.4. For each material system, four to five specimens were prepared for tensile testing and for three-point bending testing, resulting in a total of nineteen specimens. An overview of the manufactured specimens is provided in Table 7.0.

For tensile testing, the specimens were subsequently machined into strips with a reduced width of 20 mm and a thickness of 3 mm to ensure compatibility with the clamping system of the testing machine. The effective gauge length was set to 200 mm.

For bending tests, full cross-sectional specimens were used without further modification, as the geometry of the profile was considered relevant to the structural response under flexural loading.

In order to ensure full material consolidation, all specimens were preferably tested after a curing period of approximately seven days, consistent with the recommendations provided in the epoxy resin technical datasheet (Easy Composites, 2025).

7.2.1 TENSILE TEST CONFIGURATION

Tensile testing was performed using a 100 kN universal testing machine located in the Mechanical Engineering Laboratory at Delft University of Technology under supervision. The experimental procedure followed standard tensile testing practice for fibre-reinforced polymer composites.

Fig. 7.1 Test set-up tensile test at Mechanical Engineering lab (own image)

The specimens were clamped with an effective grip length of approximately 10 mm on each side, resulting in a free gauge length of 180 mm during testing. Prior to testing, specimen edges were lightly sanded to reduce stress concentrations at the grips.

Specimens were cut from 3 manufactured specimen, ensuring that the fibre orientation corresponded to the intended loading direction. Care was taken to minimise cutting-induced damage and to maintain consistent specimen geometry across all

FABRIC	NUMBER OF LAYERS	Fibre PLACE-MENT	MANUFACTURING TECHNIQUE	POST PROCESSING	NUMBER OF SAMPLES
Cross-stiched flax fibre cloth	2 / 0.36 ≈ *5.6*	Roll wrapping	Hand lamination + Vacuum bagging	At least 18h at 40 °C	5 (bending test) 5 (tensile test)
Non-woven hemp fibre mat	2 / 0.29 ≈ 6.9	Roll wrapping	Hand lamination + Vacuum bagging	At least 18h at 40 °C	4 (bending test) 4 (tensile test)

Figure 7.0 Overview of samples prepared for mechanical testing (own work).

samples. The samples tested on tensile strength are displayed in figure 7.2 and figure 7.3.

Fig. 7.2 Specimen 1-5 prepared for tensile testing (cross-stitched flax fibre cloth) (own image)

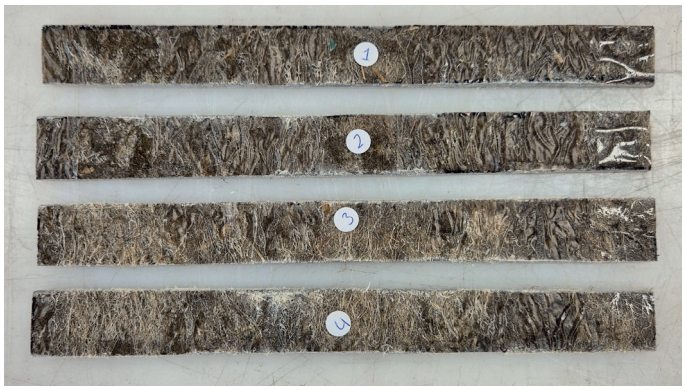

Fig. 7.3 Specimens 6-9 prepared for tensile testing (non-woven hemp fibre mat) (own image)

All tests were performed under displacement control, and force-displacement data were recorded continuously for subsequent stress–strain conversion

7.2.2 THREE-POINT BENDING TEST CONFIGURATION

Three-point bending tests were conducted using two different testing systems depending on specimen configuration.

The primary tests were performed on a 100 kN universal testing machine in the Mechanical Engineering Laboratory at Delft University of Technology. Additional tests on shortened specimens were carried out using an MF40 MKII testing machine (TecQuipment) located in the Thinklab at the Faculty of Architecture and the Built Environment.

Figure 7.4 displayes the specimens prepared for the three-point bending test at the mechanical engineering lab with on the left specimen 1-5 and on the right specimen 6-9.

Fig. 7.4 Specimens prepared for 3-point bending test (left: specimen 1-5, right: specimen 6-9) (own image)

In both configurations, the specimen was simply supported on two rollers, and a concentrated load was applied at mid-span using a loading nose. The main laboratory setup used a support span of 180 mm, while the MF40 setup used a reduced span of 80 mm due to specimen size constraints. The test set-up for both configurations is displayed in figure 7.5 and figure 7.6.

Fig. 7.5 3-point bending test set-up at the Mechanical Engineering Faculty lab (own image)

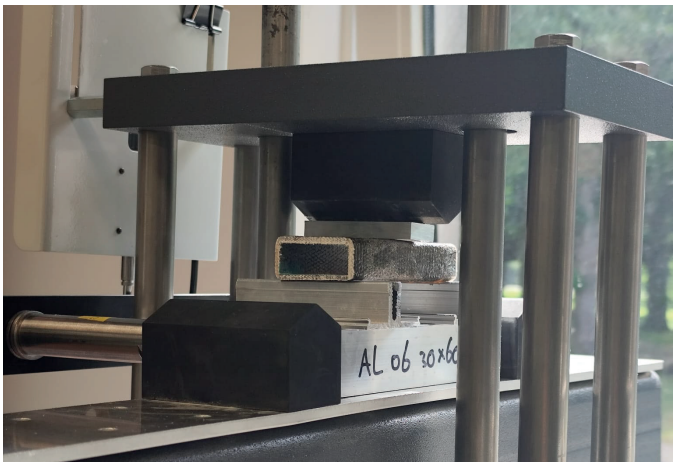

Fig. 7.6 Three-point bending test set-up at the thinklab on MF40 MKII machine (own image)

Force and displacement were recorded continuously throughout the test until either fracture or significant loss of load-bearing capacity occurred.

7.2.4 THERMAL EXPANSION TEST CONFIGURATION

Thermal expansion tests were conducted to assess the dimensional stability of the composite materials under elevated temperature conditions.

Specimens were cut to defined lengths and their initial dimensions were recorded using a digital caliper with 0.1 mm resolution. The samples were then exposed to a controlled temperature of 100°C in a laboratory oven for a fixed duration of 15 minutes. Prior to heating, all specimens were conditioned at room temperature (20.8°C).

Figure 7.7 displayed the samples prepared for the thermal expansion test.

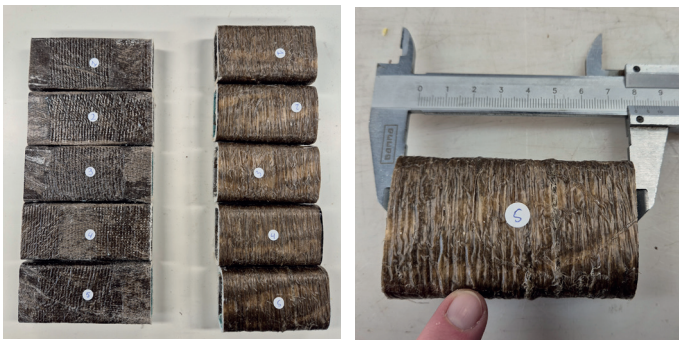

Fig. 7.7 Prepared and measuring specimens for thermal expansion test (own image)

After thermal exposure, the specimens were re-measured under identical conditions to determine dimensional changes. The coefficient of thermal expansion was subsequently determined based on the measured length variation and the applied temperature change.

7.2.5 FASTENER FIXATION CAPACITY TEST CONFIGURATION

Fastener fixation tests were conducted to evaluate the suitability of both composite systems for mechanical fastening applications.

Each specimen was prepared by drilling a pilot hole at a fixed distance from the specimen edge. Subsequently, two different fastener types commonly used in aluminium façade connections were installed into the specimens under controlled insertion depth. The two fasteners used for the test are displayed in figure 7.8.

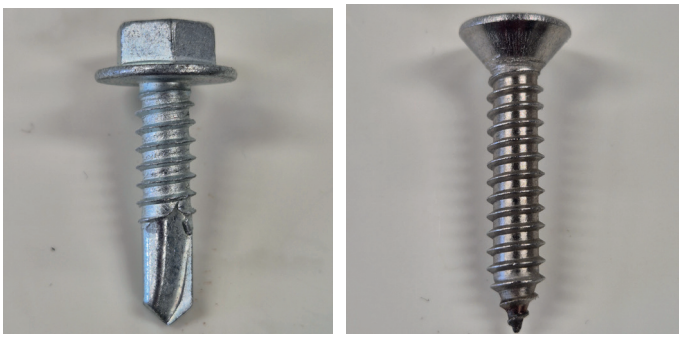

Fig. 7.8 Fasteners used for profile fixation test (left: EJOT JT6-2H-Plus-5.5 self drilling screw, right: 6mm fastener (own image)

The specimens were then mounted in a fixed vice setup as displayed in figure 7.10 and figure 7.11 and loads were applied incrementally using a suspended weight system connected via steel wire. Two loading configurations were applied:

- Axial (tensile pull-out) loading, where the fastener was loaded perpendicular to the specimen surface (figure 7.9, left)
- Shear loading, where the load was applied parallel to the specimen surface (figure 7.9, right)

The applied load was increased stepwise until either fastener slippage or complete pull-out occurred, or until the maximum available test load was reached.

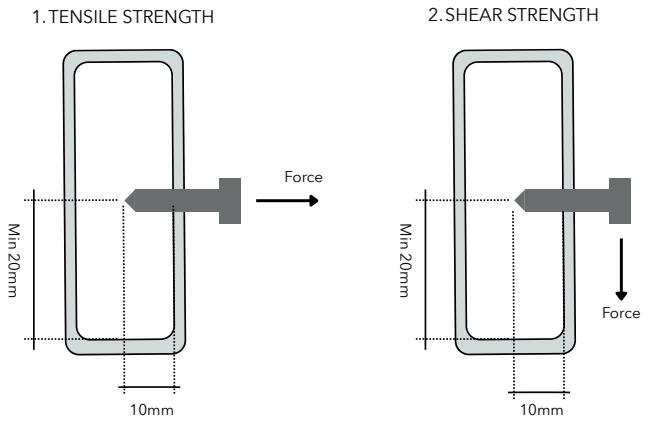

Fig. 7.9 Diagramof loading principle of fasteners for (1) tensile strength and (2) shear strength (own image).

The test set-up is displayed in figure 7.10 for axial loading and figure 7.11 for shear loading.

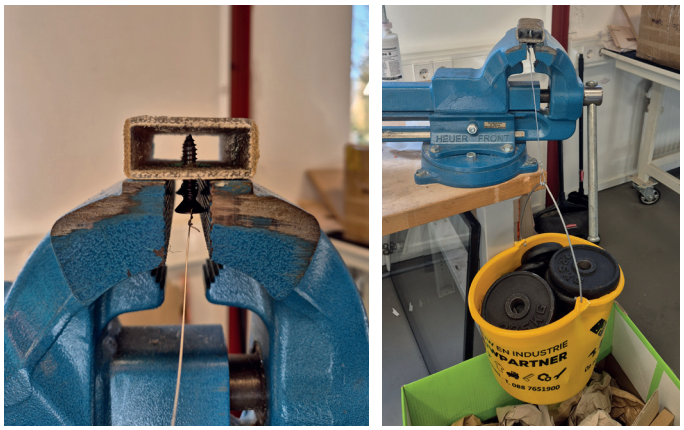

Fig. 7.10 Test set-up fastener fixation test 1(tensile) (own image)

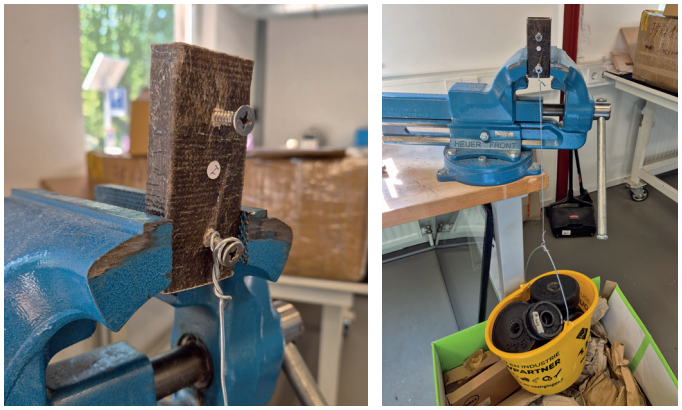

Fig. 7.11 Test set-up fastener fixation test 2 (shear) (own work)

7.3 EVALUATION OF TEST RESULTS

The mechanical test results are presented in Chapter 7.4 and form the basis for the comparative assessment of the two selected fibre reinforcement systems. The evaluation focuses on tensile behaviour, flexural performance, thermal stability, and fastener fixation capacity.

EVALUATION OF THE TENSILE TEST RESULTS

Table 7.1 displayes a comparison of the testresults of sample 1-5 and sample 6-9.

PROPERTIES	SAMPLE 1-5	SAMPLE 6-9
Average tensile strength (MPa)	*65.2*	*34.2*
Highest value tensile strength (MPa)	*99.0*	*43.1*
Spread from average tensile strength (MPa)	*21.0*	*6.7*
Average Young's Modulus (GPa) (0.01 - 0.03 strain)	*9.03*	*5.14*
Higherst value Young's Modulus (GPa)	*10.4*	*6.0*
Average elongation at break (%)	*1.0*	*0.8*
Strain at plastic deformation (mm)	*1.5 - 2.0*	*0.8 - 1.0*
Maximum force (N)	*4000-6000*	*2000-3000*

Table 7.1 Summary of results tensile test conducted at Mechanical Engineering (own work).

The tensile test results (Chapter 7.4.1) indicate a pronounced difference in mechanical consistency between the two material systems. The cross-stitched flax fibre specimens (Specimens 1–5) exhibit a relatively high scatter in ultimate tensile strength, ranging from 29 MPa to 99 MPa. This variability is most likely attributed to local heterogeneities in fibre volume fraction, manufacturing-induced defects within the cross-stitched textile architecture, and potential inconsistencies in fibre alignment during filament winding.

Despite this scatter, the average tensile strength of 65.2 MPa indicates a comparatively high load-bearing capacity. However, the observed variability implies that structural application of this material

would require conservative design assumptions and the implementation of a relatively high safety factor, which would reduce the effective utilisation of its superior strength.

In contrast, the non-woven hemp fibre mat specimens (Specimens 6–9) show a significantly narrower strength distribution, ranging from 26 MPa to 43 MPa. This lower spread indicates a more consistent mechanical response, which may be associated with a more isotropic fibre distribution and a more uniform defect distribution within the material. The average tensile strength of 34.2 MPa is approximately 1.8–2.0 times lower than that of the cross-stitched flax system.

The stiffness response, expressed through Young's modulus, follows a similar trend. The cross-stitched flax specimens reach an average modulus of 9.03 GPa, whereas the non-woven hemp specimens reach 5.14 GPa. This indicates that the flax-based system provides approximately twice the stiffness of the hemp-based system, although both materials remain significantly less stiff than conventional structural metals (≈70 GPa).

EVALUATION OF THE STRESS-STRAIN DIAGRAM

The stress–strain response of Specimens 1–5 (figure 7.18) is characterised by an initially linear elastic region followed by abrupt load drops in several specimens (notably Specimens 2–4). This behaviour is indicative of progressive internal damage mechanisms such as transverse matrix cracking and subsequent fibre bundle failure. The stepped nature of some curves suggests sequential failure events rather than a single global fracture. Specimen 1 shows an almost complete post-peak load drop, highlighting significant variability in failure progression between specimens.

The stress–strain curves of Specimens 6–9 (figure 7.19) exhibit a markedly different response, characterised by an extended yielding plateau and gradual post-yield softening. This indicates a higher capacity for plastic deformation and energy dissipation. Load levels remain relatively stable beyond approximately 1.5% strain before gradual degradation occurs. This behaviour is consistent with a non-woven fibre architecture, where fibre bridging and distributed matrix damage contribute to a more ductile failure mechanism without immediate catastrophic collapse.

FRACTURE CHARACTERISTICS

The fracture surfaces of the cross-stitched flax specimens (Figure 7.12) show a high degree of similarity in both fracture orientation and location. The fracture path is generally characterised by an initial straight propagation followed by an angled deviation. The consistency of the failure location across specimens suggests the presence of a manufacturing-related weak zone, potentially caused by local damage, discontinuities in the textile structure, or imperfections introduced during filament winding.

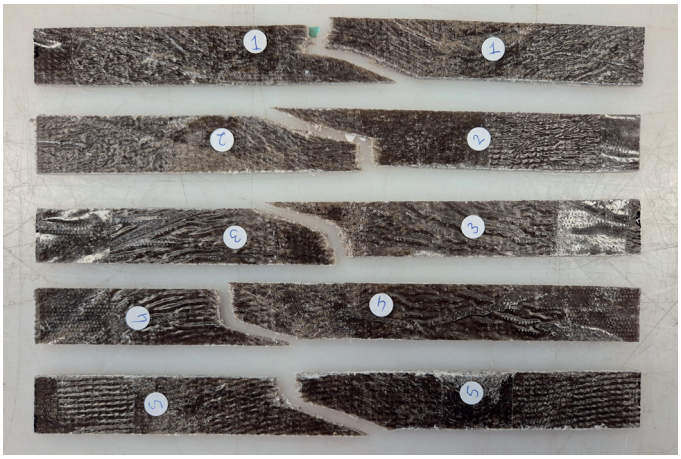

Fig. 7.12 Fracture specimen 1-5 after tensile test (own image)

In contrast, the non-woven hemp specimens (Figure 7.13) show more variability in fracture location and a more uniform distribution of failure along the gauge length. This suggests a more homogeneous stress distribution and a less localised failure mechanism, consistent with the more isotropic nature of the material.

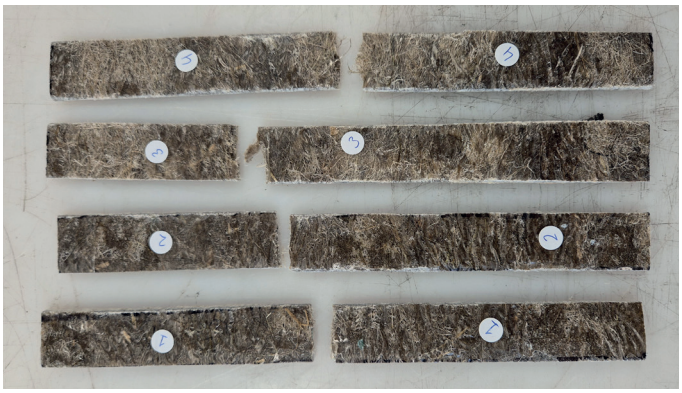

Fig. 7.13 Fracture specimen 6-9 after tensile test (own image)

EVALUATION OF THE THREE-POINT BENDING TEST RESULTS

Table 7.2 displayes the results of the three-point bending test of specimen 1-5 and specimen 6-9.

PROPERTY	SPECIMEN 1-5	SPECIMEN 6-9
Average flexural strength (MPa)	*13.8*	*37.8*
Spread from average flexural strength (MPa)	*0.9*	*3.0*
Average Young's Modulus (GPa)	*1.7*	*0.5*
Average elongation at break (%)	*16.3*	*7.6*
Average deflection at break (mm)	*6.6*	*8.9*
Average maximum force (N)	*2240*	*4069*

Table 7.2 Summary of resultsthree-point bending test (own work).

The initial bending tests on Specimens 1–5 at the MSE laboratory did not result in fracture due to insufficient global bending failure relative to local failure mechanisms at the loading nose. Instead, failure was governed by local indentation and shear-related damage prior to full structural collapse. As a result, full flexural properties could not be determined under this configuration.

To enable meaningful comparison, additional tests were performed on shortened specimens using the MF40 MKII testing machine (Thinklab), where failure was successfully achieved on the weaker axis.

The resulting flexural properties show that Specimens 6–9 achieve a significantly higher average flexural strength (37.8 MPa) compared to Specimens 1–5 (13.8 MPa under weak-axis testing conditions). However, the cross-stitched flax system exhibits a substantially higher Young's modulus (1.7 GPa versus 0.5 GPa), indicating greater stiffness but lower ultimate bending strength in the tested configuration.

The elongation at break further highlights this distinction: Specimens 1–5 reach approximately 16.3% strain, whereas Specimens 6–9 reach 7.6%, indicating that the flax-based system exhibits significantly higher deformability prior to failure under bending loads.

EVALUATION OF THE STRESS-STRAIN DIAGRAM

The stress–strain curves of specimen 1-5 (figure 7.20) demonstrate a consistent flexural response, characterised by an initial linear-elastic region followed by a gradual transition into non-linear behaviour. All specimens exhibited similar initial stiffness, indicating a relatively uniform material composition and structural performance. The presence of several local peaks and plateaus suggests progressive damage accumulation, including matrix cracking and fibre-matrix debonding, rather than immediate failure. Maximum bending stresses ranged from approximately 13 MPa to 16 MPa, while failure strains varied between 15% and 19%. Following peak stress, most specimens retained a substantial portion of their load-carrying capacity, indicating a gradual failure mechanism. Overall, the results demonstrate a ductile flexural behaviour with high deformability and good energy absorption characteristics under bending loads.

The stress–strain curves of specimen 6-9 (figure 7.21) demonstrate a combination of ductile and brittle characteristics. An initial approximately linear elastic region is observed, followed by progressive damage accumulation characterised by small load drops and plateau regions. Ultimate failure occurred suddenly in Specimens 6, 8, and 9, whereas Specimen 7 failed at a lower deformation level.

All specimens exhibited similar initial slopes, indicating a relatively consistent bending stiffness. A non-linear response developed between approximately 2 mm and 5 mm of deformation, accompanied by minor fluctuations in load. The maximum load sustained by the specimens ranged between approximately 3500 N and 4500 N.

FRACTURE CHARACTERISTICS

Figure 7.14 displayes a fractured sample of specimen 1-5. All samples fractured in a similar way.

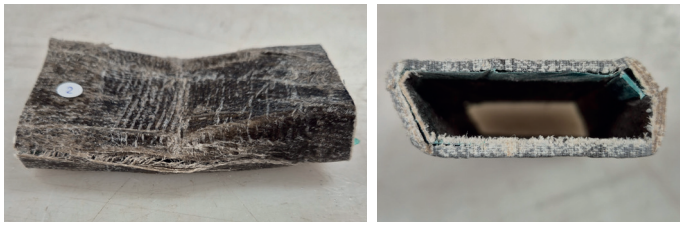

Fig. 7.14 Fractured specimens 1-5 on bending strength on the MF40 MKII test machine at the Thinklab (own image)

Figure 7.15 displayes two fractured samples of specimen 6-9.All samples fractured in a similar way.

Fig. 7.15 Fractured specimens on bending strength at mse lab (own image)

The bending test fracture patterns confirm the differences in failure mechanisms between the two material systems. In the Thinklab configuration, Specimens 1–5 show fracture dominated by shear mechanisms, with failure initiation occurring at geometric discontinuities near the profile corners rather than at the location of maximum tensile stress. This indicates a strong influence of stress concentrations introduced by the specimen geometry. Specimens 6–9, in contrast, exhibited brittle fracture under comparable loading conditions governed by maximum tensile forces.

Comparison of flexural and tensile strength values (approximately 13.8 MPa and 65.2 MPa, respectively) suggests that failure in Specimens 1–5 is primarily shear in nature, occurring at the corners of the specimen under bending load.

Comparison of flexural and tensile strength values (approximately 37.8 MPa and 34.4 MPa, respectively) suggests that failure in Specimens 6–9 is primarily tensile in nature, occurring at the lower surface of the specimen under bending load.

EVALUATION OF THERMAL EXPANSION TEST RESULTS

The thermal expansion results indicate relatively low dimensional sensitivity for both material systems. The cross-stitched flax specimens (Specimens 1–5) show an average thermal expansion coefficient of 14.91 µm/m°C, based on a measured length change of approximately 0.12 mm over 100 mm.

The non-woven hemp specimens (Specimens 6–10) show a higher thermal expansion coefficient of 22.21 µm/m°C, corresponding to a measured expansion of approximately 0.14 mm over 80 mm. This value is comparable to that of aluminium, whereas the flax-based system is closer to that of steel.

Overall, thermal expansion is not expected to be a governing design constraint for either material system. However, the cross-stitched flax composite demonstrates improved dimensional stability under thermal loading, exhibiting approximately 1.5 times lower expansion than the non-woven hemp system.

EVALUATION OF FASTENER FIXATION CAPACITY TEST RESULTS

The fastener fixation tests demonstrate that both material systems provide sufficient resistance to mechanical fastening under moderate loading conditions.

<u>Situation 1: Axial loading condition</u>

Both material systems were generally able to sustain the maximum applied load of 40 kg without fastener pull-out. Failure occurred only in the case of the EJOT JT6-2H-Plus-5.5 self-drilling screw in two specimens. This is attributed to the enlarged hole diameter created during self-drilling installation, which reduces the effective contact area and consequently lowers pull-out resistance.

The remaining fastener configurations did not exhibit failure under identical loading conditions, indicating that both material systems possess adequate axial load-bearing capacity for typical fastening applications.

Figure 7.16 displayes the material failure with the self-drilling screw at 40kg loading.

Fig. 7.16 Results profile fixation capacity test: axial loading conditions (own image).

<u>Situation 2: Shear loading conditions</u>

Under shear loading, a similar trend was observed. The self-drilling screw failed at approximately 35

kg, while the alternative fastener type sustained the maximum applied load of 40 kg without visible failure.

Figure 7.17 displayes the material failure with the self-drilling screw at 40kg loading.

These results suggest that fastener performance is more strongly influenced by installation method and local damage introduced during drilling than by intrinsic material limitations. A more controlled pull-out test using a mechanical testing machine would be required to quantify fastener resistance more accurately.

Fig. 7.17 Results profile fixation capacity test: shear loading conditions (own image)

STRENGTH COMPARISON BETWEEN SPECIMENS

To compare the material efficiency of both systems, the required cross-sectional area of the non-woven hemp composite to match the tensile capacity of the cross-stitched flax composite is estimated using:

$$F_{max} = \sigma_{uts} * A$$

Where:
F_{max} *= max force at fracture (N)*
σ_{uts} *= Ultimate tensile strength (MPa)*
A *= Cross-section area (mm²)*

Given identical specimen geometries, the required scaling factor can be expressed as:

$$A_{specimen\ 6\text{-}9} = A_{specimen\ 1\text{-}5} *(\sigma_{uts,1} / \sigma_{uts,2})$$

Using the measured average values, the required equivalent cross-sectional area for Specimens 6–9 is approximately 115.1 mm², compared to 60 mm² for Specimens 1–5. This corresponds to an equivalent thickness increase from 3 mm to approximately 5.8 mm.
Considering the non-woven mat thickness of 0.29 mm, approximately 20 winding layers would be required to achieve this equivalent strength. This corresponds to approximately 220 cm of non-woven material per specimen, compared to approximately 60 cm of cross-stitched flax material for equivalent performance.

STIFFNESS COMPARISON

The axial stiffness of a tensile specimen can be expressed as:

$$k = AE/L$$

Since the specimen length L is identical for both material systems, stiffness scaling can be simplified to:

$$A_{specimen\ 6\text{-}9} = A_{specimen\ 1\text{-}5} *(E_1 / E_2)$$

Substituting the measured elastic moduli results in a required cross-sectional area of approximately 108.4 mm² for Specimens 6–9, corresponding to a thickness of approximately 5.4 mm.

This translates to approximately 18–19 winding layers of non-woven material, or roughly 204 cm of material length, compared to 60 cm for the cross-stitched flax system to achieve equivalent stiffness.

7.4 TEST RESULTS

This chapter discusses the results from the tensile tests and three-point bending tests conducted on sample 1-5 and sample 6-9. Furthermore, important material properties are calculated.

7.4.1 TENSILE TEST RESULTS

The specimens prepared for the tensile tests are presented in Tables 7.3 and 7.4.

The results of the tensile tests conducted on specimen 1-5 are presented in Table 7.5, while the results for specimens 6-9 are presented in Table 7.6.

DENSITY OF SPECIMENS
The density of the samples are calculated through the method discribed in section 5.4. The scale used for this measurement is the digital precision scale of 10kg capacity with a precision of 0.1gr.

AVERAGE TENSILE STRENGTH
The tensile strength is determined by deviding the maximum force by the cross-sectional area of the specimen.

The specimens manufactured from the cross-stitched flax fibre composite (Specimens 1–5) exhibited an average tensile strength at failure of 65.2 MPa. In comparison, the specimens manufactured from the non-woven hemp fibre mat composite (Specimens 6–9) exhibited an average tensile strength of approximately 34.0 MPa.

VALUE SPREAD
A relatively large variation in tensile strength was observed for the cross-stitched flax fibre specimens (Specimens 1–5), with measured values ranging from 29 MPa to 99 MPa. The non-woven hemp fibre mat specimens (Specimens 6–9) showed a smaller spread in results, with tensile strengths ranging from approximately 26 MPa to 43 MPa.

ELONGATION AT BREAK
The elongation at break was determined using the following formula:

$$\varepsilon_{break} \approx dl \text{ at break} / 200$$

where ε_{break} represents the extension at failure and 200 mm corresponds to the initial gauge length of the tensile specimens. The average elongation at break of the cross-stitched flax fibre specimens (Specimens 1–5) was approximately 1.0–1.1%. The non-woven hemp fibre mat specimens (Specimens

	Fibre type	Weight of fibres (gr)	Weight of matrix(gr)	Number of layers	Weight of cut specimen (gr)	Dimensions (mm x mm)	Length sample (mm)	Density (g/cm³)
1	Cross-stitched	29	52	5	11	20 x 3	200	0.92
2	Cross-stitched	29	52	5	9	20 x 3	200	0.75
3	Cross-stitched	29	52	5	11	20 x 3	200	0.92
4	Cross-stitched	29	52	5	10	20 x 3	200	0.83
5	Cross-stitched	29	52	5	9	20 x 3	200	0.75
Average		29	52	5	10			0.83

Table 7.3 Overview of specimens for mechanical test (cross-stiched flax fibre cloth) (own work).

	Fibre type	Weight of fibres (gr)	Weight of matrix(gr)	Number of layers	Weight of cut specimen (gr)	Dimensions (mm x mm)	Length sample (mm)	Density (g/cm³)
6	Non-woven mat	35	91	7	15	20 x 3	200	1.25
7	Non-woven mat	35	91	7	15	20 x 3	200	1.25
8	Non-woven mat	35	91	7	12	20 x 3	200	1.00
9	Non-woven mat	35	91	7	12	20 x 3	200	1.00
Average		35	91	7	13.5			1.13

Table 7.4 Overview of specimens for mechanical test (non-woven mat) (own work).

Sample	Force at Break (N)	Tensile Strength at break (UTS) (MPa)	Spread from UTS (MPa)	Young's Modulus (GPa)	dl at break (mm)	Elongation at break (%)
1	*1744*	*29*	*36.2*	*10.39*	*1.6*	*0.8*
2	*4047*	*67*	*1.8*	*8.52*	*1.8*	*0.9*
3	*5934*	*99*	*33.8*	*9.53*	*2.9*	*1.5*
4	*4902*	*82*	*16.8*	*8.30*	*2.7*	*1.3*
5	*2927*	*49*	*16.2*	*8.39*	*1.2*	*0.6*
Average	*3911*	*65.2*	*21.0*	*9.03*	*2.0*	*1.0*

Table 7.5 Mechanical properties of specimens for tensile test (cross-stiched flax fibre cloth) (own work).

Sample	Force at Break (N)	Tensile Strength at break (UTS) (MPa)	Spread from UTS (MPa)	Young's Modulus (GPa)	dl at break (mm)	Elongation at break (%)
6	*2319*	*38.6*	*4.6*	*5.51*	*1.6*	*0.8*
7	*2584*	*43.1*	*9.1*	*5.99*	*1.7*	*0.9*
8	*1719*	*28.6*	*5.4*	*4.60*	*1.3*	*0.7*
9	*1593*	*26.5*	*7.5*	*4.44*	*1.6*	*0.8*
Average	*2054*	*34.0*	*6.7*	*5.14*	*1.6*	*0.8*

Table 7.6 Mechanical properties of specimens for tensile test (non-woven hemp fibre mat) (own work).

6–9) exhibited a slightly lower average elongation at break of approximately 0.8–0.9%.

YOUNG'S MODULUS

The Young's modulus was estimated from the initial slope of the stress–strain curve within the elastic region, prior to the onset of permanent deformation. The measured force-displacement data were converted to stress values using the specimen cross-sectional area of 60 mm².

The initial portion of the stress–strain curve was not perfectly linear due to factors such as minor specimen misalignment and slack within the clamping system. To ensure a consistent comparison between materials and minimise the influence of these effects, Young's modulus was determined using a strain interval between 0.001 and 0.003.

STRESS-STRAIN DIAGRAM

The stress–strain curves of Specimens 1–5 are presented in Figure 7.18, while the stress–strain curves of Specimens 6–9 are presented in Figure 7.19.

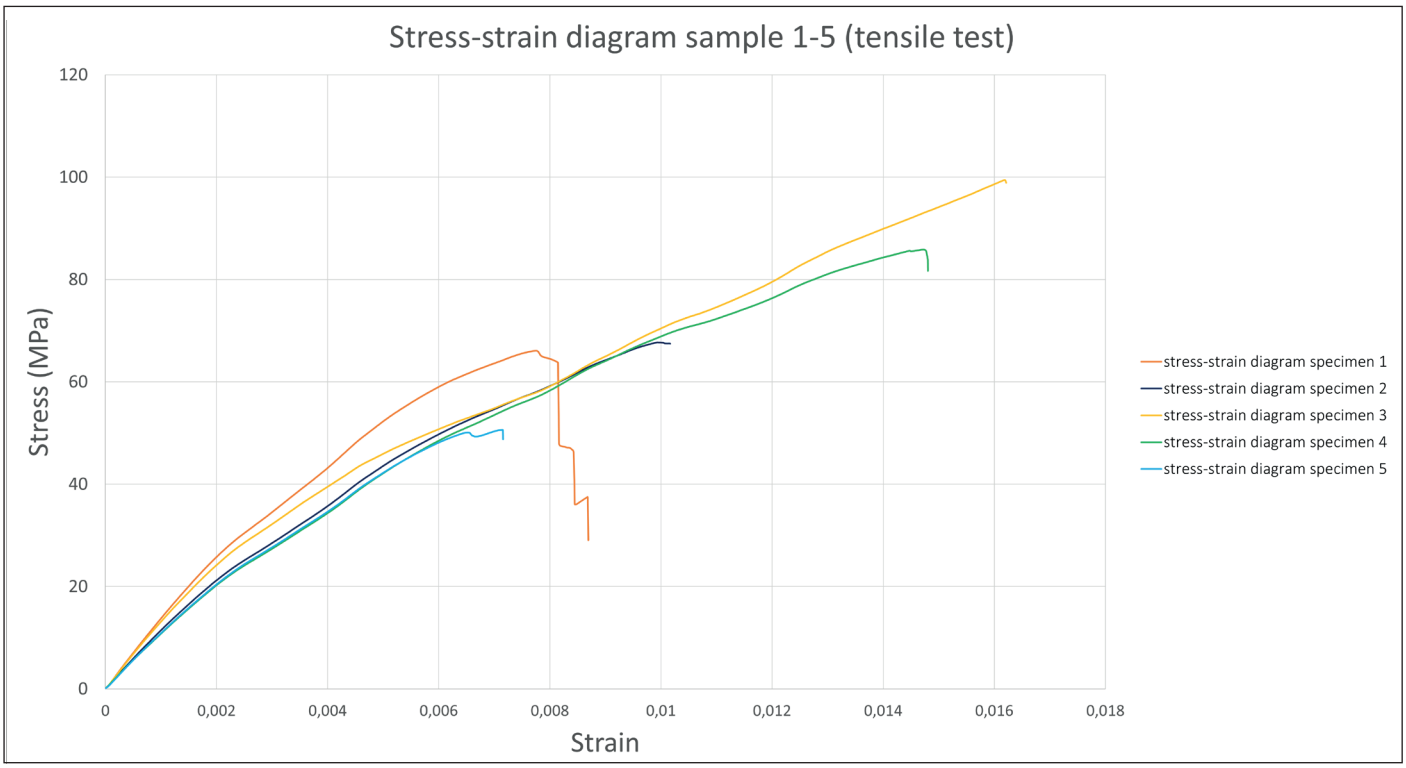

Figure 7.18. Stress to strain diagram of samples 1-5 tensile tests conducted at mse lab (own image).

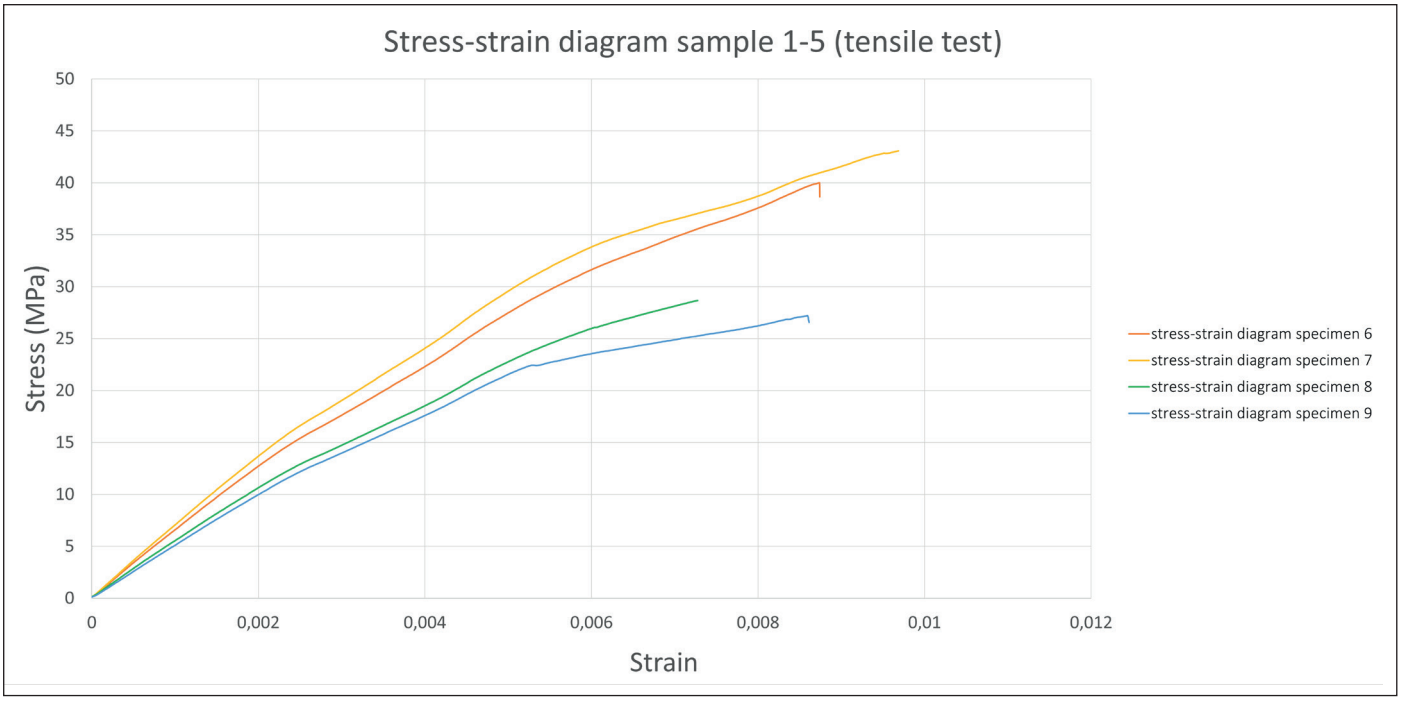

Figure 7.19. Stress to strain diagram of samples 6-9 tensile tests conducted at mse lab (own image).

7.4.2 THREE-POINT BENDING TESTS RESULTS

The specimens prepared for the three-point bending tests are presented in Tables 7.7 and table 7.8.

The three-point bending test results for the cross-stitched flax fibre specimens (specimen 1-5) are presented in Table 7.9. The results for the non-woven hemp fibre mat (specimens 6-9) are presented in Table 7.10.

FLEXURAL STRENGTH

The flexural strength was determined from the maximum force at failure F_{max}. Using the specimen geometry, the maximum bending moment was calculated as:

$$M_{max} = (F_{max} * L) / 4$$

Where:
M_{max} = *maximum bending moment (N/mm)*
F_{max} = *maximum force at fracture (N)*
L=180mm (span between supports (mm))

The bending stress at failure was calculated according to:

$$\sigma f = (M_{max} * c_y) / I$$

Where:
σf = *bending stress at fracture (MPa or N/mm²)*
M_{max} = *bending moment (N/mm)*
c_y = *distance from neutral axis to outer surface (mm)*
I = *second moment of area (mm⁴)*

The second moment of area for the rectangular hollow section was calculated for both the strong and weak bending axes using the corresponding geometric relationships.

$$I_y = (b * H^3 - b_i * h_i^3) / 12 \text{ (strong axis)}$$
$$I_y = (H * b^3 - h_i * b_i^3) / 12 \text{ (weak axis)}$$

Where:
b = *outer width*
H = *outer height*
b_i = *inner width*
h_i = *inner height*

Elastic section modulus (S) of profile:

$$c = H / 2$$
$$S = I_y / c = 2 * I_y / H$$

Flexural strength formula:

$$\sigma_{max} = M_{max} / S$$

<u>For specimen 1-5</u>
L = 80 mm
h = 48 mm
b = 26 mm
t = 3 mm
c = 13 mm

	Fibre type	Weight of fibres (gr)	Weight of matrix (gr)	number of layers	Weight of cut specimen (gr)	Dimensions (mm x mm)	Length sample (mm)	Density (g/cm³)
1	*Cross-stitched*	*10.8*	*15.1*	*5*	*26*	*48 x 26 x 3*	*100*	*0.64*
2	*Cross-stitched*	*10.8*	*15.1*	*5*	*26*	*48 x 26 x 3*	*100*	*0.64*
3	*Cross-stitched*	*11.3*	*15.7*	*5*	*27*	*48 x 26 x 3*	*100*	*0.66*
4	*Cross-stitched*	*11*	*15.1*	*5*	*26*	*48 x 26 x 3*	*100*	*0.64*
5	*Cross-stitched*	*10.4*	*14.6*	*5*	*25*	*48 x 26 x 3*	*100*	*0.61*

Table 7.7 Overview of specimens 1-5 for three-point bending test (own work).

	Fibre type	Weight of fibres	Weight of matrix	Number of layers	Weight of cut specimen (gr)	Dimensions (mm x mm)	Length sample (mm)	Density (g/cm³)
6	*Non-woven mat*	*35*	*91*	*7*	*93*	*48 x 26 x 3*	*200*	*1.13*
7	*Non-woven mat*	*35*	*91*	*7*	*91*	*48 x 26 x 3*	*200*	*1.12*
8	*Non-woven mat*	*35*	*91*	*7*	*95*	*48 x 26 x 3*	*200*	*1.16*
9	*Non-woven mat*	*35*	*91*	*7*	*95*	*48 x 26 x 3*	*200*	*1.16*

Table 7.8 Overview of specimens for three-point bending test (own work).

Sample	F_{max} (N)	M_{max}	Flexural Strength (MPa)	Spread from average flexural strength (MPa)	Deflection at F_{max} (mm)	Young's Modulus (GPa)	Strain at break (%)
1	*2100*	*42000*	*12.9*	*0.9*	*5.9*	*1.8*	*14.6*
2	*2200*	*44000*	*13.5*	*0.3*	*5.8*	*1.9*	*14.2*
3	*2100*	*42000*	*12.9*	*0.9*	*6.9*	*1.5*	*17.0*
4	*2200*	*44000*	*13.5*	*0.3*	*7.4*	*1.5*	*18.2*
5	*2600*	*52000*	*16.0*	*2.2*	*7.2*	*1.8*	*17.5*
Average	*2240*	*44800*	*13.8*	*0.9*	*6.6*	*1.7*	*16.3*

Table 7.9 Mechanical properties of specimens 1-5 from three-point bending test (own work).

Sample	F_{max} (N)	M_{max}	Flexural Strength (MPa)	Spread from average flexural strength (MPa)	Deflection at F_{max} (mm)	Young's Modulus (GPa)	Strain at break (%)
6	*4291*	*193095*	*39.9*	*2.1*	*8.7*	*0.5*	*7.7*
7	*3492*	*157140*	*32.5*	*5.3*	*7.9*	*0.5*	*6.7*
8	*4494*	*202230*	*41.8*	*4.0*	*10.1*	*0.5*	*7.9*
9	*4000*	*180000*	*37.2*	*0.6*	*9.0*	*0.5*	*7.9*
Average	*4069*	*183116*	*37.8*	*3.0*	*8.9*	*0.5*	*7.6*

Table 7.10 Mechanical properties of specimens 6-9 from 3-point bending test (own work).

I_z = *42304 mm⁴ (weak axis)*

S = *42304 / 13* = 3254.15

For specimen 6-9
L = 180 mm
h = 48 mm
b = 26 mm
t = 3 mm
c = 24 mm
I_y = *116136 mm⁴ (strong axis)*

S = *116136 /24* = 4839.00

Specimen 1-5
For the flax fibre specimens (Specimens 1–5), testing was conducted on the weak axis after the original strong-axis tests proved unsuccessful. Consequently, a second moment of area corresponding to the weak axis was used in the calculations. The average flexural strength of sample 1-5 is 13.8 MPa with values ranging from 12.9 MPa to 16 MPa.

Specimen 6-9
For the non-woven hemp fibre mat specimens (Specimens 6–9), the average flexural strength was 37.8 MPa, with individual values ranging between 32 MPa and 42 MPa.

STRAIN AT BREAK
The flexural strain at failure was calculated using:

*Strain at break = (6 * δ * d) / L^2*

where:
δ = deflection at midpoint
d = height of the specimen
L = span between supports (mm)

The cross-stitched flax fibre specimens (specimen 1-5) exhibited an average strain at break of 16.3%. The non-woven hemp fibre mat specimens (specimen 6-9) exhibited an average strain at break of 7.6%.

YOUNG'S MODULUS
Young's modulus in bending was determined from the beam deflection equation:

*δ = F_{max}*L^3 / 48*E*I*

Rearranging for (E) yields:

$E = (F_{max} * L^3 / \delta) / 48 * I$
Where:
δ. = *max deflection at fracture (mm)*
F_{max} = *maximum force at fracture (N)*
L = 180mm (span between supports (mm))
E = Young's Modulus (MPa)
I = second moment of area (mm^4)

The average Young's modulus of the cross-stitched flax fibre specimens was 1.70 GPa, with a maximum measured value of 1.89 GPa. The non-woven hemp fibre mat specimens exhibited an average Young's modulus of 0.50 GPa, with a maximum value of 0.53 GPa.

STRESS-STRAIN DIAGRAM

The stress–strain curves obtained from the three-point bending tests are presented in Figures 7.20 and 7.21 for Specimens 1–5 and Specimens 6–9, respectively.

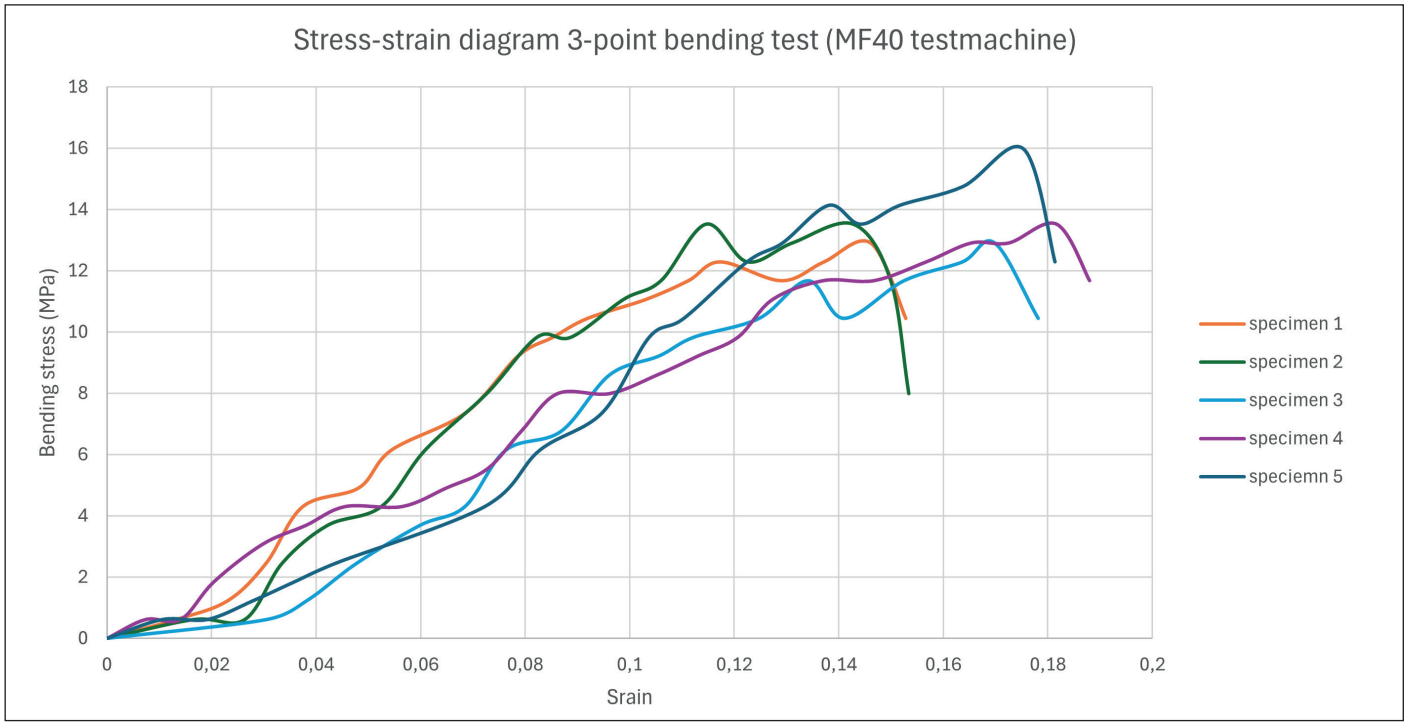

Figure 7.20. Stress to strain diagram samples 1-5 tested on bending strength (own work).

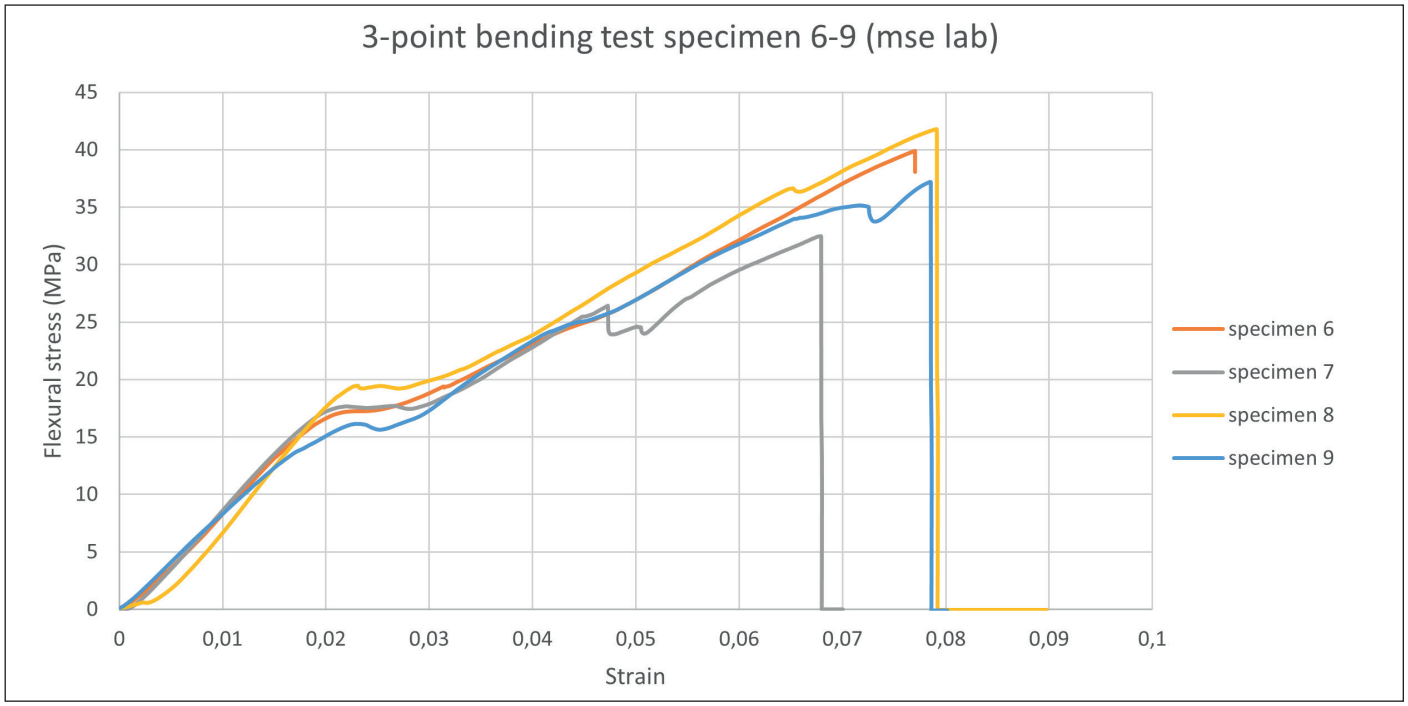

Figure 7.21. Stress to strain diagram specimen 6-9 tested on bending strength (own work).

7.4.3 THERMAL EXPANSION TEST RESULTS

The resulting dimensional changes after the thermal expansion test are presented in Tables 7.13 and 7.14.

The coefficient of thermal expansion *α* was calculated using:

$dl = L_0 * \alpha * (\Delta T)$

Where:
dl = change in object length (m)
L_0 *= initial length of the sample (m)*
α = linear exapansion coefficient (m/m°C)
ΔT = change in temperature (°C)

The results show an average thermal expansion coefficient of 14.9 µm/m°C for sample 1-5 of the cross-stitched flax fibre.

The results show an average thermal expansion coefficient of 22.2 µm/m°C for sample 6-10 of the non-woven hemp fibre mat.

Sample	Sample Length (mm)	Length sample after test (mm)	Length difference (mm)	ΔT (°C)	α (µm/m°C)
1	101.7	101.8	0.1	79.2	12.43
2	101.5	101.8	0.2	79.2	24.83
3	101.6	101.7	0.1	79.2	12.43
4	101.8	101.9	0.1	79.2	12.40
5	101.5	101.6	0.1	79.2	12.44
Average	101.62	101.76	0.12	79.2	14.91

Table 7.13 Thermal expansion of specimen 1-5 (own work).

Sample	Sample Length (mm)	Length sample after test (mm)	Length difference (mm)	ΔT (°C)	α (µm/m°C)
6	79.5	79.6	0.1	79.2	15.88
7	79.6	79.7	0.1	79.2	15.86
8	79.7	79.9	0.2	79.2	31.68
9	79.5	79.6	0.1	79.2	15.88
10	79.5	79.7	0.2	79.2	31.76
Average	79.56	79.7	0.14	79.2	22.21

Table 7.14 Thermal expansion of specimen 6-10 (own work).

7.4.4 FASTENER FIXATION CAPACITY TEST RESULTS

The preparation of the specimens for the fastener fixation tests is described in Table 7.15. A total of four fixation configurations were tested for each material. The results of the fixation tests are presented in Tables 7.14 and 7.15.

A green cell indicates that the fastener remained securely attached under the applied load, whereas a red cell indicates that the fastener failed or was pulled out at the corresponding load level.

The tests were performed at loading angles of 0° and 90° to evaluate the tensile and shear resistance of the fastener connection, respectively.

Fastner nr.	Sample tag	Discription
1	*Sample 1 / EJOT 1*	*Cross-stitched flax fibre with EJOT JT6-2H-Plus-5.5 self-drilling screw*
2	*Sample 1 / EJOT 2*	*Cross-stitched flax fibre with EJOT JT6-2H-Plus-5.5 self-drilling screw*
3	*Sample 1 / 6mm 1*	*Cross-stitched flax fibre with typical 6mm thick screw*
4	*Sample 1 / 6mm 2*	*Cross-stitched flax fibre with typical 6mm thick screw*
5	*Sample 2 / EJOT 1*	*Non-woven hemp fibre mat with EJOT JT6-2H-Plus-5.5 self-drilling screw*
6	*Sample 2 / EJOT 2*	*Non-woven hemp fibre mat with EJOT JT6-2H-Plus-5.5 self-drilling screw*
7	*Sample 2 / 6mm 1*	*Non-woven hemp fibre mat with typical 6mm thick screw*
8	*Sample 2 / 6mm 2*	*Non-woven hemp fibre mat with typical 6mm thick screw*

Table 7.15 Results profile fixation capacity test (own work).

Fastner nr.	1	2	3	4	5	6	7	8
5kg								
10kg								
15kg								
20kg								
25kg								
30kg								
35kg								
40kg								

Table 7.14 Results profile fixation capacity test 0° angle (axial loading) *(red: failure) (own work).*

Fastner nr.	1	2	3	4	5	6	7	8
5kg								
10kg								
15kg								
20kg								
25kg								
30kg								
35kg								
40kg								

Table 7.15 Results profile fixation capacity test9 0° angle (shear loading) *(red: failure) (own work).*

7.5 SUMMARY OF PHASE 2 FINDINGS

TENSILE STRENGTH
The tensile test results indicate that specimens 1–5 (cross-stitched flax fibre) exhibit significantly higher performance, achieving nearly twice the tensile strength of specimens 6–9 (non-woven hemp mat) with an average Young's modulus of 9.03 GPa compared to 5.14 GPa for specimen 6-9 (non-woven mat). Despite the observed variability, likely caused by manufacturing inconsistencies such as manual layup and resin distribution, the maximum recorded strength (99 MPa) approaches that of pure aluminium, demonstrating substantial material potential. Reducing manufacturing variability is therefore essential to fully realize this performance.

In contrast, achieving comparable tensile strength and stiffness with specimens 6–9 would require increasing the thickness from 3 mm to approximately 5.8 mm and 5.4 mm, respectively. Combined with the higher resin consumption of these specimens, the cross-stitched flax fibre composite represents a more efficient and sustainable material choice.

FRACTURE MECHANICS
From a fracture mechanics perspective, specimens 1–5 exhibit a more ductile failure behaviour, characterised by relatively lower peak loads combined with improved post-damage performance and a gradual failure progression. The three-point bending results indicate that failure is primarily governed by peak shear stresses occurring at the corners of the hollow profile geometry, identifying these regions as critical stress concentrations within the composite structure. This observation is consistent with the microscopic analysis conducted in the first experimental phase, where a reduced fibre presence was identified in the corner regions, particularly in areas formed by 90° bends during manufacturing.

In contrast, specimens 6–9 display a more brittle failure mode, with fracture occurring abruptly at higher load levels. For (semi-)structural applications, ductile failure behaviour is generally preferred, as it provides increased warning prior to ultimate failure. Furthermore, although not directly quantified in this study, the increased deformability observed in specimens 1–5 suggests a higher potential for impact resistance.

THERMAL EXPANSION
Additionally, specimens 1–5 exhibit lower thermal expansion, which is advantageous for structural applications, although both material systems expand similar to conventional metals such as aluminium and steel.

FASTENER FIXATION CAPACITY
Fastener fixation tests show adequate strength for both materials, indicating that additional reinforcement methods are unnecessary, particularly when using larger fasteners.

CONCLUSION PHASE 2
Overall, the cross-stitched flax fibre composite is considered the most suitable material system for further development. Despite the larger variation in measured tensile properties, its substantially higher tensile strength, stiffness, material efficiency, and thermal stability outweigh the advantages of the non-woven hemp fibre composite. Therefore, the cross-stitched flax fibre reinforcement was selected for the manufacture and evaluation of the final profile geometry in the subsequent experimental phase.

FURTHER ENHANCEMENTS
To further improve the structural performance of the flax fibre composite, future research should focus on increasing its resistance to local compressive and shear damage. This could be achieved by optimising the fibre architecture, increasing the fibre volume fraction, or improving laminate consolidation during manufacturing. Another promising approach is the development of hybrid composite profiles that combine flax fibres with materials such as aluminium or steel, provided that effective load transfer between the materials can be ensured.

The profile geometry should also be refined to reduce stress concentrations. The bending tests identified the profile corners as critical locations where failure initiated due to limited fibre reinforcement. Increasing the corner radii would facilitate improved fibre placement and result in a more uniform fibre distribution throughout the profile.

Finally, alternative fibre orientations should be investigated. Introducing reinforcement in multiple directions may improve shear resistance and reduce the likelihood of corner failure, thereby enhancing the overall structural reliability of the composite profile.

8. EXPERIMENTAL PHASE 3: FINAL PROFILE AND MODEL

8. EXPERIMENTAL PHASE 3: FINAL PROFILE AND MODEL

The final phase is focussed on the manufacturing and testing of a full-scale composite profile geometry representative of mullions and transoms used in curtain wall façade systems. Following manufacturing, tensile and three-point bending tests were conducted to evaluate the structural performance of the developed flax fibre/epoxy composite.

8.1 MANUFACTURING OF FINAL PROFILE GEOMETRY

MATERIAL SELECTION PHASE 3

The mechanical tests conducted in Experimental Phase 2 demonstrated that the cross-stitched flax fibre specimens (Specimens 1–5) exhibited a favourable combination of strength, ductility, and energy absorption capacity. Consequently, the cross-stitched flax fibre fabric with fibres aligned parallel to the primary loading direction was selected for manufacturing larger profile geometries representative of curtain wall mullions and transoms.

The selected profile dimensions were 100 × 50 × 4 mm.

A practical limitation of the selected flax fibre fabric is its maximum roll length of 1000 mm when oriented with the fibres parallel to the loading direction. Manufacturing a 4 mm thick profile requires approximately eleven rotations around the mould, corresponding to a total fibre length of approximately 340 cm. As a result, additional sections of fabric had to be introduced during winding.

Introducing multiple fabric sections can compromise fibre tension and increase variability between specimens. To minimise this effect, the fibre orientation in the middle section of the laminate was rotated by 90°. Since this region is located near the neutral axis during bending, it experiences lower tensile and compressive stresses. This configuration also improves the multidirectional reinforcement of the laminate. The adopted lay-up reduced the number of fabric transitions required during manufacturing. The principle is illustrated in Figure 8.0.

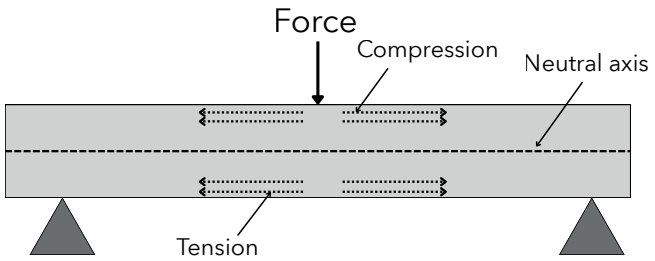

Fig. 8.0 Force distribution within the profile during bending (own image)

The selected 0°/90°/0° laminate configuration was chosen to optimise bending performance while maintaining manufacturability. In this lay-up, the outer layers consist of fibres aligned with the principal loading direction (0°), where tensile and compressive stresses are highest during bending. These outer plies therefore contribute most effectively to flexural stiffness and strength. The central 90° layer is positioned near the neutral axis, where longitudinal force is minimal; its primary role is to enhance transverse stability, improve load redistribution, and reduce crack propagation between outer layers. This hybrid configuration results in a balanced laminate with improved damage tolerance compared to a fully unidirectional lay-up, while still preserving high longitudinal load-bearing capacity.

MANUFACTURING TECHNIQUE PHASE 3

The manufacturing technique developed during Experimental Phase 2 was adopted for the final phase due to its scalability and satisfactory mechanical performance.

A practical limitation of the selected flax fibre fabric was its maximum roll length of 1000 mm when oriented with the fibres parallel to the loading direction. Manufacturing a 4 mm thick profile required approximately eleven rotations around the mould, corresponding to a total fibre length of approximately 340 cm. As a result, additional sections of fabric had to be introduced during winding.

For the larger profile geometry, a paste wax release agent was used instead of a spray-based release agent to reduce operator exposure to vapours during manufacturing. Miracle Gloss-8 mould release wax was selected. Following the manufacturer's recommendations, four layers of wax were applied before manufacturing, with

approximately 15 minutes between applications.

MIXING AND CURING CONSTANTS PHASE 2
The following manufacturing parameters were maintained throughout Experimental Phase 3:

- *Flax fibres were dried for 2 hours at 60°C before manufacturing to reduce moisture content.*
- *The fibres were allowed to cool to room temperature before use.*
- *All specimens were cured for a minimum of 18 hours at 40°C in the custom-built curing oven.*
- *A resin-to-hardener ratio of 100:30 by weight was used, following supplier recommendations.*
- *After curing, specimens were stored in airtight bags to minimise moisture absorption.*

NEW FILAMENT WINDING SET-UP
To accommodate the larger profile geometry, aluminium moulds measuring 100 × 50 × 4 mm with a length of 400 mm were obtained. The mould corners were rounded with a radius of 4 mm.

A new filament winding machine was subsequently designed and manufactured to accommodate the larger mould dimensions. New components were produced using additive manufacturing facilities at the LAMA Lab, Faculty of Architecture. The resulting winding machine is shown in Figures 8.1 and 8.2.

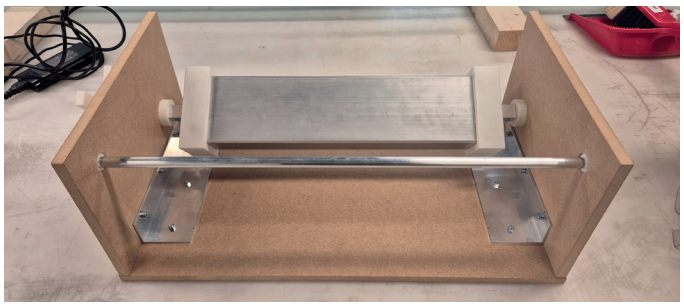

Fig. 8.1 Larger filament winding machine for the final profile geometry, overview (own image)

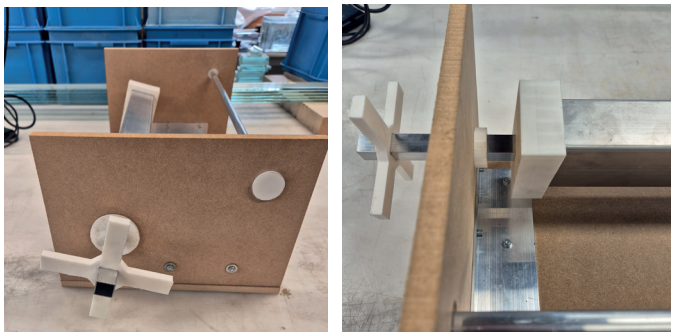

Fig. 8.2 Larger filament winding machine for the final profile geometry detailing (own image)

MANUFACTURING PROPERTIES SPECIMEN 10-15
Based on the structural calculations presented in Chapter 5.3, a composite wall thickness of 4 mm was required.

To achieve this thickness while limiting fabric transitions, the laminate consisted of:

- An inner layer with fibres oriented at 0°.
- A middle layer with fibres oriented at 90°.
- An outer layer with fibres oriented at 0°.

Approximately 60% of the fibres were therefore aligned with the principal loading direction, while 40% were oriented transversely. This lay-up is illustrated in Figure 8.3.

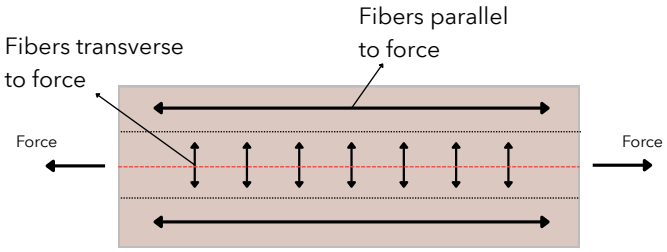

Fig. 8.3 Fibre orientation within the final profile geometry (own image)

During manufacturing, additional fibre sections were introduced by pre-wetting a 45 cm fabric strip with resin and overlapping it onto the existing laminate while maintaining tension.

Different outer-layer finishing methods were evaluated. Specimen 10 was manufactured using tightly wrapped PVC tape to provide additional external compression. A breather cloth was included to absorb excess resin during curing.

Based on previous experiments, a fibre-to-resin mass ratio of approximately 1:1.4 was expected to minimise resin accumulation. For Specimens 11–15, peel-ply and breather cloth were used as the final layer to achieve a more consistent surface finish and improved resin control.

The manufacturing properties of specimen 10-15 are displayed in table 8.0.

MANUFACTURING PROPERTIES SPECIMEN 10 -15	
Fibre type	*Cross-stitched flax fibre*
Fibre direction	*0° (inner layer),90° (middle layer), 0° (outer layer)*
Mould material	*aluminum (50x100x4mm) rounded corners*
Layers of Miracle gloss-8 wax release agent	4
Total fibre length	*≈ 340 cm*
Number of layers	*4/0.36 ≈ 11*
Total fibre weight	*≈ 230 gr*
Amount of EL2 epoxy laminating resin	*230 x 1.4 ≈ 322 gr*
Amount of AT30 slow epoxy hardener	*322 x 0.3 = 96.6 gr*
Fibre volume friction (uncut sample)	*36.2%*
Manufacturing time per specimen	*≈ 60 minutes*
Curing time (at room temperature)	*24 hours at room temperature*
Length of cut specimen	30 cm
Weight of cut specimen	≈ 450 gr

Table 8.0 Manufacturing properties of Specimens 10–10 (own work).

DEMOULDING OF SPECIMEN 10-15

The increased size of the final profile geometry required a modified demoulding procedure.

Each specimen was secured in a bench vice while protected by breather cloth to prevent surface damage. Unlike the smaller specimens, where a hammer and chisel were sufficient to release the mould, the larger surface area of the final profiles resulted in significantly higher friction forces.

To overcome this issue, a steel profile with dimensions similar to the mould was inserted and impacted with a hammer. Simultaneously moving the steel profile along the mould length distributed the applied force more effectively, allowing the mould to be removed within approximately 30 minutes.

The demoulding process is shown in Figure 8.4.

Fig. 8.4 Demoulding process of the specimen 10-15 (own image)

Figures 8.5–8.9 present the manufactured specimens.

Fig. 8.5 Result of specimen 10 (own image)

Fig. 8.6 Result of specimen 11 (own image)

Fig. 8.7 Result of specimen 12 (own image)

Fig. 8.8 Result of specimen 13 (own image)

Fig. 8.9 Result specimen 14 (own image)

EVALUATION OF SAMPLE 10-14

Specimen 10

Manufacturing Specimen 10 highlighted the difficulty of maintaining consistent fibre tension while introducing multiple fabric sections. Local fibre accumulation occurred in the middle region of the specimen, resulting in an uneven surface finish and increased manufacturing time.

The specimen mass was 575 g, indicating a relatively high resin content. The use of PVC tape also contributed to local accumulation of resin and fibres at the surface.

Cross-sectional analysis revealed several resin-starved regions where fibre bundles were insufficiently impregnated, as shown in Figure 8.10.

Fig. 8.10 Cross-section of Specimen 10 (own image)

These defects were attributed primarily to interruptions during fabric replacement. Reducing such imperfections is essential to achieve a constant wall thickness and improve the repeatability of mechanical test results.

Specimen 11-14

To improve manufacturing consistency, Specimens 11–14 were produced by two operators. One operator maintained fibre tension while the second introduced new fabric sections.

This modification significantly improved laminate quality. No voids or dry regions were observed in the cross-section of Specimen 11, and a more uniform wall thickness was achieved. Manufacturing time was reduced from approximately 65 minutes to 55 minutes.

Since the results were satisfactory, the same procedure was adopted for Specimens 12–14. Cross-sectional inspection confirmed a consistent laminate structure as shown in Figure 8.11. For these specimens, no visible voids larger than 2 mm were observed throughout the cross-section.

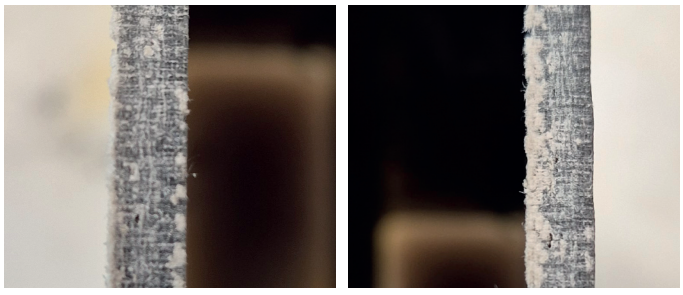

Fig. 8.11 Cross-section of Specimens 11–14 (own image)

SURFACE QUALITY ASSESSMENT

Specimen 10 exhibited significant fibre accumulation at the surface, resulting in local thickness variations between 4 mm and 6 mm. Although the PVC tape

provided additional compaction and produced a glossy finish, the resulting surface quality was inconsistent (Figure 8.12).

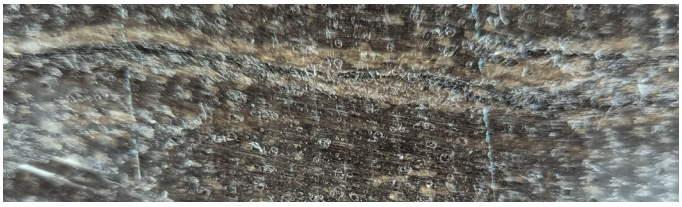

Fig. 8.12 Surface detail of Specimen 10 (own image)

To improve surface quality, Specimen 11 was manufactured using peel-ply and breather cloth as the outer layer. This produced a uniform matte finish with no significant fibre accumulation or surface defects (Figure 8.13).

Fig. 8.13 Surface detail of Specimen 11 (own image)

The improved surface quality indicates that peel-ply provides more effective resin control than non-perforated PVC tape. A cosmetic topcoat of epoxy resin could further improve the final appearance if required for architectural applications.

Because the results of Specimen 11 were promising, the same finishing method was applied to Specimens 12–14.

The surface quality of Specimens 12–14 is shown in Figures 8.14–8.16.

Fig. 8.14 Surface detail of Specimen 12 (own image)

Fig. 8.15 Surface detail of Specimen 13 (own image)

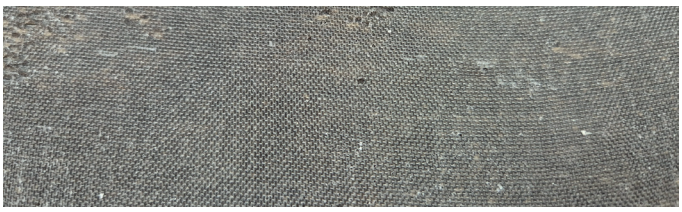

Fig. 8.16 Surface detail of Specimen 14 (own image)

8.2 MECHANICAL TEST SET-UP

8.2.1 TENSILE TEST CONFIGURATION

Tensile testing was again performed using a 100 kN universal testing machine located in the Mechanical Engineering Laboratory at Delft University of Technology under supervision. The experimental procedure followed standard tensile testing practice for fibre-reinforced polymer composites.

For the tensile tests, seven specimens were extracted from the manufactured Specimen 10. Care was taken to minimise cutting-induced damage and to ensure consistent specimen geometry across all samples. The tensile test specimens are shown in Figure 8.18. Since Specimen 10 does not exhibit a constant thickness along the profile, the cross-sectional dimensions were measured at the location of fracture in order to determine the accurate stress state at failure.

Prior to testing, the specimen edges were lightly sanded to reduce stress concentrations in the grip regions and to minimise the risk of premature failure at the clamps. The test set-up is displayed in figure 8.18.

Fig. 8.17 Specimen 10.1-10.7 prepared for tensile test (cut from specimen 10) (own image)

The first three specimens were clamped with an effective grip length of 50 mm on each side, resulting in a free gauge length of 100 mm during testing. The remaining four specimens were clamped with an effective grip length of 60 mm on each side, resulting in a reduced gauge length of 80 mm. This adjustment was necessary to prevent slippage during testing, as the clamping system used was prone to insufficient grip on the composite surface.

Fig. 8.18 Set-up tensile test at Mechanical engineering Lab, TU Delft (own image)

All tests were performed under displacement control, and force-displacement data were recorded continuously for subsequent stress–strain conversion.

8.2.2 THREE-POINT BENDING TEST CONFIGURATION

The three-point bending tests were again performed on a 100 kN universal testing machine in the Mechanical Engineering Laboratory at Delft University of Technology.

Figure 8.19 displayes Specimen 11-14 prepared for the three-point bending test.

Fig. 8.19 Specimens 11 and 12 prepared for the three-point bending test (own image)

To ensure that the relatively low hardness of the composite material does not adversely influence fracture behaviour, as observed in the mechanical tests conducted in Experimental Phase 2, a small aluminium strip (20 mm width, 8 mm height, and 60 mm length) was placed centrally on each specimen. This strip served to distribute the applied load across the full width of the specimen and to reduce local stress concentrations beneath the loading point.

During testing, each specimen was simply supported on two supports with a span of 210 mm. The load was applied at mid-span (105 mm from each support) through the aluminium strip. The experimental set-up is shown in Figure 8.20.

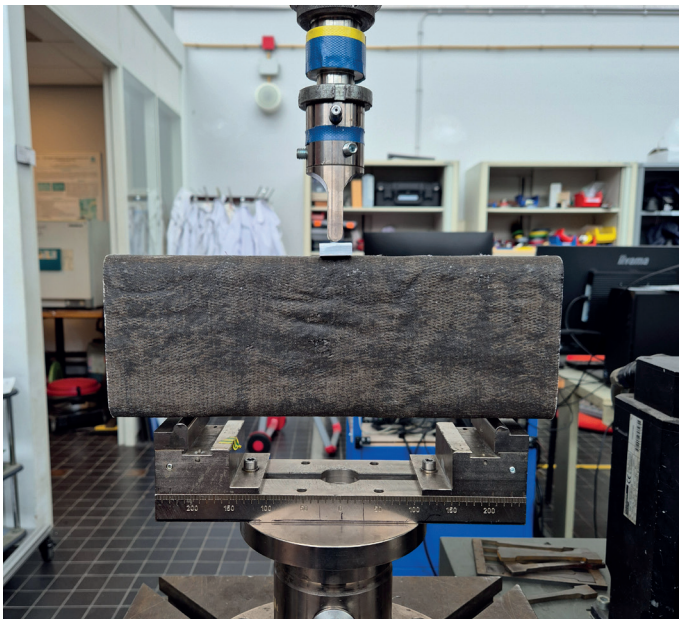

Fig. 8.20 Set-up three-point bending test at Mechanical Engineering lab, TU Delft (own image)

8.3 EVALUATION OF TEST RESULTS

EVALUATION OF THE TENSILE TEST RESULTS

The tensile tests on Specimens 10.1–10.7 exhibit a reduced scatter in tensile strength compared to the first experimental phase. This improved consistency is likely attributed to the fact that all samples were extracted from a single manufactured profile, rather than from multiple independently produced specimens. The average tensile strength was 64.7 MPa, which is comparable to, and slightly higher than, the average value obtained in Experimental Phase 2 (54.0 MPa), thereby confirming the repeatability of the material performance within expected variability limits.

The average Young's modulus was determined to be 0.83 GPa, which is significantly lower than the value obtained in the initial tensile campaign (approximately 9.0 GPa). This discrepancy is primarily associated with the measured strain response, which was considerably higher for Specimens 10.1–10.7. The increased strain is most likely not material-driven, but rather test-system induced, resulting from initial slack and compliance in the clamping system. This interpretation is supported by the stress–strain response, which shows an initially near-flat region before transitioning into a more linear segment once full grip engagement is achieved.

Table 8.1 summarises the tensile properties of Specimens 10.1–10.7 in comparison with Specimens 1–5 from Experimental Phase 2.

PROPERTIES	SAMPLE 10.1-10.8	SAMPLE 1-5 (first tests)
Average tensile strength (MPa)	*64.7*	*54.0*
Highest value tensile strength (MPa)	*78.7*	*99.0*
Spread from average tensile strength (MPa)	*10.4*	*21.0*
Average Young's Modulus (GPa)	*0.8*	*9.0*
Higherst value Young's Modulus (GPa)	*1.1*	*10.3*
Average elongation at break (%)	*5.2*	*1.0*
Average strain at plastic deformation (mm)	*10.4*	*2.0*
Average maximum force (N)	*10772*	*3911*

Table 8.1 Results of tensile test (own work).

A key observation is the substantially higher elongation at break and correspondingly lower apparent stiffness of Specimens 10.1–10.7 compared to Specimens 1–5. This is notable given that both material systems are nominally identical in terms of fibre type (cross-stitched flax), fibre-to-resin ratio (approximately 1:1.4), fibre volume fraction, and manufacturing technique.

The primary procedural difference between both experimental phases is the continuity of fibre architecture during manufacturing. In Specimens 1–5, the profile was produced using a continuous fibre lay-up, whereas Specimens 10.1–10.7 required the incorporation of multiple discrete fabric segments. This interruption likely introduced local discontinuities in fibre alignment and load transfer, as well as potential resin-rich interfaces between successive fabric sections, which may have contributed to earlier initiation of damage and increased deformation prior to failure.

EVALUATION OF THE STRESS-STRAIN DIAGRAM

The stress–strain response of Specimens 10.1–10.7 is presented in Figure 8.31 (Chapter 8.5.1). The curves exhibit an initially near-horizontal region, which is attributed to seating effects within the

clamping system and the accommodation of initial slack. Once full load transfer is established, the response becomes approximately linear, indicating a predominantly elastic fibre-dominated regime up to peak load.

Subsequently, the material reaches ultimate strength followed by a relatively abrupt loss of load-bearing capacity. Although intermediate matrix cracking was observed during testing, these events are not clearly distinguishable in the macroscopic stress–strain curves, suggesting that damage accumulation occurs progressively at a microstructural level without producing pronounced global stiffness reductions.

Despite the sudden final failure, the presence of prior matrix cracking indicates that damage initiation occurs before ultimate rupture. However, the limited resolution of the global stress–strain response prevents detailed identification of intermediate damage stages in this dataset.

FRACTURE CHARACTERISTICS

The fractured specimens are shown in Figure 8.21. Failure locations are distributed along the gauge length and are not strictly confined to the mid-span region, with several specimens also failing near or within the clamped sections. This suggests that local stress concentrations and grip-induced effects influenced the final failure location.

Fractographic inspection indicates a non-brittle failure mode dominated by fibre rupture rather than a purely resin-controlled fracture. The fracture surfaces are irregular and fibrous, which is consistent with progressive failure of the flax fibre reinforcement rather than a smooth cleavage through the epoxy matrix. This behaviour indicates that load transfer is primarily governed by fibre-dominated mechanisms at ultimate failure.

To ensure accurate stress calculation, the cross-sectional area at the fracture location was measured post-failure and used in the determination of tensile stress values, accounting for the non-uniform geometry of Specimen 10.

Fig. 8.21 Fractured tensile specimens (own image)

EVALUATION OF THE THREE-POINT BENDING TEST RESULTS

Similar to the three-point bending tests conducted on the smaller profiles in Experimental Phase 2 (Chapter 7), the larger composite profiles did not fail through global bending. Instead, failure was governed by local indentation and shear damage beneath the loading point. The aluminium strip used to distribute the load was progressively pressed into the upper flange of the profile, as shown in Figure 8.22. Consequently, local crushing and punching-shear failure occurred before the flexural capacity of the profile was reached, preventing the determination of flexural strength and stiffness.

The results indicate that the selected test configuration was unsuitable for inducing bending failure in the relatively thick flax fibre composite profiles. The combination of a short span length, a large cross-section, and the limited transverse compressive strength of the material caused local failure mechanisms to dominate.

A valid bending failure could likely only be achieved by increasing the span length or reducing the profile dimensions. The first option was beyond the scope of this project due to manufacturing limitations, while the second would effectively reproduce the smaller profile geometries already investigated in Experimental Phase 2.

Testing continued until the force-displacement response became nearly horizontal and additional displacement resulted primarily in local crushing beneath the loading strip. Although flexural

properties could not be determined, the local shear failure enabled calculation of the punching shear strength. Based on the maximum recorded force, an average punching shear strength of 8.7 MPa was obtained. This parameter is relevant for evaluating the pull-out resistance of fasteners and bolted connections in composite façade systems.

EVALUATION OF THE FORCE-DISPLACEMENT DIAGRAM

The force–displacement curves of Specimens 11 and 12 are presented in Figure 8.32 (Chapter 8.5.2). Both specimens exhibited a similar initial response, reaching approximately 6 kN at a displacement of 8–10 mm. This indicates that the profiles initially behaved as relatively stiff structural members capable of distributing the applied load.

Beyond this point, the responses diverged. Specimen 11 reached a maximum force of approximately 7.7 kN at a displacement of 12 mm, whereas Specimen 12 plateaued at approximately 6.3 kN. Following the peak load, both specimens exhibited a gradual reduction in load-carrying capacity with several distinct force drops.

These drops indicate progressive damage development, including matrix cracking, fibre-matrix debonding, local delamination, and crushing beneath the loading strip. Rather than failing catastrophically, both specimens continued to carry substantial loads after damage initiation, demonstrating a relatively high degree of damage tolerance and energy absorption.

FRACTURE CHARACTERISTICS

Figure 8.22 presents the specimens after testing.

Fig. 8.22 Tested specimens after three-point bending (left: Specimen 11, right: Specimen 12) (own image)

The observed damage confirms that failure was governed by local punching-shear and indentation rather than global bending. The aluminium strip penetrated the upper flange, creating a local crushed region beneath the loading point. Shear cracks developed around the perimeter of the loaded area, forming a punched section within the laminate.

No complete fracture of the profile occurred, and the lower flange remained intact throughout the test. This indicates that local compressive and shear failure developed before tensile rupture could occur on the underside of the profile.

Inspection of the damaged region revealed crushed fibres, local delamination, and fibre pull-out around the indentation zone. These features indicate progressive energy dissipation through damage accumulation rather than brittle fracture of the epoxy matrix. After unloading, partial elastic recovery was observed, although permanent deformation remained beneath the loading strip.

Overall, the fracture characteristics correspond closely with the force–displacement response and demonstrate a progressive, damage-tolerant failure mode. Although conventional flexural properties could not be obtained, the results highlight the material's ability to absorb energy and retain residual load-carrying capacity after damage initiation.

8.4 MANUFACTURING OF THE FACADE MODEL

The final outcome of this research is a curtain wall façade model incorporating the developed plant-fibre composite profiles. The profile configuration that demonstrated the highest mechanical performance, most consistent fibre-resin distribution, and best surface quality during the experimental programme was selected for the model.

As established in Chapter 5.5, a rectangular hollow section measuring 50 × 100 × 5 mm is required to satisfy the tensile, wind, and self-weight loads acting on a 1.5 × 3.0 m curtain wall section. Consequently, the same 50 × 100 mm aluminium mould used during Experimental Phase 3 was employed for manufacturing the façade profiles. The mould corners were rounded with a radius of 4 mm to facilitate fibre placement and reduce stress concentrations.

REQUIRED MATERIALS FOR FACADE MODEL

The following components were obtained from curtain wall façade manufacturer RAICO for the construction of the façade model:

1. A sealing system consisting of EPDM rubber seals and an insulation block, as shown in Figure 8.23.

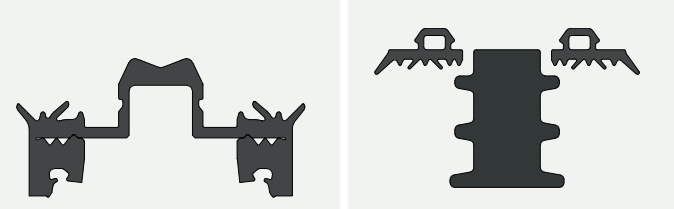

Fig. 8.23 Rubber sealing system (left: interior seal, right: insulation block) (RAICO, 2025).

2. Aluminium interior and exterior pressure profiles, shown in Figures 8.24 and 8.25.

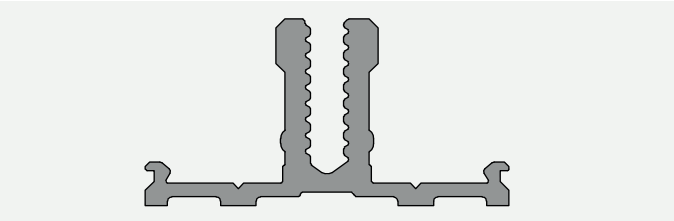

Fig. 8.24 Aluminum interior base profile (RAICO, 2025).

Fig. 8.25 Aluminum pressure profile (RAICO, 2025).

3. Standard 6 mm mechanical fasteners, identical to those evaluated in the fastener tests of Experimental Phase 2 (Figure 7.8, right).

4. Glazing panels manufactured from 5 mm thick acrylic sheets. Real glass was not used to avoid unnecessary weight in the presentation model. The glazing assembly represents a triple-glazed HR++ unit with a 20 mm cavity. The inner pane consists of two laminated 5 mm acrylic sheets, while the outer pane consists of a single 5 mm sheet. A black-painted timber spacer with an aluminium cap was used to simulate the glazing spacer system.

EXTERIOR CAP

The exterior cap of a curtain wall façade is not a primary structural component and is therefore subjected to lower mechanical demands than the mullions and transoms. In addition, it can be replaced relatively easily during maintenance. However, the component remains exposed to weathering and must therefore provide adequate environmental resistance.

For this reason, a non-woven hemp fibre mat reinforced with epoxy resin was selected for the exterior cap. Although this material exhibits lower mechanical properties than the cross-stitched flax fibre composite, it provides sufficient strength for this application while maintaining a natural appearance and reducing material costs. The relatively high resin content of the non-woven laminate is expected to improve moisture and weather resistance due to the protective properties of the epoxy matrix.

A dedicated mould was designed and manufactured using additive manufacturing techniques at the LAMA Lab, Faculty of Architecture, TU Delft. The manufacturing parameters used for the exterior cap are presented in Table 8.2.

MANUFACTURING PROPERTIES EXTERIOR CAP	
Fibre type	*Non-woven hemp fibre mat*
Fibre direction	*undirectional*
Mould material	*PETG*
Layers of Miracle gloss-8 wax release agent	4
Total fibre used	*≈ 150 cm x 35cm*
Number of layers	*3/0.29 ≈ 10.1*
Total fibre weight	*≈ 92 gr*
Amount of EL2 epoxy laminating resin	*92 x 2 ≈ 184 gr*
Amount of AT30 slow epoxy hardener	*184 x 0.3 = 55.2 gr*
Manufacturing time per specimen	*≈ 45 minutes*
Fibre volume fraction (uncut sample)	*23.4%*
Curing time (at room temperature)	*24 hours at room temperature*

Length of cut specimen	30 cm
Weight of cut specimen	≈ 184 gr

Table 8.2 Manufacturing properties of the exterior cap (own work).

The resulting component is shown in Figures 8.26 and 8.27.

Fig. 8.26 Exterior cap for façade model (own image)

Fig. 8. 27 Cross-section of exterior cap for façade model (own image)

CONNECTING PARTS

To connect the composite mullions and transoms, a timber connector block was fabricated and machined to match the internal geometry of the composite profiles. The corners of the block were rounded to correspond with the internal radii of the profiles. The connector was fixed to the mullion using long mechanical fasteners, after which the transoms were positioned around the connector and secured with screws.

In commercial curtain wall systems, mullions and transoms are typically connected using aluminium connector profiles. Although such a connection would provide greater structural capacity, a timber connector was selected for this model to minimise the use of aluminium and demonstrate the feasibility of a façade system with a reduced environmental impact.

RESULT OF FACADE MODEL

The completed façade model is presented in Figures 8.28–8.30. Figure 8.28 presents a front view, Figure 8.29 shows the cross-section of the system, and Figure 8.30 provides an overall view of the assembled façade model.

The completed façade model demonstrates the technical feasibility of integrating bio-based composite profiles within a conventional curtain wall façade system. The model shows that the developed flax fibre–epoxy profiles can accommodate standard façade components, including glazing, sealing systems, pressure plates, and mechanical connections, while significantly reducing the amount of aluminium required in the primary structure.

Fig. 8.28 Front view of façade model (own image)

Fig. 8.29 Cross-section of façade model showing: (1) flax fibre–epoxy mullion and transom profiles, (2) timber connector profile, (3) aluminium base profile, (4) rubber sealing system, (5) insulation block, (6) glazing spacer, (7) aluminium pressure profile, and (8) hemp fibre–epoxy exterior cap (own image)

Fig. 8.30 Overview of completed façade model (own image)

8.5 TEST RESULTS

This chapter discusses the results from the tensile tests conducted on sample 10.1-10.7 and three-point bending tests conducted on specimen 11-14. Furthermore, important material properties are calculated.

8.5.1 TENSILE TEST RESULTS

The specimens prepared for the tensile tests are presented in Tables 8.3.

The results of the tensile tests conducted on specimen 10.1-10.8 are presented in Table 8.4.

DENSITY OF SPECIMENS
The density of the samples are again calculated through the method discribed in section 5.4. The scale used for this measurement is the digital precision scale of 10kg capacity with a precision of 0.1gr.

AVERAGE TENSILE STRENGTH
The tensile strength is determined by deviding the maximum force by the cross-sectional area of the specimen.

The specimens manufactured samples during phase three exhibited an average tensile strength at failure of 64.7 MPa. In comparison, the specimens manufactured of the similar fibre type and reinforcement in the second experimental phase exhibited an average tensile strength of 65.2 MPa.

VALUE SPREAD
A lower variation in tensile strength was observed for specimens 10.1-10.7 compared to the first mechanical tests (specimen 1-5), with measured values ranging from 42 MPa to 79 MPa.

ELONGATION AT BREAK (%)
The elongation at break for the samples is calculated with the following formula:

$$\varepsilon_{break} \approx dl \text{ at break} / 200$$

where ε_{break} represents the extension at failure and 200 mm corresponds to the initial gauge length of the tensile specimens. The average elongation at break of specimen 10.1-10.7 is 5.2%.

YOUNG'S MODULUS
The Young's modulus was estimated from the initial slope of the stress–strain curve within the elastic region, prior to the onset of permanent deformation. The measured force-displacement data were converted to stress values using the cross-sectional area of the specimen displayed in table 8.3. The initial portion of the stress–strain curve was not perfectly linear due to factors such as minor specimen misalignment and slack within the clamping system. To ensure a consistent comparison between materials and minimise the influence of these effects, Young's modulus was determined using a strain interval as displayed in table 8.5.

Sample	Weight of fibres (gr)	Weight of matrix(gr)	Number of layers	Weight of cut specimen (gr)	Dimensions (mm x mm) *	Length sample (mm)	Density (g/cm^3)
10.1	*13.8*	*19.3*	*11.1*	*33*	*30 x 5.5*	*200*	*1.00*
10.2	*12.1*	*16.9*	*11.1*	*29*	*30 x 5.3*	*200*	*0.91*
10.3	*12.9*	*18.1*	*11.1*	*31*	*30 x 5.2*	*200*	*0.99*
10.4	*11.7*	*16.3*	*11.1*	*28*	*30 x 5.0*	*200*	*0.93*
10.5	*14.6*	*20.4*	*11.1*	*35*	*30 x 5.3*	*200*	*1.10*
10.6	*12.5*	*17.5*	*11.1*	*30*	*30 x 4.8*	*200*	*1.04*
10.7	*12.5*	*17.5*	*11.1*	*30*	*30 x 4.6*	*200*	*1.09*
Average	*12.6*	*17.7*		*29.9*			*0.99*

** Thickness values are the values from the thickness measurements from table 8.5*

Table 8.3 Overview of sample 10.1-10.7 prepared for tensile testing (own work).

Sample	Force at Break (N)	Tensile Strength at break (UTS) (MPa)	Spread from av. UTS (MPa)	Young's Modulus (GPa)	dl at break (mm)	Elongation at break (%)
10.1	*9871*	*62.1*	*0.4*	*1.1*	*7.7*	*3.9*
10.2	*8717*	*42.7*	*19.0*	*0.4*	*14.0*	*7.0*
10.3	*10968*	*69.0*	*7.3*	*0.9*	*11.6*	*5.8*
10.4	*12749*	*78.7*	*17.0*	*1.1*	*9.6*	*4.8*
10.5	*11575*	*68.9*	*7.2*	*0.9*	*10.1*	*5.1*
10.6	*10230*	*55.0*	*6.7*	*0.5*	*11.1*	*5.6*
10.7	*11294*	*76.8*	*15.1*	*1.0*	*8.8*	*4.4*
Average	*10772*	*64.7*	*10.4*	*0.8*	*10.4*	*5.2*

Table 8.4 Mechanical properties of sample 10.1-10.7 obtained from tensile testing (own work).

Sample	Thickness of sample at fracture (mm)	Strain range	Number of values within strain range
10.1	5.5	0.06 - 0.08	1020
10.2	5.3	0.08 - 0.12	1693
10.3	5.2	0.10 - 0.12	1020
10.4	5.0	0.10 - 0.12	780
10.5	5.3	0.12 - 0.14	780
10.6	4.8	0.08 - 0.12	1538
10.7	4.6	0.10 - 0.12	780

Table 8.5 Sample thickness at fracture point and accomodating strain range (own work).

STRESS-STRAIN DIAGRAM

The stress–strain curves of Specimens 10.1-10.7 are presented in Figure 8.31.

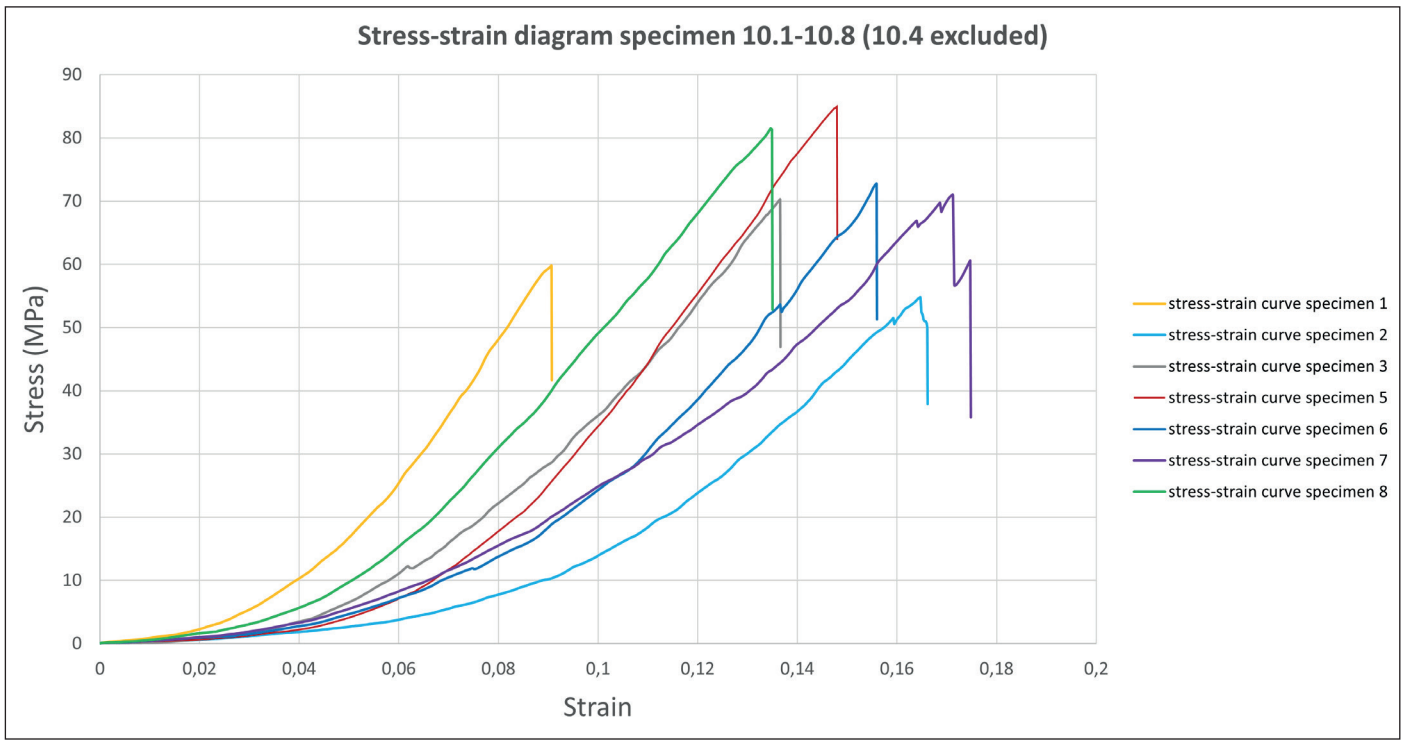

Fig. 8.31 Stress to strain diagram of tensile test of samples 10.1-10.7 (own image).

8.5.2 THREE-POINT BENDING TEST RESULTS

The specimens prepared for the three-point bending tests are presented in Table 8.6.

During the three-point bending tests conducted in the Mechanical Engineering Laboratory, the specimens could not be fractured through global bending failure. Instead, failure was governed by local damage mechanisms occurring beneath the loading nose. Even after placing an aluminium strip between the loading nose and the composite material to distribute the applied load over a larger area and reduce stress concentrations, local indentation and shear-related damage occurred before complete structural failure could be achieved. Consequently, the flexural strength and other full flexural properties could not be determined using this test configuration.

Nevertheless, the observed shear damage in the upper flange of the profile enabled the determination of the impact shear strength of the composite material. This parameter is relevant for assessing the pull-out resistance of fasteners and bolts embedded in the composite structure.

IMPACT SHEAR
The impact shear stress of the specimens was calculated using:

$\tau = F / A$

Where:
τ = the impact shear (Pa or MPa)
F = the maximum force (N)
A = the surface area of the composite material (mm^2)

The shear area was determined based on the cross-sectional area subjected to the applied load. Due

Specimen	Weight of fibres (gr)	Weight of matrix (gr)	number of layers	Weight of cut specimen (gr)	Dimensions (mm x mm)	Length sample (mm)	Density (g/cm^3)
11	*228*	*417*	*11.1*	*437*	*110 x 60 x 5*	*300*	*0.91*
12	*216*	*393*	*11.1*	*434*	*110 x 60 x 5*	*300*	*0.90*

Table 8.6 Overview of specimens for three-point bending test (own work).

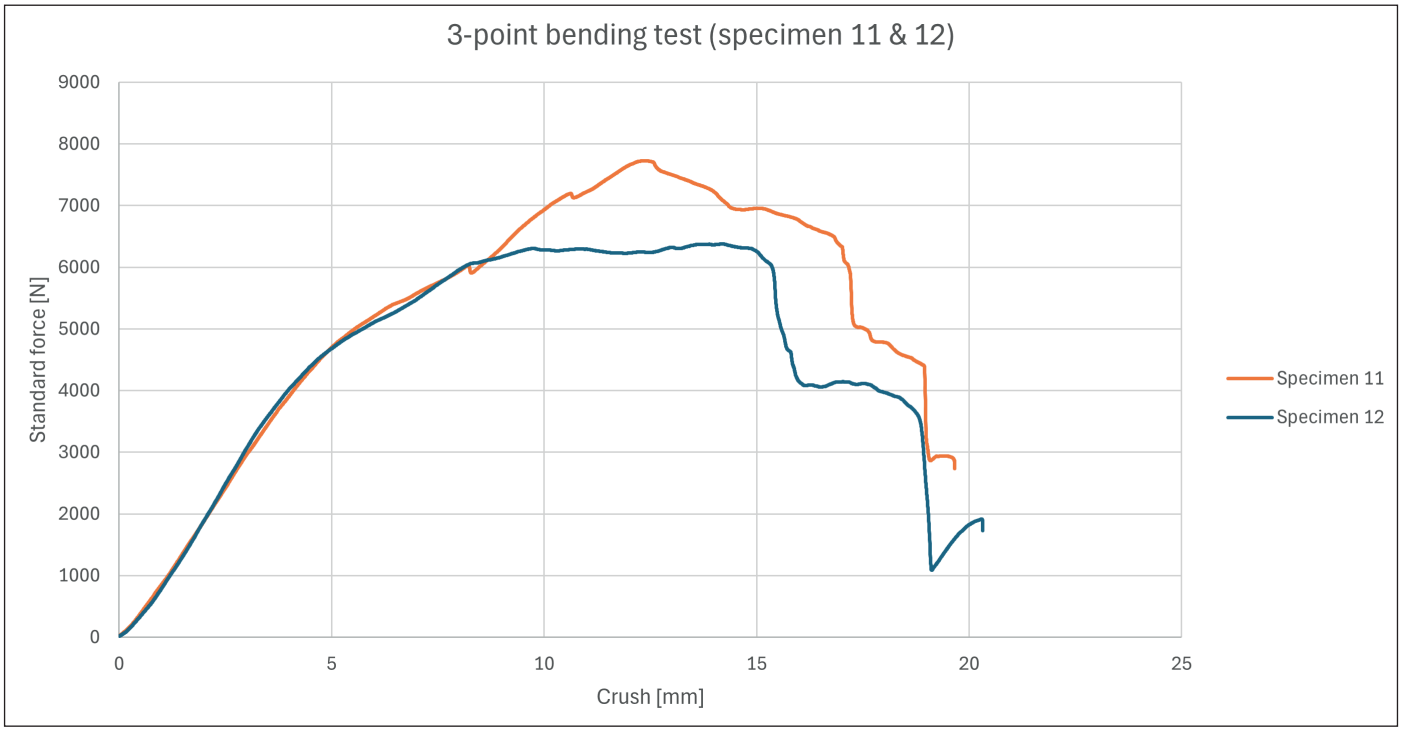

Fig. 8.32. Force to displacement diagram of three-point bending test specimen 11 and 12 (own image).

to the presence of the aluminium strip, the load was distributed across the width of the profile, resulting in a punched region that generated shear around the perimeter of the loaded area rather than along a single shear plane. The shear area was therefore calculated as:

$A_s = P * t$

Where:
A_s = Shear area (mm2)
P = area of applied force (mm)
t = thickness of the material (mm)

For specimen 11 and 12 this is calculated as follows:

$A_s = 2(60 + 20) * 5 = 800mm^2$

$\tau = F / 800mm^2$

The maximum force was obtained from the experimental test data. The resulting impact shear stresses are presented in Table 8.7.

Specimen	Max force (N)	Crush at max force (mm)	Impact shear τ (MPa)
11	7505	13.0	9.4
12	6375	13.9	8.0
Average	6940	13.5	8.7

Table 8.7 Results of specimens 11 and 12 (own work).

8.6 SUMMARY OF PHASE 3 FINDINGS

MANUFACTURING MULLION AND TRANSOM PROFILE GEOMETRY

The results of Experimental Phase 3 show that manufacturing the final mullion and transom geometry was successfully achieved, but only through careful adaptation of the production method to the limitations of the selected textile reinforcement. The cross-stitched flax fibre composite was again identified as the most suitable material system, since the tensile tests confirmed that it retained a favourable balance between strength, ductility and damage tolerance at the larger profile scale. At the same time, the production of the 50 × 100 × 4 mm geometry required multiple fabric sections, which introduced additional manufacturing complexity and made fibre continuity more difficult to control.

The comparison between the manufactured specimens clearly demonstrates that process control had a direct influence on the final laminate quality. Specimen 10 showed local fibre accumulation, resin-rich regions and non-uniform thickness, indicating that interruptions during fabric replacement can adversely affect the internal structure of the profile. In contrast, specimens 11–14 were manufactured with improved handling and more consistent tension, resulting in better consolidation, fewer visible defects and a more uniform surface quality. This confirms that the final profile geometry is technically feasible, but also that repeatability depends strongly on the manufacturing sequence and the coordination between operators.

MECHANICAL STRENGTH OF PROFILES

The tensile test results show that the larger cross-stitched flax fibre profiles still provide a high level of mechanical performance. The average tensile strength of the final specimens was 64.7 MPa, which is slightly higher than the average value obtained in the previous experimental phase. This indicates that scaling up the profile geometry did not lead to a loss in tensile capacity, and that the material system remained structurally effective when transferred to a larger application-oriented section. The lower scatter in tensile strength also suggests improved consistency, which is an important advantage for future structural use.

Although the measured average Young's modulus was considerably lower than in the earlier phase, this should be interpreted with caution. The initial part of the stress-strain curves was influenced by seating effects, initial slack and clamping compliance, which reduced the apparent stiffness of the specimens. Once full load transfer had been established, the profiles behaved in a more stable and load-bearing manner. The tensile response therefore still supports the conclusion that the cross-stitched flax fibre composite is capable of carrying substantial loads, but that testing conditions and grip behaviour must be considered carefully when interpreting stiffness values.

The bending tests did not result in a conventional global flexural failure. Instead, the larger profiles failed locally by indentation and punching shear beneath the loading point. This shows that the profiles possessed sufficient strength to resist bending loads for a considerable period, but that the test configuration was not suited to develop full flexural rupture. Even so, the results remain valuable because they demonstrate the structural robustness of the profile and provide a useful indication of local compressive and shear capacity, which is highly relevant for façade applications and connection design.

FRACTURE MECHANICS OF PROFILES

From a fracture mechanics perspective, the final profiles exhibited a progressive and damage-tolerant failure mechanism rather than a sudden brittle collapse. In the tensile tests, fracture was accompanied by irregular and non-planar surfaces, which indicates that failure was governed by fibre rupture, matrix cracking and local fibre-matrix debonding. The fact that failure locations were distributed along the gauge length, and in some cases near the grips, further suggests that local stress concentrations and clamping effects influenced the final fracture process. This behaviour is consistent with a textile composite in which the reinforcement architecture and the quality of load transfer play a decisive role.

The bending tests revealed a different but equally informative failure mode. Instead of a complete fracture of the profile, local indentation occurred at the loading point, followed by shear cracking and crushing of the upper flange. The aluminium strip distributed the applied load to some extent, but the composite still failed locally once the transverse compressive and shear stresses became too high. Importantly, the specimens continued to carry load after damage initiation, which indicates progressive failure and substantial energy absorption. For structural applications, this is preferable to brittle

fracture, because it provides warning before final failure and allows the material to retain residual load-bearing capacity after local damage has occurred.

GENERAL CONCLUSION

Overall, the third experimental phase confirms that the cross-stitched flax fibre composite is suitable for further development as a bio-based façade profile material. The final geometry could be manufactured successfully, the tensile performance remained strong, and the fracture response showed a favourable progressive failure mode. Although the bending tests revealed limitations in local compressive and shear resistance, the material system still demonstrated sufficient structural potential for curtain wall applications. Consequently, the experimental phase provides a strong basis for continued refinement of the profile design and its integration into sustainable façade systems.

9. PROFILE VALIDATION & PERFORMANCE ASSESSMENT

9. PROFILE VALIDATION & PERFORMANCE ASSESSMENT

This chapter discusses the mechanical strength, visual appearance, durability, maintenance and end-of-life potential of the flax-fibre/epoxy profiles manufactured during this project. These properties are then compared to that of conventional building materials used for the construction of façade systems like aluminum, steel and engineered timber. In addition, the composite profiles are assessed in relation to the EU building codes for curtain wall façades and the upscaling of the manufacturing technique is discussed during this chapter.

First, a life-cycle assessment (LCA) is performed on the manufacturing and use of the plant-fibre composite profiles to obtain the Global Warming Potential (GWP) of the flax-fibre/epoxy composite profiles.

9.1 LIFE CYCLE ASSESSMENT OF PROFILES

Figure 9.0 displays the components of a Life Cycle Assessment (LCA). An LCA is a modelling tool used to quantify the environmental impacts of products and processes (Eckelman & Nunberg, 2026). For the manufactured profiles in this project, an LCA is performed to assess the carbon footprint of the product and to determine whether these profiles are environmentally preferable compared to alternative materials such as aluminium, steel, or wood.

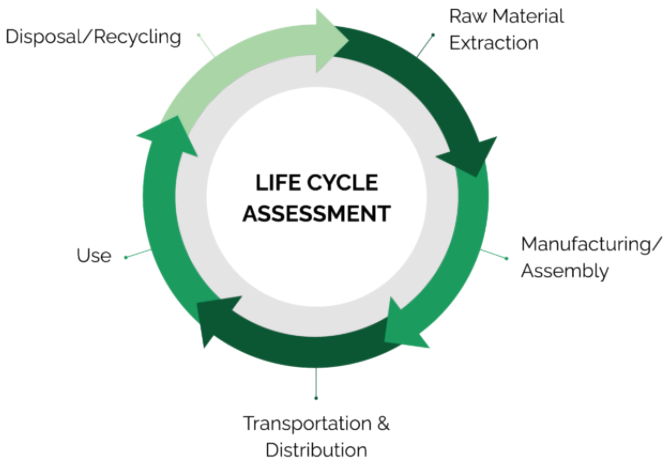

Fig. 9.0. Components of a life cycle assessment (Eckelman & Nunberg, 2026)

The LCA consists of five stages. Stage A1 covers raw material extraction from nature via mining, drilling, or harvesting. Materials are then refined and transported to manufacturing (A2), where they are combined and packaged (A3). After production, transport to site occurs (A4), followed by use (A5), which may last decades or only a short period depending on the product. The final stage is end-of-life treatment (Eckelman & Nunberg, 2026).

RAW MATERIAL EXTRACTION (A1)

The components of the plant-fibre profiles are natural flax fibre and a two-component thermosetting epoxy resin.

NATURAL FLAX FIBRE

Flax fibre is 100% European, sourced from Normandy, France. After harvesting, dew retting is applied by laying flax on the ground to decompose non-fibrous material. This is followed by scutching, hackling, and drying. Scutching removes woody parts, hackling aligns and cleans fibres, and drying reduces moisture (Balasubramanian M. et al., 2024).

At Eco-Technilin (Normandy), flax is processed into non-woven mats or woven textiles using industrial equipment (Temafa, 2024). The cross-stitched fibre used here is chemically untreated, while industrial flax is often treated for bonding, moisture resistance, or fire resistance.

The material is distributed via EasyComposites Europe (Rijen, Netherlands). Flax fibre typically requires 2–5 times less energy than glass fibre, and its production is often considered carbon neutral or negative due to CO_2 uptake during growth (Easycomposites, 2025).

Lopez-Arraiza et al. (2025) reported a climate footprint of 1.15 kg CO_2-eq per kg of flax fibre in a study on ship hulls using flax fibre and bio-epoxy. The study identified electricity consumption as the primary contributor to environmental impact, indicating that the use of renewable energy could significantly improve sustainability. Barth & Carus (2015) reported a lower total global warming potential (GWP) of 0.80 kg CO_2-eq per kg flax fibre (cradle to gate).

For this study, the average of the two reported values is used. Therefore, the GWP for flax fibre production is assumed to be 0.97 kg CO_2-eq per kg.

2-COMPONENT EPOXY RESIN

A two-component thermosetting epoxy resin is used in the production of the plant-fibre profiles. CarbonCloud (2026) reports a total lifecycle footprint of 11.96 kg CO_2-eq per kg epoxy resin. The main constituents include sodium hydroxide (NaOH), bisphenol A (BPA), and epichlorohydrin (ECH). Of the total emissions, 5.31 kg CO_2-eq per kg (44%) is attributed to fossil resource extraction and use, 0.06 kg CO_2-eq per kg (0.5%) to transport, and 6.59 kg CO_2-eq per kg (55%) to refining processes.

The fibre-to-resin ratio used in this study is 1:1.4. The climate impact of 1 kg of composite material is therefore calculated as follows:

0.417 kg flax fibre × 0.97 kg CO_2-eq/kg = 0.40 kg CO_2-eq/kg

0.583 kg epoxy resin × 11.96 kg CO_2-eq/kg = 6.98 kg CO_2-eq/kg

This results in a total GWP of 7.38 kg CO_2-eq per kg of flax fibre/epoxy composite, excluding transport to the manufacturing site.

TRANSPORTATION OF RAW MATERIAL (A2)

After extraction and refinement, materials are transported to the composite profile manufacturer in Delft. For this study, transport emissions are calculated for delivery from Normandy, France (flax fibre, 563 km) and Rijen, the Netherlands (epoxy resin, 83 km), resulting in a total transport distance of 646 km.

A 3.5–7.5 metric ton lorry is assumed. Michelin (2025) reports average emissions of 0.35 kg CO_2-eq per km for this vehicle class, resulting in 226.10 kg CO_2-eq for full transport. However, assuming a full load capacity of 3,500 kg, the transport impact is distributed across the load, resulting in 0.07 kg CO_2-eq per kg of composite material.

MANUFACTURING OF PROFILES (A3)

The production of plant-fibre composite profiles involves several auxiliary materials and processes, including:

- Oven heating (2 hours at 60 °C) for fibre drying and post-curing
- Resin application using rollers or brushes
- Aluminium moulds (reusable)
- Vacuum bagging materials (single use per profile)

No heavy industrial machinery is used; therefore, the environmental impact of manufacturing is assumed to be negligible compared to raw material production and transport.

TRANSPORTATION TO BUILDING SITE (A4)

For this study, a hypothetical construction site is located in Amsterdam. Transport is carried out using a 32-ton lorry with a payload capacity of 20 tons and standard dimensions (L = 12 m, W = 2.5 m, H = 2.5 m).

Profiles are assumed to measure 100×50×5mm with a length of 2 m and are transported on Europallets (0.8×1.2×0.15m). Approximately 30 pallets fit per truck, with 10 profiles per 2 pallets, resulting in 150 profiles per shipment (total mass ≈ 450 kg). Each 2m profile weighs approximately 3 kg (based on Chapter 8, Table 8.2).

The transport distance from Delft to Amsterdam is approximately 70 km. Michelin (2025) reports emissions of 0.5 kg CO_2-eq per km for heavy-

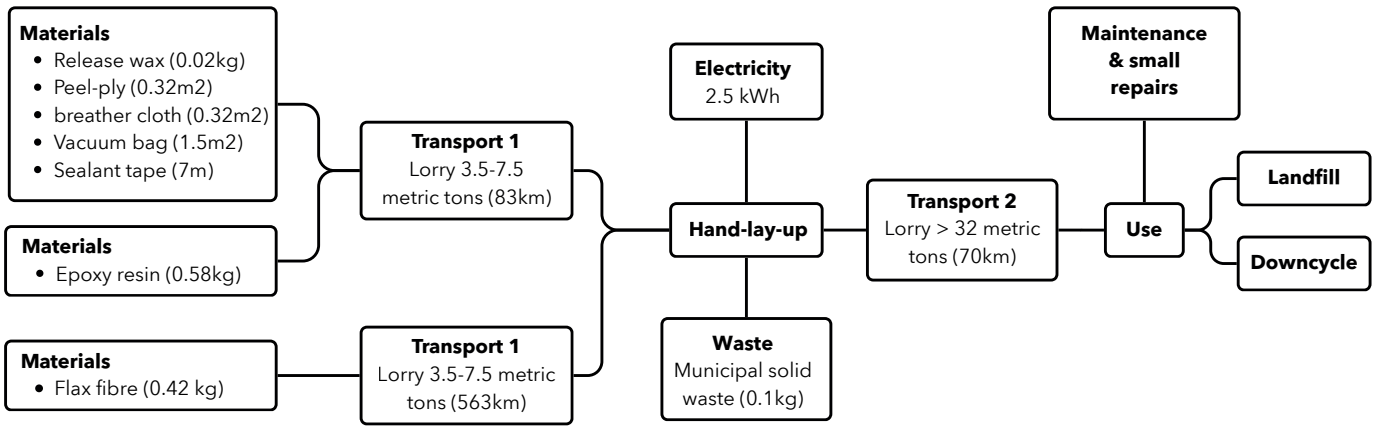

Fig. 9.1 Life cycle data of 1kg flax-fibre/epoxy composite profile (adapted from Lopez-Arraiza et al., (2025))

duty trucks (>7.5 tons). Due to the low mass of the composite, transport emissions are reduced, resulting in 0.07 kg CO_2-eq per kg of composite material.

USE (A5)
During use, maintenance, repair, and storage conditions are critical. Profiles should be stored dry prior to installation to prevent moisture ingress. Epoxy resin provides high resistance to moisture, chemicals, and UV radiation. Therefore, properly manufactured profiles are expected to have a service life of at least 30 years with minimal replacement.

Since the profiles are installed behind glazing in curtain wall façades, direct UV exposure and moisture are limited. Nevertheless, periodic inspection is required to detect cracking or fibre–matrix debonding. Maintenance includes dry cleaning, visual inspection, marking potential defects, and periodic mechanical testing under controlled conditions. Non-compliant profiles may be repaired by applying an additional epoxy layer to restore surface protection. The epoxy system cures at room temperature, enabling rapid on-site repairs.

END-OF-LIFE POTENTIAL (EOL) OF PROFILES
Flax fibre is biodegradable under landfill conditions, whereas thermosetting epoxy resin is not. Once cured, epoxy cannot be remelted or reprocessed like thermoplastics, limiting material reuse.

Biodegradation tests of plant-fibre/epoxy composites show that soil exposure leads to microbial attack and epoxy degradation, causing microcracks and increased moisture ingress. This promotes fibre swelling and fungal growth, significantly reducing mechanical performance, but does not fully decompose the composite (G. Rajeshkumar et al., 2022). To address end-of-life challenges, three recycling routes have been developed: mechanical, thermal, and chemical recycling (Mu Q. et al., 2022).

Mechanical recycling involves crushing composites for use as filler material but is energy intensive. Chemical recycling uses solvent-based processes such as solvolysis or acid treatment to recover resin components. Thermal recycling involves combustion of organic fibres for energy recovery, while inorganic residues may be reused in cement applications (G. Rajeshkumar et al., 2022).

These methods are primarily developed for glass- and carbon-fibre composites and are less suitable for natural-fibre composites. Efficient chemical recycling of epoxy thermosets remains challenging due to slow decomposition rates and difficulty in recovering reusable components under mild conditions (Mu Q. et al., 2022). As a result, a significant portion of current flax-fibre/epoxy composites is incinerated for energy recovery.

An alternative end-of-life route is reuse in non-structural applications such as façade elements or wall components. Until fully biodegradable thermoset systems are available, disposal is expected to rely on mechanical separation and energy recovery using renewable energy sources.

ECO AUDIT ASSESSMENT
The Eco Audit tool in Ansys® Granta EduPack is used to evaluate total energy use and carbon emissions of the flax fibre/epoxy composite. Input data is provided in Appendix F.

Figure 9.2 shows the distribution of energy use and climate impact over the lifecycle of 1,000 kg of composite material. The results indicate that stage A1 (raw material extraction) is the dominant contributor to both energy use and CO^2 emissions. This is primarily driven by epoxy resin production, as shown in Table 9.0, where epoxy accounts for 88.6% of total emissions and flax fibre for 11.4%.

OVERVIEW RESULTS LCA
The LCA results from Ansys® Granta EduPack are compared with literature values and manual calculations. Differences in A1 results are primarily due to the epoxy resin dataset used in EduPack, which reports 6.49 kg CO_2-eq per kg compared to 11.96 kg CO_2-eq per kg from CarbonCloud (2026).

For manufacturing, EduPack assumes a filament winding process with an energy demand of 9 MJ/kg and a climate impact of 0.60 kg CO_2-eq/kg.

Table 9.1 displayes the result of the LCA of the flax-fibre/epoxy composite profiles manufactured during this project.

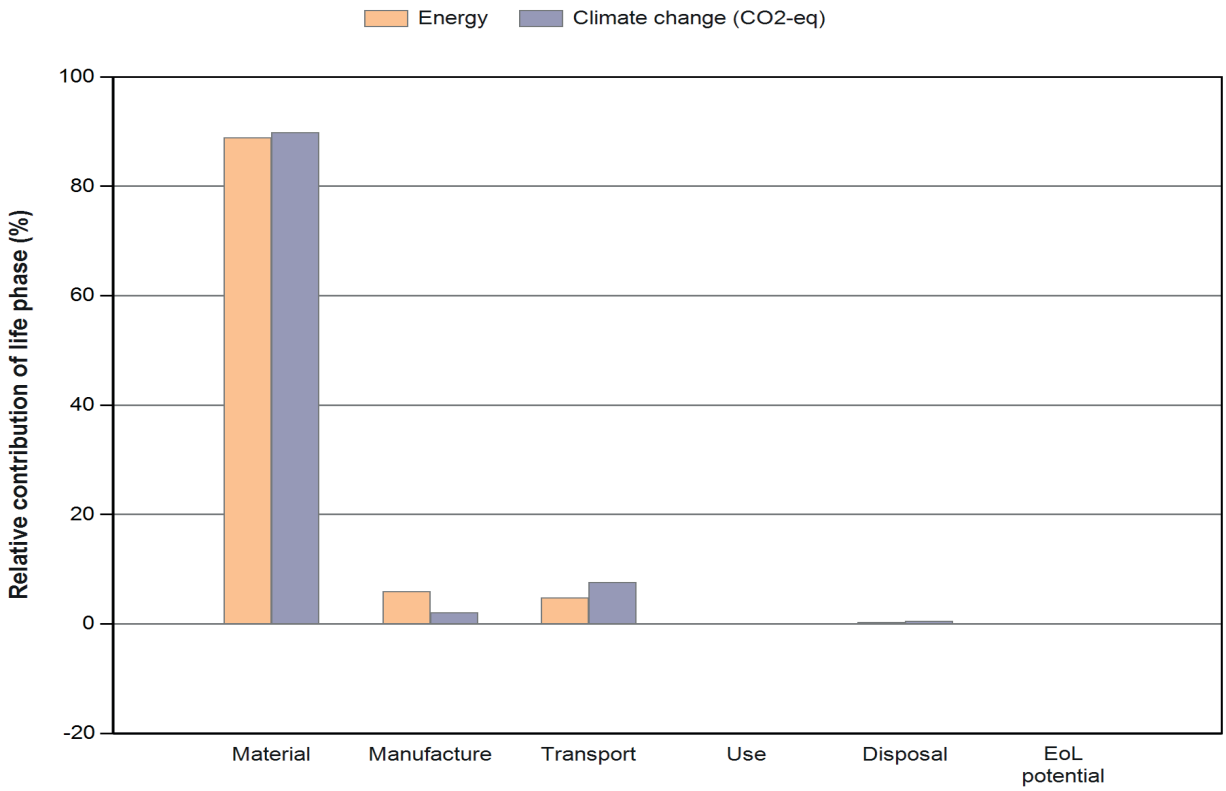

Fig 9.2. Result ECO AUDIT Assessment of flax-fibre/epoxy composite profiles (Generated by Ansys® Granta EduPack 2025)

Component	Material	Recycled content* (%)	Part mass (kg)	Qty.	Total mass processed** (kg)	Climate change (CO_2-eq) (kg)	%
Flax fibre	Flax fibre	Virgin (0%)	420	1	460	520	11.4
Epoxy resin	Epoxy resin (heat resistant)	Virgin (0%)	580	1	650	4000	88.6
Total				2		4520	100

* Typical: Includes 'recycle fraction in current supply'
** Where applicable, includes material mass removed by secondary processes

Table 9.0. Eco Audit tool result details stage A1 (Generated by Ansys® Granta EduPack 2025)

RESULT LCA OF FLAX-FIBRE/EPOXY COMPOSITE PROFILE		
LCA Stage	**GWP (own) (kg CO_2-eq per kg)**	**GWP (Edupack software) (kg CO_2-eq per kg)**
Raw material extraction (A1)	7.38	4.52
Transportation of raw material (A2)	0.065	0.378
Manufacturing of profiles (A3)	0.6	0.1
Transportation to building site (A4)	0.07	0.0073
Use (A5)	Low maintenance / small repairs	Product life: 30 years
Disposal	Downcycling, combustion for energy recovery, Landfill	0.024
Total GWP	8.12	5.03

Table 9.1 LCA results flax-fibre epoxy profiles (own work)

9.2 COMPARISON WITH CONVENTIONAL BUILDING MATERIALS

A comparison is made between the flax-fibre/epoxy composite profiles and conventional materials used for similar façade profile applications. This chapter evaluates Global Warming Potential (GWP), durability, visual appearance, mechanical strength, and end-of-life potential of the composite against aluminium, steel, solid and engineered timber profiles. A flax-fibre/bio-epoxy variant is included for future reference. Data are obtained from scientific literature and Ansys® Granta EduPack 2025.

9.2.1 GLOBAL WARMING POTENTIAL

Table 9.2 presents the kg CO_2-eq per kg for raw material extraction and profile production for each material. Oceanic region data are used, as this is considered a likely implementation region due to economic conditions and innovation drivers.

FLAX-FIBRE/EPOXY PROFILE

As calculated in Chapter 9.1, production of 1 kg flax-fibre composite (A1–A2) results in 7.38 kg CO_2-eq/kg. In stage A3 (manufacturing), an electric oven is used for fibre drying and curing (2 hours at 60°C), contributing approximately 0.60 kg CO_2-eq/kg (Clever Carbon, 2025). The total GWP is therefore approximately 8.10 kg CO_2-eq/kg.

FLAX-FIBRE/BIO-EPOXY PROFILE

A bio-epoxy can be used as a future alternative. Several bio-based epoxies are commercially available and show significant reductions in CO^2 emissions compared to petroleum-based resins. LCA studies indicate reductions of 28–34% (average 31%)(Lopez-Arraiza et al., 2025). In addition, biomass-derived resins from waste or by-products reduce environmental impact without competing with food production.

Applying this reduction to the epoxy contribution from Section 9.1 results in a GWP of 5.09 kg CO_2-eq/kg for raw materials. Adding manufacturing (0.60 kg CO_2-eq/kg) gives a total GWP of 5.69 kg CO_2-eq/kg.

ALUMINUM PROFILE

The GWP of aluminium depends on alloy composition and surface treatment. For this study, 6060-T6 aluminium used by STABALUX for curtain wall profiles is used (STABALUX, 2025). Ansys® Granta EduPack reports 13.30 kg CO_2-eq/kg (virgin grade) and 9.72 kg CO_2-eq/kg (typical grade).

European Aluminium (2024) reports 9.70 kg CO_2-eq/kg for European production (cradle-to-gate), consistent with EduPack typical values. The extrusion process to manufacture the profile geometry adds approximately 0.38 kg CO_2-eq/kg, resulting in a total range of 10.10–13.30 kg CO_2-eq/kg.

Hoxha et al. (2025) report regional averages of 11.80 kg CO_2-eq/kg for oceanic regions. Raw material supply (A1) contributes about 88–97% (average 92.5%) to this GWP. This results in approximately 10.92 kg CO_2-eq/kg for A1–A2 and 0.88 kg CO_2-eq/kg for production.

STEEL PROFILE

The steel used for the curtain wall mullions and transoms by STABALUX is galvanized S280 steel (STABALUX, 2025). EduPack reports 3.16 kg CO_2-eq/kg (virgin grade) and 2.24 kg CO_2-eq/kg (typical grade). Profile forming via hot extrusion to manufacture the profile geometry adds 1.47 kg CO_2-eq/kg, resulting in a total of 4.63 kg CO_2-eq/kg.

For a more general GWP for steel, Worldsteel Association (2025) reports an average of 2.18 kg CO_2-eq/kg for steel with <10% scrap content, with lower values possible at higher scrap rates (>70%).

In addition, Hoxha et al. (2025) report regional values of 3.70 kg CO_2-eq/kg for Oceanic regions. Stage A1 (raw material extraction) contributes 81–91% (average 86%), while stage A3 (manufacturing) contributes 3–13% (average 7%). This corresponds to 3.18 kg CO^2-eq/kg (Stage A1–A2) and 0.26 kg CO_2-eq/kg (production). EPD Hub (2025) reports 2.54 kg CO_2-eq/kg (A1–A3) for steel hollow sections, with 2.48 kg CO_2-eq/kg from raw materials and 0.05 kg CO_2-eq/kg from transport and manufacturing.

SOLID AND ENGINEERED TIMBER PROFILE

Hybrid and natural materials, such as engineered timber products derived from timber, can be associated with CO_2 sequestration during the growth phase prior to felling, or after felling and during tree regrowth. This is referred to as storage of biogenic carbon, and in the former case is represented as a negative GWP value during the

MATERIAL	GWP (A1-A2) (kg CO_2-eq/kg)	GWP (A3) (kg CO_2-eq/kg)	TOTAL GWP (A1-A3) (kg CO_2-eq/kg)	REFERENCES
Flax-fibre/Epoxy profiles	*7.38*	*≈ 0.6*	*≈ 8.1*	*(Lopez-Arraiza, A., et al., 2025), (Barth & Carus, 2015) Clever Carbon, 2025*
Flax-fibre/ Bio-Epoxy profiles	*5.09*	*≈ 0.6*	*≈ 5.69*	*(Lopez-Arraiza, A., et al., 2025) Clever Carbon, 2025*
Aluminum profiles	*9.7 - 10.9*	*0.38 - 0.88*	*10.1 - 13.3*	*European Aluminum, (2024) Hoxha E. et al. (2025) Ansys® Granta EduPack*
Steel profiles	*2.48 - 3.18*	*0.046 - 0.26*	*2.18 - 4.63*	*Hoxha E. et al. (2025) WorldSteel Association (2025) EPD Hub (2025) Ansys® Granta EduPack*
Solid and engineered Timber profiles	*≈ 0.58*	*≈ 0.17*	*-1.48 (when sources from sustainably managed forests and stored in biomass) - 0.48*	*Hoxha E. et al. (2025) Rubner Holding A.G.-s.p.a (2023) Burdett, S., et al., (2026) Ansys® Granta EduPack*

Table 9.2. Climate footprint material comparison (own work)

A1 module of an LCA (assuming timber is sourced from sustainably managed forests) (Burdett, S., et al.,. 2026). For this study, a solid pine profile is used from the Ansys® Granta EduPack. Pine wood in EduPack shows 0.29 kg CO_2-eq/kg (virgin and typical grade production).

Rubner Holding A.G. (2023) reports 1.48 kg CO^2-eq/kg (Stage A1–A3) for glulam beams (spruce, pine, larch, Douglas fir), assuming incineration in biomass energy recovery. Burdett S. et al. (2026) report fossil emissions of 0.16–0.49 kg CO_2-eq/kg (average 0.33 kg CO_2-eq/kg), consistent with ICE and EduPack datasets. EduPack reports 0.48 kg CO_2-eq/kg for glulam (virgin and typical production).

9.2.2 DURABILITY

Table 9.3 presents expected service life for each material. The durability of flax-fibre/epoxy is highly dependent on environmental conditions.

Oun A. et al. (2024) report a 60% strength retention after 190 hours at 30°C in hygrothermal conditions. Other studies indicate up to 50% strength loss after 5 years in harsh outdoor exposure. Benzart K. (2019) shows that moderate humidity (50–75% RH) can have limited effects on tensile properties, with slight strength increases observed due to post-curing at elevated temperatures. This deviation in results shows that extensive research into the long-term durability of flax-fibre/epoxy composites need to be conducted before they can be used in oudoor environments.

For the intended application (indoor or semi-protected curtain wall environments), limited UV exposure, controlled humidity, and moderate temperatures are expected. A service life of 30–40 years is therefore assumed with appropriate maintenance.

Material	Expected service life (years)	Reference
Flax / epoxy curtain wall framing	30 - 40	Estimation based on Benzart. K., (2019) and Oun. A et al., (2024)
Flax / bio-epoxy curtain wall framing	30 - 40	Estimation based on Benzart. K., (2019)and Oun. A et al., (2024)
Aluminum curtain wall framing	43 - 75	Cerclos, 2015 Reynaers Aluminum (2022)
Steel curtain wall framing	83	Cerclos, 2015
Timber curtain wall framing	65	Cerclos, 2015

Table 9.3. Expected service life of structural frame member materials (own work)

ENHANCING THE DURABILITY OF FLAX-FIBRE/ EPOXY COMPOSITE PROFILES

Fibre surface treatments can improve the initial hygrothermal response of flax-fibre/epoxy composites; however, no consistent long-term improvement is observed under prolonged ageing. This is primarily due to degradation of both the polymer matrix and the fibre–matrix interface under hygrothermal conditions. As a result, the effectiveness of physical and chemical fibre surface modifications (see Chapter 3.1.4) is limited over extended service life. Therefore, alternative strategies are required to improve long-term performance under moisture and temperature exposure.

Oun A. et al. (2024) demonstrate that long-term durability can be improved through the incorporation of nanomaterials. Accelerated ageing tests show that hybrid composites containing 0.5% graphene nanoparticles retain at least 57% of flexural strength and 49% of interlaminar shear strength after the equivalent of 100 years in service under hygrothermal conditions at 30°C. Similarly, Khotbehsara et al. (2020) report that epoxy systems filled with fire retardants and fly ash, exposed to 98% relative humidity at elevated temperatures, retain most mechanical properties. This is attributed to reduced moisture uptake and an increased glass transition temperature (Tg). Overall, these studies indicate that the incorporation of filler materials or nano-reinforcements can significantly enhance the long-term durability of flax-fibre/epoxy composites in harsh environmental conditions.

9.2.3 MECHANICAL STRENGTH

The mechanical performance of the flax-fibre/epoxy composite profiles is compared with conventional façade materials using Ansys® Granta EduPack.

Figure 9.3 presents tensile strength as a function of density. The average tensile strength obtained in this study ranged from 54.0 MPa during experimental phase 2 to 64.7 MPa for the final profile geometry in experimental phase 3, with peak values reaching 99 MPa and 78.7 MPa, respectively. These values are comparable to high performance plastics but remain significantly lower than those of engineering composites and metals. A red dot labeled 1. in figure 9.3 represents the tensile strength of the flax-fibre/epoxy composite material obtained during this project.

Figure 9.4 compares Young's modulus and density. The highest measured stiffness was approximately 9.0 GPa, while the larger profiles achieved an average of 0.83 GPa. The lower stiffness of the final specimens is likely influenced by test-related factors, including grip slippage and increased strain measurements. Therefore, the Young's Modulus of the smaller profiles best represents the value for

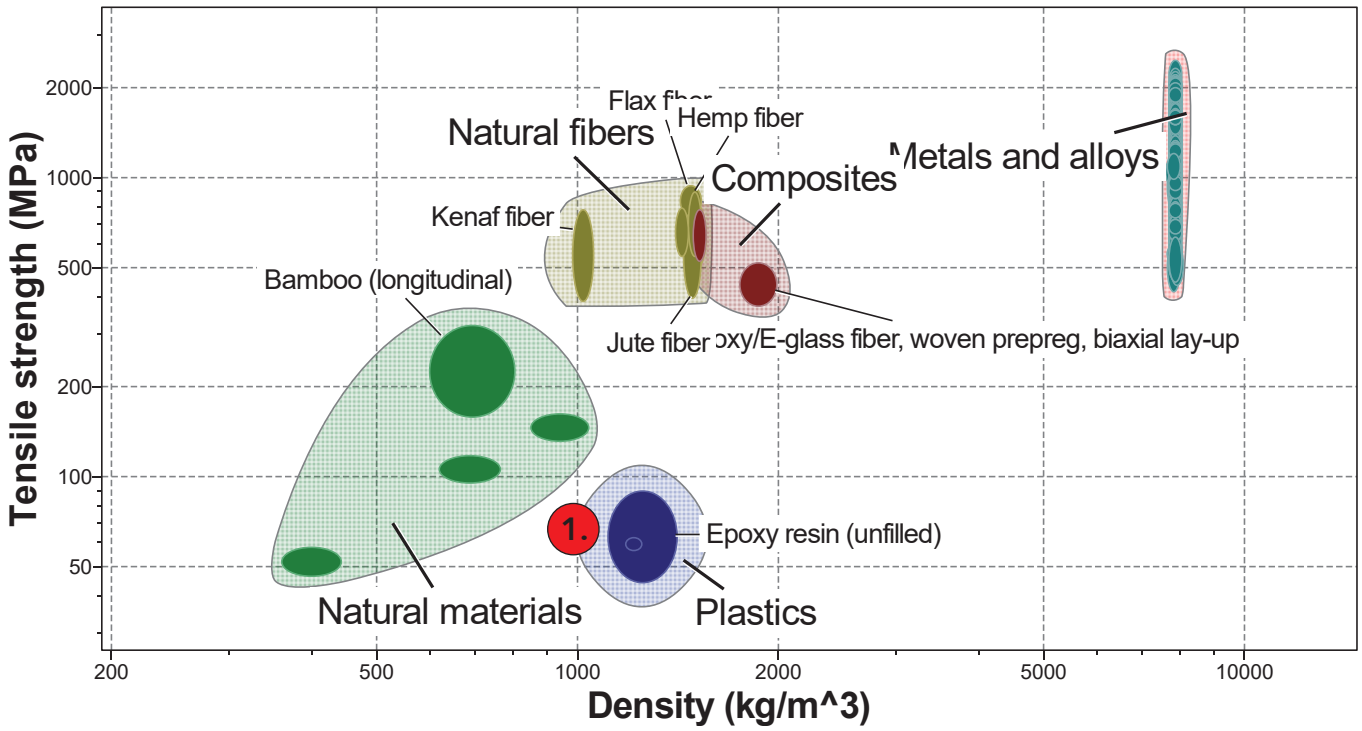

Fig. 9.3. Plot of tensile strength as a function of density using Ansys® Granta EduPack (Generated by Ansys® Granta EduPack)

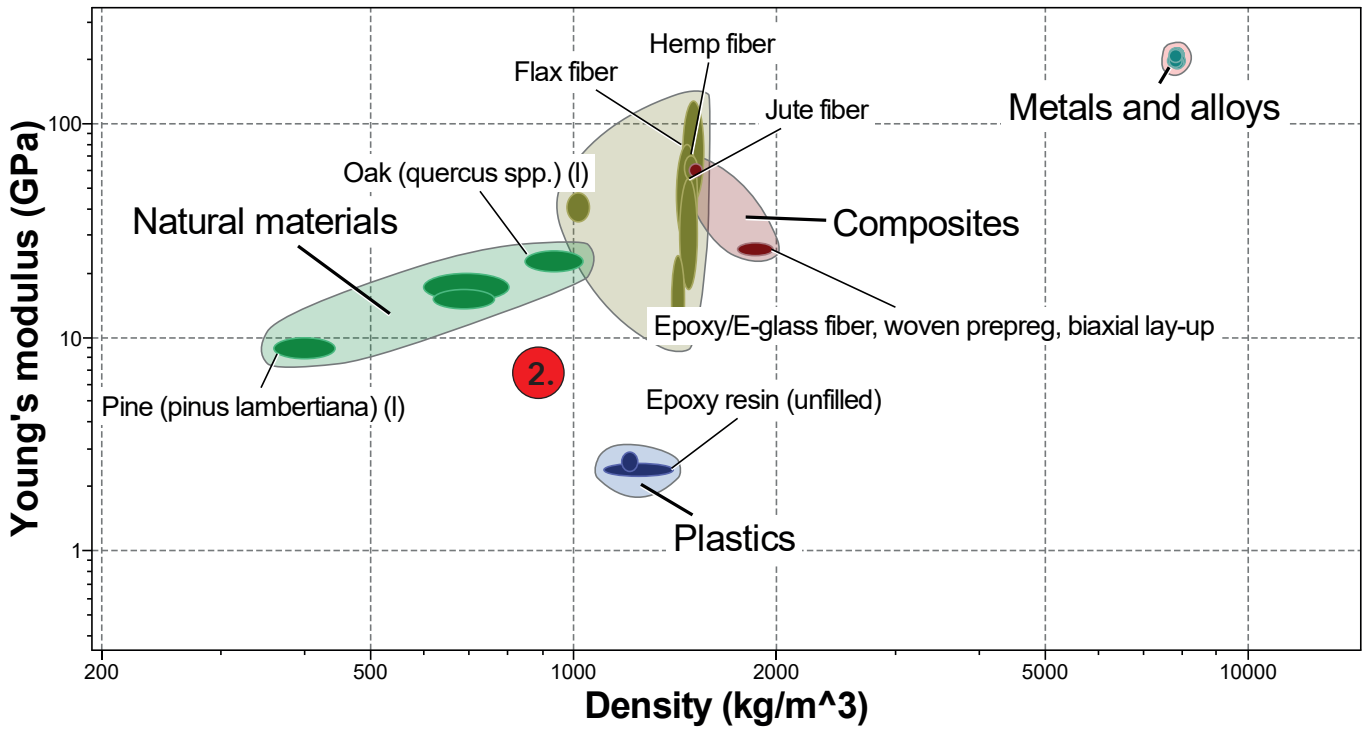

Fig. 9.4. Young's Modulus plotted against density using Ansys® Granta EduPack (Generated by Ansys® Granta EduPack)

stiffnes of the composite material and is displayed with a red dot labeled 2. in figure 9.4. Overall, the material exhibits a lower stiffness than metals and synthetic composites but remains stiffer than neat epoxy resin. Combined with its relatively high strain-to-failure and progressive damage behaviour, this indicates a material with good energy absorption capacity rather than high structural stiffness.

COMPARISON OF THE MECHANICAL STRENGTH TO THE LITERATURE

Several studies on flax-fibre-reinforced composites were reviewed to benchmark the mechanical performance obtained during this project.

M. Rask et al. (2012) investigated filament-wound flax/polypropylene composites with a fibre volume fraction of 37%. Tensile strengths between 110 MPa and 169 MPa were reported.

Q. Liu and M. Hughes (2008) examined woven flax-fibre/epoxy laminates manufactured using a manual lay-up process. Tensile strengths ranged from 52 MPa to 126 MPa in the warp direction and from 29 MPa to 62 MPa in the weft direction.

M. Assarar (2011) studied 11-ply unidirectional flax-fibre/epoxy laminates produced using prepreg and hot-press technology. Tensile strengths of approximately 370 MPa and failure strains around 1.8% were reported before water ageing.

F. Duc et al. (2014) manufactured unidirectional flax-fibre/epoxy laminates using resin transfer moulding (RTM). Tensile strengths of 250–280 MPa and Young's modulus values of 15–20 GPa were obtained.

Although all studies used flax-fibre reinforcement, the reported properties vary considerably due to differences in fibre architecture, fibre volume fraction, specimen geometry, and manufacturing technique. Direct comparison is therefore difficult, as the specimens in this project were cut from filament-wound rectangular hollow sections rather than flat composite panels.

A clear trend is visible: composites manufactured using automated techniques such as hot pressing and RTM generally achieve substantially higher strength and stiffness than manually produced laminates. These methods provide improved fibre alignment, reduced void content, and better fibre–matrix consolidation.

The tensile strength achieved in this study (64.7 MPa) falls within the lower range reported in the literature but corresponds closely to the results of

Liu and Hughes (2008), who also used a manually manufactured flax-fibre/epoxy system. The Young's modulus of 9.03 GPa obtained during Experimental Phase 2 is likewise below the values reported for highly consolidated laminates but remains within the range commonly reported for manually produced natural-fibre composites.

Overall, the comparison suggests that the relatively modest mechanical properties obtained in this project are primarily linked to the manufacturing method rather than the intrinsic potential of flax-fibre reinforcement. Improved consolidation techniques, higher fibre volume fractions, and enhanced fibre alignment are expected to significantly increase both tensile strength and stiffness in future developments.

9.2.4 VISUAL APPEARANCE

The external appearance of curtain wall façades is primarily defined by glazing and aluminium caps. Aluminium is typically selected due to its low weight and its ability to achieve a wide range of surface finishes and colours through coatings. Even in timber or bamboo façade systems, aluminium caps are often preferred because they provide superior weather resistance compared to natural material alternatives.

In the case of plant-fibre composites, the cap component could also be manufactured from the composite material itself, provided it is properly designed and protected. This approach can create a more natural visual expression of the façade, as illustrated in Figure 9.7. A key advantage of using plant-fibre composites is that surface appearance can be controlled directly through the mould surface and the final manufacturing layer. The mould texture is transferred to the final part, potentially eliminating the need for additional coating or galvanising steps compared to aluminium components.

The interior appearance is also strongly influenced by the surface finish of the profiles. Aluminium and steel profiles are typically coated to achieve a matte finish, as shown in Figure 9.5. The choice between matte or glossy finishes depends on factors such as building type, location, and client preference. Figure 9.6 shows a timber curtain wall façade, while Figure 9.7 presents a flax-fibre/epoxy composite curtain wall façade.

Fig 9.5 Aluminum curtain wall façade (KAWNEER. (n.d.) and Aluwood, (2025) (edited image))

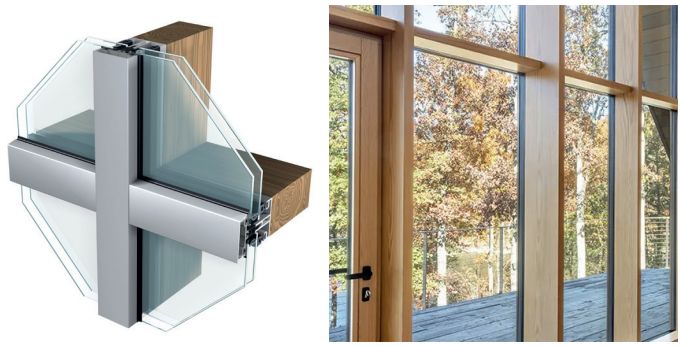

Fig 9.6 Timber curtain wall façade (Alwiti b.v. (2026) and Aluwood, (2025))

Fig 9.7 Flax-fibre/epoxy composite curtain wall façade (own image and Aluwood, (2025) (edited image))

9.2.5 END-OF-LIFE POTENTIAL

The end-of-life potential of curtain wall façade materials is based on data from Ansys® Granta EduPack and supporting scientific literature.

FLAX-FIBRE/EPOXY PROFILE

The end-of-life options for flax-fibre/epoxy composites are discussed in Chapter 9.1 and include reuse, downcycling into aggregates, thermal treatment (combustion), or landfill. Landfill is considered the least favourable option due to the non-biodegradable thermoset epoxy matrix. Fully closed-loop recycling is not currently feasible. For this study, energy recovery via combustion is

assumed for the flax-fibre/epoxy profiles.

To estimate the GWP of combustion, data from epoxy-infused carbon fibre composite (woven and unidirectional lay-up) is used as a proxy, as its structure is comparable to the flax composite. Ansys® Granta EduPack reports 3.33 kg CO_2-eq/kg for this process. Although carbon fibre requires higher combustion energy than flax fibre, the epoxy fraction dominates the emissions; therefore, this value is considered representative for the flax-fibre/epoxy system.

ALUMINUM PROFILE
The end-of-life potential of aluminium depends on alloy type and surface treatment. While aluminium is fully recyclable in principle, façade profiles are often contaminated by coatings and mixed materials, reducing recycling efficiency.

For this study, 6060-T6 aluminium (STABALUX curtain wall profiles) is used. Ansys® Granta EduPack indicates that aluminium is functionally recyclable, with an associated GWP of 3.06 kg CO_2-eq/kg. Remaining fractions may still be landfilled, while combustion is not applicable for energy recovery.

European Aluminium (2024) reports that remelting of post-use aluminium results in approximately 0.26 kg CO_2-eq/kg aluminium ingot, highlighting the strong benefits of recycling compared to primary production

STEEL PROFILE
As with aluminium, steel end-of-life performance depends on alloy composition and coatings. For this study, galvanized and coated S280 steel (STABALUX curtain wall profiles) is considered.
According to Ansys® Granta EduPack, the steel is partially recyclable, with approximately 40% downcycling and a GWP of 0.85 kg CO_2-eq/kg for end-of-life processing. Remaining material may end up in landfill, while combustion for energy recovery is not typically applied.

Burdett S. et al. (2026) note that steel reuse offers the lowest environmental impact, with emissions of approximately 0.05 kg CO_2-eq/kg when reused directly after collection, cleaning, and certification. Increased scrap recovery and the use of electric arc furnaces (EAFs) can further reduce impacts significantly.

SOLID AND ENGINEERED TIMBER PROFILE
Timber end-of-life scenarios depend on whether solid or engineered wood is used for the production of the profiles.

For solid pine (EduPack), end-of-life routes include downcycling into particle materials (≈0.02 kg CO_2-eq/kg) or combustion for energy recovery (≈1.85 kg CO_2-eq/kg). Due to its biodegradability, a significant share may also end up in landfill.

For engineered timber (glulam), EduPack reports downcycling into particles with a GWP of approximately 0.25 kg CO_2-eq/kg, and combustion with a GWP of approximately 1.82 kg CO_2-eq/kg. Similar to solid timber, landfill remains a common end-of-life route despite its biodegradability.

Table 9.4 summarizes the end of life potentials of the different building materials with its GWP for the processes that occur at the end-of-life of the building materials.

Material	**End-of-life potential (EOL)**	**GWP for recycling (kg CO2-eq./kg)**
Flax-fibre/ (bio-) epoxy profiles	*Complete reuse, downcycling, heat combustion for energy, landfill*	*≈ 3.33 (heat combustion)*
6060 T6 Aluminum profiles	*Reuse, functional recycling (35%)*	*≈ 3.06*
Galvanized and coated Steel profiles	*Reuse, downcycling (40%)*	*≈ 0.85*
Solid timber profiles	*Downcycling, heat combustion for energy, landfill*	*≈ 0.02 (downcycling) ≈ 1.85 (combustion)*
Engineered timber profiles	*Downcycling, heat combustion for energy, landfill*	*≈ 0.25 (downcycling) ≈ 1.82 (combustion)*

Table 9.4. Result end-of-life potential of profiles (own work)

9.3 COMPLIENCE WITH EUROPEAN CURTAIN WALL CODES

This chapter evaluates the flax-fibre/epoxy composite profiles manufactured in this project against EU building regulations for curtain wall systems discribed in chapter 4.3 with focus on mechanical performance and fire safety. In addition, the profiles are assessed to the set performance criteria of chapter 5.1 regarding sustainability.

RESISTANCE TO WIND LOAD (2kN/M)

''Accoring to DIN EN 13116 (Curtain walls - Resistance to windload-Performance requirements). Max deflection must not exceed L/200 or 15 mm if L≤3000mm'' (STABALUX, 2026).

For the tested profile (L = 300 mm), the allowable midspan deflection is:

L/200 = 300/200 = 1.5 mm

To relate the applied load to the standard wind load of 2 kN/m, the line load is converted to a point load over the specimen length:

2000 N/m × 0.3 m = 600 N

Experimental results (Chapter 8) show a midspan displacement of 0.8 mm at 600 N for specimens 11 and 12. This is well below the allowable limit of 1.5 mm, indicating compliance with the deflection requirement.

RESISTANCE TO SELF WEIGHT

''Accoring to EN 1991-1-1. Maximum deflection of any horizontal primary beam due to vertical loads not exceeding L/500 or 3mm (depends on which is the smallest value)'' (STABALUX, 2026).

The measured density of the manufactured profiles (Chapters 7 and 8) is approximately 1.0 g/cm³, which is about 2.7 times lower than aluminium (2.7 g/cm³). Even if increased thickness is required to achieve comparable stiffness, the resulting self-weight remains significantly lower than steel or aluminium profiles.

However, structural performance of the system is strongly dependent on connection behaviour, which was not investigated in this study and should be addressed in future work.

IMPACT RESISTANCE

''Accoring to DIN EN 14019 (curtain walling -impact resistance). Pendulum is caused to impact with critical points of the facade construction (central mullion, central transom, intersection between mullion/transom, etc.) from a certain height for the purpose of this test. Permanent deformation of the facade is permitted. But falling parts, holes or cracks are prohibited''(STABALUX, 2026).

Impact resistance is commonly related to fracture toughness, which describes resistance to crack propagation. Brittle materials exhibit low fracture toughness, while ductile materials show higher resistance to crack growth and sudden failure.

Although fracture toughness was not directly measured during this project, three-point bending tests (Chapters 7 and 8) indicate ductile material behaviour. Specimens 11 and 12 (chapter 8) showed permanent deformation at approximately 6000 N central load. Combined with the relatively low Young's modulus, this suggests good energy absorption and potential impact damping behaviour, consistent with natural fibre composites.

Optimisation of epoxy content is critical, as the matrix governs ductility and fracture behaviour and therefore directly influences impact resistance.

FIRE RESISTANCE

''If demanded explicitly, the curtain wall must include suitable devices that inhibit the spread of fire and smoke through openings in the curtain wall construction by means of the installation of structural base plates on the connections in all levels. '' Validation from expert assessment.''(STABALUX, 2026).

Flax fibres are not inherently fire resistant, and epoxy resins generally degrade at elevated temperatures. Standard two-component epoxies typically resist temperatures up to approximately 230°C. However, fire-resistant epoxy systems are available, such as Sicomin SR 1122 and SR 1124 (Sicomin, 2026), designed for structural applications.

Fire performance can be improved through:

- flame-retardant additives in the epoxy matrix
- fibre surface treatments (e.g. silane treatments, see Chapter 3.1.4)
- fire-resistant coatings
- insertion of fire-resistant cores within hollow sections

Nevertheless, fire resistance must be experimentally validated if the profiles are to be used in façade systems.

BUILDING AND THERMAL MOVEMENT

"The design of the curtain wall must be capable of absorbing thermal movements and movements of the structure in such a way that destruction of facade elements or impairment of the performance characteristics do not occur"(STABALUX, 2026).

Thermal expansion testing (Chapter 7) shows a coefficient of 14.9 µm/m°C for the cross-stitched flax-fibre/epoxy composite. This is comparable to steel and significantly lower than aluminium, indicating good dimensional stability under temperature variations. Since larger profiles use the same fibre architecture and similar fibre-to-resin ratios, comparable thermal behaviour can be assumed.

An additional advantage of flax fibres is their inherent damping capacity, which is widely exploited in applications such as skis and skateboards. Although not directly tested in this study, this property suggests potential for good vibration and movement absorption in façade applications when properly manufactured.

9.4 FULFILMENT OF PERFORMANCE CRITERIA

The set performance criteria of chapter 5.1, related to material performance, embodied carbon and visual performance are related to the results of the testresults and Life-Cycle Assessment of the profiles.

MATERIAL PERFORMANCE

The aluminium alloy employed in the STABALUX AL mullion and transom profiles was selected as the reference benchmark for evaluating material performance in terms of mechanical strength. The benchmark values consist of a tensile strength of 220 MPa, a yield strength of 160 MPa, and a Young's modulus of 68 GPa. The experimental results obtained during this project, however, indicate that the plant-fibre composite material exhibits significantly lower mechanical strength compared to these reference values.

The relatively modest tensile strength, yield strength, and Young's modulus of the composite material can likely be attributed to several factors inherent to the manufacturing process. These include the manual filament-winding technique, fibre waviness and potential damage introduced during manual lay-up, structural discontinuities within the profile, and the absence of external consolidation pressure during curing. Collectively, these factors negatively affect fibre alignment, increase void content, and reduce the efficiency of fibre–matrix bonding. Consequently, the tensile strength achieved in this project is comparable to that of engineered plastics and unfilled epoxy resins. Furthermore, the cross-stitched flax fibre used in this study exhibits a reported tensile strength of 255 MPa according to the manufacturer, which is considerably lower than the tensile strength range of 500–1000 MPa for individual flax fibres reported by Ansys® Granta EduPack.

The thermal expansion test conducted during Experimental Phase 2 yielded a coefficient of thermal expansion of 14.9 µm/m°C. This value is significantly lower than that of the aluminium alloy used in the STABALUX AL system, which has a coefficient of 24 µm/m°C. These results indicate that, despite its lower mechanical performance, the composite material demonstrates favourable thermal stability characteristics.

EMBODIED CARBON OF PROFILES

A durability-related performance target was defined during this project, aiming to achieve a 70% reduction in the embodied carbon of the structural profiles (51.5 $kgCO_2$-eq/m). This resulted in a target value of 15.3 $kgCO_2$-eq/m for the manufactured plant-fibre composite profiles.

The LCA conducted in Section 9.1 indicates a total Global Warming Potential (GWP) of 8.12 $kgCO_2$-eq/kg for the flax-fibre/epoxy composite material. The production of one meter of profile requires approximately 1.5 kg of material (approximately 450 g for a 300 mm profile). Based on these values, the embodied carbon can be estimated at 12.2 $kgCO_2$-eq/m per profile. This value is below the established performance criterion of 15.3 kg CO_2-eq/m.

SURFACE QUALITY

Due to time constraints within the scope of this project, the surface quality of the final flax-fibre/epoxy composite profile from experimental phase 8 was not assessed using microscopic analysis.

However, no surface perforations are visible to the naked eye. The application of a final peel-ply layer resulted in a rough surface finish, which may increase the susceptibility of the fibres to moisture uptake.

In contrast, the use of a perforated film produced a glossy surface finish on the flax-fibre specimens, as illustrated in Figure 9.8. Microscopic evaluation of these specimens, conducted during experimental phase 2 (Figure 9.10), revealed minimal surface perforations at 100× magnification. This indicates a relatively smooth outer surface with a reduced potential for moisture absorption.

Fig. 9.8 Surface quality of using a perforated film (own image)

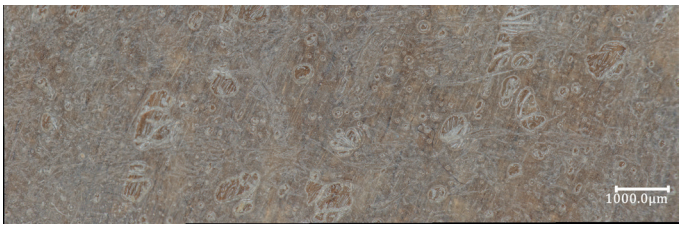

Fig. 9.10 Microscopic assessment specimen, 100x (own image)

9.5 UPSCALABILITY OF THE MANUFACTURING PROCESS

The following chapter discusses upscaling the manufacturing process used during this thesis project to manufacture larger quantities of profiles. For this study, it is assumed 2.5m long profiles will be manufactured with dimensions of 100 x 50 x 5mm used primarily for semi-structural façade applications. The target production volume is set to 40 profiles per day. A flowchart of the process is displayed in figure 9.8 at the end of this chapter.

The transition from laboratory-scale production to semi-industrial manufacturing of 2.5m flax fibre epoxy profiles requires substantial modifications to ensure process stability, particularly in relation to resin handling, fibre conditioning, and demoulding. The implementation of automated winding systems, controlled resin dispensing, and mechanical demoulding is essential to achieve the targeted production rate of forty profiles per day while maintaining consistent mechanical performance and safety standards.

1. PREPARING AND CLEANING OF FIBRES

Prior to processing, flax fibre material is subjected to a controlled cleaning procedure to reduce contamination and improve process consistency. At industrial scale, the fibre is handled in a roll-to-roll configuration and passed through a cleaning station equipped with compressed air knives and a vacuum extraction system. This process removes dust, loose particles, and minor fibre defects that could negatively influence impregnation quality and interfacial bonding.

After cleaning, the fibre is visually inspected under controlled lighting conditions to identify major defects or irregularities. The cleaned material is subsequently rewound onto storage spools to maintain handling efficiency and to prevent recontamination prior to drying and impregnation.

2. FIBRE DRYING

Moisture content in natural fibres such as flax has a critical influence on the mechanical performance and durability of fibre-reinforced composites. Therefore, the cleaned fibre is dried in a convection oven at approximately 60 degrees celsius for a minimum of two hours. At industrial scale, this process is implemented as a batch or continuous drying operation depending on production demand.

Following drying, the fibres are transferred to a controlled storage environment with reduced relative humidity, typically below 30 percent, to prevent moisture reabsorption. To ensure continuity of production, a buffer stock of pre-dried fibres is maintained, allowing decoupling of the drying process from the manufacturing line.

3. MANUFACTURING OF THE PROFILES

The manufacturing of 2.5 m hollow profiles is based on an automated filament winding process adapted for natural fibre reinforcement. The aluminium mandrel, corresponding to the desired hollow profile geometry, is mounted on a motor-driven rotating system capable of maintaining controlled rotational speeds along the full length of the mandrel.

Fibre is supplied from tension-controlled creels and guided through a resin impregnation system. In the scaled-up configuration, manual resin application is replaced by a controlled epoxy delivery system consisting of metering pumps and a static mixing unit. This ensures consistent resin-to-fibre ratio and reduces variability associated with manual brushing.

During production, the mandrel rotates continuously while the impregnated fibre is applied in a controlled winding pattern. The winding process is supported by a traversing mechanism to ensure uniform axial coverage along the entire 2.5 m length. Epoxy resin is prepared in small, sequential batches to accommodate the limited pot-life of approximately 115 minutes. Two alternating mixing stations are used to maintain continuous production without exceeding the usable life of the resin.

Strict temperature control is maintained in the manufacturing area to ensure stable resin viscosity and consistent impregnation quality. Local exhaust ventilation is implemented at the impregnation zone to ensure operator safety and to control exposure to volatile organic compounds.

4. CURING AND DEMOULDING

Following fibre winding, the composite structure remains on the mandrel for curing. For industrial consistency, the mandrel with the wound composite is transferred directly into a temperature-controlled curing oven. The curing cycle is performed at 60 degrees celsius for approximately six hours, followed by controlled cooling to minimize residual stresses and deformation.

Demoulding of the cured profiles is performed using a mechanical extraction system rather than manual impact methods. A hydraulic or mechanical pulling system is used to remove the mandrel axially from the composite structure. To facilitate release, the mandrel surface is treated with an appropriate release coating or an equivalent industrial release agent. This method reduces the risk of damage to the composite material, particularly given the increased length of 2.5 m profiles.

5. CUTTING, TRIMMING AND FINISHING

After demoulding, the profiles are transferred to a cutting station where end trimming is performed. Approximately ten percent of material is removed from both ends to eliminate defects and edge irregularities resulting from the manufacturing process. Cutting is carried out using guided abrasive or diamond saw systems mounted on linear rails to ensure dimensional accuracy and repeatability.

Following cutting, the profiles are cleaned using compressed air and, if necessary, lightly finished to remove residual resin or fibre protrusions. This stage ensures that the profiles meet aesthetic and dimensional requirements for façade applications.

6. QUALITY CONTROL, STORAGE AND TRANSPORT PREPARATION

Quality control is implemented throughout the production chain, with particular focus on fibre quality, impregnation consistency, void content, and dimensional accuracy. Non-destructive evaluation methods such as visual inspection and, where available, ultrasonic testing are applied to ensure structural integrity.

Finished profiles are stored in a controlled environment with stable humidity and temperature conditions to prevent post-curing degradation or moisture uptake. Due to the length of the profiles, they are stored in horizontal racks designed to avoid deformation under self-weight.

For transport, the profiles are packaged with protective end caps and secured within rigid support frames to prevent mechanical damage. Batch tracking is implemented to ensure traceability from raw material to final product.

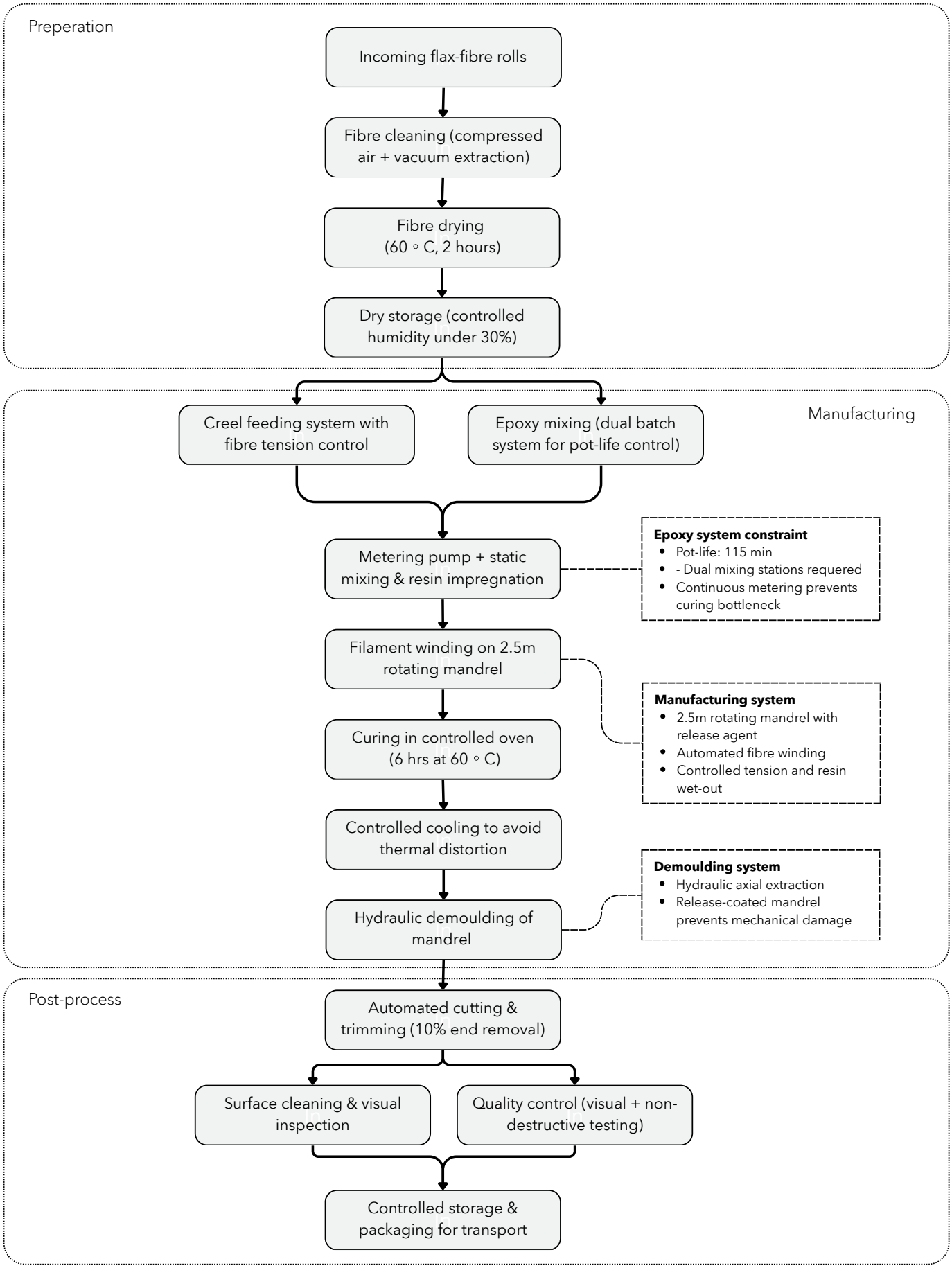

Figure 9.8. Flowchart of upscaled manufacturing process flax-fibre/epoxy composite profiles (own flowchart)

9.6 SUMMARY OF VALIDATION RESULTS

The Life Cycle Assessment of the flax-fibre/epoxy composite profiles demonstrates that the environmental impact is primarily driven by raw material production, with epoxy resin being the dominant contributor to overall carbon emissions. Although flax fibre itself has a relatively low environmental burden and contributes to CO_2 uptake during cultivation, this benefit is largely offset by the impact of the thermosetting resin system. Transport and manufacturing stages contribute only marginally to the total footprint. Nevertheless, the developed profiles achieve an embodied carbon of approximately 12.2 kg CO_2-eq/m, which remains below the predefined performance target of 15.3 kg CO_2-eq/m, representing a reduction of more than 70% compared to conventional structural profiles. The profiles are expected to achieve a service life exceeding 30 years with limited maintenance requirements, while end-of-life treatment remains problematic due to the limited recyclability of thermoset composites. Consequently, future developments should focus on lower-impact and more recyclable resin systems to further improve overall sustainability.

When compared to conventional materials, the flax-fibre/epoxy profiles manufactured in experimental phase 3 show an intermediate global warming potential of approximately 8.1 kg CO_2-eq/kg, which is lower than aluminium (10.1–13.3 kg CO_2-eq/kg) but higher than steel (≈4.6 kg CO_2-eq/kg) and timber (0.29–1.48 kg CO_2-eq/kg). The use of available bio-epoxy can further reduce this value to approximately 5.69 kg CO_2-eq/kg, improving its relative environmental performance. However, in terms of durability, the composite underperforms compared to aluminium, steel, and timber without a fully biodegradable resin matrix, with an estimated service life of 30–40 years and limited long-term stability under hygrothermal exposure.

The tensile strength is comparable to unfilled epoxy resins and engineered plastics, but remains below values typically reported for engineered flax-fibre composites. Similarly, the measured Young's modulus of 9.03 GPa exceeds that of neat epoxy but is significantly lower than that of metals and highly optimised fibre-reinforced systems, resulting in a lightweight material with moderate stiffness and relatively high deformability. Despite these limitations, the composite shows a favourable strength-to-weight ratio and progressive failure behaviour, which is beneficial for semi-structural façade applications.

Comparison with literature confirms that the obtained mechanical properties fall within the lower range of flax-fibre composites and are consistent with manually manufactured systems. The comparatively modest performance achieved in this study is therefore primarily attributed to manufacturing constraints, including fibre waviness, resin-rich regions, and the absence of external consolidation pressure, rather than the intrinsic potential of the material.

Assessment against EU building regulations shows that the profiles meet key requirements for wind load resistance and self-weight, with measured deflection and density offering clear advantages. In addition, the visual performance of the profiles indicates that no surface perforations are visible to the naked eye, suggesting an acceptable surface integrity for façade applications. However, microscopic assessment was not conducted for the final profiles, and the use of peel ply resulted in a relatively rough surface finish that may increase susceptibility to moisture uptake. In contrast, earlier specimens produced with perforated film demonstrated a smoother and less permeable surface, indicating potential for improved durability through process optimisation. Although not tested during this project, impact behaviour and thermal movement remain to be verified. Fire resistance remains a critical limitation, and full compliance cannot be confirmed without further testing and material modification. Overall, while the profiles show potential for façade applications, particularly due to their low weight and acceptable structural and environmental performance, their application is constrained by fire safety, recyclability, surface durability, and long-term behaviour.

Finally, the upscaling of the manufacturing process demonstrates that semi-industrial production is feasible, provided that strict process control is implemented. The introduction of automated fibre handling, controlled resin dosing, filament winding, and temperature-regulated curing is essential to ensure consistency and repeatability. Proper fibre conditioning and storage are also required to prevent moisture-related defects, while mechanical demoulding improves product integrity. In conclusion, the proposed upscaling approach enables reliable and scalable production while preserving the mechanical and environmental performance required for façade applications.

10. CONCLUSION & DISCUSSION

10. CONCLUSION, DISCUSSION AND REFLECTION

10.1 OVERALL CONCLUSION

This study set out to investigate whether non-wood plant-fibre reinforced composites can be developed into manufacturable façade profile geometries that meet the mechanical, environmental, and regulatory requirements of aluminium curtain wall systems. The research was motivated by the growing demand for low-carbon building envelope solutions and the absence of systematic investigations into the translation of plant-fibre composites into aluminium-like hollow section profiles for stick-built curtain wall applications. Through a structured programme of literature review, material selection, iterative experimental development, and profile validation, this thesis demonstrates that flax-fibre/epoxy composite profiles represent a technically feasible and environmentally promising alternative to conventional aluminium façade profiles, while also identifying clear limitations that must be addressed before practical application can be realised.

FIBRE AND MATRIX SELECTION

The literature review and material selection phase established that bast fibres, specifically flax, hemp, and jute, are the most suitable non-wood plant fibres for load-transferring façade profile applications, owing to their favourable specific strength and stiffness, high aspect ratios, and relative commercial availability. Among the matrix systems considered, a low-viscosity two-component epoxy resin was selected for its mechanical performance, good fibre-wetting characteristics, and compatibility with the thermal sensitivity of plant fibres. These findings directly address the first and second sub-research questions, confirming that flax and cross-stitched fabric architectures in a thermoset epoxy matrix constitute the most appropriate system for structural composite profile development within the boundary conditions of this study. The selection was deliberately grounded in commercial availability and processing feasibility, ensuring that the chosen system could be realistically translated into manufactured components under laboratory conditions.

ITERATIVE MANUFACTURING DEVELOPMENT

A central methodological contribution of this research is the iterative and systematic refinement of the manufacturing process across three experimental phases. Rather than adopting a single fixed production method, the study progressively developed and adapted the manufacturing approach in response to observed limitations, thereby generating transferable knowledge about the process-property relationships governing plant-fibre composite profile production.

In the first experimental phase, the filament wrapping technique was identified as the most suitable method for producing rectangular hollow sections from fabric reinforcement. Early trials using manual rotation or a stationary vice bench resulted in insufficient fibre tension, fibre slippage, and resin spillage, confirming that process stability is a prerequisite for achieving adequate laminate quality. The introduction of a custom-built filament winding machine in subsequent specimens significantly improved consolidation and surface quality, demonstrating the direct influence of equipment control on product integrity. Aluminium was established as the preferred mould material due to its strength, thermal expansion behaviour during curing, and facilitated demoulding, while peel ply and perforated release film were identified as surface finish options with distinct functional consequences for moisture resistance and secondary bonding.

The second experimental phase provided a systematic mechanical comparison between cross-stitched flax fibre and non-woven hemp mat reinforcements at the coupon level. Cross-stitched flax fibre composites demonstrated substantially higher tensile strength and an average Young's modulus of 9.03 GPa, compared to 5.14 GPa for the hemp mat specimens, alongside lower thermal expansion and more ductile failure behaviour. These results provided the material-level evidence required to select the cross-stitched flax fibre system for the final profile geometry, and simultaneously confirmed that manually manufactured specimens are susceptible to variability arising from fibre waviness, inconsistent resin distribution, and the absence of external consolidation pressure.

The third experimental phase represented the critical step of transferring the selected material system to the full-scale 50 × 100 × 4 mm mullion and transom geometry. This phase confirmed that manufacturing the final profile geometry is technically feasible, which constitutes the primary finding of this study. The successful production of specimens 11–14, characterised by improved consolidation, fewer visible defects, and more uniform surface quality compared to the initial

specimen 10, demonstrated that process consistency can be achieved when fibre handling, tension control, and operator coordination are carefully managed. The average tensile strength of the final profiles reached 64.7 MPa, marginally exceeding the average value recorded in the preceding phase, indicating that upscaling the geometry did not compromise tensile capacity. The bending tests, which resulted in local indentation and punching shear failure rather than global flexural rupture, further confirmed the structural robustness of the profiles under transverse loading and provided relevant data on local compressive and shear resistance for façade connection design.

MECHANICAL PERFORMANCE

The mechanical performance of the developed profiles is characterised as low-to-moderate but structurally meaningful within the context of semi-structural façade applications. The tensile strength is comparable to that of engineered plastics, and the measured Young's modulus of 9.03 GPa exceeds that of neat epoxy and is comparable to structural timber, though it remains significantly below that of aluminium and steel. Comparison with published literature confirms that the obtained properties fall within the lower range reported for flax-fibre composites, consistent with the expected performance of manually manufactured systems and the relatively low tensile capacity of the cross-stitched flax fibres used. The relatively modest values are therefore attributed primarily to manufacturing constraints, including fibre waviness, resin-rich regions, discontinuities, and the absence of external consolidation pressure, rather than to any fundamental limitation of the material system itself.

Importantly, the progressive and damage-tolerant failure behaviour observed across all experimental phases, characterised by non-planar fracture surfaces, fibre pull-out, and continued load-carrying capacity after damage initiation, is considered a key functional advantage for façade applications, where early warning of structural distress is preferable to sudden brittle collapse. In addition, the comparatively low coefficient of thermal expansion (14.9 µm/m°C), significantly below that of aluminium, indicates favourable thermal stability, supporting the material's suitability for façade applications despite its lower mechanical strength.

ENVIRONMENTAL PERFORMANCE

The Life Cycle Assessment conducted in the validation phase indicates a total Global Warming Potential (GWP) of 8.12 kg CO_2-eq/kg for the flax-fibre/epoxy composite material, corresponding to an embodied carbon of approximately 12.2 kg CO_2-eq/m for the manufactured profile. This value is below the predefined performance target of 15.3 kg CO_2-eq/m, representing a reduction exceeding 70% relative to the reference aluminium profile. The environmental impact is dominated by epoxy resin production, which largely offsets the carbon sequestration benefit associated with flax fibre cultivation. In comparative terms, the profiles exhibit an intermediate global warming potential which is lower than that of aluminium (10.1–13.3 kg CO_2-eq/kg) but higher than steel (≈4.6 kg CO_2-eq/kg) and timber (0.29–1.48 kg CO_2-eq/kg). The substitution of conventional epoxy with commercially available bio-epoxy has the potential to reduce the GWP to approximately 5.69 kg CO_2-eq/kg, which would substantially improve the relative environmental positioning of the material system.

REGULATORY AND DURABILITY ASSESSMENT

Assessment against applicable European building regulations confirms that the profiles meet key performance criteria relevant to curtain wall applications, including wind load resistance and self-weight requirements. The measured deflection and material density offer quantifiable advantages in the context of lightweight façade design. However, fire resistance remains a critical unresolved limitation: without fire-retardant treatment or material modification, full compliance with European fire performance requirements cannot be confirmed. Long-term durability under hygrothermal exposure also constitutes a significant uncertainty. Although an estimated service life of 30–40 years is considered feasible based on available literature, the inherent moisture sensitivity of plant fibres, the limited recyclability of thermoset matrix systems, and the relatively rough surface finish resulting from peel-ply application all present barriers to unconditional deployment in outdoor façade environments. The visual performance assessment confirmed the absence of surface perforations visible to the human eye, while earlier specimens produced with perforated release film demonstrated a smoother and less moisture-permeable surface, indicating that surface quality can be improved through deliberate process selection.

MANUFACTURING SCALABILITY

The upscaling analysis conducted in the validation

phase confirms that semi-industrial production of the developed profiles is conceptually feasible, provided that the process control measures identified throughout the experimental programme are systematically implemented. Automated fibre handling, controlled resin dosing, filament winding, and temperature-regulated curing are identified as essential conditions for achieving the consistency and repeatability required for structural façade components. Proper fibre conditioning and storage protocols are additionally required to mitigate moisture-related defects prior to processing.

OVERALL FEASIBILITY ASSESSMENT

Returning to the main research question, this study demonstrates that non-wood plant-fibre reinforced composites, specifically cross-stitched flax fibre in a low-viscosity epoxy matrix, can be developed into manufacturable façade profile geometries with mechanical, environmental, and geometric properties that are relevant to aluminium curtain wall applications. The embodied carbon target was met, the final profile geometry was successfully manufactured, and the mechanical performance is structurally meaningful for semi-structural façade use. Nevertheless, the profiles do not yet constitute a direct, drop-in replacement for aluminium curtain wall members. Critical limitations remain in the areas of fire resistance, long-term hygrothermal durability, and end-of-life recyclability, each of which must be resolved before the material system can be considered for certified façade applications. The results of this study should therefore be interpreted as a proof of concept and a methodologically structured foundation for continued material and process development, rather than as a validated product ready for immediate deployment.

10.2 DISCUSSION

The discussion addresses the main findings of the project, outlines directions for further research, and positions the work within its broader societal and professional context, followed by a reflection on the graduation process.

10.2.1 INTERPRETATION OF THE RESULTS

The results of this project show that non-wood plant-fibre reinforced composites, and specifically cross-stitched flax-fibre/epoxy profiles, can be manufactured in façade-relevant hollow geometries with mechanically meaningful and environmentally favourable performance, but that they are not yet ready to replace aluminium curtain wall profiles in practice. The work thus moves plant-fibre composites from a predominantly material-level concept towards an application-scale proof of concept. Under controlled conditions, the iterative experiments demonstrate that a filament-wound flax-fibre profile can achieve tensile strengths comparable to engineered plastics, display stable and progressive failure, and realise more than a 70% reduction in embodied carbon per metre relative to a reference aluminium mullion. Together, these outcomes answer the main research question in a cautiously positive way: plant-fibre composites can meet several mechanical and environmental requirements of aluminium curtain wall systems, provided that the application remains semi-structural and that current limitations are explicitly recognised.

These results matter for several reasons. They provide concrete evidence that the embodied carbon associated with façade profiles can be reduced substantially without radical changes in façade geometry or design principles. By showing that a 50 × 100 × 4 mm hollow section in flax-fibre/epoxy can be both manufactured and structurally characterised, the project offers a tangible alternative to aluminium within the established typology of mullions and transoms. The work also underscores the importance of manufacturing route, process control, and testing conditions in realising the potential of bio-based composites. The progression from unstable manual wrapping to controlled filament winding, and the associated improvements in laminate quality and tensile performance, indicate that process development is a central determinant of achievable properties rather than a secondary technical detail.

The mechanical test results from experimental phases 2 and 3 are considered valid and reliable, as they were obtained in a specialised laboratory at the Department of Mechanical Engineering of TU Delft under appropriate supervision. Differences in tensile strength between smaller and larger profiles with comparable fibre content and reinforcement are attributed primarily to the use of a different clamping system, while the three-point bending tests on the MF40 MKII testing machine provide only an approximate indication of flexural behaviour compared with the more accurate tensile data from the universal 100 kN testing machines. Finally, the combined use of mechanical testing,

life cycle assessment, and basic regulatory checks yields a more complete feasibility picture than single-focus studies, clarifying not only what the material can achieve in principle, but how it aligns with the constraints of European façade practice.

At the same time, the results are constrained in scope and cannot answer several important questions. The experiments were conducted on a limited number of specimens and relied on largely manual manufacturing, so the reported properties describe carefully produced prototypes rather than statistically robust industrial production. They cannot capture the full variability, defect rates, or quality control challenges that may arise at scale. The bending tests did not produce a classical global flexural failure and were influenced by local indentation and test equipment limitations, so the flexural properties of the profiles remain only partially characterised. Long-term performance is inferred mainly from literature, as no dedicated ageing or hygrothermal exposure tests were performed on the manufactured profiles; definitive statements on service life, creep, and moisture-induced degradation cannot therefore be made. Fire behaviour was not experimentally assessed, and recyclability was examined qualitatively through the known constraints of thermoset systems rather than through detailed end-of-life scenarios. Moreover, the study focuses mainly on a single material system of a cross-stitched flax fibre in a specific epoxy, and only one profile geometry, so it does not support general conclusions for all plant-fibre composites, resin systems, or façade typologies.

In summary, the project demonstrates that flax-fibre/epoxy façade profiles are technically feasible and environmentally promising at prototype scale and clarifies the conditions under which they could contribute to low-carbon curtain wall design. The results are significant because they translate an abstract sustainability ambition into a tested material–geometry combination and highlight the crucial roles of manufacturing and testing in bridging the gap between material potential and practical application. However, unresolved issues regarding long-term durability, fire performance, industrial-scale reproducibility, and generalisation to other systems define the limits of the present conclusions and set the agenda for future research.

10.2.2 RECOMMENDATION FOR FURTHER RESEARCH

The findings of this study provide a solid foundation for continued development of plant-fibre composite profiles for load-bearing façade applications, while also indicating clear priorities for future work. The most immediate need is the refinement of the manufacturing process to obtain more consistent laminate quality. Reducing the number of fabric interruptions during wrapping. For example by using longer continuous textile rolls or alternative reinforcement strategies. This would improve fibre continuity, decrease local weak zones, and enhance the repeatability of mechanical properties along the profile. In parallel, better control of resin distribution and compaction pressure during curing is essential to limit resin-rich regions and dry fibre zones, both of which contributed to property scatter in the experimental phases.

From the perspective of mechanical characterisation, the bending behaviour of the full-scale profiles requires more targeted investigation. The configuration used in experimental phase 3 resulted in local indentation and punching shear rather than global flexural failure, so the true flexural stiffness and bending strength remain insufficiently defined. A revised test setup with a longer span or alternative loading arrangement would allow these parameters to be quantified more accurately. In addition, the long-term mechanical response under hygrothermal exposure, including moisture cycling, elevated temperature, and UV radiation, should be examined systematically, given the known sensitivity of plant-fibre composites to climatic conditions in outdoor applications.

Regarding the material system, future research should prioritise replacing conventional epoxy with bio-based or more recyclable resins. The Life Cycle Assessment identified epoxy as the dominant driver of environmental impact, and the adoption of currently available bio-epoxy systems could reduce the global warming potential from 8.12 kg CO_2-eq/kg to approximately 5.69 kg CO_2-eq/kg. Fire resistance remains a critical limitation, so the development of fire-retardant treatments or the integration of inherently flame-resistant constituents is a prerequisite for regulatory acceptance in façade applications. Finally, the behaviour of connections (particularly fastener interaction and long-term deformation at the profile-to-connector interface)

deserves dedicated investigation, as these regions govern structural reliability in assembled curtain wall systems and were only indirectly addressed in this study.

10.2.3 SOCIETAL IMPACT

The results of this research are most relevant to low- and mid-rise façade renovation, where the load-bearing components of curtain wall systems provide a realistic entry point for bio-based composites. The manufactured flax-fibre/epoxy profiles demonstrate that plant-fibre composites can be formed into geometries comparable to conventional aluminium mullions and transoms and can satisfy several key requirements for façade use. Nevertheless, direct practical application is unfeasible. Mechanical performance, fire resistance, long-term hygrothermal durability, and end-of-life recyclability remain unresolved, meaning that the profiles cannot yet be considered for certified building applications. At this stage, the findings primarily inform material developers, composite manufacturers, and façade engineers working on early-stage systems rather than immediate market deployment.

The principal innovation of the project lies in the systematic translation of plant-fibre composites into hollow-section façade profiles through an iteratively refined manufacturing method. Moving beyond coupon-level investigations, the filament wrapping process developed for rectangular hollow mullions represents a concrete step towards application-scale components. The project is further distinguished by its integrated assessment of mechanical performance, environmental impact, regulatory constraints, and scalability, whereas existing studies generally treat these aspects separately.

In relation to sustainable development, the study shows that an embodied carbon reduction of more than 70% compared with aluminium profiles is achievable, with scope for further improvement through the adoption of bio-epoxy resins. In the European construction context, where façades contribute significantly to embodied carbon in both new buildings and renovations, this points to a credible pathway towards lower-impact envelopes. At the same time, the reliance on a thermoset epoxy matrix limits recyclability and circularity, so part of the environmental benefit is offset and the development of more circular resin chemistries remains essential.

The project aligns closely with broader societal and regulatory efforts to decarbonise the construction sector, including ambitions expressed in the European Green Deal and tightening building performance regulations. It addresses the concrete challenge of upgrading an ageing building stock through façade renovation, a context in which bio-based profiles could eventually substitute conventional systems. The work also intersects wider debates on agricultural resource use, fibre sourcing, and the credibility of “natural” or “bio-based” materials, underscoring that sustainability claims must be supported by transparent, life cycle-based evidence rather than assumptions.

If the identified limitations can be resolved, plant-fibre composite profiles have the potential to reduce the embodied carbon of the built environment, particularly in renovation projects requiring façade replacement. Their lower density compared with aluminium offers practical benefits for handling, transport, and connection design. For now, however, the impact on the built environment remains prospective: the study provides a technically grounded proof of concept rather than an immediately deployable solution, and its eventual influence will depend on further material development, regulatory validation, and industry uptake.

10.2.4 REFLECTION ON THE GRADUATION PROCESS

This graduation project was carried out in a studio focused on sustainable building technologies and innovative material applications in architecture and engineering. The topic of plant-fibre composite façade profiles sits at the intersection of structural engineering, façade engineering and material science. Its interdisciplinary nature required combining insights from composite mechanics, manufacturing engineering, life cycle assessment, and European building regulations, which broadened the scope but also demanded a wide-ranging and self-directed research strategy.

The research approach was shaped by a clear gap in the literature: although plant-fibre composites are often well characterised at material level, their translation into complex façade profiles under controlled manufacturing conditions had not been systematically studied. In response,

a structured experimental methodology was adopted, progressing from material selection and coupon-level characterisation to full-scale profile manufacturing and validation. This iterative strategy was chosen deliberately, so that manufacturing insights from each phase could inform the next, building a more robust and transferable body of knowledge than a single-phase programme would have allowed.

Overall, the iterative experimental approach proved well suited to the research objectives. Each phase generated concrete findings that directly informed subsequent decisions. The manufacturing process led to profiles of measurably improved quality by the third phase. At the same time, the approach revealed limitations: mechanical testing was constrained by available equipment, and microscopic assessment of the final profiles could not be completed within the available time. These constraints are understood as boundary conditions rather than methodological flaws and form a clear basis for the recommendations for future work.

The relationship between research and design in this project is primarily instrumental. The research findings directly informed the design of the composite profile geometry, the manufacturing route, and the proposed curtain wall integration strategy. The selection of a 50 × 100 × 4 mm rectangular hollow section as reference geometry was based on a structural calculation for a representative curtain wall section, ensuring that the experimental work remained anchored in a realistic design scenario. In turn, the façade integration model developed during the validation phase illustrates how the experimentally characterised profiles could be incorporated into a conventional stick-built curtain wall system, closing the loop between material research and façade application.

Several ethical issues emerged during the project. The most concrete concern relates to the use of epoxy resin as matrix material. Epoxy systems contain substances such as bisphenol A-based diglycidyl ether and amine hardeners, which are classified as skin sensitisers and potential endocrine disruptors, and thus pose occupational health risks if not handled correctly. All resin processing followed the manufacturer's safety instructions, with appropriate personal protective equipment throughout. Even so, the toxicity of conventional epoxy represents a genuine ethical limitation of the proposed material system and strengthens the argument for safer, bio-derived resin alternatives in future research. More broadly, presenting flax fibre as a sustainable material requires careful context: although its cultivation generally has a relatively low environmental burden, land use, agricultural practices, and supply chain transparency remain important factors in any life cycle-based sustainability claim.

11. REFERENCES

11. REFERENCES

Ahmad, A. F., Abbas, Z., Obaiys, S. J., & Zainuddin, M. F. (2018). Effect of untreated fibre loading on the thermal, mechanical, dielectric, and microwave absorption properties of polycaprolactone reinforced with oil palm empty fruit bunch biocomposites. *Polymer Composites,* 39(S3), E1778–E1787. https://doi.org/10.1002/pc.24792

Ahmad, F., Choi, H. S., & Park, M. K. (2014). A review: Natural fibre composites selection in view of mechanical, light weight, and economic properties. *Macromolecular Materials and Engineering*, 300(1), 10–24. https://doi.org/10.1002/mame.201400089

Ahmad, W., McCormack, S. J., & Byrne, A. (2025). Biocomposites for sustainable construction: A review of material properties, applications, research gaps, and contribution to circular economy. *Journal of Building Engineering*, 105, 112525. https://doi.org/10.1016/j.jobe.2025.112525

Akil, H. M., Omar, M. F., Mazuki, A. A. M., Safiee, S., Ishak, Z. A. M., & Abu Bakar, A. (2011). Kenaf fiber reinforced composites: A review. *Materials & Design*, 32(8–9), 4107–4121. https://www.sciencedirect.com/science/article/pii/S0261306911002639

AlMaadeed, M. A. A., Ponnamma, D., & El-Samak, A. A. (2020). Polymers to improve the world and lifestyle: Physical, mechanical, and chemical needs. In M. A. A. AlMaadeed, D. Ponnamma, & M. A. Carignano (Eds.), *Polymer science and innovative applications (pp. 1–19*). Elsevier. https://doi.org/10.1016/B978-0-12-816808-0.00001-9

Alsuhaibani, E. (2025). Mechanical and ultrasonic evaluation of epoxy-based polymer mortar reinforced with discrete fibres. *Polymers*, 17(9), 1250. https://doi.org/10.3390/polym17091250

Aluwood. (2025). Aluwood gordijngevels [Image]. https://www.aluwood.com.tr/nl/

Alwiti B.V. (2026). Aluminium hout vliesgevels [Image]. http://www.aluhout.nl/service

Aravindh, M., Sathish, S., Prabhu, L., Raj, R. R., Bharani, M., Patil, P. P., Karthick, A., & Luque, R. (2022). Effect of various factors on plant fibre-reinforced composites with nanofillers and its industrial applications: A critical review. *Journal of Nanomaterials*, 4455106. https://doi.org/10.1155/2022/4455106

Arinze, R. U., Oramah, E., Chukwuma, E. C., Okoye, N. H., Eboatu, A. N., Udeozo, P. I., Chris-Okafor, P. U., & Ekwunife, M. C. (2023). Reinforcement of polypropylene with natural fibres: Mitigation of environmental pollution. *Environmental Challenges,* 11, 100688. https://doi.org/10.1016/j.envc.2023.100688

Arumugam, S., Sultan, M. T., Kandasamy, J., Shahar, F. S., Md Shah, A. U., Sebaey, T., & Khan, T. (2022). Natural fibre composites. I*n Encyclopedia*. https://encyclopedia.pub/entry/22712

Asfaw, N. T., Absi, R., Labouda, B. A., & Abbassi, I. El. (2024). Assessment of the thermal and mechanical properties of bio-based composite materials for thermal insulation: A review. *Journal of Building Engineering*, 97, 110605. https://doi.org/10.1016/j.jobe.2024.110605

Assarar, M., Scida, D., El Mahi, A., Poilâne, C., & Ayad, R. (2011). Influence of water ageing on mechanical properties and damage events of two reinforced composite materials: Flax fibres and glass fibres. *Materials & Design*, 32(2), 788–795. https://www.sciencedirect.com/science/article/pii/S0261306910004590

Awais, H., Nawab, Y., Amjad, A., Anjang, A., Akil, H. Md., & Abidin, S. Z. M. (2021). Environmental benign natural fibre reinforced thermoplastic composites: A review. *Composites Part C: Open Access*, 4, 100082. https://doi.org/10.1016/j.jcomc.2020.100082

Baker, M. I., Walsh, S. P., Schwartz, Z., & Boyan, B. D. (2012). A review of polyvinyl alcohol and its uses in cartilage and orthopedic applications. *Journal of Biomedical Materials Research Part B: Applied Biomaterials*, 100B(5), 1451–1457. https://doi.org/10.1002/jbm.b.32694

Balasubramanian, K., Sultan, M. T. H., & Rajeswari, N. (2018). Manufacturing techniques of composites for aerospace applications. In M. Jawaid & M. Thariq (Eds.), *Sustainable composites for aerospace applications (Woodhead Publishing Series in Composites Science and Engineering*, Chapter 4, pp. 55–67). Woodhead Publishing. https://doi.org/10.1016/B978-0-08-102131-6.00004-9

Balasubramanian, M., Saravanan, R., & Sathish, T. (2024). Exploring natural plant fibre choices and treatment methods for contemporary composites: A comprehensive review. *Results in Engineering*, 24, 103270. https://doi.org/10.1016/j.rineng.2024.103270

Balaji, A., Karthikeyan, B., & Sundar Raj, C. (2015). Bagasse fibre – The future biocomposite material: A review. *International Journal of ChemTech Research*, 7(1), 223–233.

Balavigna Weaving Mills Private Limited. (n.d.). Bamboo fibre at best price in Dindigul – ID: 3666608. ExportersIndia. https://www.exportersindia.com/product-detail/bamboo-fibre-3666608.htm

Barth, M., & Carus, M. (2015). Carbon footprint and sustainability of different natural fibres for biocomposites and insulation material. https://pantanova.nl/wp-content/uploads/2015/05/pantanova_multihemp_nova_carbon-footprint-of-natural-fibres.pdf

Belaguli Mahesh, M., Biligere Sathish, M., Rangaswamy, M., Jamadar, N. S., Puttegowda, M., & Ballupete Nagaraju, S. (2026). Advancements in 3D printed hemp-PLA composites: A sustainable approach for additive manufacturing. *Next Research*, 3, 101168. https://doi.org/10.1016/j.nexres.2025.101168

Biron, M. (2018). Thermoplastics and thermoplastic composites. In Thermoplastics and thermoplastic *composites (3rd ed., Chapter 4: Detailed accounts of thermoplastic resins)*. https://doi.org/10.1016/B978-0-08-102501-7.00004-7

Biron, M. (2018). Thermoplastics and thermoplastic composites. In Thermoplastics and thermoplastic composites *(3rd ed., Chapter 5: Thermoplastic processing)*. https://doi.org/10.1016/B978-0-08-102501-7.00005-9

Birdsupply.nl. (n.d.). Sisal fibre, de webshop in nestmaterialen. https://www.birdsupply.nl/sisal-fibre-500-gram.html

Boafo, F. E., Kim, J.-H., & Kim, J.-T. (2016). Performance of modular prefabricated architecture: Case study-based review and future pathways. *Sustainability*, 8(6), 558. https://www.mdpi.com/2071-1050/8/6/558

Boafo, F. E., Kim, J.-T., Ahn, J., Kim, S., & Kim, J.-H. (2021). Slim curtain wall spandrel integrated with vacuum insulation panel: A state-of-the-art review and future opportunities. *Journal of Building Engineering*, 42, 102445. https://doi.org/10.1016/j.jobe.2021.102445

Boppana, S. B., Ramachandra, C. G., Kumar, K. P., & Ramesh, S. (2024). Structural composite materials. *Composites Science and Technology*. https://doi.org/10.1007/978-981-99-5982-2

Bourmaud, A., Beaugrand, J., Shah, D. U., Placet, V., & Baley, C. (2018). Towards the design of high-performance plant fibre composites. *Progress in Materials Science*, 97, 347–408. https://doi.org/10.1016/J.PMATSCI.2018.05.005

Burdett, S., Arora, M., & Myers, R. J. (2026). Sustainable materials selection with emerging structural materials. *Materials Sustainability*, 4, 13. https://doi.org/10.1038/s44296-026-00099-7

Campbell, F. C. (2010). Thermoset composite fabrication processes. In Structural composite materials (pp. 119–182). *ASM International*. https://doi.org/10.31399/asm.tb.scm.t52870119

CarbonCloud. (2026). Epoxy resin. https://apps.carboncloud.com/climatehub/product-reports/id/9346344592306

Cerclos. (2015). Typical life expectancy of building components. https://etoolglobal.com/wp-content/uploads/2015/10/BuildingComponentLifeExpectancy.pdf

Chand, N., & Rohatgi, P. K. (1992). Potential use, mechanical and thermal studies of sabai grass fibre. *Journal of Materials Science Letters*, 11, 578–580. https://doi.org/10.1007/BF00728614

Charai, M., Salhi, M. O., Horma, O., Mezrhab, A., Karkri, M., & Amraqui, S. (2022). Thermal and mechanical characterization of adobes bio-sourced with Pennisetum setaceum fibres and an application for modern buildings. *Construction and Building Materials*, 326, 126809. https://doi.org/10.1016/j.conbuildmat.2022.126809

Chichane, A., Boujmal, R., & El Barkany, A. (2024). Towards a green and ecological revolution: Review of natural reinforcing bio-composites and bio-hybrid composites. *Polymers and Polymer Composites*, 32. https://doi.org/10.1177/09673911241226578

Chou, T.-W., & Ko, F. K. (1989). Textile structural composites. *Elsevier Science Publishers B V*. https://doi.org/10.1002/adma.19890011016

Clark, D. (2019). What colour is your building?: Measuring and reducing the energy and carbon footprint of buildings (1st ed.). *RIBA Publishing*. https://doi.org/10.4324/9780429347733

Clever Carbon. (2025). The carbon footprint of everyday items. https://clevercarbon.io/carbon-footprint-of-common-items

Clyne, T. W., & Hull, D. (2019). An introduction to composite materials. Cambridge University Press.

Cole, R. J., & Kernan, P. C. (1996). Life-cycle energy use in office buildings. *Building and Environment*, 31(4), 307–317. https://doi.org/10.1016/0360-1323(96)00017-0

Costa, A. R. M., Almeida, T. G., Silva, S. M. L., Carvalho, L. H., & Canedo, E. L. (2015). Chain extension in poly(butylene adipate-co-terephthalate): Inline testing in a laboratory internal mixer. *Polymer Testing*, 42, 115–121. https://doi.org/10.1016/j.polymertesting.2015.01.007

Cotton, S. (n.d.). Barley straw archives - Dynamic Ag. Dynamic Ag. https://www.dynamicag.com.au/tag/barley-straw/

Dai, J., Peng, Y., Teng, N., Liu, Y., Liu, C., Shen, X., & Liu, X. (2018). High-performing and fire-resistant biobased epoxy resin from renewable sources. *ACS Sustainable Chemistry & Engineering*, 6(6), 7589–7599. https://doi.org/10.1021/acssuschemeng.8b00439

Dehghani, A., Madadi Ardekani, S., Al-Maadeed, M. A., Hassan, A., & Wahit, M. U. (2013). Mechanical and thermal properties of date palm leaf fibre reinforced recycled poly(ethylene terephthalate) composites. *Materials & Design*, 52, 841–848. https://doi.org/10.1016/j.matdes.2013.06.022

Delgado-Aguilar, M., Vilaseca, F., Tarrés, Q., Julián, F., Mutjé, P., & Espinach, F. X. (2018). Extending the value chain of corn agriculture by evaluating technical feasibility and the quality of the interphase of chemo-thermomechanical fibre from corn stover reinforced polypropylene biocomposites. *Composites Part B: Engineering*, 137, 16–22. https://doi.org/10.1016/j.compositesb.2017.11.006

Di Landro, L., & Janszen, G. (2014). Composites with hemp reinforcement and bio-based epoxy matrix. *Composites Part B: Engineering*, 67, 220–226. https://doi.org/10.1016/j.compositesb.2014.07.021

EasyComposites Europe. (2025). 100 g non-woven hemp fibre reinforcement mat, 480 mm wide. https://www.easycomposites.eu/100g-non-woven-hemp-fibre-mat

EasyComposites Europe. (2025). Flax fibre reinforcement in composites. https://www.easycomposites.eu/learning/flax-fibre-in-composites

Easy Composites. (2025). Resins and gelcoats – Easy Composites Europe. https://www.easycomposites.eu/resins-and-gelcoats

Eckelman, M., & Nunberg, S. (2026). Life cycle assessment explained. *STiCH*. https://stich.culturalheritage.org/life-cycle-assessment-explained/

Ekomia. (2025). Coconut fibre. Ekomia. https://ekomia.de/en/blogs/materialien-sammlung/kokosfaser

Elfaleh, I., Abbassi, F., Habibi, M., Ahmad, F., Guedri, M., Nasri, M., & Garnier, C. (2023). A comprehensive review of natural fibres and their composites: An eco-friendly alternative to conventional materials. *Results in Engineering*, 19, 101271. https://doi.org/10.1016/j.rineng.2023.101271

EPD Hub. (2025). Environmental product declaration in accordance with EN 15804+A2 & ISO 14025 / ISO 21930: Hollow sections, Tobnoy Oy. Performed with OneClick LCA. https://www.tibnor.fi/medias/EPD-Hollow-sections.pdf

European Aluminium. (2024). Environmental profile report for the European aluminium industry: Life cycle inventory (LCI) data for aluminium production and transformation processes in Europe. https://european-aluminium.eu/wp-content/uploads/2024/11/2024-11-07-European-Aluminium-EPR-2024-Executive-Summary.pdf

European Bioplastics. (2020). Bioplastic materials. https://www.european-bioplastics.org/bioplastics/materials/

Evaluation of the diameter influence on the tensile strength of pineapple leaf fibres (PALF) by Weibull method. (n.d.). *ResearchGate*. https://www.researchgate.net/figure/Pineapple-fibres-PALF-extracted-from-the-leaves-of-Ananas-comosus_fig4_298424144 (Accessed December 19, 2025)

Exel Composites. (2025, December 17). Data sheets and specifications – Exel Composites. https://exelcomposites.com/data-sheets-and-specifications/

Fan, M., & Fu, F. (2017). Advanced high strength natural fibre composites in construction. *Woodhead Publishing Series in Composites Science and Engineering* (Vol. 74). https://doi.org/10.1016/C2014-0-03942-1

Fan, M., & Weclawski, B. (2017). Long natural fibre composites. In M. Fan & F. Fu (Eds.), Advanced high strength natural fibre composites in construction (Chapter 6, pp. 141–177). *Woodhead Publishing*. https://doi.org/10.1016/B978-0-08-100411-1.00006-6

Faruk, O., Bledzki, A. K., Fink, H. P., & Sain, M. (2012). Biocomposites reinforced with natural fibres: 2000–2010. *Progress in Polymer Science*, 37(11), 1552–1596. https://doi.org/10.1016/S0079-6700(12)00039-1

Figueiredo, A., Vela, G., Ascensão, G., Vettorazzi, E., Vicente, R., & Oliveira, M. (2025). Development of an innovative biocomposite using coconut fibres and bio-based binder for thermal and acoustic applications in buildings. *Journal of Cleaner Production*, 491, 144834. https://doi.org/10.1016/j.jclepro.2025.144834

Fook, L., & Yatim, J., (2015). Mechanical properties of kenaf fiber reinforced concrete with different fiber content and fiber length. *Journal of Asian Concrete Federation*. 1. 11. 10.18702/acf.2015.09.1.11.

Fujimaki, T. (1998). Processability and properties of aliphatic polyesters "BIONOLLE" synthesized by polycondensation reaction. *Polymer Degradation and Stability*, 59(1–3), 209–214. https://doi.org/10.1016/S0141-3910(97)00220-6

Garfield Aluminium. (2025). Prijsontwikkeling op de aluminium markt. https://www.garfield.nl/nl-nl/aluminium-prijs

George, M., Chae, M., & Bressler, D. C. (2016). Composite materials with bast fibres: Structural, technical, and environmental properties. *Progress in Materials Science,* 83, 1–23. https://doi.org/10.1016/j.pmatsci.2016.04.002

Geremew, A., De Winne, P., Demissie, T. A., & De Backer, H. (2022). Characterization of wheat straw fibre grown around Jimma Zone, Ethiopia. *Journal of Natural Fibres,* 20(1). https://doi.org/10.1080/15440478.2022.2134268

Gowman, A., Picard, M., Lim, L., Misra, M., & Mohanty, A. (2019). Fruit waste valorization for biodegradable biocomposite applications: A review. *BioResources, 14(4)*. https://doi.org/10.15376/biores.14.4.Gowman

Guedes Soares, C., & Salvado, F.C. (Eds.). (2026). Innovations in Maritime Technology and Engineering: Volume 1 (1st ed.). *CRC Press*. https://doi.org/10.1201/9781003795490

Guna, V., Ilangovan, M., Adithya, K., Koushik, C. V., Srinivas, C. V., Yogesh, S., Nagananda, G. S., Venkatesh, K., & Reddy, N. (2019). Biofibres and biocomposites from sabai grass: A unique renewable resource. *Carbohydrate Polymers*, 218, 243–249. https://doi.org/10.1016/j.carbpol.2019.04.085

Hagel, S., & Schütt, F. (2024). Reinforcement fibre production from wheat straw for wastepaper-based packaging using steam refining with sodium carbonate. *Clean Technologies*, 6(1), 322–338. https://doi.org/10.3390/cleantechnol6010016

Hanway, J. (1993). How a corn plant develops. Special Publication 48, Iowa Agricultural and Home Economics Experiment Station Publication 1966, 48, 1–18. https://www.aces.edu/wp-content/uploads/2022/03/ANR-2863-How-Corn-Plant-Develops_PROOF_022422aL-G.pdf

Hemp from Own Cultivation. (n.d.). Topp Textil GmbH. https://www.topp-textil.de/en/sustainability/hemp-from-own-cultivation

Hoxha, E., Birgisdottir, H., & Röck, M. (2025). Climate impact of EU building materials: Data compilation and statistical analysis of global warming potential in environmental product declarations. *Sustainable Production and Consumption*, 54, 64–74. https://www.sciencedirect.com/science/article/pii/S2352550924003580

IJIRA. (n.d.). Jute – Fibre of the future. https://ijira.org.in/jute-fibre-of-the-future/

ILVO. (n.d.). Een waardeketen voor maïsstro in de bio-economie in Vlaanderen? https://ilvo.vlaanderen.be/en/news/a-value-chain-for-maize-straw-in-the-bioeconomy-of-flanders

Intertek. (2024). EN 13830: Curtain walling – Product standard. https://www.intertek.com/building/standards/en-13830/

Islam, S., Hasan, M. B., Kodrić, M., Motaleb, K. Z. M. A., Karim, F., & Islam, M. R. (2025). Mechanical properties of hemp fibre-reinforced thermoset and thermoplastic polymer composites: A comprehensive review. *SPE Polymers*, 6(1). https://doi.org/10.1002/pls2.10173

Islam, S., Karim, F., & Islam, M. R. (2024). Assessing the consequences of water retention on the structural integrity of jute fibre and its composites: A review. *SPE Polymers*, 5(4), 457–480. https://doi.org/10.1002/pls2.10142

Jawaid, M., & Abdul Khalil, H. P. S. (2011). Cellulosic/synthetic fibre reinforced polymer hybrid composites: A review. *Carbohydrate Polymers*, 86, 1–18. https://doi.org/10.1016/J.CARBPOL.2011.04.043

Jayaraman, K. (2003). Manufacturing sisal–polypropylene composites with minimum fibre degradation. *Composites Science and Technology*, 63, 367–374. https://doi.org/10.1016/S0266-3538(02)00217-8

Jia, Y. (2020). Durability of flax fibre/bio-epoxy sustainable composites for structural application (Doctoral dissertation, Technische Universität Hamburg). https://tore.tuhh.de/bitstream/11420/4967/1/Yunlong%20Jia%20-%20dissertation%20for%20library.pdf

Jian, J., Xiangbin, Z., & Xianbo, H. (2020). An overview on synthesis, properties and applications of poly(butylene adipate-co-terephthalate) (PBAT). *Advanced Industrial and Engineering Polymer Research*, 3(1), 19–26. https://doi.org/10.1016/j.aiepr.2020.01.001

Kabir, M. M., Wang, H., Lau, K. T., & Cardona, F. (2012). Chemical treatments on plant-based natural fibre reinforced polymer composites: An overview. *Composites Part B: Engineering*, 43, 2883–2892. https://doi.org/10.1016/j.compositesb.2012.04.053

Kambli, N., Basak, S., & Deshmukh, R. (2021). Cornhusk fibres, its properties, and value addition. In N. Ibrahim & C. M. Hussain (Eds.), *Green chemistry for sustainable textiles (Chapter 31, pp. 471–480)*. Woodhead Publishing. https://doi.org/10.1016/B978-0-323-85204-3.00006-3

Kanaginahal, G., Shahapurkar, K., Kakkamari, P., Rajeshwari, S., Chenrayan, V., Magi, M., Tirth, V., Algahtani, A., Bhaviripudi, V., Venkatachalam, V., Umarfarooq, M. A., & Singh, B. (2026). Jute fiber and its composites: Processing, properties, and applications. *Journal of*

Natural Fibers, 23. https://doi.org/10.1080/15440478.2026.2635010

Kasturi Coconut Processing. (n.d.). Coir fibre bales. https://www.kasturicoconutprocessing.com/coir-fibre-bales.htm

Kawneer. (n.d.). AA 100 FR brandwerend vliesgevelsysteem [Image]. https://www.kawneer.nl/producten/vliesgevels/aa-100-fr

Kazmierczak, K., & Hershfi, M. (2010). Review of curtain walls, focusing on design problems and solutions. *In Proceedings of BEST2 Conference*. Portland, OR, USA. http://karol.us/BEST2.pdf

Kelly, J. W. (2024). Crystal Palace: Study reveals secret of 190-day Victorian build. BBC News. https://www.bbc.com/news/articles/cy0ll41l9pno

Khalid, M. Y., Al Rashid, A., Arif, Z. U., Ahmed, W., Arshad, H., & Zaidi, A. A. (2021). Natural fibre reinforced composites: Sustainable materials for emerging applications. *Results in Engineering*, 11, 100263. https://doi.org/10.1016/J.RINENG.2021.100263

Khan, T., Hameed Sultan, M. T. B., & Ariffin, A. H. (2018). The challenges of natural fibre in manufacturing, material selection, and technology application: A review. *Journal of Reinforced Plastics and Composites*, 37(11), 770–779. https://doi.org/10.1177/0731684418756762

Khotbehsara, M. M., Manalo, A., Aravinthan, T., Ferdous, W., Nguyen, K. T., & Hota, G. (2020). Ageing of particulate-filled epoxy resin under hygrothermal conditions. *Construction and Building Materials*, 249, 118846. https://doi.org/10.1016/j.conbuildmat.2020.118846

Kieffer, V,. & Santana, R.. (2025). Influence of additives use from natural sources on the mechanical performance of post-consumer HDPE composites reinforced with natural fibers. *Materials Research*. 28. 10.1590/1980-5373-mr-2024-0610.

Kumar, S., Das, R., & Parida, S. (2025). Evaluation of mechanical properties of Sabai grass (Eulaliopsis binata) fibres and epoxy resin composite laminates using fly ash as filler material. *Journal of Composites Science*, 9, 38. https://doi.org/10.3390/jcs9010038

Kumar, S., Das, R., & Parida, S. K. (2024). Strength evaluation of alkali treated Sabai grass (Eulaliopsis binata) fibres and its reinforced composites. P*roceedings of the Institution of Mechanical Engineers, Part C: Journal of Mechanical Engineering Science*, 238(12), 5739–5751. https://doi.org/10.1177/09544062231220533

Laribi, M. A. (2018). Caractérisation et modélisation micromécanique du comportement des matériaux composites SMC sous chargement thermomécanique de type quasi-statique et fatigue (Doctoral thesis). École Nationale Supérieure d'Arts et Métiers, Paris, France.

Lau, A. K., & Hung, A. P. (2017). Natural fibre-reinforced biodegradable and bioresorbable polymer composites. Woodhead Publishing. https://nl1lib.org/book/2918570/99a2a5?dsource=recommend

LETI. (2020). Embodied carbon primer: Supplementary guidance to the climate emergency design guide. Low Energy Transformation Initiative. https://www.leti.uk/_files/ugd/252d09_8ceffcbcafdb43cf8a19ab9af5073b92.pdf

Liu, Q., & Hughes, M. (2008). The fracture behaviour and toughness of woven flax fibre reinforced epoxy composites. *Composites Part A: Applied Science and Manufacturing*, 39(10), 1644–1652. https://www.sciencedirect.com/science/article/pii/S1359835X08001929

Livne, A., Wosten, H. A. B., Pearlmutter, D., & Gal, E. (2022). Fungal mycelium bio-composite acts as a CO_2-sink building material with low embodied energy. *ACS Sustainable Chemistry & Engineering, 10(37)*, 12099–12106. https://doi.org/10.1021/acssuschemeng.2c01314

Lopez-Arraiza, A., Essamari, L., Iturrondobeitia, M., Boullosa-Falces, D., & Justel, D. (2025). Life cycle assessment of glass fibre versus flax fibre reinforced composite ship hulls. *Scientific Reports*, 15(1). https://doi.org/10.1038/s41598-025-00811-y

Mahajan, A., Binaz, V., Singh, I., & Arora, N. (2022). Selection of natural fibre for sustainable composites using hybrid multi-criteria decision making techniques. *Composites Part C: Open Access*, 7, 100224. https://doi.org/10.1016/j.jcomc.2021.100224

Mahmudul, A., Alimuzzaman, S., Shah, D., & Rahman, A. N. M. M. (2018). Physico-mechanical, thermal and biodegradation performance of random flax/polylactic acid and unidirectional flax/polylactic acid biocomposites. *Fibers*, 6(4), 98. https://doi.org/10.3390/fib6040098

Make. (2024, January 5). Embodied carbon in curtain walls. Make Architects. https://www.makearchitects.com/thinking/embodied-carbon-in-curtain-walls/

MakeItFrom. (2020). 6060-T66 aluminum: Mechanical properties. https://www.makeitfrom.com/material-properties/6060-T66-Aluminum

Majorel, M. (2024). Different uses of flax fibre and innovations. Safilin. https://www.safilin.fr/uses-of-flax-fibre-and-innovations/?lang=en

Mallick, P. K. (2008). Fibre reinforced composites: Materials, manufacturing, and design. *Taylor & Francis Group*. https://www.taylorfrancis.com/books/mono/10.1201/9781420005981/fiber-reinforced-composites-mallick

MallonLinen. (2026). Good tow flax fibre. https://mallonlinen.co.uk/product/good-tow-flax-fibre/

Mathur, V.K.,(2006), Composite materials from local resources, *Construction and Building Materials*. V*olume 20*, Issue 7. Pages 470-477, ISSN 0950-0618. https://doi.org/10.1016/j.conbuildmat.2005.01.031.

McKeen, L. (2012). Renewable resource and biodegradable polymers. In L. McKeen (Ed.), *The effect of sterilization on plastics and elastomers (Chapter 12)*. Elsevier. https://doi.org/10.1016/B978-1-4557-2598-4.00012-5

Mekonnen, T., Mussone, P., Khalil, H., & Bressler, D. (2013). Progress in bio-based plastics and plasticizing modifications. *Journal of Materials Chemistry A*, 1(43), 13379–13398. https://doi.org/10.1039/c3ta12555f

Michelin. (2025). How to calculate your fleet's carbon footprint. https://connectedfleet.michelin.com/blog/calculate-co2-emissions/

Mohammed, A. A. B. A., Hasan, Z., Omran, A. A. B., Kumar, V., Elfaghi, A. M., Ilyas, R., … & Sapuan, S. (2022). Corn: Its structure, polymer, fibre, composite, properties, and applications. *Polymers*, 14(20), 4396. https://doi.org/10.3390/polym14204396

Morten, R., Bo, M., Bent, S. F., Julie, F. L., Martyniuk, M., & Lauridsen, E. M. (2012). In situ observations of microscale damage evolution in unidirectional natural fibre composites. *Composites Part A: Applied Science and Manufacturing*, 43(10), 1639–1649. https://www.sciencedirect.com/science/article/pii/S1359835X12000656

Mu, Q., An, L., Hu, Z., & Kuang, X. (2022). Fast and sustainable recycling of epoxy and composites using mixed solvents. *Polymer Degradation and Stability*, 199, 109895. https://doi.org/10.1016/j.polymdegradstab.2022.109895

Mustapha, R., Rahmat, A. R., Abdul Majid, R., & Mustapha, S. N. H. (2019). Vegetable oil-based epoxy resins and their composites with bio-based hardener: A short review. *Polymer-Plastics Technology and Materials*, 58(12), 1311–1326. https://doi.org/10.1080/25740881.2018.1563119

Muthuraj, R., Misra, M., & Mohanty, A. K. (2018). Biodegradable compatibilized polymer blends for packaging applications: A literature review. *Journal of Applied Polymer Science*, 135(24), 45726. https://doi.org/10.1002/app.45726

Mwaikambo, L. Y. (2006). Review of the history, properties and application of plant fibres. *African Journal of Science and Technology (AJST)*, Science and Engineering Series, 7, 120–133.

Nechita, P., & Ionescu, Ş. M. (2018). Investigation on the thermal insulation properties of lightweight biocomposites based on lignocellulosic residues and natural polymers. *Journal of Thermoplastic Composite Materials*, 31(11), 1497–1509. https://doi.org/10.1177/0892705717738300

Neitzel, N., Eder, M., Hosseinpourpia, R., Walther, T., & Adamopoulos, S. (2023). Chemical composition, particle geometry, and micro-mechanical strength of barley husks, oat husks, and wheat bran as alternative raw materials for particleboards. *Materials Today Communications*, 36, 106602. https://doi.org/10.1016/j.mtcomm.2023.106602

NEN. (2023). NEN-EN 12020-2:2023 en. https://www.nen.nl/nen-en-12020-2-2023-en-305338

Ntrivala, M. A., Pitsavas, A. C., Lazaridou, K., Baziakou, Z., Karavasili, D., Papadimitriou, M., Ntagkopoulou, C., Balla, E., & Bikiari, D. N. (2025). Polycaprolactone (PCL): The biodegradable polyester shaping the future of materials – A review on synthesis, properties, biodegradation, applications and future perspectives. *European Polymer Journal*, 234, 114033. https://doi.org/10.1016/j.eurpolymj.2025.114033

Oil palm fibre. (n.d.). ETawau. https://www.etawau.com/OilPalm/OilPalmFibre.htm

Oksman, K., Skrifvars, M., & Selin, J. F. (2003). Natural fibres as reinforcement in polylactic acid (PLA) composites. *Composites Science and Technology*, 63(9), 1317–1324. https://doi.org/10.1016/S0266-3538(03)00103-9

Oun, A., Alajarmeh, O., Manalo, A., Abousnina, R., & Gerdes, A. (2024). Durability of hybrid flax fibre-reinforced epoxy composites with graphene in hygrothermal environment. *Construction and Building Materials*, 420, 135584. https://doi.org/10.1016/j.conbuildmat.2024.135584

Overend, M., et al. (unpublished). Material selection, fabrication and performance of continuous flax fibre composites with high bio-based content. Unpublished manuscript, received through personal communication.

Paolette, I., & Nastri, M. (2024). Executive design of the façade systems: Typologies and technologies of the advanced building envelopes (Chapter 2). I*n SpringerBriefs in applied sciences and technology*. https://doi.org/10.1007/978-3-031-44893-5

Peças, P., Carvalho, H., Salman, H., & Leite, M. (2018). Natural fibre composites and their applications: A review. *Journal of Composites Science*, 2(4), 66. https://doi.org/10.3390/jcs2040066

Peters, S. T. (2013). Handbook of composites. *Springer Science & Business Media*. https://scholar.google.com/scholar_lookup?title=Handbook%20of%20composites&publication_year=2013&author=S.T.%20Peters

Petroudy, S. R. D. (2017). Physical and mechanical properties of natural fibres. In M. Fan & F. Fu (Eds.), High strength natural fibre composites in construction (pp. 59–83). Woodhead Publishing. https://doi.org/10.1016/B978-0-08-100411-1.00003-0

PHA Sourcing. (2025). What is bagasse? https://pha-sourcing.com/what-is-bagasse/

Philip, S., Keshavarz, T., & Roy, I. (2007). Polyhydroxyalkanoates: Biodegradable polymers with a range of applications. J*ournal of Chemical Technology and Biotechnology*, 82(3), 233–247. https://doi.org/10.1002/jctb.1667

Pracucci, A., Vandi, L., Morganti, L., Gallego Fernández, A., Nunez Diaz, M., Navarro Muedra, A., Győri, V., Kouyoumji, J.-L., & Astudillo Larraz, J. (2024). Design and simulation for technological integration of bio-based components in façade system modules (Version 1) [Preprint]. Preprints.org. https://doi.org/10.20944/preprints202403.1552.v1

Puițel, A. C., Tofanica, B. M., & Gavrilescu, D. A. (2020). Fibrous raw materials from agricultural residues. In V. I. Popa (Ed.), *Pulp production and processing: High-tech applications (pp. 49–72)*. Walter de Gruyter GmbH & Co KG.

Raftoyiannis, I. (2012). Experimental testing of composite panels reinforced with cotton fibres. *Open Journal of Composite Materials*, 2, 27–33. https://doi.org/10.4236/ojcm.2012.22005

Raggousis, M. (2016). Demystifying the fly-by curtainwall parapet. Walls & Ceilings Online. https://digitaledition.wconline.com/november-2022/demystifying-the-fly-by-curtainwall-parapet/

Raico Bautechnik GmbH. (2025). THERM+ H-I – Timber façade. https://www.raico.de/en/products/facades-content/timber/therm-h-i.html

Rahman, M. D. H., & Bhoi, P. R. (2021). An overview of non-biodegradable bioplastics. *Journal of Cleaner Production*, 294, 126218. https://doi.org/10.1016/j.jclepro.2021.126218

Rajeshkumar, G., Seshadri, S.A., Keerthi, T.K.G. (2022). Recycling and Biodegradation Studies of Epoxy/Natural Fiber Composites. In: Mavinkere Rangappa, S., Parameswaranpillai, J., Siengchin, S., Thomas, S. (eds). *Handbook of Epoxy/Fiber Composites*. Springer, Singapore. https://doi.org/10.1007/978-981-19-3603-6_49

Ramesha, M., Palanikumarb, K., & Reddy, K. H. (2017). Plant fibre based bio-composites: Sustainable and renewable green materials. https://doi.org/10.1016/j.rser.2017.05.094

Rana, A. K., Mandal, A., & Bandyopadhyay, S. (2003). Short jute fibre reinforced polypropylene composites: Effect of compatibiliser, impact modifier and fibre loading. *Composites Science and Technology*, 63, 801–806. https://doi.org/10.1016/S0266-3538(02)00267-1

Raw banana fibre – Handicraft usage, eco-friendly, affordable price. (n.d.). Musa Agro Industries. https://www.musaagroindustries.com/raw-banana-fibre-8588667.html

Reynaers Aluminium. (2022). The life cycle of aluminium. https://www.reynaers.com/inspiration/stories/sustainability/life-cycle-aluminium

Rosales-Calderon, O., & Arantes, V. (2019). A review on commercial-scale high-value products that can be produced alongside cellulosic ethanol. *Biotechnology for Biofuels*, 12(1), 240. https://doi.org/10.1186/s13068-019-1529-1

Rubner Holding A.G.-s.p.a. (2023). Environmental product declaration as per ISO 14025 and EN 15804+A2: Glued laminated timber (update). https://www.ibu-epd.com

Saba, N., Paridah, M. T., & Jawaid, M. (2015). Mechanical properties of kenaf fibre reinforced polymer composite: A review. *Construction and Building Materials*, 76, 87–96. https://www.sciencedirect.com/science/article/pii/S0950061814012628

Samanth, M., & Bhat, K. S. (2023). Conventional and unconventional chemical treatment methods of natural fibres for sustainable biocomposites. *Sustainable Chemistry for Climate Action*, 3, 100034. https://doi.org/10.1016/j.scca.2023.100034

Samantaray, P. K., Little, A., Haddleton, D. M., McNally, T., Tan, B., Sun, Z., … Wan, C. (2020). Poly(glycolic acid) (PGA): A versatile building block expanding high performance and sustainable bioplastic applications. *Green Chemistry*, 22(13), 4055–4081. https://doi.org/10.1039/D0GC01394C

Sanders, R. M. (2006). Curtain walls: Not just another pretty facade. *Journal of Architectural Technology*, 23, 1–8. https://www.hoffarch.com/wp-content/uploads/Journal-Vol-23-N-1.pdf

Shanmugam, V., Mensah, R. A., Försth, M., Sas, G., Restás, A., Addy, C., Xu, Q., Jiang, L., Neisiany, R. E., Singha, S., George, G., Jose, E. T., Berto, F., Hedenqvist, M. S., Das, O., & Ramakrishna, S. (2021). Circular economy in biocomposite development: State-of-the-art, challenges and emerging trends. *Composites Part C: Open Access*, 5, 100138. https://doi.org/10.1016/j.jcomc.2021.100138

Shelly, D., Lee, S., & Park, S. (2025). Hemp fibre and its bio-composites: A comprehensive review part I–characteristics and processing. *Advanced Composites and Hybrid Materials*, 8, 252. https://doi.org/10.1007/s42114-025-01314-0

Sicomin. (2026). Fire resistant epoxy resins. https://sicomin.com/en/epoxy-products/epoxy/fire-resistant/

Singh, S. P., Dutt, A., & Hirwani, C. K. (2023). Experimental and numerical analysis of different natural fibre polymer composite. *Materials and Manufacturing Processes*, 38(3), 322–332. https://doi.org/10.1080/10426914.2022.2136379

SpecialChem. (2021). Polyethylene furanoate (PEF) material guide: Bio-based polymer. https://www.specialchem.com/plastics/guide/polyethylene-furanoate-pef-bioplastic

Spyridonos, E., & Dahy, H. (2025). Application of natural fibre pultruded profiles in diverse lightweight structures and architectural scenarios. *Architecture, Structures and Construction*, 5(2). https://doi.org/10.1007/s44150-024-00118-y

STABALUX. (2025). Things to know (Aluminium). https://www.stabalux.com/wp-content/uploads/PDF/en/9.0%20Aluminium_Wissenswertes_EN.pdf

Temafa, D. (2024). Boosting Eco-Technillin's flax fibre production. *Technical Textiles*. https://technical-textiles.textiletechnology.net/news/news/dilo-temafa-boosting-eco-technilins-flax-fibre-production-35980

The Editors of Encyclopædia Britannica. (2017). Bast fibre. Encyclopædia Britannica. https://www.britannica.com/technology/bast-fibre

Todor, M. P., Rackov, M., Kiss, I., & Cioata, V. G. (2022, February). Composite solutions with recycled textile wastes. *Journal of Physics: Conference Series*, 2212(1), 012030. IOP Publishing.

TVF. (n.d.). Cotton fibre types. https://www.tvfinc.com/article/cotton-fibre-types-and-traits/

Udisi, B., Osman, F., Gorgolewski, M., Saunders, K., Devraj-Kizuk, R., & Kemp, S. (2024). *IOP conference series: Earth and environmental science*, 1363, 012070. https://doi.org/10.1088/1755-1315/1363/1/012070

USDA.gov. (2025). World agricultural production. Economics, Statistics, and Market Information System. https://esmis.nal.usda.gov/publication/world-agricultural-production

Väisänen, T., Das, O., & Tomppo, L. (2017). A review on new bio-based constituents for natural fibre-polymer composites. *Journal of Cleaner Production*, 149, 582–596.

Vigneshwaran, S., Sundarakannan, R., John, K. M., Johnson, R. D. J., Prasath, K. A., Ajith, S., Arumugaprabu, V., & Uthayakumar, M. (2020). Recent advancement in the natural fibre polymer composites: A comprehensive review. *Journal of Cleaner Production*, 277, 124109. https://doi.org/10.1016/J.JCLEPRO.2020.124109

Wang, Z., & Zhu, G. (2023). Development of the temperature-dependent constitutive model of glass fibre reinforced polypropylene composites. *Materials and Manufacturing Processes*, 38, 295–305. https://doi.org/10.1080/10426914.2021.2016817

Wimmers, G., Klick, J., Tackaberry, L., Zwiesigk, C., Egger, K., & Massicotte, H. (2019). Fundamental studies for designing insulation panels from wood shavings and filamentous fungi. *BioResources*, 14(3), 5506–5520. https://bioresources.cnr.ncsu.edu/resources/fundamental-studies-for-designing-insulation-panels-from-wood-shavings-and-filamentous-fungi/

Worldsteel Association. (2025). Sustainability indicators report 2025. https://worldsteel.org/wider-sustainability/sustainability-indicators/

Yan, L., Chouw, N., & Jayaraman, K. (2014). Flax fibre and its composites – A review. *Composites Part B: Engineering*, 56, 296–317. https://www.sciencedirect.com/science/article/pii/S1359836813004228

Yan Cheong, H., Brambilla, A., Gasparri, E., Kuru, A., & Sangiorgio, A. (2024). Life cycle assessment of curtain wall facades: A screening study on end-of-life scenarios. *Journal of Building Engineering*, 84, 108600. https://doi.org/10.1016/j.jobe.2024.108600

Yang, H. S., Kim, H. J., Son, J., Park, H. J., Lee, B. J., & Hwang, T. S. (2004). Rice-husk flour filled polypropylene composites: Mechanical and morphological study. *Composites Structures*, 63(3–4), 305–312. https://www-sciencedirect-com.tudelft.idm.oclc.org/science/article/pii/S026382230300179X

Zafar, F., & Sharmin, E. (2012). Polyurethane. In Polyurethane. InTech. http://dx.doi.org/10.5772/2416

Zhang, L., Fairbanks, M., & Andrew, T. L. (2017). Rugged textile electrodes for wearable devices obtained by vapor coating off the shelf, plainwoven fabrics. *Advanced Functional Materials*, 27. https://doi.org/10.1002/adfm.201700415

Zhang, X. Y., Fu, W. Y., Duan, C. T., Xiao, H., Shi, M. W., Zhao, N., & Xu, J. (2013). Superhydrophobicity determines the buoyancy performance of kapok fibre aggregates. *Applied Surface Science*, 266, 225–229. https://doi.org/10.1016/j.apsusc.2012.11.153

Zhang, Y., Liu, X., Wan, M., Zhu, Y., & Zhang, K. (2024). Recent development of functional bio-based epoxy resins. *Molecules*, 29(18), 4428. https://doi.org/10.3390/molecules29184428

Zheng, Y., Wang, J.,Zhu, Y., Wang, A.,(2015). Research and application of kapok fiber as an absorbing material: A mini review, *Journal of Environmental Sciences, Volume 27*, Pages 21-32,ISSN 1001-0742, https://doi.org/10.1016/j.jes.2014.09.026.

12. APPENDIX

A. PROPERTIES OF NON-WOOD PLANT FIBRES

PROPERTIES OF BAST FIBRES

FIBRE	DENSITY (g/cm³)	YOUNGS MODULUS (GPa)	TENSILE STRENGTH (MPa)	ELONGATION AT BREAK (%)	COST	REFERENCE
Flax	*1.38*	*50-70 (60)*	*343–1035 (689)*	*1.2–3 (2.1)*	+++	*Peças et al., 2018 Mahajanet al., 2022*
Hemp	*1.5*	*30-60 (45)*	*580–1110 (845)*	*1.6–4.5 (3.05)*	++	*Peças et al., 2018 Mahajanet al., 2022*
Jute	*1.5*	*20-55 (37,5)*	*187–773 (480)*	*1.5–3.1 (2.3)*	+	*Peças et al., 2018 Mahajanet al., 2022*
Kenaf	*1.2*	*22-60 (41)*	*295–930 (612.5)*	*2.7–6.9 (4.8)*	+	*Peças et al., 2018 Mahajanet al., 2022*
Ramie	*1.44*	*61.4–128 (94.7)*	*400–938 (669)*	*2–4 (3)*	++	*Peças et al., 2018*
Bam-boo	*0.6–1.1 (0.85)*	*17–89 (53)*	*270–862 (566)*	*1.3–8 (4.65)*	+	*Peças et al., 2018*

PROPERTIES OF FRUIT AND GRASS FIBRES

FIBRE	DENSITY (g/cm³)	YOUNGS MODULUS (GPa)	TENSILE STRENGTH (MPa)	ELONGATION AT BREAK (%)	COST	REFERENCE
Coir	*1.2*	*6*	*175*	*15–25 (20)*	+	*Peças et al., 2018*
Oil Palm	*0.7-1.55 (1.13)*	*0.5-9 (4.75)*	*80-400 (240)*	*8-25 (16.5)*	+	*Shelly et al., 2025*
Bagasse	*1.2*	*11-27 (19)*	*20-290 (155)*	*1.1*	+	*Shelly et al., 2025*
Sabai	*0.6-0.9 (0.75)*	*9.8*	*76*	*38.1*	+	*Kumar et al., 2024*

PROPERTIES OF LEAF AND SEED FIBRES

FIBRE	DENSITY (g/cm³)	YOUNGS MODULUS (GPa)	TENSILE STRENGTH (MPa)	ELONGATION AT BREAK (%)	COST	REFERENCE
Abaca	*1.5*	*31.1–33.6 (32.35)*	*430–813 (621.5)*	*2.9*	+	*Peças et al., 2018*
Sisal	*1.2*	*9–22 (15.5)*	*507–855 (681)*	*1.9–3 (2.45)*	++	*Peças et al., 2018*
Pineapple	*1.5*	*60–82 (71)*	*170–1627 (898.5)*	*1–3 (2)*	+	*Peças et al., 2018*
Cotton	*1.21*	*6–10 (8)*	*287–597 (442)*	*2–10 (6)*	+++	*Peças et al., 2018*
Kapok	*1.3*	*1.7-4.0 (2.85)*	*45-93 (69)*	*1.2-4.0 (2.6)*	+	*Shelly et al., 2025 Mwaikambo, 2006*

+ = 0 - 1000 US$/ton
++ = 1000 - 2500 US$/ton
+++ = > 2500 US$/ton
Numbers between brackets () are averages.

PROPERTIES OF STALK FIBRES

FIBRE	DENSITY (g/cm^3)	YOUNGS MODULUS (GPa)	TENSILE STRENGTH (MPa)	ELONGATION AT BREAK (%)	COST	REFERENCE
Corn (maize)	*1.42*	-	-	-	+	*Mohammed et al., 2022*
Rice straw	*1.4*	*3.3-12.5 (7.9)*	*150-200 (175)*	*3.2-4.6 (3.9)*	+	*Shelly et al., 2025*
Wheat straw	*1.49*	*3.7-4.8 (4.25)*	*59-140 (99.5)*	*2.0-5.0 (3.5)*	+	*Shelly et al., 2025*

ADDITIONAL PROPERTIES OF PLANT FIBRES

Fibre	DIAMETER (µm)	LENGTH (mm)	ASPECT RATIO (µm)	DENSITY (g/cm^3)	STRAIN AT BREAK (%)	SPECIFIC STRENGTH ($MPa/g/cm^3$)	SPECIFIC MODULUS ($GPa/g/cm^3$)	MOISTURE ABSORPTION (%)	COST	REFERENCE
Flax	*5-38 (21.5)*	*10-65 (35.5)*	*1651.2*	*1.38*	*1.4*	*832.5*	*36*	*7*	+++	*Mahajanet al., 2022*
Hemp	*10-51 (30.5)*	*5-55 (30)*	*983.6*	*1.5*	*1.6*	*360*	*47.3*	*8*	++	*Mahajanet al., 2022*
Jute	*5-25 (15)*	*0.8-6 (3.4)*	*226.7*	*1.5*	*1.8*	*411*	*14*	*10*	+	*Mahajanet al., 2022*
Kenaf	*12-36 (24)*	*1.4-11 (6.2)*	*258.3*	*1.2*	*1.6*	*641*	*36.6*	*9.1*	+	*Mahajanet al., 2022*
Ramie	*18-80 (49)*	*40-250 (145)*	*2959.2*	*1.44*	*1.2*	*465*	*65.8*	*11*	++	*Peças et al., 2018*
Bamboo	*25-88 (56.5)*	*1.5-4 (2.75)*	*48.7*	*0.6–1.1 (0.85)*	*1.73*	*383.1*	*22.1*	*8*	+	*Mahajanet al., 2022*
Coir	*7-30 (18.5)*	*0.3-3 (1.65*	*89,2*	*1.2*	*20*	*145.8*	*5*	*10*	+	*Peças et al., 2018*
Oil Palm		-	-	*0.7-1.55 (1.13)*	*16.5*	*212.4*	*4.2*	-	+	*Shelly et al., 2025*
Bagasse	*200-400 (300)*	-	-	*1.2*	*1.1*	*129.2*	*15.8*	*8.8-10 (9.4)*	+	*Shelly et al., 2025*
Sabai	-	-	-	*0.6-0.9 (0.75)*	*38.1*	*101.3*	*50.8*	-	+	*Kumar et al., 2024*
Abaca	*10-30 (20)*	*4.6-5.2 (4.9)*	*245*	*1.5*	*2.9*	*414.3*	*21.6*	*14*	+	*Peças et al., 2018*
Sisal	*7-47 (27)*	*0.8-8 (4.4)*	*163*	*1.2*	*2.45*	*567.5*	*12.9*	*11*	++	*Peças et al., 2018*
Pine apple	*8-41 (24.5)*	*3-8 (5.5)*	*224.5*	*1.5*	*2*	*599*	*47.3*	*14*	+	*Peças et al., 2018*
Cotton	*12-35 (23.5)*	*15-56 (35.5)*	*1510.6*	*1.21*	*6.5*	*264.9*	*8*	*33.5*	+++	*Mahajanet al., 2022*
Kapok	*23.6*	-	-	*1.3*	*2.6*	*53.1*	*2.1*	-	+	*Shelly et al., 2025 Mwaikambo, 2006*

Maize	-	-	-	*1.42*	-	-	-	-	+	*Shelly et al., 2025*
Rice	-	-	-	*1.4*	*3.9*	*125*	*2.8*	-	+	*Shelly et al., 2025*
Wheat	*84-94 (89)*	-	-	*1.49*	*3.5*	*66.8*	*2.3*	-	+	*Shelly et al., 2025*
Perfor-mance criteria	-	-	*>250*	*2.7*	*9.1*	*81.5*	*25.9*	*<10*	< +++	-

+ = 0 - 1000 US$/ton
++ = 1000 - 2500 US$/ton
+++ = > 2500 US$/ton
Numbers between brackets () are averages.

B. PROPERTIES OF POLYMER MATRICES

PROPERTIES OF SYNTHETIC THERMOSETS							
SYNTHETIC THERMOSET	**DENSITY (g/cm³)**	**TENSILE STRENGTH (MPa)**	**TENSILE MODULUS (GPa)**	**ELONGATION AT BREAK (%)**	**COST (eur/kg)**	**AVAILABLE TO BUY**	**NEEDED EQUIPMENT / USAGE**
Polyester	1.1-1.43	34.5-103.5	2.1-3.45	1-5	5-10	Marine-supply retailers, DIY craft stores	-MEKP catalyst needed -Accurate dropper or syringe (very important) -Ventilation is critical - Used for boats, surfboards, molds
Vinyl esters	1.08	90	3.5	4.0	10-15	Some specialty shops	- MEKP catalyst - Scale or catalyst dispenser - Ventilation is critical - Use for stronger, more durable laminates than basic polyester
Epoxy resin	1.2-1.3	55-130	2.75-4.10	6-9	20-25	Widely available	-Hardener needed (fixed ratio) - Release agents (for molds) - Used for DIY carbon/fibreglass parts, tooling, coatings
Poly utherane	1.24	20.7	2.8	8	10-15	Often hobby grade	- 2 part resin (often moisture-sensitive) - Precise scale, dry containers - Used for patterns, molds, cores
Mechanical properties of synthetic thermosets (Mallick, 2008 and Zafar et al., 2012 and Fan et al., 2017; Biron, 2018; Easycomposites, 2025).							
PROPERTIES OF SYNTHETIC THEMOPLASTICS							
PE	-	-	-	-	-	Sheets/ pellets	- Heat gun or precise oven - Compression mold or press - Non-stick mold - Used for impact-resistant panels, tanks, cores
PP	0.13	70-85	5	600	0.9-2	Sheets/ pellets	- Heat gun or precise oven - Compression mold or press - Non-stick mold - Used for automotive panels, structural thermoplastic composites
PVC	1.3	12	-	400	1-2	Sheets/ pellets	- Heat gun or precise oven - Compression mold or press - Non-stick mold - Used for rigid sheets, pipes, panels, non-structural composites
PMMA	1.2	70	3.5	10	2.1-2.2	Sheets/ pellets	- Reinforcement: Particulate fillers, short fibres - Used as a matrix in simple composites (e.g., optical or transparent composites)
PS	1.05	60	3.5	4	1.5-2.5	Sheets/ pellets	- Impact modifiers, plasticizers (for some grades) - Used in composites like wood-plastic composites (WPC) when blended with wood flour or plant fibres or can be reinforced with glass or carbon in injection molded parts if modified
HDPE	0.97	30-40	0.5-1.1	500-700	1-2	Pellets, sheets, and recycled stock.	-Most common thermoplastics in wood-plastic composites.

PEEK	1.32	100	3.9	150	50-75	Industrial only (advanced material	Need high-temp processing: Industrial extruder or high-temp 3D printer (~340+ °C)
ABS	1.15	60	3	100	1.5-3	Sheets/ pellets	- Coupling agentrecommended - 220–250 °C melt region - Used for consumer/automotive parts with added reinforcement

Mechanical properties of synthetic thermoplastics (Mallick, 2008 and Zafar et al., 2012 and Fan et al., 2017; Biron, 2018; Easycomposites, 2025).

PROPERTIES OF BIOPLASTICS							
PBAT	1.18-1.3	21	15-130	670	1.3-1.4	Limited	- Need plasticizers (often pre-added) - Need campatibilizers for fibres - Used in flexible biocomposites and not for high-load applications.
Bio-epoxy	-	60-68	2.64-3.04	5.3-5.8	20-25	Widely available/ sold as DIY resin kits	- Need hardener - replacement for petroleum based epoxy resin, used with natural fibres
PCL	1.07-1.2	4-785	0.21-0.44	20-1000	-	Available as pellets, sheets	- Low-temperature biocomposites -Used for medical, educational, biodegradable parts
PBS	-	-	-	-	-	Limited	- Need coupling agents - Used in natural-fibre composites - Good balance of strength and biodegradability
PVOH	-	-	-	-	-	Easy available as powder, film or filament	- Needs plasticizers (glycerol) - Often used as binder or film, not structural, used in paper composites. - Moisture sensitive
Bio-PE	0.9-0.96	8-35	0.2-1.4	-	1.3-1.8	Very limited	-Same as PE - needs coupling agents (maleic anhydride PE)
Bio-PP	0.9	21-43	1.1-1.55	-	20	Very limited	- Same as PP - Needs stabalizers - Used for automotive industry
Bio-PET	1.3-1.48	47-72	2.25-4.14	-	2.4-3.2	Limited	- Same as PET
PLA	1.27	59	1.28	-	4-20	Available as filament, pellets and sheets	- Needs plasticizers for toughness - Most used for extrusion - Rigid, brittle, most common biodegradable plastic
PHA	-	-	-	-	-	Very limited	- Needs precise temperature control - Needs plasticizers Used for high-end medical and packaging applications
PGA	-	-	-	-	-	Very limited	- Not hobby-friendly, needs controlled processing -Used for high-end medical applications
Starch Blend	-	-	-	-	-	Available as films and pellets	- Needs plasticizers (glycerol) - Used for packaging materials and Low structural demandig applications

*Properties of bioplastics (*Rahman & Bhoi, 2021; *Easycomposites, 2025;* Jian et al, 2020; Ntrivala et al. 2025*)*

PROPERTIES OF PLANT-FIBRE COMPOSITES					
Reinforcement	**Matrix**	**Tensile strength (MPa)**	**Flexural strength (MPa)**	**Young's Modulus (GPa)**	**Reference**
Flax	PP	27.3±0.2	40.9±0.6	3.90	*Yan, L et al. (2014)*
Flax	epoxy	132 (+/- 4.5)	15 (+/- 0.6)	/	*Arbelaiz, A. (2005)*
Flax (aligned)	PLA	83.0 ± 5.0	130.0 ± 5.0	9.9 ± 1.0	*Mahmudul, A. et al. (2018)*
Flax (random)	PLA	151.0 ± 7.0	215.0 ± 7.2	18.5 ± 2.0	*Mahmudul, A. et al. (2018)*
Hemp	PP	34	41.5	2.30	*Islam, S et al. (2025)*
Hemp	HDPE	27.4	37.1	2.02	*Islam, S et al. (2025)*
Hemp	polyester	33.0	54.0	5.00	*Islam, S et al. (2025)*
Hemp	PLA	44.63	90	/	*Islam, S et al. (2025)*
Jute	Epoxy	60	/	8	*Kanaginahal, G. et al. (2026)*
Jute (12 ply)	PLA	43.11	/	1.12	*Kanaginahal, G. et al. (2026)*
Kenaf	PP	42	71	/	*Akil, H.M., (2011)*
Kenaf (15%)	Polyester	57.95	/	3.69	*Saba, N. et al. (2015)*

C. MANUFACTURING PROCESSES COMPARISON

FABRICATION METHOD	THERMOSET OR THERMOPLASTIC RESIN	ADVANTAGES	LIMITATIONS	REFERENCE
Compression molding	• Thermosets • Thermoplastics	• Needs few investments: the mold and press are relatively inexpensive • Reinforcement–woven fabric (UD/BD), short fibres, chopped fibres, and chopped strand mats.	• Yields very low output rates. • Needs high labor costs. • Is consequently suited for small outputs. • Risks inducing voids and internal stresses if some air cannot escape. • Does not adapt well to the use of inserts • Often needs a finishing step.	Biron M., (2018)
High-pressure injection molding	• Thermoplastics	• Permits total automation of the process and high output rates • Has the cheapest labor costs • Is suited for mass production. For standard mass-production parts, it is the cheapest process. • Normally, the whole surface of the part has a good finish, which removes the need for finishing operations. • Apart from particular cases of resins filled with fibres and other acicular or lamellar fillers, the parts are isotropic if there are no residual constraints. • Overmolding and comolding can be used.	• Has the highest mold and press prices. • The optimization of the molding parameters can be difficult; part warpage and shrinkage are sometimes difficult to predict. • The part sizes are limited by the mold size and the machinery performances	Biron M., (2018)
Extrusion	• Thermoplastics	• The output is medium or high, varying from kg/h to t/h. • The section sizes are limited by the die size and/or the machinery size. The length is unlimited. • Several extruders can be arranged to fabricate multimaterial profiles.	• The cost of the tools and machinery depends on its sophistication but are usually expensive. Each tool is appropriate for a single section. • Arrangements of reinforcements are limited. • The parts are often anisotropic. Properties are different in the processing and transverse directions. • The aspect is correct for the outer surface but cuts are rough.	Biron M., (2018)
Autoclave curing	• Thermoplastics • Thermosets	• Uniform dispersal of resin within the matrix • Controlled dilution of resin • Smooth finishing	• Expensive tools • Higher procesing and maintanance expenses • Not appropriate for small components • Requires a highly skilled worker, because most of the steps are done manually. • It also requires time, up to several hours, thus increasing the labor cost for the composite manufacturing. • Can induce fibre buckling or wrinkles in parts due to the pressure	Biron M., (2018)
Oven curing	• Thermoplastics • Thermosets	• Tooling less expensive than autoclave curing	• Part size limited to oven size	Biron M., (2018)

Thermoforming	• Thermoplastics	• Cheap tools and molds. • Convenient for processing from prototype to mass-production parts • Allows the processing of large parts such as car body parts, refrigerator inner doors, domestic inner doors, and so on. • Large choice of machinery from very simple lab models to very sophisticated lines.	• Wall thicknesses are not controllable. • Parts must be simple with restricted shapes. • Limited choice of thermoplastics • Tolerances can be broad • Sheets are expensive, and wastes are significant. • Finishing is often necessary.	Biron M., (2018)
Wet hand lay-up	• Thermosets	• Capable of making very large parts • minimal tooling costs • curing at room temperature • Can be combined with other techniques to obtain higher strength like vacuum bagging or autoclave curing • Mould can be made of wood, plaster, sheet metal or glass. • Works great with epoxies	• Labor intensive • Mould is necessary for good fibre placement. • Does not work great without mats or fabrics. • Surface of tooling side is as smooth as the mould itself.	Campbell F.C., (2010)
Filament winding	• Thermosets • Thermoplastics	• The reinforcement levels can reach 60%75%, even 80%, making it possible to obtain excellent mechanical characteristics • The properties can be enhanced in chosen directions by modifying the winding angle • Part sizes can be significant.	• Heavy instruments • Limited design and shapes • The reinforcement placement must be carefully calculated	Biron M., (2018) Campbell F.C., (2010)
Pultrusion	• Thermoplastics • Thermosets	• Excellent mechanical properties in the profile axis • Practically unlimited length • Smooth surfaces except cut ends • continuous production.	• Exclusively profile manufacturing • Limited sizes in transverse section • Unidirectional reinforcement • Limited reinforcement choice • Significant investments	Biron M., (2018)
Low-temperature Vacuum bagging	• Thermosets	• Less mixing errors • Minimal tooling cost • Great with low-temperature resin matrices • The vacuum makes degassing easier and reduces bubbles and other voids • It is possible to use a heated oven to accelerate consolidation.	• Low temperature curing often takes a long time • Trapped air can form bubbles in resin • Necessity to tailor the bag according to the part and mold shapes • Part size limited by the mold size.	Biron M., (2018) Campbell F.C., (2010)
Resin transfer molding (RTM)	• Thermosets	• Smooth finish on both surfaces. • Can obtain high fibre volumes • Fabricating three-dimensional structures requiring tight dimensional tolerances on several surfaces. • Cycle times can be very short • Lower labor intensity and skill levels • Considerable design flexibility	• Tooling cost is high • Mold and tool design critical to part quality • Mold filling permeability based on limited permeability data base • Preform and reinforcement alignment in mold is critical. • Production quantities typically range from 100 to 5000 parts.	Campbell F.C., (2010)
Vacuum assisted resin transfer molding (VARTM)	• Thermosets	• Excellent surface finishes on tool side • Tooling less expensive than RTM	• Requires low viscosity resins • Lower fibre volumes normally obtained	Campbell F.C., (2010)

D. CURTAIN WALLING - EUROPEAN BUILDING CODES

PERFORMANCE CRITERIA	EU BUILDING CODE
Building code - Curtain wall standard	According to DIN EN 13830 / NEN-EN 12153:2023 en
Resistance to windload - horizontal load of 2KN/m^2	Accoring to DIN EN 13116 (Curtain walls - Resistance to windload-Performance requirements). Max deflection must not exceed L/200 or 15 mm if L≤3000mm, L/300 or 5mm if 3000mm < L < 7500mm and L/250 if L ≥7500mm during a measurement according to EN 13166.
Self-weight	Accoring to EN 1991-1-1. Maximum deflection of any horizontal primary beam due to vertical loads not exceeding L/500 or 3mm (depends on which is the smallest value)
Air permeability (Pa)	Accoring to DIN EN 12152 (Curtain walling - Air permeability - Performance requirements and classification) and DIN EN 153 (Curtain walling - Air permeability - test methods)
Impact resistance	Accoring to DIN EN 14019 (curtain walling -impact resistance). Pendulum is caused to impact with critical points of the facade construction (central mullion, central transom, intersection between mullion/transom, etc.) from a certain height for the purpose of this test. Permanent deformation of the facade is permitted. But falling parts, holes or cracks are prohibited.
Watertightness (Pa)	Accoring to DIN EN 12154 and DIN EN 12155 (curtain walling - Watertightness - Performance requirements and classification; Laboratory test under static pressure).
Airborne sound insulation (dB)	Accoring to EN ISO 140-3 for each property
Heat transmittance (W/m2.K)	Accoring to prEN 13947
Fire resistance of full configuration	Accoring to DIN EN 1363 (Fire resistance tests) and DIN EN 1364-3 (Fire resistance tests for non-load-bearing elements. Part 3: Curtain walling. Full configuration (complete assembly).
Fire resistance of part configuration	According to EN 1364-4 Fire resistance tests for non-load-bearing elements. Part 4: Curtain walling. Part configuration.
Fire spread	No codes. “If demanded explicitly, the curtain wall must include suitable devices that inhibit the spread of fire and smoke through openings in the curtain wall construction by means of the installation of structural base plates on the connections in all levels.” Validation from expert assessment.
Fire classification	According to EN 13501-1 Fire classification of construction products and building elements - Part 1: Classification using data from reaction to fire tests.
Durability	No codes, validtion must be provided by an expert assessment.
Seismic safety	“If necessary in the specific case, the seismic safety must be determined according to the Technical Specifications or other requirements defined for the location of use.” Validation must be provided for each property.
Thermal shock resistance	“A suitable glass, e.g. hardened or pre-tensioned glass according to European standards, must be used insofar as the glass is required to exhibit resilience to temperature fluctuation.” Validation must be provided for each property and refers exclusively to the glass installed in the property.
Building and thermal movement	“The design of the curtain wall must be capable of absorbing thermal movements and movements of the structure in such a way that destruction of facade elements or impairment of the performance characteristics do not occur

Resistance to dynamic horizontal loads	The curtain wall must withstand dynamic horizontal loads at the level of the sillpiece according to EN 19911-1." The value is expressed in [kN] at height (H in [m]) of the sillpiece.

EN 13830: Curtain walling - product Standards (adapted from STABALUX, 2025; Intertek, 2024)

E. RESULTS MICROSCOPIC ASSESSMENT

SAMPLE	DISCRIPTION OF SAMPLE
1	*Cross-stiched flax fibre cloth around aluminum mould using roll wrapping + vacuum bagging, fibre parallel to force.*
2	*Non-woven mat around aluminum mould using roll wrapping + vacuum bagging, random fibre direction.*
3	*Flax fibre yarn around aluminum mould using filament winding + vacuum bagging, fibre direction transverse to force.*

SAMPLE	MICROSCOPY	ANALYSIS
<u>Sample 1</u> Center of cross-section 200x 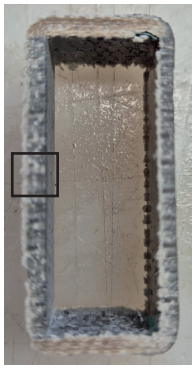	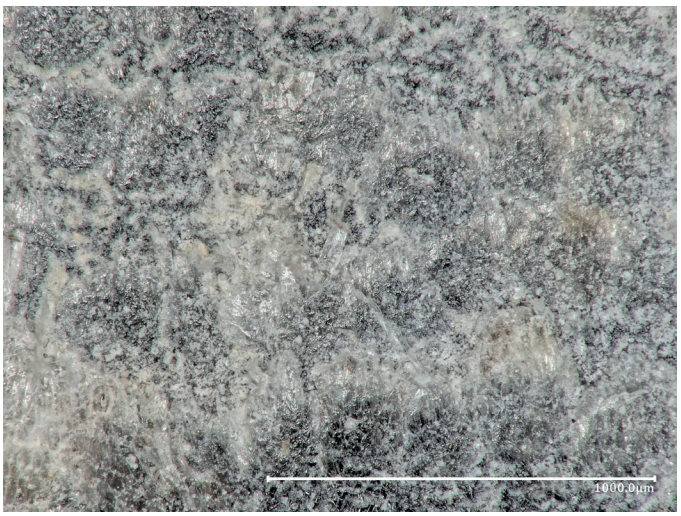 *200x microscopic view of sample 1, center of cross-section*	The brown line indicates a distinct fibre layer, which alternates with a resin-rich layer. No significant air voids or regions lacking either fibres or resin are observed in this cross-sectional view.
<u>Sample 1</u> Interior edge of cross-section 100x 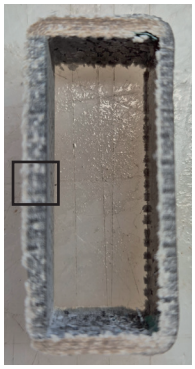	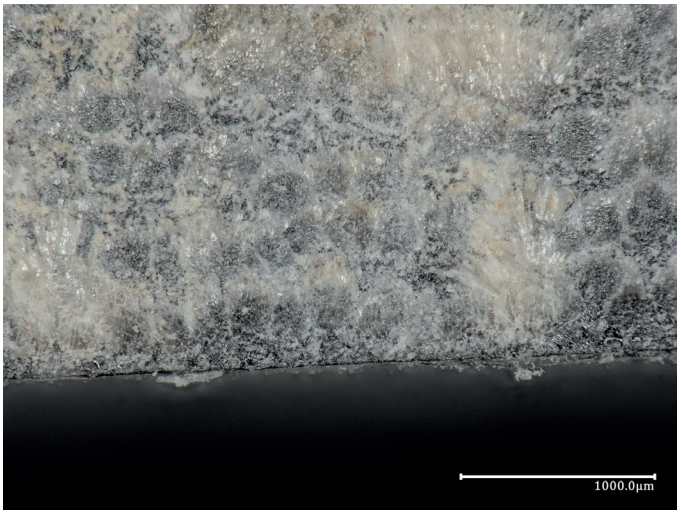 *100x microscopic view of sample 1, interior edge*	The interior edge of the sample is predominantly flat, with minimal presence of loose fibres. However, local clustering of fibre material is observed.

SAMPLE	MICROSCOPY	ANALYSIS
Sample 1 Exterior edge of cross-section 100x 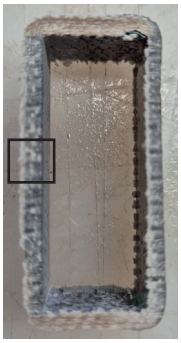	 *100x microscopic view of sample 1, exterior edge*	The exterior edge of the sample is rough, with protruding fibres extending from the surface. Fibre clustering is again observed in regions where the resin content is relatively low within the cross-section.
Sample 1 Corner view of cross-section 200x 	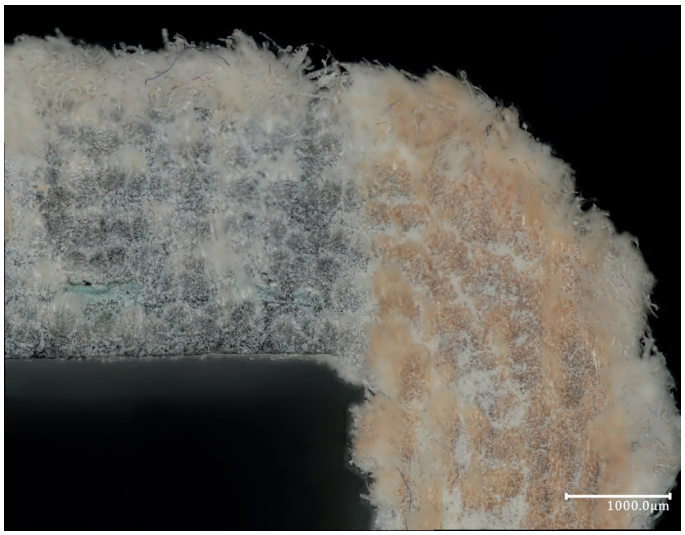 *200x microscopic view of sample 1, corner view*	The corner exhibits a clear difference in coloration between the two adjacent sides. The entire exterior surface appears rough, while the interior edge on one side is also characterised by a rough surface texture.
Sample 1 Zoomed in image of corner view of cross-section 200x 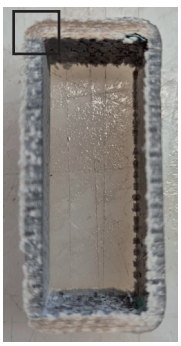	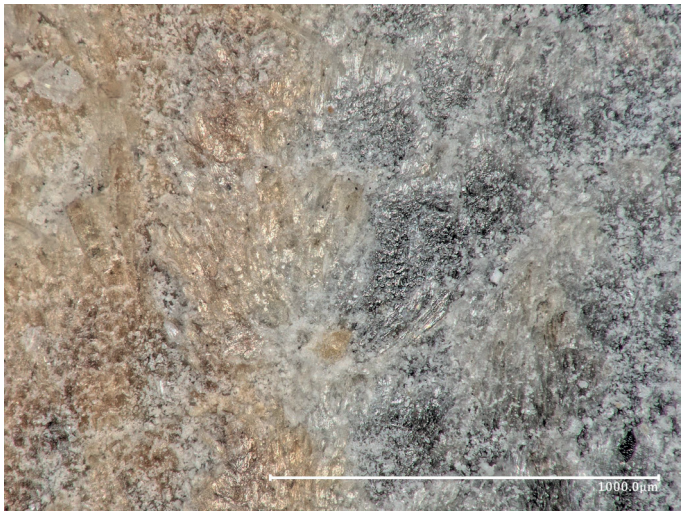 *200x microscopic view of sample 1, corner view , middle*	This image shows a magnified view of the corner region. A reduced fibre presence is observed at the interface between the brown and grey areas.

SAMPLE	MICROSCOPY	ANALYSIS
<u>Sample 1</u> Surface quality of sample 100x 	 *100x microscopic view of sample 1, surface view*	The surface of the sample appears largely uniform to the naked eye; however, microscopic inspection reveals small voids lacking resin. Within these voids, the fibre structure is clearly exposed.
<u>Sample 2</u> Center of cross-section 200x 	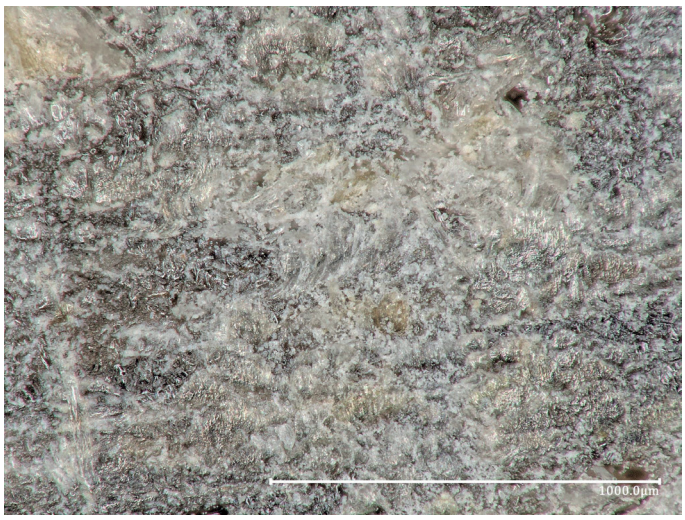 *200x microscopic view of sample 2, center of cross-section.*	The non-woven hemp fibre mat sample exhibits an uneven fibre-to-resin distribution. Small variations in fibre coloration are visible, which may indicate the presence of multiple fibre types within the sample.
<u>Sample 2</u> Interior edge of cross-section 100x 	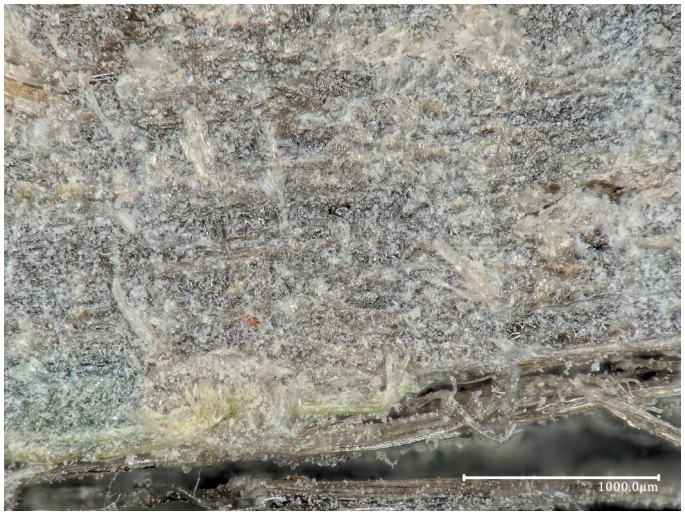 *100x microscopic view of sample 2, interior edge.*	The interior edge of the sample exhibits an uneven surface quality, with several loose fibre strands present. The fibre-to-resin distribution appears comparable to that observed in the central region of the sample.

SAMPLE	MICROSCOPY	ANALYSIS
Sample 2 Exterior edge of cross-section 100x 	 *100x microscopic view of sample 2, exterior edge.*	The exterior edge of the sample appears rougher than the interior edge. In this region, minor variations in coloration are also visible.
Sample 3 Center of cross-section 200x 	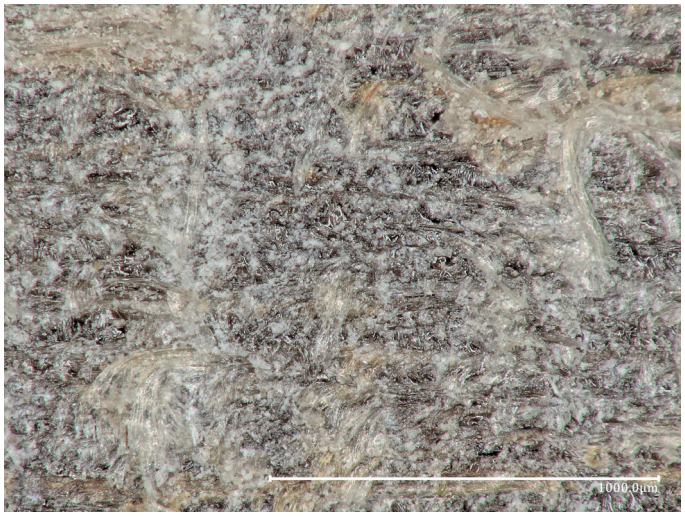 *200x microscopic view of sample 3, center of cross-section*	The central region of the cross-section of Sample 3 appears similar to that of Sample 2, with an uneven fibre-to-resin distribution observed. As in Sample 2, minor variations in fibre coloration are also present.
Sample 3 Interior edge of cross-section 100x (locally delaminated) 	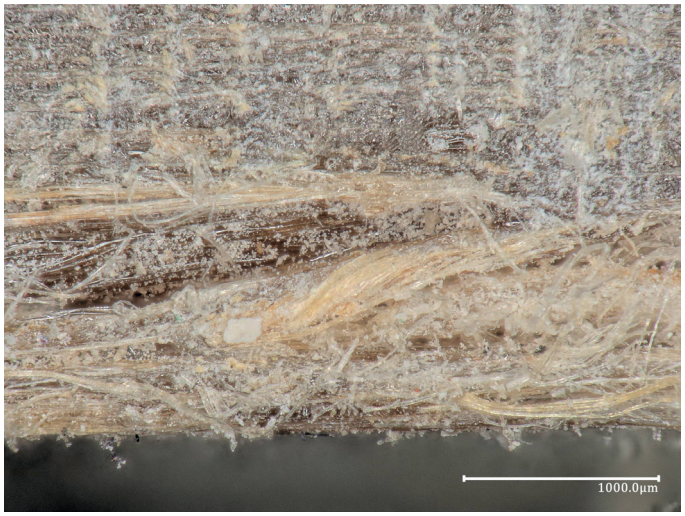 *100x microscopic view of sample 3, interior edge, locally delaminated part.*	The interior edge of Sample 3 exhibits localised delamination, where fibres appear to have detached from the composite structure. Nevertheless, the edge remains relatively smooth, with no significant fibre protrusion observed.

SAMPLE	MICROSCOPY	ANALYSIS
Sample 3 Exterior edge of cross-section 100x (worst section) 	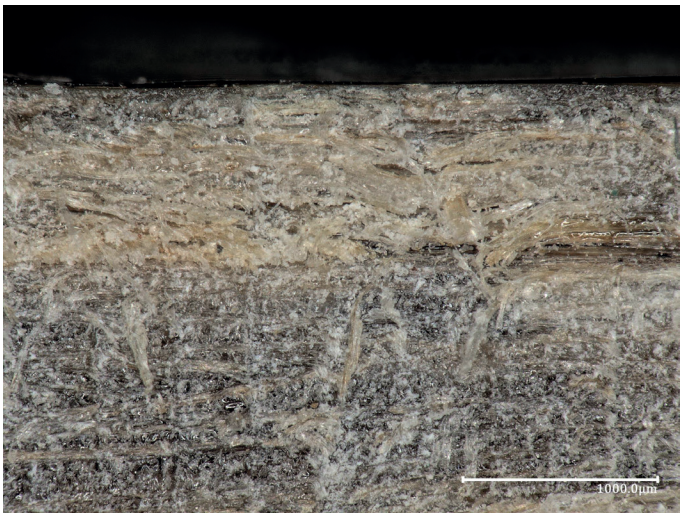 *100x microscopic view of sample 3, exterior edge, locally delaminated part.*	The exterior surface of Sample 3 appears smooth overall but shows localised delamination in this region. A distinct boundary is visible between the central area and the edge region.
Sample 3 Exterior edge of cross-section 100x (best section) 	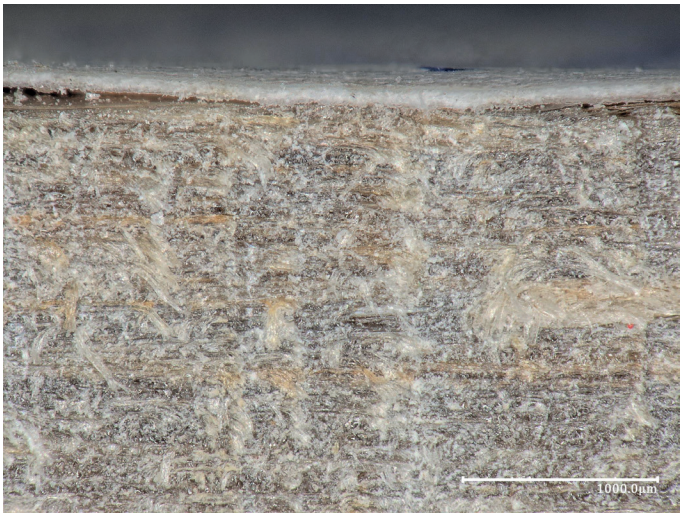 *100x microscopic view of sample 3, outer edge,best result.*	The exterior edge of another region of Sample 3 exhibits a smooth surface without signs of delamination. The fibre layers are slightly visible through the surface.

F. RESULT ECO AUDIT ASSESSMENT

Ansys GRANTA EDUPACK

Eco Audit Report

Product name	Flax fibre/epoxy composite
Country of use	Netherlands
Product life (years)	30

Summary:

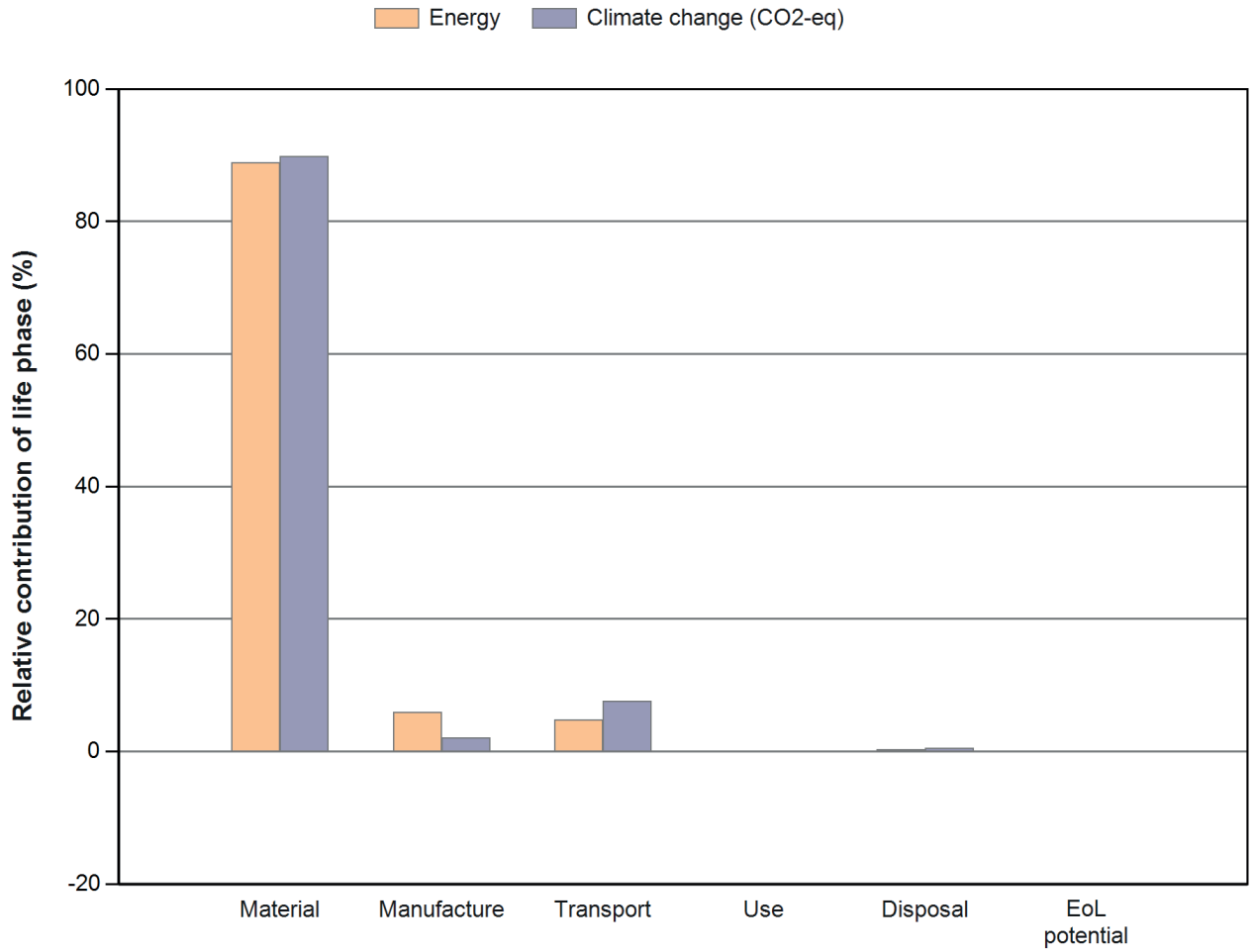

Energy details Climate change (CO2-eq) details

Phase	Energy (MJ)	Energy (%)	Climate change (CO2-eq) (kg)	Climate change (CO2-eq) (%)
Material	1,06e+05	88,9	4,52e+03	89,9
Manufacture	7,11e+03	6,0	102	2,0
Transport	5,73e+03	4,8	383	7,6
Use	0	0,0	0	0,0
Disposal	340	0,3	23,8	0,5
Total (for first life)	**1,19e+05**	**100**	**5,03e+03**	**100**
End of life potential	-46,6		-3,26	

Ansys
GRANTA EDUPACK

Eco Audit Report

Climate Change (CO2-eq) Analysis

Summary

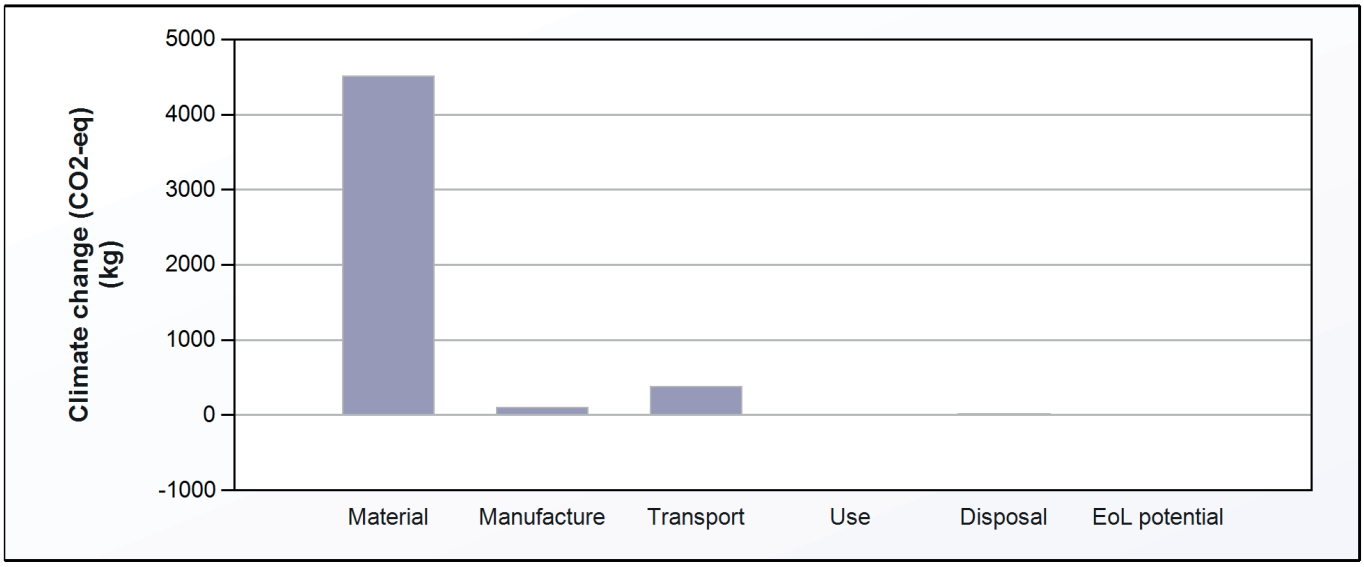

	CO2 (kg/year)
Equivalent annual environmental burden (averaged over 30 year product life):	168

Detailed breakdown of individual life phases

Material:

Summary

Component	Material	Recycled content* (%)	Part mass (kg)	Qty.	Total mass processed** (kg)	Climate change (CO2-eq) (kg)	%
Flax fibre	Flax fiber	Virgin (0%)	4,2e+02	1	4,6e+02	5,2e+02	11,4
Epoxy resin	Epoxy resin (heat resistant)	Virgin (0%)	5,8e+02	1	6,5e+02	4e+03	88,6
Total				**2**	**1,1e+03**	**4,5e+03**	**100**

*Typical: Includes 'recycle fraction in current supply'

**Where applicable, includes material mass removed by secondary processes

***User-defined material

Manufacture:

Summary

Component	Process	% Removed	Amount processed	Climate change (CO2-eq) (kg)	%
Flax fibre	Fabric production	-	4,6e+02 kg	96	94,4
Flax fibre	Cutting and trimming	10	46 kg	1,1	1,0
Epoxy resin	Custom: Filament wrapping*	-	6,5e+02 kg	3,9e-07	0,0
Epoxy resin	Cutting and trimming	10	65 kg	1,5	1,5
Profile joining	Fasteners, large	-	6e+02	3,1	3,1
Total				**1e+02**	**100**

*User-defined process

Transport:

Summary

Breakdown by transport stage

Stage name	Transport type	Distance (km)	Climate change (CO2-eq) (kg)	%
Transport Flax fibre to manufacturer	Truck 3.5-7.5t, EURO 6	5,6e+02	3,3e+02	85,5
Transport Epoxy resin to manufacturer	Truck 3.5-7.5t, EURO 6	83	48	12,6
Transport profiles to building site	Truck >32t, EURO 6	70	7,3	1,9
Total		**7,2e+02**	**3,8e+02**	**100**

Breakdown by components

Component	Mass (kg)	Climate change (CO2-eq) (kg)	%
Flax fibre	4,2e+02	1,6e+02	41,7
Epoxy resin	5,8e+02	2,2e+02	58,3
Total	**1e+03**	**3,8e+02**	**100**

Use:

Summary

Relative contribution of static and mobile modes

Mode	Climate change (CO2-eq) (kg)	%
Static	0	
Mobile	0	
Total	**0**	**100**

Disposal:

Summary

Component	End of life option	% recovered	Climate change (CO2-eq) (kg)	%
Flax fibre	Landfill	0,0	5,8	24,5
Epoxy resin	Downcycle	80,0	18	75,5
Total			**24**	**100**

EoL potential:

Component	End of life option	% recovered	Climate change (CO2-eq) (kg)	%
Flax fibre	Landfill	0,0	0	0,0
Epoxy resin	Downcycle	80,0	-3,3	100,0
Total			**-3,3**	**100**

Notes:

Summary

Appendix

User-defined materials:

Custom processes:

Name	Type	Energy	Unit	Climate change (CO2 -eq)	Unit
Custom: Filament wrapping	Primary	9	MJ/kg	6e-10	kg/kg